



Manson, John Russell (1994) *The development of a predictive procedure for localised three dimensional river flows*. PhD thesis.

<http://theses.gla.ac.uk/1124/>

Copyright and moral rights for this thesis are retained by the author

A copy can be downloaded for personal non-commercial research or study, without prior permission or charge

This thesis cannot be reproduced or quoted extensively from without first obtaining permission in writing from the Author

The content must not be changed in any way or sold commercially in any format or medium without the formal permission of the Author

When referring to this work, full bibliographic details including the author, title, awarding institution and date of the thesis must be given

THE DEVELOPMENT OF A PREDICTIVE PROCEDURE FOR LOCALISED THREE DIMENSIONAL RIVER FLOWS.

Phd.

© John Russell Manson, June 1994.

Department of Civil Engineering
Rankine Building
University of Glasgow
Glasgow G12 8LT
Scotland

For Jeanie

Remember, when discoursing about water, to induce first experience then reason.....Leonardo da Vinci, 1452-1519

Abstract

This thesis contains the formulation, development and initial tests of a computer model for the prediction of fully three dimensional turbulent free surface flows typically found at localised areas of river systems. It is the intention that the model will be used to predict flow situations which are fully three dimensional. The model is, therefore, tested against a fully three dimensional test case of flow in a two-stage meandering channel. However, the model is not intended simply to be for computing flows in meandering river channels. Rather the model is intended to be used in a variety of problems which are outlined in the thesis.

A comprehensive literature review of other relevant mathematical model studies is given and practical aspects of mathematical modelling of fluids in civil engineering is summarised. The need for the present model is argued. Particular consideration is given to the representation of turbulence in the physical system and the numerical solution method used to solve the mathematical system. The numerical method proposed draws on existing research however it introduces some novel concepts. It is contrasted with the well known SIMPLE algorithm. Importantly, the present model is demonstrated to be superior to traditional finite volume codes for time dependent problems. The need for an operator splitting approach to cope with the advection terms is highlighted.

The Reynolds Averaged Navier-Stokes equations form the basis of the physical system. The Reynolds stresses are represented by two different stress-strain relationships: (1) a linear relationship and (2) a non-linear relationship. These relationships rely on an eddy viscosity and a turbulence time-scale which are calculated from two characterising turbulence quantities, a velocity squared scale, k , and an inverse length scale, ϵ . These quantities are computed from differential transport equations. Non-linear stress-strain relationships are relatively new and, it has been argued by their originators, require application to several different problems to fully ascertain their potential for future use. The author addresses this demand by applying them to two new problems. These are flow in a plenum chamber and open channel flow over a backward facing step.

The equations are solved by an operator splitting method which, it is argued, allows for an accurate and realistic treatment of the troublesome advection terms at low spatial resolutions. This is thought to be essential since for three dimensional problems owing to computer time limitations achieving grid independent solutions with low order schemes is at present very difficult. The advantage of the present approach is demonstrated with reference to a simple one dimensional analogue. Traditional discretisation methods are shown to be poorer than the present method at small time steps (advective Courant numbers less than unity) and highly inaccurate at high timesteps (advective Courant numbers greater than unity) particularly at low spatial resolutions. The conclusions of this study have serious repercussions for researchers using traditional finite volume codes for unsteady flows although the consequences for steady flow computation are not clear. A method for dealing with the Oldroyd derivative terms in the non-linear model is

also suggested. The pressure-velocity coupling is achieved by means of a projection method which involves forming a Poisson equation for the pressure. The Poisson equation is solved by a preconditioned conjugate gradient method. The method represents the free surface with a rigid lid assumption which presently limits its applicability however many flows in civil engineering can be simulated with this assumption.

Because of computing overheads the model is initially applied to two dimensional problems to ascertain its usefulness. The model is tested with reference to a benchmark solution proposed by the IAHR. Both linear and non-linear turbulence models are tried. The mean flow field and turbulence fields are shown to be predicted at least as successfully as other numerical codes using the linear model. When the non-linear model is tried better predictions for the level of the turbulent kinetic energy are forthcoming. The model is further tested by application to several situations of importance in civil engineering, including: open channel flow over a backward facing step, flow in a settling chamber and flow over a slot. This last problem is particularly important and exhibits some of the mechanisms which occur in the cross-over region in a meandering two-stage channel. Modelling the important mechanisms are therefore treated in detail. Interestingly flow mechanisms are shown to be highly dependent on the aspect ratio of slot. A full understanding of these mechanisms is argued to be an important pre-cursor to understanding the cross-over region in a meandering two stage channel.

Finally, a fully three dimensional application is presented. Over bank flow in a single meander two-stage channel is modelled. The three dimensional simulation sheds some light on the physical processes occurring in such systems. The cross-over region is the main focus of attention. The computations show that, in agreement with experiment, a vigorous expulsion of the main channel fluid occurs with a consequently large proportion of the main channel fluid ending up on the flood plain. The model predictions for the surface elevation compare favourably with experimental results predicting local maximums in the main channel immediately before the flood plain bank and local minimums immediately after the bank. Unfortunately, certain features are not predicted by the numerical model. Noticeably, the recirculations in the main channel in the cross-over region are not reproduced although a reverse flow at the channel bed is observed. This flaw in the results is almost certainly due to an inadequate grid resolution. Plausible predictions for the turbulent kinetic energy distribution are also obtained which suggest that turbulence generated by high velocity gradients in the cross-over region is carried onto the oncoming flood plain. The results so far are promising although clearly more research has to be done. The most important areas of future research are therefore outlined.

Preface

The Development of a Predictive Procedure for Localised Three Dimensional River Flows

Thesis submitted in partial fulfillment of the requirements of the degree of Doctor of Philosophy in the Department of Civil Engineering, University of Glasgow.

Declaration

I declare that this thesis is a record of original work carried out solely by myself in the Department of Civil Engineering at the University of Glasgow in the period October, 1990 to October, 1993. This thesis has not been presented elsewhere in consideration for a higher degree.

John Russell Manson, B.Eng., June 1994.

Acknowledgements

I wish to sincerely thank Dr Gareth Pender for supervising this research project. His wise advice, criticism and encouragement were greatly appreciated throughout the duration of this project. My thanks also go to Dr Alan Ervine for his helpful advice and his encouragement.

I wish to thank Professor David Muir-Wood for allowing me to undertake this research in his Department and the Science and Engineering Research Council for funding this research in the form of a departmental studentship.

I wish to thank my colleagues for encouragement and helpful discussions along the way. In particular I wish to thank: Dr Paul Addison, Dr James Wark, Dr Manuel Lorena, Dr Trevor Davies and Mr John Fisher.

I am grateful to the staff of the Computer Services Department for their help.

Outwith Glasgow University I would like to thank Dr Bassam Younis and Dr Davor Cokljat, of City University, London for a helpful meeting in the early stages of this project. I would also like to thank Dr Steve Wallis of Heriot-Watt University for his encouragement.

I will be eternally grateful to my wife, my parents and my friends and family whose support and encouragement enabled the completion of this research.

Finally, I wish to thank a late friend, Mr Peter McCrae, for introducing me to computational hydraulics and for introducing me to Dr Gareth Pender. His enthusiasm for civil engineering hydraulics inspired those who knew him.

Table of Contents

- 1.0 Chapter 1 Introduction 1
 - 1.1 Background 1
 - 1.2 Aims of the Research Project 3
 - 1.3 Review of River Engineering 7
 - 1.3.1 River Flows and Engineering Problems 7
 - 1.3.2 Traditional or Non-computer Based Design Methods 8
- 2.0 Chapter 2 Review of Numerical Models for River Engineering 19
 - 2.1 Background to Computer Based Design Methods 19
 - 2.2 Review of Present River Models 21
 - 2.3 Hydrostatic Models 22
 - 2.3.1 Assuming a Hydrostatic Pressure 22
 - 2.3.2 Area Averaged Models - One Dimensional River Models 24
 - 2.3.3 Depth Averaged Models 26
 - 2.3.4 Quasi-Three Dimensional Models 28
 - 2.3.5 Width Averaged Models 30
 - 2.4 Non-Hydrostatic Models 30
 - 2.4.1 Pressure Solution 31
 - 2.4.2 Free Surface Treatment 31
 - 2.4.3 Three Dimensional - Rigid Lid 33
 - 2.4.4 Three Dimensional - Free Surface Tracking 35
 - 2.4.5 Two Dimensional - Vertical Plane Modelling - Rigid Lid 36
 - 2.4.6 Two Dimensional - Vertical Plane Modelling - Free Surface Tracking 37
 - 2.5 Fully Developed Flow Models 37
 - 2.5.1 Fully Developed Depth Averaged Flow Models 38
 - 2.5.2 Fully Developed Three Dimensional Flow Models 40
- 3.0 Chapter 3 Foundations for River Hydraulics 47
 - 3.1 Physical Laws 47
 - 3.1.1 Coordinate System and Control Volume 47
 - 3.1.2 Underlying Assumptions 48
 - 3.1.3 Conservation of Mass 48
 - 3.1.4 Conservation of Momentum 49
 - 3.1.4.1 Body Forces 51
 - 3.1.4.2 Surface Forces 51
 - 3.1.4.3 The Body Force Vector 53
 - 3.1.4.4 The Stress Tensor 54
 - 3.1.5 Viscous Stresses 56
 - 3.1.5.1 The Fluid at Rest 56
 - 3.1.5.2 Stress - Deformation Laws 57
 - 3.1.6 Boundary Conditions 60
- 4.0 Chapter 4 Turbulence and its Representation 64
 - 4.1 Laminar and Turbulent Flow 64
 - 4.2 Representing Turbulent Flow 65
 - 4.2.1 Full Simulation 67
 - 4.2.2 Large Eddy Simulation Models (LES) 67
 - 4.3 Reynolds Proposal 68
 - 4.3.1 Reynolds Stresses 70
 - 4.4 Turbulence Modelling 71
 - 4.4.1 Zero Reynolds Stress Models ? 72
 - 4.4.2 A Stress-Strain Relationship for Turbulent Flows 73

4.4.3	Models Based on Algebraic Formula	74
4.4.4	Models Based on One Differential Transport Equation	77
4.4.5	Models Based on Two Differential Transport Equations	79
4.4.5.1	Considerations for Depth Averaged Modelling	81
4.4.6	Non-Linear Stress-Strain Relationships	82
4.4.6.1	Baker and Orzechowski (1983)	82
4.4.6.2	Speziale's Model (1987)	83
4.4.6.3	Other Non-Linear Models	85
4.4.7	Discussion of Non-linear Stress-strain Relationships	85
4.4.8	Reynolds Stress Transport Models (RSTM)	87
4.4.8.1	Algebraic Stress Models (ASM)	87
4.5	Boundary Conditions for Turbulent River Flows	88
4.5.1	Near Wall Turbulent Flow Characteristics	88
4.5.2	Free Surface Turbulent Flow Characteristics	91
4.6	Strategy for a Three Dimensional River Model	93
5.0	Chapter 5 The Present Model	97
5.1	System of Equations	97
5.1.1	Boundary Conditions and Model Constants	98
5.2	Mathematics of the Equations	99
5.3	Solving the Hydrodynamic Equations	100
5.3.1	Co-ordinate System and Grid Aspects	101
5.3.2	Overview of Solution Technique	103
5.3.3	Treatment of the Advection Terms in Step 1	105
5.3.4	Treatment of the Diffusion Terms in Step 1	108
5.3.5	Treatment of the Pressure Terms and Continuity in Step 2	114
5.4	Solving the Turbulence Equations	119
5.4.1	Treatment of Advection and Diffusion	120
5.4.2	Treatment of Turbulence Source and Sink Terms	120
5.5	Boundary Conditions	123
5.6	Accuracy	125
5.7	Stability	126
5.8	Computer Aspects	127
6.0	Chapter 6 Numerical Tests and Model Verification	135
6.1	Pure Advection Tests	136
6.1.1	Eulerian Methodology	137
6.1.2	Lagrangian Methodology	140
6.1.3	Results of Different Schemes	143
6.1.3.1	Courant Number Less Than One	145
6.1.3.2	Courant Number Greater Than One	146
6.2	Flow in a Plenum Chamber - Boyle and Golay (1983)	148
6.2.1	Geometry, Grid and Boundary Conditions	148
6.2.2	Results	149
6.3	Open Channel Flow over a Backward Facing Step - Nakagawa and Nezu (1987)	152
6.3.1	Geometry, Grid and Boundary Conditions	152
6.3.2	Model Results and Discussion	153
6.4	Flow in a Settling Tank - Iman and McCorquodale (1983)	157
6.4.1	Geometry, Grid and Boundary Conditions	158
6.4.2	Model Results and Discussion	159
6.5	Open Channel Flow over a Slot	161
6.5.1	Geometry, Grid and Boundary Conditions	162
6.5.2	Model Results and Discussion	162
6.6	Conclusions from Initial Numerical Trials	164
7.0	Chapter 7 Three Dimensional Applications	220
7.1	Overview	220
7.2	Flow Mechanisms in Meandering Two-Stage Channels	221
7.3	Description of the Present Problem	224
7.3.1	Grid and Boundary Conditions	225
7.4	Results	226
7.4.1	Primary Velocity Field	226
7.4.2	Secondary Velocity Field	227
7.4.3	Water Surface Elevation	228

7.4.4 Turbulence Characteristics 228

7.5 Conclusions from Results 229

8.0 Chapter 8 Closure 242

8.1 Summary of Work and Conclusions 242

8.1.1 Conclusions Regarding Numerical Methods 243

8.1.2 Conclusions Regarding Turbulence Modelling 244

8.1.3 Conclusions Regarding Two Dimensional Applications 245

8.1.4 Conclusions Regarding Three Dimensional Application 245

List of Illustrations

Figure 1.	Computer Speeds and Performances	16
Figure 2.	Overbank flow in straight river reaches - Principal Mechanisms	17
Figure 3.	Divided channel approach	17
Figure 4.	Overbank flow in meandering river reaches - Principal Mechanisms	18
Figure 5.	Complex localised flow at a bridge	18
Figure 6.	Typical fully developed depth averaged flow model results	44
Figure 7.	Typical fully developed three dimensional flow model results	45
Figure 8.	The coordinate system	62
Figure 9.	Mass and momentum balance	62
Figure 10.	Forces on small element	63
Figure 11.	Deformation of Fluid	63
Figure 12.	Laminar and Turbulent Flow	94
Figure 13.	Time Trace of Velocity in a River at Point A	94
Figure 14.	Eddy viscosity in uniform flow	95
Figure 15.	Eddy viscosity in localised non-uniform flows	95
Figure 16.	The 'staircase' approximation	128
Figure 17.	Alternative grids and variable placement	128
Figure 18.	Characteristic Curves	129
Figure 19.	Computational Cell for Stress Terms	129
Figure 20.	Convergence Curve for Gauss-Seidel Operator for Stress	130
Figure 21.	Computational Cell for Pressure Calculation	131
Figure 22.	Five point diagonal square and associated uncoupling problem	131
Figure 23.	Convergence Curve for PCGM for Pressure Solution (Res2, Pdel)	132
Figure 24.	Curves Depicting Attainment of Steady State	133
Figure 25.	Eulerian Grid	167
Figure 26.	Characteristic Curves in One Dimension	167
Figure 27.	Characteristic Curves in Two Dimensions	168
Figure 28.	Results from Implicit Schemes - Upwind, Central	169
Figure 29.	Results from more Implicit Schemes - QUICK, SMART	170
Figure 30.	Results from Implicit Schemes - Upwind, Central	171
Figure 31.	Results from Implicit Schemes - QUICK, SMART	172
Figure 32.	Results from Explicit schemes - QUICKEST, TAKACS	173
Figure 33.	Results from Lagrangian Schemes - Linear and Cubic Interpolation	174
Figure 34.	Implicit Schemes - Upwind, Central - High Courant Number	175
Figure 35.	Implicit Schemes - QUICK, SMART - High Courant Number	176
Figure 36.	Implicit Schemes - Upwind, Central - High Courant Number	177
Figure 37.	Implicit Schemes - QUICK, SMART - High Courant Number	178
Figure 38.	Lagrangian Schemes - Cubic Interpolation - High Courant Number	179
Figure 39.	Geometry and Computational Details	181
Figure 40.	Predicted By Linear Model - Vectors and Contours of normalised k	182
Figure 41.	Predicted By Other Research Group - Vectors and Contours of k	183

Figure 42. Comparison with experimental data - Velocity Profiles	184
Figure 43. Comparison with experimental data - Normalised k Profiles . . .	185
Figure 44. Predicted By Non-Linear Model - Vectors and Contours of normalised k	186
Figure 45. Comparison with experimental data - Normalised k Profiles . . .	187
Figure 46. Geometry and Computational Details	189
Figure 47. Velocity vectors within the recirculation zone	190
Figure 48. Comparison of Linear Model with experiment - Turbulence Intensity	191
Figure 49. Comparison of Linear Model with experiment - Turbulence Intensity	192
Figure 50. Comparison of Linear Model with experiment - Turbulence Intensity	193
Figure 51. Comparison of Linear Model with experiment - Reynolds stresses	194
Figure 52. Comparison of Linear Model with experiment - Reynolds stresses	195
Figure 53. Comparison of Linear Model with experiment - Reynolds stresses	196
Figure 54. Comparison of Non-linear Model with experiment - Turbulence Intensity	197
Figure 55. Comparison of Non-linear Model with experiment - Turbulence Intensity	198
Figure 56. Comparison of Non-linear Model with experiment - Turbulence Intensity	199
Figure 57. Comparison of Non-linear Model with experiment - Reynolds Stresses	200
Figure 58. Comparison of Non-linear Model with experiment - Reynolds Stresses	201
Figure 59. Comparison of Non-linear Model with experiment - Reynolds Stresses	202
Figure 60. Geometry and Computational Details	204
Figure 61. Results for Linear Model - Velocity Vectors and K	205
Figure 62. Results for Linear Model - Viscosity and Length Scale	206
Figure 63. Comparison with experimental data - U Profiles	207
Figure 64. Comparison with experimental data - U Profiles	208
Figure 65. Comparison with experimental data - U Profiles	209
Figure 66. Water Surface Profile Results of Jasem (1990)	211
Figure 67. Flow Results of Fujita et al (1991)	212
Figure 68. Computational Grids	213
Figure 69. Velocity Vectors at Differing Aspect Ratios	214
Figure 70. K Values at differing Aspects Ratios	215
Figure 71. Eddy Viscosity Values at differing Aspects Ratios	216
Figure 72. Turbulent Length Scale Values at differing Aspects Ratios	217
Figure 73. Normalised Surface Pressure Profiles	218
Figure 74. The Problem Geometry, after Kiely (1989)	231
Figure 75. Computational Grid Details	232
Figure 76. Velocity Profiles - Predicted	233
Figure 77. Velocity Profiles - Observed	234
Figure 78. Streamlines - Predicted and Observed by	235
Figure 79. Lateral Velocity Vectors in Cross-over region - Pred and Obs . .	236
Figure 80. Comparison of water surface level	237
Figure 81. Comparison of turbulence above bankfull level	238
Figure 82. Staircase approximation	239
Figure 83. Possible grid for future study	240

List of Tables

Table 1.	Expressions for C	10
Table 2.	Investigations for uniform depth averaged flow in compound channels	40
Table 3.	Investigations for fully developed three dimensional flow	42
Table 4.	Model Constants for Standard Linear Model	80
Table 5.	Non-linear Model Constants	83
Table 6.	Wall Friction Relationships	89
Table 7.	Typical values of Nikuradse's equivalent sand grain size	90
Table 8.	Summary of boundary conditions	99
Table 9.	Model Constants	99
Table 10.	Summary of grid types	102
Table 11.	Source terms due to stress terms	110
Table 12.	Implicit Schemes	138
Table 13.	Explicit Schemes	140
Table 14.	Hydraulic Parameters for experiment ST3 after Nakagawa and Nezu (1987)	152
Table 15.	Predictions for the recirculation length in step heights	155
Table 16.	Summary of some other fully three dimensional model applications	221

Notation

A Cross-sectional area of river channel

P Wetted Perimeter of river channel

R Hydraulic Radius of river channel

h Depth of water

η Water stage, $h + z_o$

f Friction factor

δ Shear layer width

λ Darcy-Weisbach friction factor ($4f$), pressure weighting factor and also non-dimensional eddy viscosity (NEV)

θ Angle river bed makes with horizontal

S_o River bed slope

S_f Friction slope (rate of loss of energy)

\bar{U} Cross-sectionally averaged velocity of river

ρ Water density

$\bar{\tau}_b$ Average bed shear stress

τ_{bx} Average bed shear stress in x direction

τ_{by} Average bed shear stress in y direction

τ_{ij} Stress tensor

F Fraction of Fluid Volume (VOF Method)

H Height above datum (Height function method)

$\bar{\nu}_t$ Depth averaged turbulent viscosity

g gravitational acceleration

α Energy correction factors

α_{ij} Constants in Bakers Model

$C_{1,2,3}$ Constants in Bakers Model

$a_{1,2,3}$ Constants in Bakers Model

T Timescale of large eddies, $(\frac{k}{\varepsilon})$

p' Turbulent fluctuation of pressure

E Additive constant in log-law

B , Roughness Factor in log-law

k^+ Non-dimensional Nikuradse's k ,

z^+ Non-dimensional wall distance

κ Von Karmans Wall Constant

$\overset{\circ}{D}_{ij}$ Oldroyd derivative

β Momentum correction factors

C Friction coefficient

k_s Nikuradse's Equivalent Sand roughness

n Manning's coefficient

t time

x, y, z co-ordinate directions

w_o Typical vertical velocity

u_o Typical horizontal velocity

h_o Typical depth

L_o Typical length scale

u^* Friction velocity

P^{atm} Atmospheric pressure

$\delta x, \delta y, \delta z$ Small spatial distances

g_x, g_y, g_z Body accelerations

f_x, f_y, f_z Body forces

$c, c_{shallow}$ Water wave celerities

σ Ratio of celerity of general wave to celerity of shallow wave

P Pressure

U_o Normalising velocity

L_o Normalising length scale
 δ_{ij} Kronekar delta
 F_x Depth averaged body force in x direction
 F_y Depth averaged body force in y direction
 T_{xx}, T_{yy} Depth averaged normal stresses
 T_{xy} Depth averaged shear stress
 η Water surface elevation
 k Kinetic energy of the turbulent fluctuations $= \frac{1}{2}(\overline{u'^2} + \overline{v'^2} + \overline{w'^2})$
 ε Dissipation rate of the Kinetic energy of the turbulent fluctuations
 ν_t Turbulent viscosity
 μ Dynamic molecular viscosity
 ν Kinematic molecular viscosity
 ε_{ij} Mean strain rate tensor based on instantaneous velocity field
 σ_{ij} Stress tensor
 D_{ij} Mean strain rate tensor based on time averaged velocity field
 $\overline{u'_i u'_j}$ Reynolds stress
 Δx Computational Grid spacing in x direction
 Δy Computational Grid spacing in y direction
 Δz Computational Grid spacing in z direction
 $U_{i,j,k}$ Instantaneous velocity components in i,j,k directions
 $u_{i,j,k}$ Time averaged velocity components in i,j,k directions
 $u'_{i,j,k}$ Turbulent fluctuation of velocity components in i,j,k directions
 P Instantaneous pressure
 p Time averaged pressure
 ϕ Time averaged effective pressure incorporating normal turbulent stress and gravitational potential $(\frac{P}{\rho} + \frac{2}{3}k - gx_j)$
 l,m,n Computational grid indices (subscripts)

i, j, k Tensor notation indices
 $n, aux, n + 1$ Computational time indices (superscripts)
 a_{l+1}, a_{l-1} Computational coefficients
 b_{m+1}, b_{m-1} Computational coefficients
 c_{n+1}, c_{n-1} Computational coefficients
 Ω Relaxation parameter
 c_μ Constant in linear k- ε model
 $c_{1\varepsilon}$ Constant in model
 $c_{2\varepsilon}$ Constant in model
 σ_k Constant in model
 σ_ε Constant in model
 c'_μ Additional constants
 c'_d Additional constants
 C_D Constant in Speziale's Model
 C_E Constant in Speziale's Model

1.0 Chapter 1 Introduction

1.1 *Background*

In recent years the use of numerical methods for solving engineering problems in hydraulics have become very popular. Improved computer hardware, its low cost availability and greatly improved user interfaces are the primary reasons for this. Mathematical descriptions of engineering problems previously considered too complicated to be tackled are being re-evaluated in light of this. At both the high performance computer level (mainframes and supercomputers) and the low performance computer level (desktop computers) these advances in speed and useability seem set to continue at pace, see figure 1. These advances in computability must be tempered however, at least in river engineering, with the uncertainties prevalent in most river hydraulics problems. After all the solution to any problem is only as good as the most questionable step in the calculation. The uncertainties in a river engineering problem are considerably higher than in aeronautical or mechanical engineering fluid mechanics problems. In these disciplines the problem geometry is usually man-made, therefore regular and may be specified with reasonable confidence. Similarly, the boundary conditions are generally straightforward and therefore introduce little or no error. This is not so in river engineering problems which are set in the natural environment, usually take place over longer timescales and in many cases are interlinked with probabilistic hydrological predictions. In addition most river beds are mobile and

our present understanding of how the changing bed forms affect resistance is far from complete.

Despite these difficulties there are certainly instances when it is beneficial to learn from the research that has been done in the refined modelling fields of aeronautical and mechanical engineering computational fluid mechanics. In particular many problems in civil engineering involve complex three dimensional flow fields which interact strongly (and non-linearly) with the associated turbulence and scalar fields (temperature, concentration of species etc). Examples of such flows are, flow over a slot or steep-sided trench, secondary flows in channels, plumes and jets in the near field, hydraulic jumps, short crested waves, breaking waves and localised flow at hydraulic structures. The non-hydrostatic pressure field in these situations prevents, or at least casts some doubt on the validity of, the St.Venant or two-dimensional depth-averaged analysis which have focussed the attentions of civil engineering researchers for the last three decades. The non-uniform velocity in the vertical and lateral directions and the associated secondary motions in planes normal to the main flow direction are typically taken account of by correction factors, mixing coefficients, effective dispersion terms or lumped resistance coefficients. While these simplified approaches have an important place as predictive tools they are, undoubtedly, an approximation. Models based on them may be suitably calibrated (i.e. adjustment of the empirical coefficients) until they give reasonable results but, often, in doing so the underlying physics is conveniently 'forgotten'. The danger of forgetting the underlying physics has been highlighted by Townson (1991) and a similar argument (albeit in a slightly different context) has been expounded by Samuels (1990). Basically, this process of calibration should not be continued outwith reasonable limits where different physical laws should be adopted. The limits however are not clearly defined and can often be liberally interpreted and then ingeniously justified. The alternative

then is to move to the other end of the modelling spectrum. That is, to include much more theory in the model formulation in the hope that more flow physics will be correctly reproduced. In general, the more underlying theory included in mathematical models the more universal its application. Unfortunately, they will also tend to be more computationally demanding. Finding a balance between computational requirements and accuracy of results (or physical realism) is a recurring question in computer modelling. A persisting no-go area of computational river engineering is the prediction of very localised highly three dimensional flows which are still the domain of physical models. It is the intention of this research to explore the development of models for these situations.

1.2 Aims of the Research Project

The aim of this research project was to begin the development of a computer code for three dimensional numerical modelling in river applications. This was the first stage in a longer term research strategy of the Department of Civil Engineering at Glasgow University. The work was inspired by the Science and Engineering Research Council (SERC) funded programme on the Flood Channel Facility (FCF) at HR Wallingford and the perceived need by the river engineering community to have available a numerical model capable of simulating these flows. The intention of the research was more general however in that it was decided to develop a code capable of application to other localised three dimensional problems as well as the two stage channel investigations of the FCF programme.

Initially the possibility of using or adapting one of the commercially available three-dimensional hydrodynamic codes such as PHOENICS, FLUENT or HARWELL-FLOW3D was investigated. Following an initial literature review this option was ruled out for the following reasons:

1. Each of these codes come from a background of mechanical engineering and their development has therefore largely ignored parallel developments in civil and environmental engineering. Only now is this being rectified. These codes adopt turbulence models based on the early turbulence modelling research of Launder and Spalding at the Imperial College Department of Mechanical Engineering although in updated form. These models may be too advanced or not advanced enough for civil engineering problems but this has not yet been fully quantified.
2. These codes are based on traditional finite volume methods (SIMPLE or one of its derivatives) which have been around since 1972. The initial literature review revealed that it may be more advantageous to investigate the suitability of other algorithms reported in the literature, most notably those based on the work of the Los Alamos Group (e.g. Amsden and Harlow (1970)) and the operator splitting (or fractional step) approach of of the Electricite de France (e.g. Viollet, Benque and Goussebaile (1983)). Independently, each research group has developed or adopted an algorithm and then tended to concentrate on its application. There appears to be little consideration given by research groups to other completely different methodologies once they have a code that 'works'. This means that research groups may not be aware of the differences between their codes and other available codes. This has been addressed, to some extent, in this thesis by outlining the advantages of the present approach (operator splitting) over traditional finite volume methods. This is highlighted in chapter 6.
3. Published results comparing experimental and numerical results for relatively simple cases show varying degrees of agreement, although the investigators use similar numerical methods and turbulence models, see section 6.3.2. In most

cases the differences can be attributed to subtle differences in the codes or in the grid used. There are also instances in the literature where misapplication on the part of the users has resulted in erroneous results. This leads to the conclusion that it would be unwise to base a three year research programme on the use of a computer code of which one's understanding of its operation is limited by documentation in users manuals. The same conclusion applies to the Department's plans to extend the programme beyond one PhD programme.

4. In the U.K. computational fluid dynamics (CFD) community fully three dimensional simulations are carried out almost exclusively with variants of the SIMPLE algorithm (a traditional finite volume code). Only if different research groups adopt different numerical algorithms to solve the same problems will truly independent verification of the underlying physics result. It will be demonstrated that traditional finite volume discretisation of the advection terms is not always suitable, see chapter 6.

The decision was therefore taken to develop a new three-dimensional code. This will of course contain certain limitations when compared with the commercially available codes, but at least the limitations will be fully understood. In addition, however, it provides the opportunity to implement algorithms which may prove better than the existing codes.

The specific research objectives of the project were therefore to:

1. Undertake a literature review extending to all branches of engineering to identify a suitable solution algorithm to achieve the simulation of the flows described above.

2. Develop a numerical code for the solution of the fully three dimensional Reynolds Averaged Navier-Stokes equations. The model should be capable of simulating fully three dimensional turbulent flow with a free surface as would be found at localised river features and hydraulic structures.
3. Critically review the treatment of the advection terms which are known to be troublesome. Identify a suitable treatment of the terms.
4. Critically review turbulence models applied to other engineering problems. Select those suitable for the aims of this project and verify these against data sets from simplified two-dimensional problems representative of civil engineering problems.
5. Apply the code to a fully three dimensional flow problem to ascertain its usefulness.

It was decided at an early stage that the certain features would be outwith the scope of the current project and form part of future model developments. These led to the following recommendations:

1. To develop the code using rectilinear elements rather than curvilinear. This decision was taken as it was believed that the feasibility of the coding should be demonstrated first using the simpler rectilinear formulation.
2. The computer used for the present purposes in this project was the IBM 3090 mainframe available at Glasgow University. During the project it was recognised that this machine was reaching the end of its useful life, indeed it is to be decommissioned in July, 1994. Significant improvements in computer speed could be achieved by porting the code to a more modern machine.

However, this would have seriously detracted from the present research effort since time would be required to mount the code on a new machine. It was therefore decided to accept the limitations of the IBM mainframe and for this project to concentrate on hydraulic and numerical aspects of the problem. Upgrading to a more powerful computer could form part of a follow on project.

3. To initially represent the free surface using the rigid lid approximation. An algorithm for tracking variations in the free-surface would have required an upgrade of the computer facilities, see (2) above.

1.3 Review of River Engineering

1.3.1 River Flows and Engineering Problems

Flows which enter the river system from direct surface runoff and through ground percolation are continually varying. Likewise, where flow leaves the system - at the sea - the water elevation is continually varying owing to gravitational effects of the moon on the large water mass in the oceans. With these boundary conditions estimated civil engineers are required to predict water levels and flow rates throughout the river system and the effects of changes made to the river. It can be appreciated that river engineers are never dealing with exactly steady, uniform flow despite the large number of solution techniques based on this assumption. Many engineering predictions are concerned with river modification works. For example, if a bridge is placed at some point in the river system, what effect does that have on water levels upstream and downstream ? How will sediment erosion and deposition characteristics alter ? Will the dispersion characteristics of the river change ?

Since early times the river engineer has been concerned with the prediction of water quantity and its distribution. Predictions of water quality received little or no attention. This is because society was more concerned with the supply of water and the control of flooding with their more immediate effect upon human lives than with the safe and clean disposal of waste waters. There has, in the past, been a notion that rivers and estuaries have an infinite dilution potential because of their enormous volume. In recent years this idea has gradually lost credence and society has come to appreciate that wastewater disposal to the hydrosphere must be properly managed. Falconer (1992) gives reasons for this change in public perception. The role of civil engineers has had to change accordingly with predictions of water quality now required for most new river and estuary developments. This has a very important effect on engineering research. This is because for water quality predictions there is a much greater dependence on the turbulence representation than there is for water level and flow predictions which, for the most part, can be conceptualised adequately as a balance between bed friction and the action of gravity through the water surface slope. In order to make more accurate predictions of solute mixing a better understanding of turbulence characteristics will be required. Mathematical models of solute transport will similarly benefit by adopting more sophisticated turbulence closures, Falconer and Li (1992).

1.3.2 Traditional or Non-computer Based Design Methods

Computer based solutions are discussed in chapter 2. However, before doing this it is interesting to review some of the traditional or non-computer based solution methods.

Rivers are much longer than they are broad or deep. Traditionally therefore they have been considered as one dimensional bodies. Classical equations describing

steady, uniform river flow have been proposed in different forms at different times but they more or less say the same thing : the component of water weight acting down the slope is balanced by the resisting force due to friction generated at the river bed and walls, Henderson (1966). For a short reach of channel δx , with cross-sectional area, A , and a mean boundary shear stress $\bar{\tau}_b$ acting over the wetted perimeter P , the resisting force is $\bar{\tau}_b \delta x P$. The weight of this element is $\rho g A \delta x$ thus the weight component in the flow direction is $\rho g A \delta x S_o$ where S_o is the slope of the channel (which must be small for the above to hold true) and g is the gravitational acceleration. Equating these gives $\bar{\tau}_b = \rho g \left(\frac{A}{P} \right) S_o$. This simple model is, at present, entirely theoretical. To proceed, however, we must postulate how $\bar{\tau}_b$ relates to the mean flow velocity. In doing this empirical relations are introduced. If the mean boundary shear stress depends on the mean kinetic energy per unit volume as can be shown by dimensional analysis then,

$$\bar{\tau}_b = f \frac{1}{2} \rho \bar{U}^2 = \rho g \left(\frac{A}{P} \right) S_o \quad [1.1]$$

In the above model \bar{U} represents the mean flow velocity in the channel and f is a roughness parameter obtained from experimental observations. The boundary shear stress is sometimes described by an pseudo-velocity termed the friction velocity, $\frac{\bar{\tau}_b}{\rho} = u^{\star 2}$. For an infinitely wide channel the ratio A/P equals the flow depth, h , and for a pipe of diameter, D , flowing just full the ratio A/P becomes $D/4$. If the pipe-flow becomes pressurised then the slope must re-defined as the hydraulic gradient of the piezometric head. For pipes therefore it is convenient to study the empirical parameter, $4f$ which is equivalent to λ , the Darcy-Weisbach coefficient. The behaviour of this parameter has been studied extensively for pipe flow, but has led to some confusion by having two friction factors, one being four times the other. Indeed f and λ are both referred to as the Darcy-Weisbach

coefficient in different literature sources although strictly only λ is. Re-writing equation 1.1 in terms of flow velocity,

$$\overline{U} = \sqrt{\frac{2g}{f}} \sqrt{(\frac{A}{P})S_o} \tag{1.2}$$

or

$$\overline{U} = C \sqrt{RS_o} \tag{1.3}$$

where $R = A/P$, the hydraulic radius, and $C = \sqrt{2g/f}$ is a friction coefficient. Expressions for C have been proposed in different forms over the years, by Chezy in 1768, Manning in 1891, Colebrook-White in 1939 and Williamson in 1959 among others. These contributions are all described by Henderson (1966). The friction coefficient, C , is taken to be constant or a function of the cross-sectional geometry and the boundary roughness, see table 1. In table 1 n is the Manning’s roughness coefficient and k_s is the Nikuradse equivalent sand size.

Originator	Expression for C
Chezy	Constant
Manning	$\frac{R^{1/6}}{n}$
Colebrook-White	$\sqrt{\frac{2g}{f}}$ where $f = \lambda/4$ and $\lambda^{-1/2} = -2\log(14.8R/k_s)$
Williamson	$26.4(R/k_s)^{1/6}$

Table 1. Expressions for C: Fully developed rough turbulent flow over a fixed bed

Re-writing in terms of discharge, Q , instead of velocity,

$$Q = CA \sqrt{RS_o} \tag{1.4}$$

or

$$Q = K\sqrt{S_o} \quad [1.5]$$

where K is known as the conveyance of the river channel. An equation like 1.5 is usually the first recourse of a civil engineer dealing with a river problem. Their use in isolation is limited, however, since exactly steady, uniform flow, over a fixed bed almost never occurs in practice. They do however provide a first approximation which allows the design process (which is generally trial and error) to begin.

Where the river is steady but non-uniform then the discharge, Q , is constant but the water depth changes with distance. The problem then is to determine the water level throughout the river system subject to an imposed water level at some point. A fuller description of this calculation is given by Henderson (1966). In brief it may be shown by considering an energy balance between two sections of a gradually varying river channel that,

$$\alpha_1 \frac{Q^2}{2gA_1^2} + h_1 + z_1 = \alpha_2 \frac{Q^2}{2gA_2^2} + h_2 + z_2 + \delta x \bar{S}_f \quad [1.6]$$

where

$$\bar{S}_f = \text{Avg}(S_{f1}, S_{f2}) \quad [1.7]$$

and α is an energy correction factor, h is the river depth, z is the bed elevation and S_f is termed the friction slope and represents the rate of energy loss per unit distance. It may be manipulated from equation 1.5 or a variant thereof by assuming that friction characteristics are the same in uniform and non-uniform flows. $\text{Avg}()$ is some averaging function the simplest being arithmetic averaging,

$$\text{Avg}(x_1, x_2) = 0.5 \times (x_1 + x_2) \quad [1.8]$$

although other averaging functions may be more appropriate to different kinds of gradually varied flow profiles, Laurenson (1985). It will be appreciated that if the water depth is known at one section then equation 1.6 may be solved to provide the depth at another section since the bed elevations are known and the areas and friction slopes may be written as functions of the flow depth. This process may be continued in a piecewise fashion until the river profile is established.

There are however reaches of the river where the above theory has to be modified. The basic resistance equation described above does not perform well in predicting the resistance characteristics in natural river sections which have a main channel in which the river flows most of the time and flood plains which are usually only inundated during periods of high precipitation. When this flood plain inundation occurs the flow characteristics of the river can change quite drastically especially if the main channel is not aligned with the flood plain direction. This is the norm for natural channels. In such cases the standard resistance equations have to be modified to take account of this. Traditional methods involve dividing the channel into compartments, computing the conveyance of each compartment and then summing to obtain the total channel conveyance. These concepts are illustrated in figures 2 and 3. These traditional treatments for channels with floodplains have been shown to be unreliable often resulting in errors of as much as 30% in flow predictions for a given depth, Myers and Brennan (1990). Therefore in recent years a research programme, aimed at understanding the principle flow mechanisms and producing practical guidelines for prediction calculations, has been carried out at Hydraulics Research, Wallingford and a number of Universities in the U.K. under the auspices of the Science and Engineering Research Council. The full conclusions of this research programme are not recapitulated here instead reference is made to Ackers (1991) who reviews

available methods and produces design recommendations. More elaborate computer based solutions to this problem will be dealt with in chapter 2.

The uniform flow analysis is strictly only valid for long straight rivers. Of course real rivers are not like that and contain many localised deviations from this ideal, for example at river bends or at river structures (bridges, weirs, pipeline trenches, groynes etc). These points on the river are termed 'transitions' by Henderson (1966) who defines them as usually short features which produce a local change in the state of flow. Although short, such transitions may affect the river for a significant distance upstream and downstream. At these points zones of recirculation may form and secondary motions may become significant. Although river bends sometimes occur in isolation and therefore could be considered a 'transition' this is unusual and more commonly they tend to occur in a series of quasi-periodic meanders and therefore constitute a slightly different case. Willetts (1991) and Sellin, Ervine and Willetts (1992) give some insight into this problem and suggest possible solution strategies. Figure 4 shows some of the important mechanisms of over bank flow in meandering channels.

For the general case of localised non-uniform, non-fully developed flow, which may be caused by natural or man-made river geometries, a different approach to quantifying energy losses is therefore required. Such regions are traditionally treated by replacing equation 1.6 with a local loss formula which has been derived experimentally for the particular river structure. For example at a bridge, figure 5, Yarnell's classic equations may be used, see Henderson (1966). Other examples of localised flow laws are given by Henderson (1966) or Chow (1959). The problem with such empirical laws is that although many experiments have been undertaken there are so many different types of bridge configuration and different settings in the river due to local bathymetry that a completely universal equation cannot be

produced. The same, of course, goes for any type of river structure. In addition to relying on these empirical equations for stage-discharge relationships we also have to rely on these studies to give some indication of the localised effects at the structure (bed shear stresses, local velocities etc). Therefore, if the actual structure being designed differs from the configuration of the classical studies (and usually this is inevitable owing to the local bathymetry) then unreliable predictions would result. These problems are therefore usually resolved by recourse to physical model studies.

The foregoing is a brief summary of traditional design methods in river engineering. The description is by no means exhaustive but gives a flavour of what has been possible in the past. Other problems which can be approached by a hand calculation have been omitted in the interests of brevity (in particular unsteady calculations - flood routing, tidal calculations). Henderson (1966) or Chow (1959) give full descriptions. Fischer et al (1979) describe some hand calculations for solute transport problems. It is worth pointing out that despite the rapid advances in computer software and numerical methods these traditional methods have served civil engineers well for many years and will continue to be used routinely in design offices. They may seem simplistic compared to the complex computer models which are now abundant but as a first approximation they are often adequate for predicting flow and water levels. They have been less successful in solute transport predictions where there is less confidence in the physical laws adopted and there is a consequently greater variance in the model coefficients. They are generally poor for calculating localised effects and recourse is usually taken to a building a physical model of the situation, Samuels (1985). A recent example of this eventuality is given by Kaya and McNally (1991). Physical models are expensive and inflexible. In addition it is often particularly difficult (if not impossible) to incorporate the correctly scaled level of turbulent mixing. They are

less favoured now in comparison to mathematical models for many applications although there are certain circumstances where they are the only alternative. They also have an important advantage in public relations. The non-expert, who is generally financing hydraulic improvements, usually finds it easier to accept that a small scale model of a river or estuary behaves like its larger prototype than an abstract set of equations. This intuition is not well founded and will lessen as computer modelling matures but it still is a consideration.

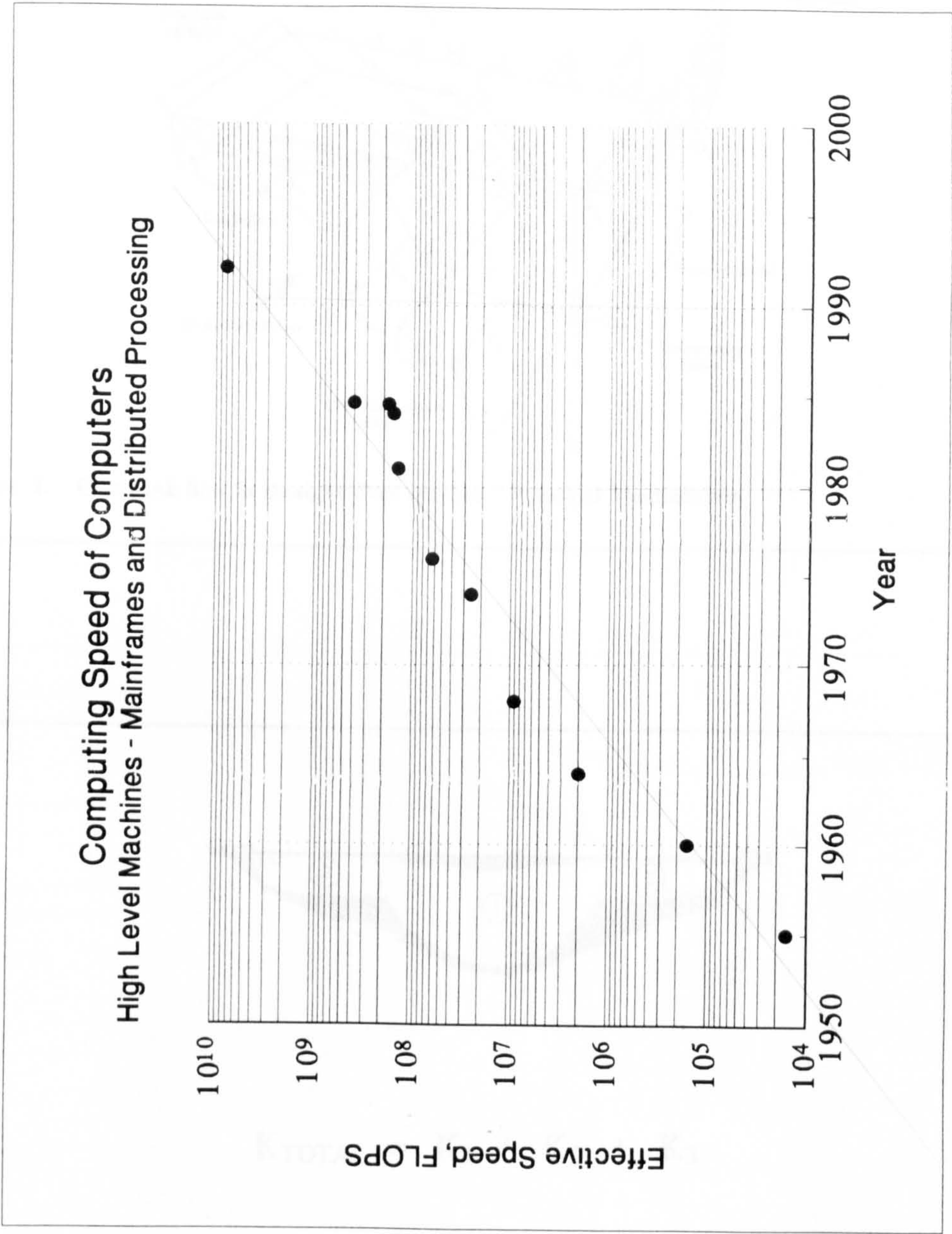
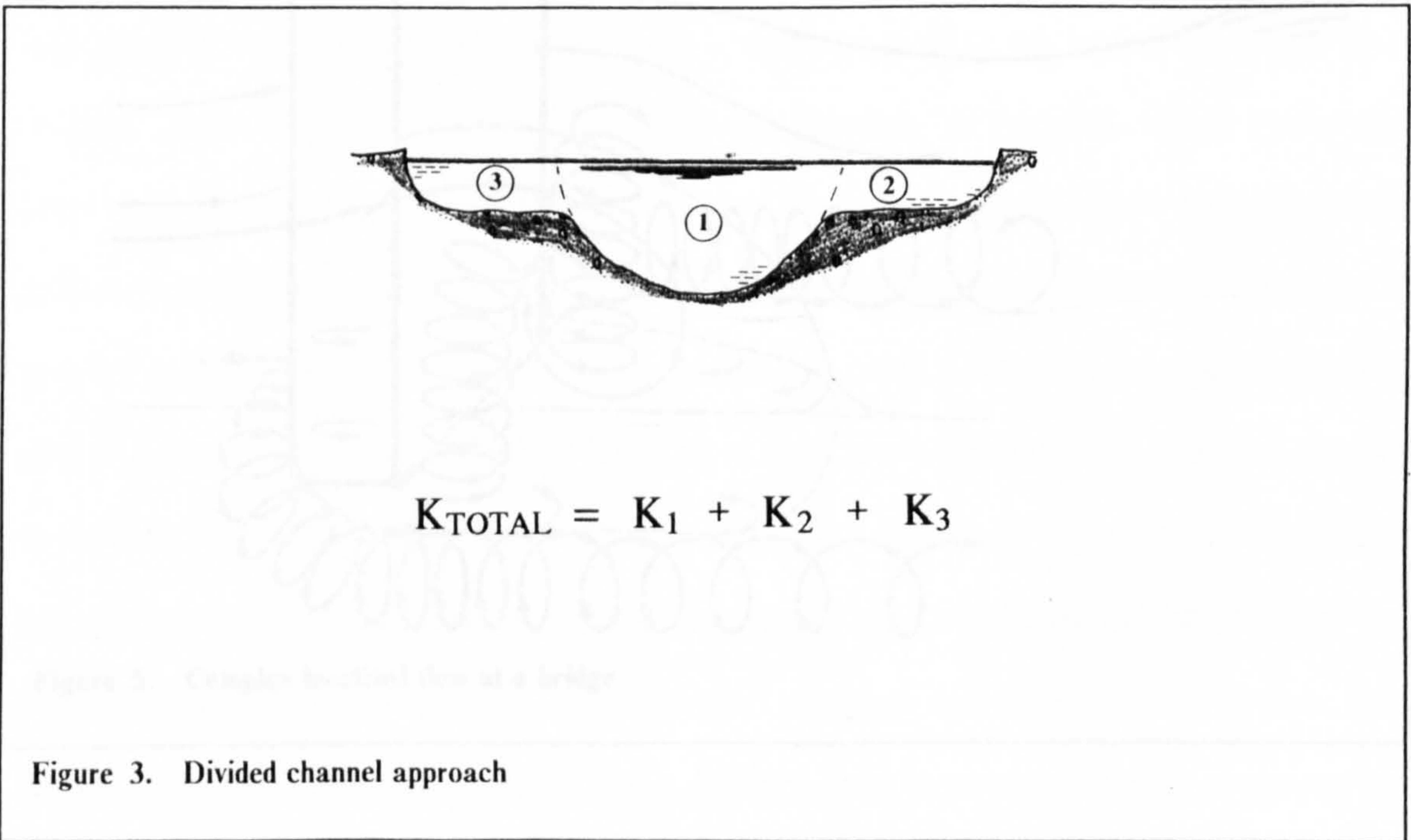
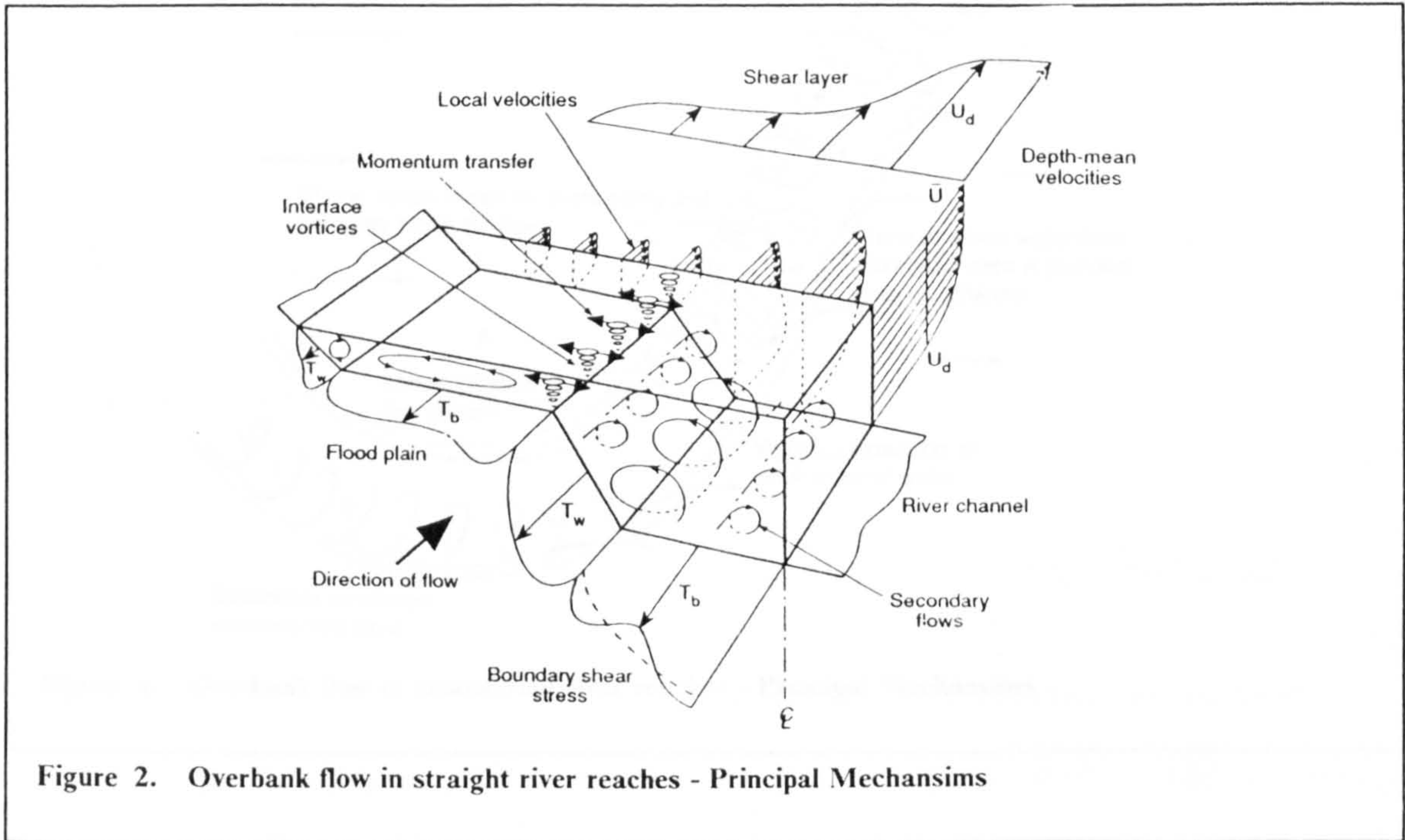
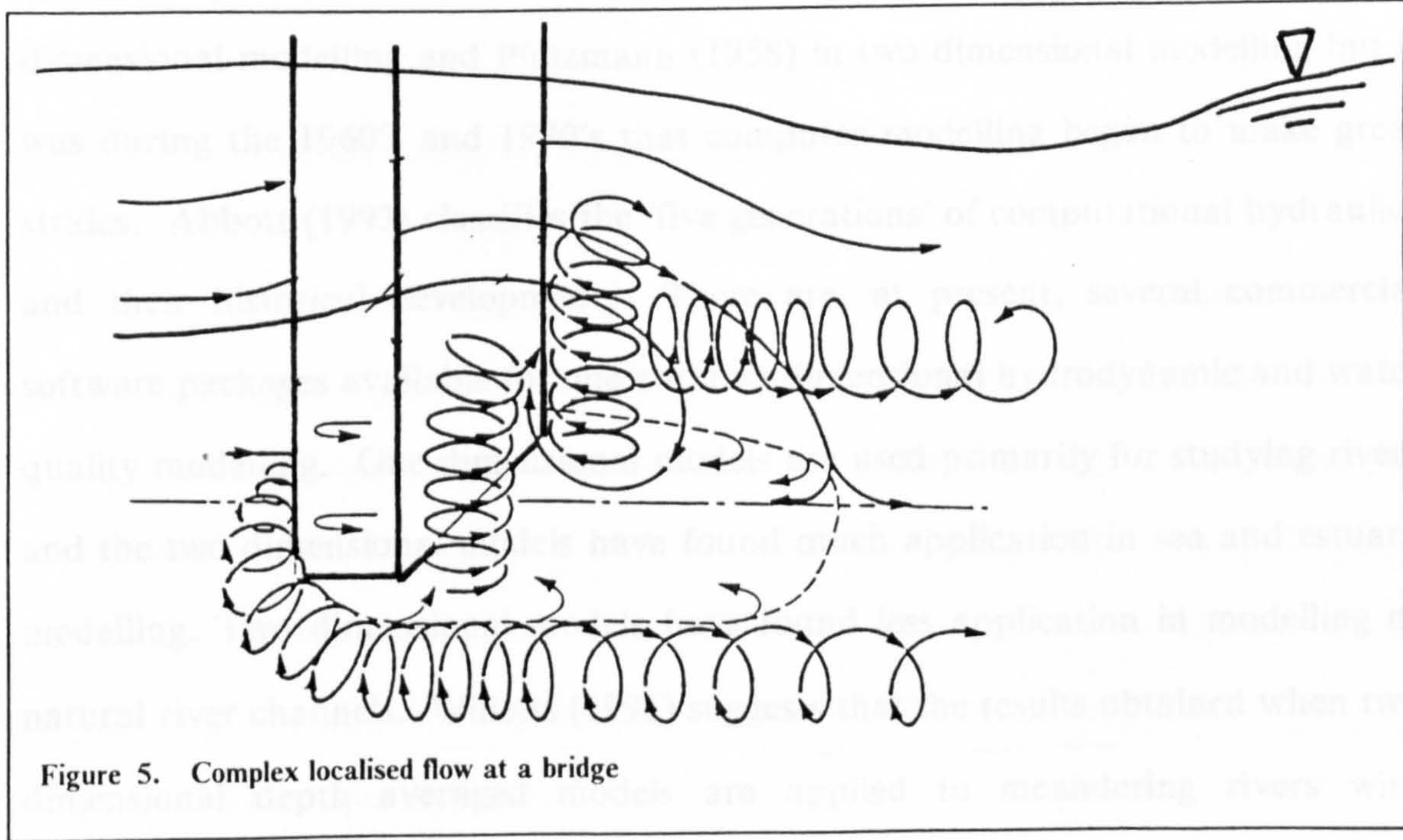
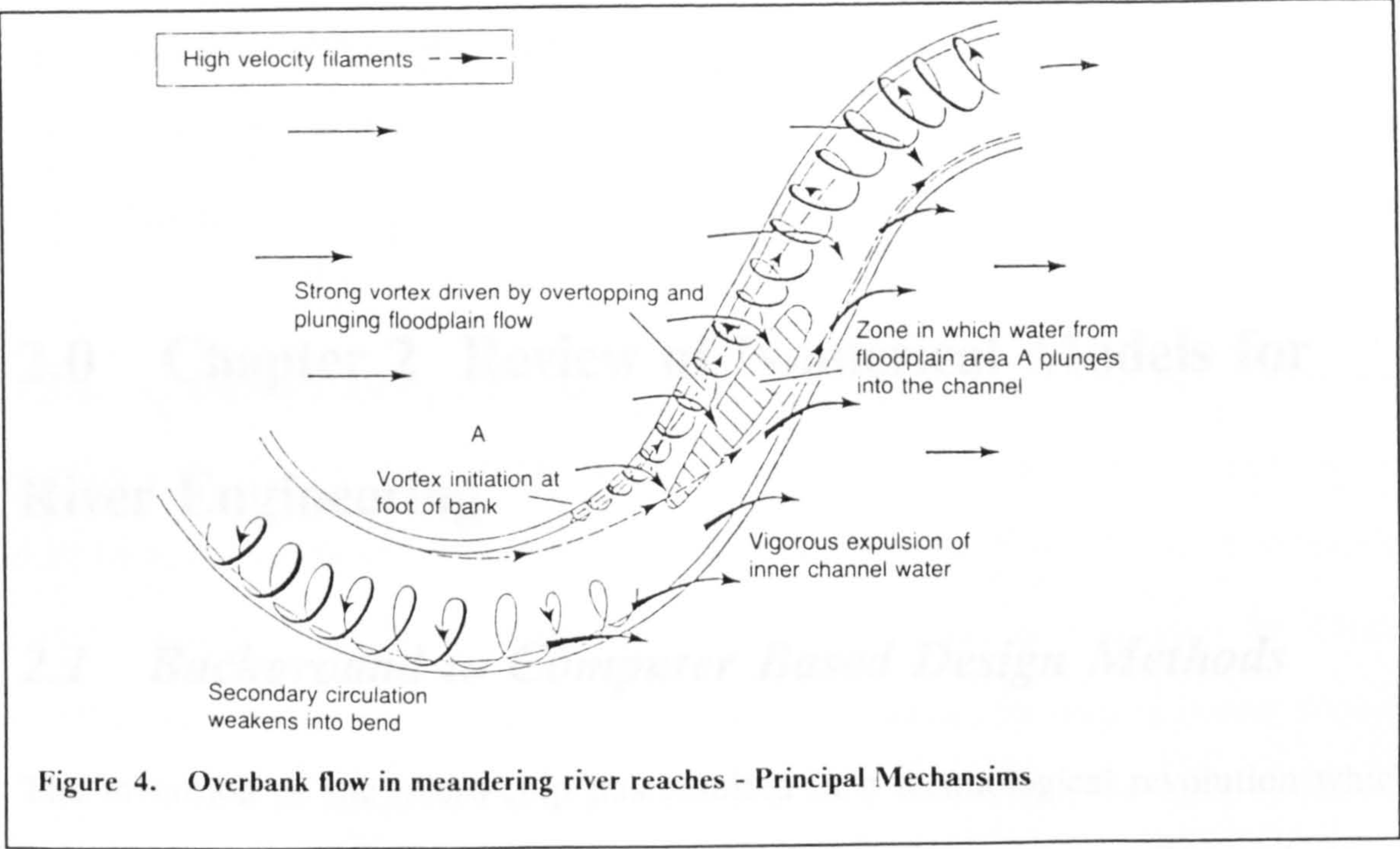


Figure 1. Computer Speeds





2.0 Chapter 2 Review of Numerical Models for River Engineering

2.1 Background to Computer Based Design Methods

The invention of the micro-chip has resulted in a technological revolution which has affected many areas of society and is continuing to do so. The techniques available in river engineering and environmental management have changed dramatically. Early computer based solutions include Preissmann (1960) in one dimensional modelling and Platzmann (1958) in two dimensional modelling but it was during the 1960's and 1970's that computer modelling began to make great strides. Abbott (1993) classifies the 'five generations' of computational hydraulics and their historical development. There are, at present, several commercial software packages available for one and two dimensional hydrodynamic and water quality modelling. One dimensional models are used primarily for studying rivers and the two dimensional models have found much application in sea and estuary modelling. Two dimensional models have found less application in modelling of natural river channels. Willetts (1991) suggests that the results obtained when two dimensional depth averaged models are applied to meandering rivers with floodplains are 'fortuitous' and Cunge (1989), in a keynote address, suggests that there are a limited number of circumstances in which a two dimensional model may be applied to a river engineering problem since,

....when a river engineering problem cannot be approached by a 1-D schematisation, most likely it includes 3-D features (such as helicoidal secondary currents) which should be taken into account and typical 2-D hypotheses of horizontal velocities are not sufficient.....

There is also an increasing concern that for pollution transport problems, particularly if the pollutants are not neutrally buoyant, then only three dimensional models can truly represent the phenomena. Indeed two dimensional depth averaged models can give very misleading results as discussed by Thorn (1993). He presents a case study of a warm water discharge from a power station where the results obtained from a depth averaged model and the results from a three dimensional model are in sharp contrast and would lead to very different design recommendations. This study highlights the false economy of employing the less expensive two dimensional models when they are really not applicable. It also shows that the choice of using a two dimensional or using a three dimensional model for a particular study is not always obvious a priori.

Over the same time period that civil engineers were concentrating their efforts on the development and application of one dimensional and two dimensional depth averaged models mechanical and aeronautical engineers were using computer models to study the complexities of fluid turbulence and its effects on mechanical engineering problems. In order to do this they have had to develop numerical procedures for solving the mathematical systems governing these flows. The two schools of model development seem to have developed almost independently providing a wealth of literature on the subject. There is now evidence in the research literature that these two schools of thought may be converging with civil engineering researchers including more sophisticated turbulence models into their codes, Falconer and Li (1992), while mechanical engineering researchers are

adapting their numerical algorithms to the application to civil engineering problems, Reeve and Hiley (1992), and Rajar (1992).

In summary, one dimensional river models are (and will remain) the workhorse in the civil engineering design office. When their use becomes untenable or at least questionable owing to the complexity of the local flow field then suitably calibrated two dimensional models, although not strictly representing the flow physics, may provide some additional predictions. However when these also become inapplicable recourse is usually made to physical models. The aim of this research is to provide a viable numerical model alternative to physical models for the case of highly localised three dimensional flows.

2.2 Review of Present River Models

This review is chiefly concerned with studies of flows with a free surface as this is the main area of this research effort. The representation of the turbulent stresses has not been treated in detail in this chapter since the models that are described here could in theory be implemented with a variety of different turbulence models. Therefore, detailed discussion of turbulence modelling is postponed until chapter 4. The models in this chapter are set apart by other more fundamental differences.

This review has been split up into three model categories. Models that assume hydrostatic pressure, those that do not assume hydrostatic pressure and models that assume fully developed flow. Strictly the fully developed flow model is a sub-category of both hydrostatic and non-hydrostatic flow models, however, its relevance to river engineering warrants it a separate treatment in this discussion.

2.3 *Hydrostatic Models*

The Navier-Stokes equations are most often found in civil engineering in a simplified form, the commonest simplification being that the vertical momentum equation is reduced to a statement of hydrostatic pressure, i.e. negligible vertical motions. Models that assume hydrostatic pressure are termed shallow water models since, as it will be demonstrated, they should only be used to simulate shallow water waves whose celerity is given by \sqrt{gh} where h is the water depth. There are basically three alternatives for modelling shallow water waves: area averaged river models, depth averaged models and quasi-three dimensional models.

2.3.1 Assuming a Hydrostatic Pressure

In this approach the vertical momentum equation is reduced to,

$$\frac{\partial P}{\partial z} = -\rho g \quad \text{Natural co-ordinate system} \quad [2.1]$$

by neglecting the local and advective acceleration terms as well as neglecting the Reynolds stress gradients. Neglecting these terms reduce the universality of the model. If this assumption is made, and further it is assumed that the fluid is well mixed throughout its depth, i.e. the density is uniform, then equation 2.1 may be integrated to give pressure as a linear function of the depth below the water surface,

$$P = P_{atm} + \rho g(\eta - z) \quad [2.2]$$

where P_{atm} is the atmospheric pressure at the water surface, η is the water surface elevation above some datum and z is the depth below the datum. This means that pressure may be eliminated as a dependent variable in favour of water elevation and the pressure gradients in the horizontal momentum equations become

independent of the vertical co-ordinate. This greatly simplifies the equations at the expense of generality. The question remains: when is it valid to assume hydrostatic pressure ? A rough indication may be given by an order of magnitude analysis which weighs the importance of vertical accelerations against gravity. Liggett (1975) has carried out this order of magnitude analysis and concludes that in order for the assumption of hydrostatic pressure to be valid, $\frac{h_o}{L_o}$, must be less than some assigned tolerance value, where h_o is some representative depth and L_o is some feature length. This assigned tolerance value depends on the problem and also on the accuracy the user is prepared to accept but some general guidelines may be obtained by consideration of linear wave theory. The celerity of a linear oscillatory wave is given by,

$$c = \sqrt{\frac{gL}{2\pi} \tanh\left(\frac{2\pi h}{L}\right)} \quad [2.3]$$

as summarised by Townson (1991). The celerity of a shallow water wave (hydrostatic pressure) is given by,

$$c_{shallow} = \sqrt{gh} \quad [2.4]$$

obtained from 2.3 by letting $\frac{h}{L}$ tend to a small number. Therefore, the ratio of the celerities calculated by these two formula is,

$$\sigma = \sqrt{\frac{\tanh(2\pi \frac{h}{L})}{2\pi \frac{h}{L}}} \quad [2.5]$$

Thus for the hydrostatic pressure assumption to be valid to within 2 percent ($\sigma = 0.98$) the ratio of the water depth to wave length must be less than 0.055. This places a restriction on the range of waves that may be modelled with any form of the shallow water equations.

If the flow phenomenon is not an oscillatory wave but has significant vertical motions a different way of testing the validity of hydrostatic pressure assumption must be defined. Following Liggett (1975),

$$\frac{w_o}{u_o} = \frac{h_o}{L_o} \quad [2.6]$$

where w_o is a typical vertical velocity and u_o is a typical horizontal velocity. Thus, instead of basing the accuracy criteria on h_o/L_o it may be possible to base it on w_o/u_o . Thus to assume hydrostatic pressure with an accuracy of 2% the ratio of vertical to horizontal velocity should be less than 5%. This criterion merely serves as a very rough indication and more work is required to categorically prescribe limits where hydrostatic models may be applied and when fully three dimensional models should be used. However it does give some indication of the validity of the hydrostatic pressure assumption.

2.3.2 Area Averaged Models - One Dimensional River Models

These models are the workhorse of the civil engineering hydraulics industry. Indeed there are several computer packages available which are based on this type of model. In addition to the hydrostatic pressure assumption these models assume that only the streamwise component of horizontal velocity is important so that equations describing conservation of mass and momentum in only one dimension, along the river's longitudinal axis, are required. A formal derivation of the physical laws which these models are based on is given by Yen (1973) in which the Reynolds Averaged Navier-Stokes equations are averaged over the river cross-sectional area. These laws are (adapted from Yen (1973)),

$$B \frac{\partial \eta}{\partial t} + \frac{\partial Q}{\partial x} = q \quad [2.7]$$

Conservation of Mass

$$\frac{\partial Q}{\partial t} + \frac{\partial}{\partial x} \left(\frac{\beta Q^2}{A} \right) + gA \frac{\partial \eta}{\partial x} + \frac{A \bar{\tau}_b}{\rho R} = 0 \quad [2.8]$$

Conservation of Momentum

In these equations Q is the river discharge, η is the water stage, B is the flow top width, q is the lateral inflow per unit length, A is the flow area and R is the hydraulic radius. In these models, $\bar{\tau}_b$ and β are empirical parameters which must be specified. $\bar{\tau}_b$ is often termed the mean boundary shear stress but perhaps should be renamed the mean effective boundary shear stress because in practice it is only rarely determined by the value of the bed roughness alone. It is replaced in the above equation by some functional relationship which relates it to the river discharge derived from equation 1.1. β is a momentum correction factor which takes account of the fact that the velocity distribution over the cross section is non-uniform. These variables represent the effects of turbulence in a lumped parameter sense. Boundary conditions usually consist of specified flow hydrographs at upstream boundaries and specified water stages (which may be tidally varying) or rating curves at downstream boundaries although alternative boundary conditions are possible. These equations, when furnished with suitable initial conditions may be solved by a numerical method to give flows and stages throughout the river. This is not described in detail here. Cunge, Holly and Verwey (1980) give a fuller description.

These models are well proven and appear to work well for what they were designed for, i.e. calculating the stage and flow throughout river systems. They do not, however, give much detailed information at local points on the river. At certain points of the river, e.g. bridges or local expansions or contractions, the equations as given above are not representative and local empirical laws must be applied. This is similar to what must be done in traditional solutions at these points and therefore has the same consequences, see section 1.3.2.

2.3.3 Depth Averaged Models

When both horizontal velocity components are important but strong vertical mixing is promoted by bed roughness, leading to an almost uniform velocity in the vertical, then it is possible to derive a depth averaged form of the Reynolds Averaged Navier-Stokes Equations. For a description of the depth averaging process, see Wark (1990). The depth averaged equations may be written in a natural co-ordinate system,

$$\frac{\partial \eta}{\partial t} + \frac{\partial \bar{U}h}{\partial x} + \frac{\partial \bar{V}h}{\partial y} = 0 \quad [2.9]$$

Conservation of Mass

$$\frac{\partial \bar{U}h}{\partial t} + \beta \left[\frac{\partial}{\partial x} (\bar{U}\bar{U}h) + \frac{\partial}{\partial y} (\bar{U}\bar{V}h) \right] + gh \frac{\partial \eta}{\partial x} + \frac{\tau_{bx}}{\rho} + F_x - \frac{1}{\rho} \left[\frac{\partial}{\partial x} T_{xx} + \frac{\partial}{\partial y} T_{xy} \right] = 0 \quad [2.10]$$

Conservation of Momentum in X Direction

$$\frac{\partial \bar{V}h}{\partial t} + \beta \left[\frac{\partial}{\partial x} (\bar{V}\bar{U}h) + \frac{\partial}{\partial y} (\bar{V}\bar{V}h) \right] + gh \frac{\partial \eta}{\partial y} + \frac{\tau_{by}}{\rho} + F_y - \frac{1}{\rho} \left[\frac{\partial}{\partial x} T_{yx} + \frac{\partial}{\partial y} T_{yy} \right] = 0 \quad [2.11]$$

Conservation of Momentum in Y Direction

η is the water elevation, \bar{U} and \bar{V} are the depth averaged velocities in the horizontal directions, β is the momentum correction factor, h is the water depth, τ_{bx} is the bed shear stress in the horizontal directions, $F_{x,y}$ represents some external body force and T_{xx} , T_{xy} , *etc* are the horizontal stresses. These are described in more detail in chapter 4 where turbulence modelling is introduced. Appropriate boundary conditions are specification of flow or water elevation, some combination of the two or some relationship describing the flow at water/land interfaces (zero flow normal to the land and some relationship between flow and stress tangential to the land).

This type of model has been applied by Platzmann (1958) for predicting storm surges in lakes, Leendertsee (1967) for predicting the effects of underwater explosions, Kuipers and Vreugdenhil (1973) for a variety of steady state problems including river channels and Falconer (1984) for flow and water quality prediction in tidal embayments.

Natural river channels tend to have very irregular courses. The river banks meander in a quasi-periodic but irregular line often with the river width varying simultaneously. Although there are studies in the literature which utilise a cartesian computational grid and therefore approximate the river bends with a staircase like boundary, Vreugdenhil and Wijnbenga (1982), it may be more appropriate to use a technique which can take account of the irregular geometry with less approximation. Candidates for this are the finite element method, as applied by Samuels (1985) or Su, Wang and Alonso (1980), applying a finite difference technique to the shallow water equations after transforming them to a suitably boundary fitted co-ordinate system, Wijnbenga (1985), or a finite volume procedure, Lai and Yen (1992). These are only examples of what has been achieved - there are many other studies in the literature using this basic model. The

work of McGuirk and Rodi (1978) deserves mention as one of the earliest applications of a more sophisticated turbulence model to the depth averaged flow equations however this will be discussed more fully in chapter 4.

These equations appear to work well for vertically well-mixed, nearly horizontal flow in which the horizontal velocity components are nearly uniform in the vertical and there are negligible vertical motions. However, as mentioned in the previous chapter, this cannot always be assumed particularly in highly localised river flows.

2.3.4 Quasi-Three Dimensional Models

The equations used are the continuity equation, the x and y direction momentum equations and the hydrostatic relation. Sometimes it is advantageous to non-dimensionalise the equations in terms of the water depth. Most applications of these models so far have been for water bodies with large horizontal dimensions compared to the depth such as lakes and estuaries. However, there have been some studies of river channels. Liggett (1969) has applied this type of model to computing lake circulation. Falconer, George and Hall (1991) also describe an application of this type of model to a shallow, homogeneous lake. Leendertse (1973) has applied this type of model to computing flow and water quality in seas and estuaries. Van der Kuur et al (1989), present a version of Leendertse's basic scheme in a boundary fitted co-ordinate system and have used it for simulating flows in tidal bays. Koutitas and O'Connor (1980) has used a quasi-three dimensional model to investigate wind driven circulations in Thessalonki Bay. This study highlights the difference between various turbulence models for calculating the vertical shear stresses due to turbulent mixing. Blumberg and Mellor (1983) have proposed a model of this type for computing flow and water quality in open seas and Galperin and Mellor (1990) have applied the same model to predicting river-estuary system circulations. Blumberg, Galperin and O'Connor (1992) have

further applied it to computing velocity profiles in river channels. Hall, Shiono and Falconer (1992) have presented a quasi-three dimensional model which they have applied to an idealised tidal embayment and claim greater computationally efficiency than other three dimensional models currently in use. A quasi-three dimensional model has been introduced by Janin, Lepeintre and Pechon (1992) which is based on an operator splitting approach utilising the finite element method. Benque, Hauguel and Viollet (1982) describe the application of a quasi-three dimensional model to computing flow patterns in a river channel with a skewed trench with gently sloping sides. Recently Ammer and Valentin (1993) have applied the quasi-three dimensional equations with the finite element method to river flows with floodplains. The preliminary results presented were not very encouraging but clearly this approach with suitable refinement and improvement should eventually provide a useful quasi-three dimensional river model. Shimizu, Yamaguchi and Itakura (1990) have applied a hydrostatic pressure three dimensional model to predicting flow and sediment transport for in bank meandering channels. Their results highlight the importance of computing the pressure driven secondary motions for sediment transport.

Once again only a selection of applications of these quasi-three dimensional models is given. These models allow the prediction of a wider variety of flows than the depth averaged models. They provide more flow information and allow for a more realistic treatment of vertical mixing however they are not applicable when vertical accelerations become significant and/or when the stress gradients in the vertical become important. In the selection of studies given above various levels of turbulence closure have been adopted ranging from zero to two equation models. These will be discussed in chapter 4.

2.3.5 Width Averaged Models

Finally, for completeness, width averaged models are briefly considered. These models are a simplification of the quasi-three dimensional models when the flow can be considered uniform or nearly uniform over the channel width. The quasi-three dimensional equations can then be averaged over the channel width. For a fuller description see Hamilton (1974). This type of model has found use in application to nearly prismatic tidal channels which are stratified due to a salt wedge intrusion.

2.4 *Non-Hydrostatic Models*

The equations upon which these types of model are founded are presented and explained in chapters 3 and 4.

Due to computing overheads many studies have not retained all terms in the Reynolds Averaged Navier-Stokes equations where they could reasonably be argued not to be important. Therefore the model equations were not fully elliptic in all directions. Parabolic and partially parabolic equations have been employed more often than the fully elliptic ones. Another device which allow these type of models to be studied with less computational effort is to study the case of a flow in an infinitely wide channel when the problem reduces to a two dimensional problem in the vertical plane. It, however, retains many of the characteristics of the fully three dimensional problem, notably the non-hydrostatic pressure distribution and the interaction of all the turbulent stresses. In non-hydrostatic models the vertical momentum equation is retained in its entirety. This introduces two problems: (1) How do you solve for pressure ? and (2) How do you treat the free surface ?

2.4.1 Pressure Solution

Various algorithms for the pressure solution have been proposed in the past. Patankar and Spalding (1972) and Patankar (1980) describe what has come to be known as the SIMPLE algorithm. The algorithm has several offshoots (SIMPLER, SIMPLEC, PISO) but they work on approximately the same principle. Fletcher (1988) describes the method. Using a guessed pressure field the momentum equations are solved to estimate the velocity field. The amount by which this velocity field deviates from satisfying the continuity equation is then used as a source for calculating a correction to the guessed pressure field which in turn is used to make a better attempt at solving the momentum equations. This procedure is repeated until the solution converges. The algorithm used in the present model is not based on the SIMPLE algorithm but rather is based on a projection method. This algorithm is described in detail in chapter 5.

2.4.2 Free Surface Treatment

In these models there are two commonly used treatments of the free surface dynamics. In the rigid lid approximation the free surface is replaced by an artificial plane surface parallel to the horizontal axes at some defined equilibrium water elevation. A non-zero pressure is allowed to develop at the surface and this in some way represents the height of water that would be present if the surface was completely free. Thus the effect of the free surface on the internal flow is captured. However, it will be appreciated that there is some amount of fluid above the rigid lid that is omitted. McGuirk and Rodi (1977) and Leschziner and Rodi (1979) suggest that the rigid lid approximation is valid as long as the superelevated regions are not greater than 10% of the total channel depth. The commonly used alternative to this is a surface tracking procedure which has been proposed in various forms and is computationally much more demanding. Most free surface

tracking models are related in some way to the original work of Harlow and Welch (1965). In this method, which became known as the Marker and Cell (MAC) method, they suggested that the fluid could contain many marker particles whose co-ordinate position is recorded. These particles could then, at each timestep, be moved according to the local fluid velocity components. Using the new co-ordinates of these particles a new fluid region could be assigned in terms of the Eulerian computational mesh. This procedure was found to be computationally too demanding and subsequently was replaced with a different method which was similar but less demanding of computing time. In this method, the Volume of Fluid (VOF) method, Nichols, Hirt and Hotchkiss (1980), instead of marker particles each computational cell was assumed to contain some fraction of fluid, F . Thus full cells had F equal to one and empty cells had F equal to zero. Cells with some fluid had F less than one but greater than zero. The F variable could then be advected as a Lagrangian invariant according to,

$$\frac{\partial F}{\partial t} + u \frac{\partial F}{\partial x} + v \frac{\partial F}{\partial y} + w \frac{\partial F}{\partial z} = 0 \quad [2.12]$$

where (u,v,w) are the local fluid velocities. Once F is known throughout the domain then the mesh may be reconfigured. The advantage of the MAC and VOF method is that they allow arbitrary unrestricted deformation of the fluid including the case of wave breaking. If the simulation of wave breaking is not required then a simpler procedure is the height function method (HF), Hirt and Nichols (1981), in which the new free surface is computed as the height, H , above some datum by the following expression,

$$\frac{\partial H}{\partial t} + u \frac{\partial H}{\partial x} + v \frac{\partial H}{\partial y} = w \quad [2.13]$$

at each timestep and then the mesh reconfigured. These surface tracking approaches appear to require fairly fine meshes and this may lead to high computer times..

2.4.3 Three Dimensional - Rigid Lid

In this and the following section fully three dimensional problems are considered, that is, when there are significant motions in all three co-ordinate directions. Baker (1974) presents a finite element method model for predicting flow and pollutant transport in a idealised natural river channel. The model is based on the Reynolds Averaged Navier-Stokes equations in stream function-vorticity form but uses the parabolic flow assumption to simplify the problem. A simple zero equation turbulence model is employed and plausible results are obtained. Unfortunately there does not appear to be any follow up studies using this model. Rastogi and Rodi (1978) describe an early application of a three dimensional hydrodynamic model which uses the rigid lid assumption. They solve the Reynolds Averaged Navier-Stokes equations in primitive variable form (velocity and pressure) in three dimensions with a relatively sophisticated two equation model of turbulence. They apply the model to the prediction of flow and heat in a rectangular river channel subject to a heated co-axial slot discharge at the channel centre. Importantly, they adopt a simplified form of the equations, the fully parabolic form, which although computationally efficient does not allow the prediction of recirculations in the streamwise direction. Leschziner and Rodi (1979) present an extension of the method to a partially parabolic case where the pressure terms are taken elliptically yet the other diffusion terms are taken parabolically. With this extension and also the introduction of a mixture of cartesian and cylindrical polar coordinate systems the model can be applied to the case of in bank flow in a idealised channel bend. Demuren and Rodi (1986) further enhance this model by

introducing a transport equation for a neutrally buoyant pollutant in addition to considering a higher order treatment of the troublesome advection terms. They restrict their investigation to in bank flows in which they assume that no recirculation in the streamwise direction occurs. They consider both single and multiple meander geometries. Demuren (1989) has also incorporated a sediment transport model. Demuren and Rodi (1983) present a fully elliptic version of the model of Rastogi and Rodi (1978) for predicting the effects of a side discharge into a rectangular channel. This study highlights the importance of using higher order treatments of the advection terms for advection dominated flows. Miyata and Yamada (1992) present a model which they use to predict flow patterns in a bay with an island. The fully elliptic three dimensional equations are used. They utilise a very simple turbulence model which is not entirely appropriate, however, they argue that it at least produces the correct flow phenomena. There are many important studies that, like Miyata and Yamada (1992), only produce these so called phenomenological results. The use of a rigid lid is an approximation here since the free surface is tidally varying however since the depth of ocean being modelled is very much larger than the tidal range plausible results may be obtained. Novelli, Dekeyser and Fraunie (1992) also present a full elliptic three dimensional model for predicting ocean circulations but they incorporate a more sophisticated two equation model of turbulence. They also allow a 'mesh vertical deformation' of the surface according to the kinematic condition thus the rigid lid assumption is relaxed somewhat.

There appears to be few applications of the fully elliptic three dimensional equations with the rigid lid approximation to localised river modelling in the literature. This is mainly due to computing overheads but may also be due to inadequacies in the rigid lid approach since in many river problems the free surface varies steeply. The study of McGuirk and Rodi (1977) gives some indication of the

range of validity of the rigid lid assumption but clearly more research is required in this area to ascertain comprehensively the limitations of the rigid lid assumption for various flow configurations.

2.4.4 Three Dimensional - Free Surface Tracking

If the rigid lid approach is considered invalid then some form of surface determination algorithm must be employed. Three dimensional computations of fluid flow with free surface tracking are rare in the literature. This is because, in addition to the computation that must be done in the internal fluid, the new position of the free surface at each timestep must be computed and the computational mesh reconfigured appropriately as discussed earlier. Nichols and Hirt (1972) present a model which employs the height function method for free surface tracking. The model is applied to the problem of wave propagation in a rectangular channel and to computing free surface flow around submerged obstacles. The fluid is assumed inviscid by arguing that the inertial forces are balanced by the pressure and body forces. In a river engineering context a study worthy of mention is the one by Davis and Deutsch (1980) in which they model the flow through a Parshall flume in three dimensions using the VOF method for surface tracking. This problem is essentially a balance between inertial, body and pressure forces so that the treatment of the turbulent stress terms is not crucial. The model predicts flow patterns and water surface elevations over a Parshall flume at various flow rates. Miyata and Nishimura (1985) present a model based on the MAC method for simulating non-linear waves around moving ships. As in the previous study the treatment of the turbulent stresses is not considered important. Miyata, Sato and Baba (1987) consider the same problem in a generalised boundary fitted co-ordinate system. Miyata (1986) considers the same model for flow conditions which involve wave breaking. All these models are

computationally demanding because they are three dimensional and involve a surface tracking procedure. To also include a more realistic turbulence representation would make this situation worse and this may be why very simple turbulence representations (if any) are used. Indeed these studies have often used a numerical treatment of the advection terms which is known to introduce a high level of numerical diffusion. Presumably, therefore, the results can only be considered to be phenomenological.

2.4.5 Two Dimensional - Vertical Plane Modelling - Rigid Lid

Many of the vertical features (non-hydrostatic pressure, vertical shear stress gradients etc) can still be studied without resorting to fully three dimensional modelling by studying vertical plane problems. This may be appropriate if lateral variations can be assumed negligible. There have been many more studies of this type than of fully three dimensional problems probably because of the lower computing times required. Among those vertical plane studies that employ the rigid lid assumption are Alfrink and Van Rijn (1982) who use this type of model for simulating flow over a steep sided trench. They employ a two equation model for representing the turbulent stresses and solve the equations on a boundary fitted grid with an operator splitting approach. The vertical plane model with a rigid lid has also been used by Mendoza and Shen (1990) and Sajjadi and Aldridge (1993) for studying the flow characteristics over river bed dunes. Different turbulence closures are used in each investigation. The vertical plane model has found much application in modelling the characteristics of settling tanks and mixing chambers owing to the two dimensionality of the flow field, Zhou and McCorquodale (1992), Lyn, Stamou and Rodi (1992), Stamou, Adams and Rodi (1989) and Lyn and Zhang (1989). These studies, however, seem to concentrate on improving the accuracy of solution and including more physical processes for the steady state

case. There is a need, however, to look at long term unsteady simulations in these water and wastewater treatment plants. This is discussed further in chapter 6.

2.4.6 Two Dimensional - Vertical Plane Modelling - Free Surface Tracking

The two dimensional version of the models in section 2.4.4 are much more amenable to computation. Indeed Lemos (1992) has carried out this type of computation on a personal computer. He has studied wave breaking using the VOF method for surface tracking and has also further developed the model to incorporate a two equation model of turbulence. Heinrich (1992) has used a similar technique for studying non-linear waves generated by submarine and aerial landslides. Kothe and Mjolsness (1992) have also used this technique with some computational enhancements to study low speed flow problems in mechanical engineering. They use a simple zero equation turbulence model.

2.5 Fully Developed Flow Models

Fully developed flow models are models of flow in which there are no changes in the longitudinal direction. Therefore, they compute the velocity, turbulence and shear stress distribution for a given cross-sectional shape, boundary roughness and uniform bed slope. These models have found much application in river engineering providing practical predictions as well as enlightenment on the flow and turbulence mechanisms in natural and man-made river channels. They are strictly only applicable to fully developed flow conditions when the channel is long and straight enough to allow a longitudinal equilibrium (uniform flow) to be reached. They provide much better predictions for gross flow properties for two-stage river channels than traditional uniform flow formulae however it should be noted that their range of applicability is strictly no greater than the uniform flow formulae. It should be possible to introduce ad-hoc correction factors to take account of

non-uniform flow as can be done for the traditional formula, however, this should be done cautiously. These models are based on simplified forms of either the three dimensional equations or the two-dimensional depth averaged equations. They are simplified to the case of steady fully developed steady flow in a prismatic channel by assuming that all velocity derivatives in the x-direction are zero as are all temporal derivatives. If the secondary motions are ignored also (usually in depth averaged models) then the lateral and vertical velocities are assumed zero also. Haque (1959) gives a formal discussion of the fully developed depth averaged flow problem while Gosman and Rapley (1980) give an excellent account of the general principles of the fully developed three dimensional flow problem.

2.5.1 Fully Developed Depth Averaged Flow Models

These models utilise the two dimensional depth averaged equation set 2.9-11 with the simplifications noted above. With these simplifications introduced the model equation becomes,

$$gh \frac{\partial \eta}{\partial x} + \frac{\tau_{bx}}{\rho} - \frac{1}{\rho} \frac{\partial}{\partial y} T_{xy} = 0 \quad [2.14]$$

If η , the water elevation is written as the sum of the water depth, h and bed level z_o and it is assumed that the water depth is constant along the river's longitudinal axis(uniform flow) and the water elevation is constant along the river's lateral axis then,

$$\frac{\partial h}{\partial x} = 0 \text{ and } \frac{\partial z_o}{\partial x} = -S_o \text{ (The channel slope)}$$

Thus the depth averaged fully developed flow equation simplifies to the following,

$$-ghS_o + \frac{1}{\rho} \tau_{bx} - \frac{1}{\rho} \frac{\partial}{\partial y} T_{xy} = 0 \quad [2.15]$$

Equation 2.25 and variants of it have been used to predict the lateral velocity variation and bed shear stress in compound channels by various investigators, see table 2. Equation 2.25 has been solved by different numerical methods, for different dependent variables (depth averaged velocity, \bar{U} , or unit flow, q) and using different closures for the bed and lateral shear stress terms. In all these attempts the lateral shear stress term has been treated with an eddy viscosity closure,

$$T_{xy} = h \bar{\nu}_t \frac{\partial \bar{U}}{\partial y} \quad [2.16]$$

although different methods of computing the eddy viscosity have been proposed. The different lateral shear stress expressions constitute the turbulence model and are discussed in more detail in chapter 4.

Investigator(s)	Dependent Variable	Eddy Viscosity ($\bar{\nu}_t$)	Numerical Solution
Vreugdenhil and Wijnbenga (1982)	\bar{U}	$\bar{\nu}_t$ assumed constant	finite difference
Wormleaton (1988)	\bar{U}	$\bar{\nu}_t = c\delta\Delta\bar{U}$	finite difference with Newton-Raphson iteration for non-linearity
Shiono and Knight (1988)	\bar{U}	$\bar{\nu}_t = \lambda hu^*$	finite analytic
Wark, Samuels and Ervine (1990)	$q = \bar{U}h$	$\bar{\nu}_t = \lambda hu^*$	finite difference with Newton-Raphson iteration for non-linearity
Keller and Rodi (1988)	\bar{U}	$\bar{\nu}_t$ given by k- ϵ model	finite volume

Table 2. Investigations for uniform depth averaged flow in compound channels:

λ has been termed the lateral non-dimensional eddy viscosity with values given by Fischer et al (1979). c is a constant, δ is a length scale related to the shear layer width and $\Delta\bar{U}$ is the velocity difference across the shear layer, Wormleaton (1988).

2.5.2 Fully Developed Three Dimensional Flow Models

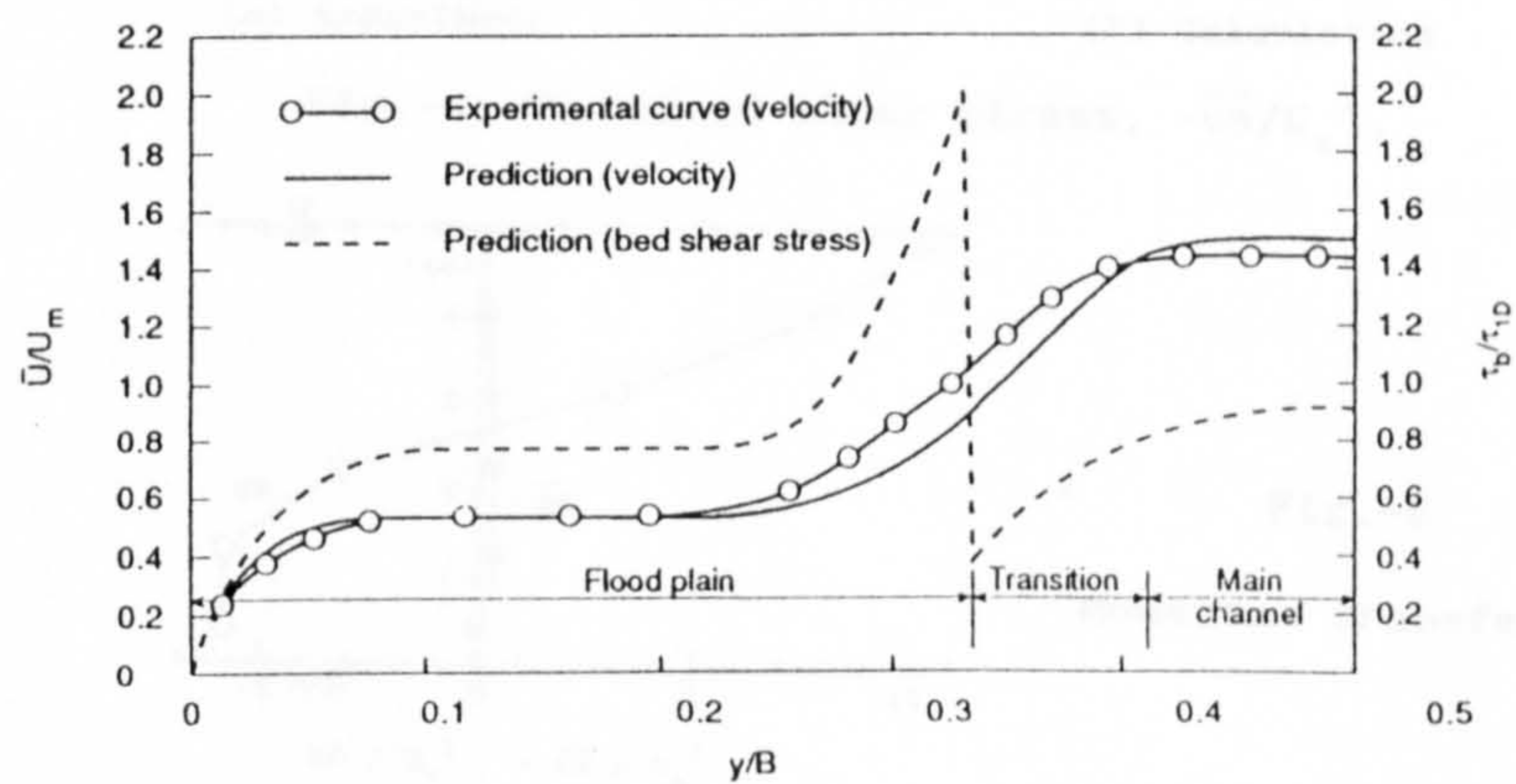
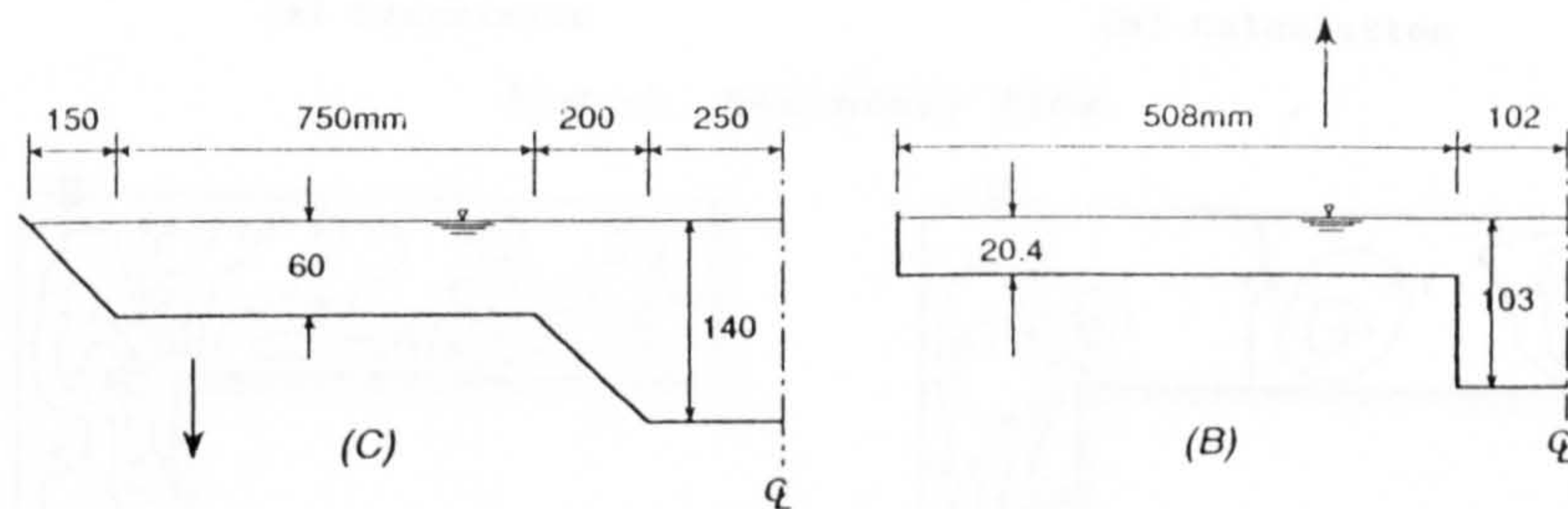
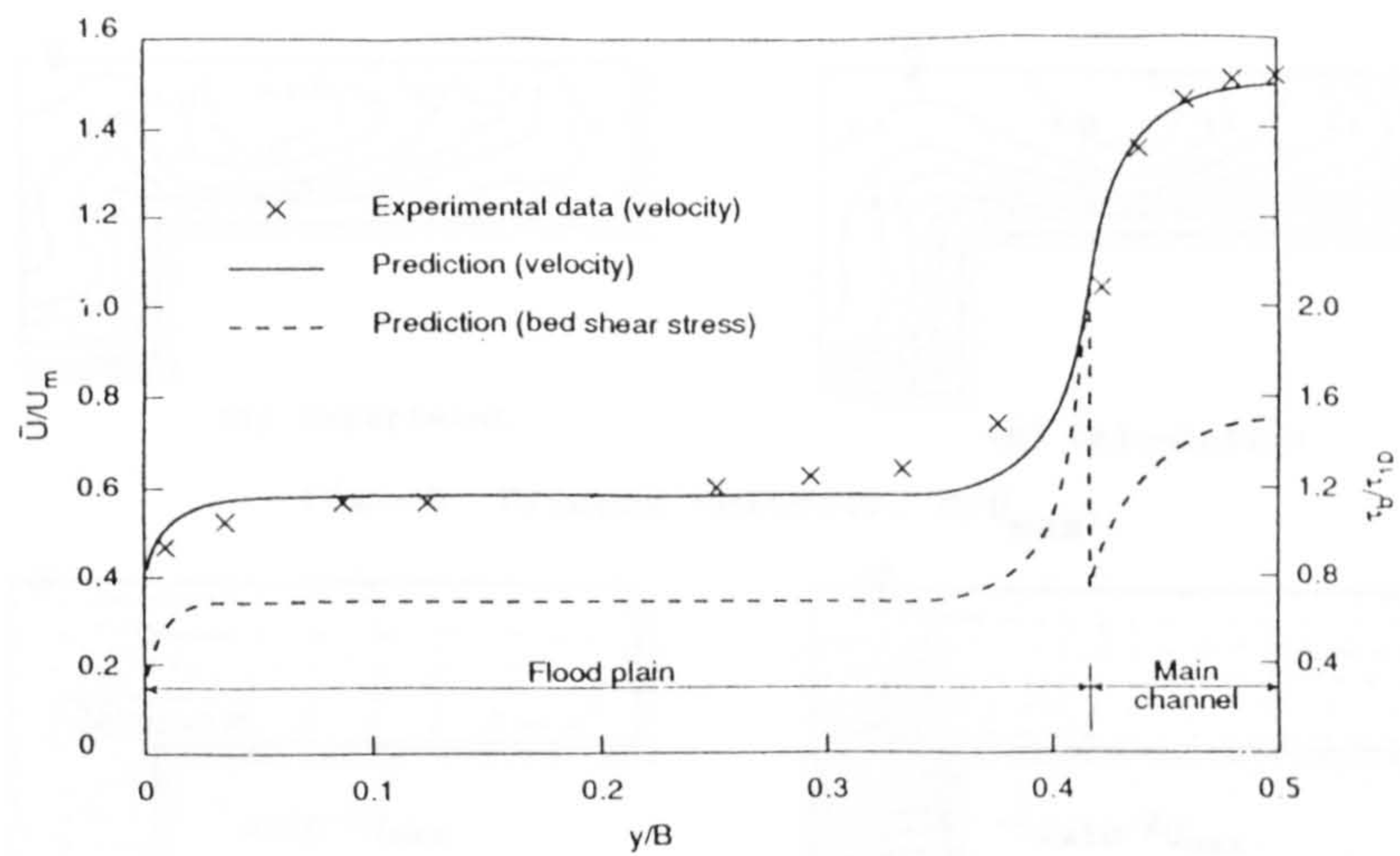
This type of model has been applied to compound channel flow by Krishnappan and Lau (1986), Kawahara and Tamai (1989), Prinos (1990), Naot, Nezu and

Nakagawa (1993), Lin and Shiono (1992), Prinos (1992), and Cokljat (1993) among others. This type of model has also been applied to simple channels by Naot and Rodi (1982) and Younis and Abdellatif (1989) who also considered its effect on sediment transport predictions. Nearly all applications of this type of model have used virtually the same numerical solution technique which is outlined by Krishnappan and Lau (1986). The numerical method is based on the SIMPLE algorithm suitably simplified for the parabolic flow case. A selection of some of these studies are detailed in table 3.

Investigator(s)	Numerical Method	Turbulence Model	Comments
Krishnappan and Lau (1986)	Parabolic Finite Volume	Algebraic Stress Model (ASM)	Comparisons with experimental data indicated that the model could predict discharge, velocity distributions and bed shear stress distributions adequately. No detail was given on secondary motion prediction.
Cokljat (1993)	Parabolic Finite Volume	Reynolds Stress Transport Model (RSTM) and Non-linear k- ϵ (NKE) model	Results indicated that the both turbulence models could predict secondary velocities, turbulence quantities, discharge, velocity distributions and bed shear stress distributions very well with the RSTM superior.
Lin and Shiono (1992)	Parabolic Finite Volume	Algebraic Stress Model (ASM), Non-linear k- ϵ model (NKE) and linear k- ϵ model	A scalar transport equation is also solved to represent a pollutant and perhaps not surprisingly significant differences are observed between the linear k- ϵ model (no secondary motion) and the other two models which predict secondary motion.
Naot, Nezu, Nakagawa (1993)	Parabolic Finite Volume	Algebraic Stress Model (ASM)	Comparisons with experimental data indicated that the model could predict secondary velocities, turbulence quantities, discharge, friction factors and bed shear stress distributions very well.

Table 3. Investigations for fully developed three dimensional flow

“ These studies deal with the prediction of secondary motions induced by the non-equivalence of the normal Reynolds stresses. The main focus of these studies, therefore, lies on the turbulence representation employed which is discussed more fully in chapter 4. Two interesting studies of fully developed duct flow which is very similar to open channel flow prediction warrant mention owing to the different numerical solution approach taken. Gerard (1974) and Baker and Orzechowski (1983) both use the finite element which may or may not be more efficient for accurately modelling complex geometries.



After Keller and Rodi (1988)

Figure 6. Typical fully developed depth averaged flow model results

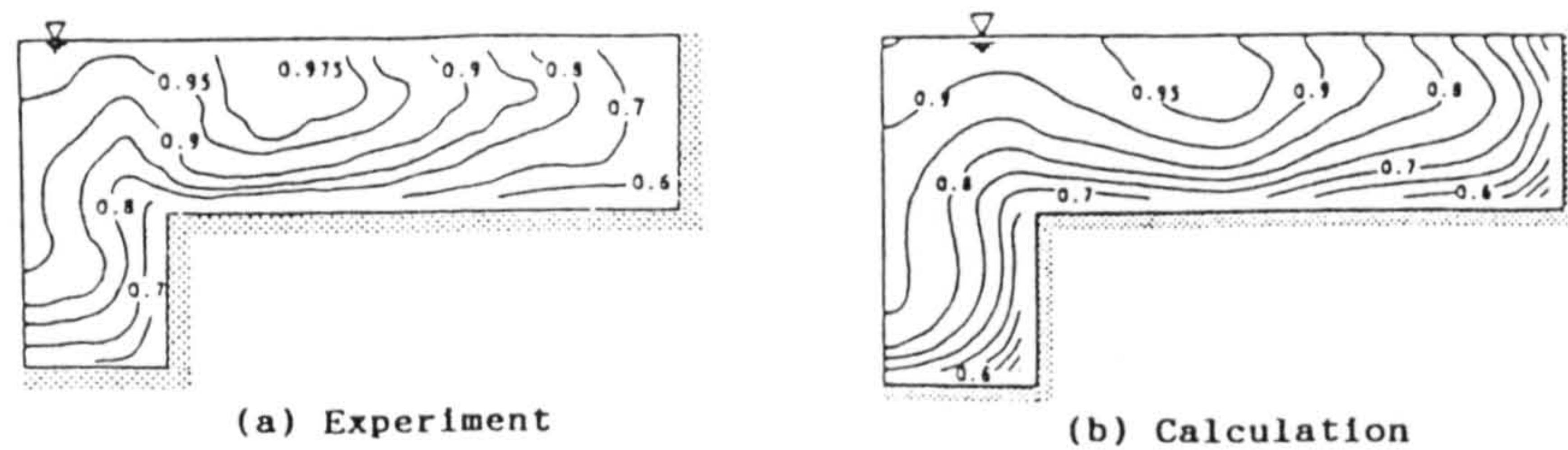


Fig.-2 Primary velocity, U/U_{\max} .

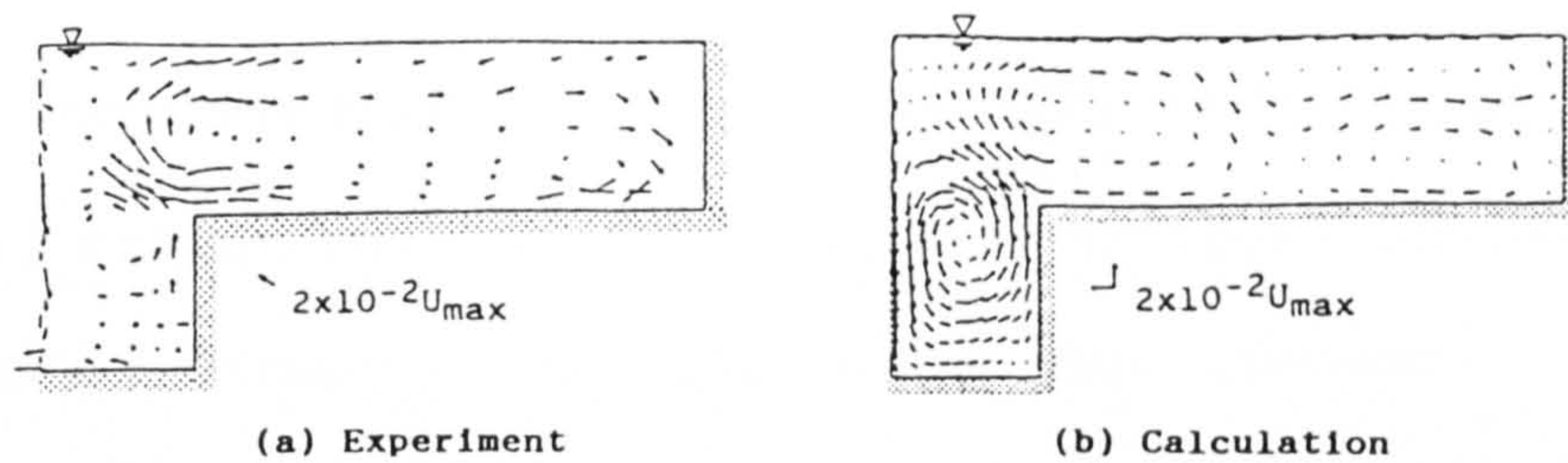


Fig.-3 Secondary flow.

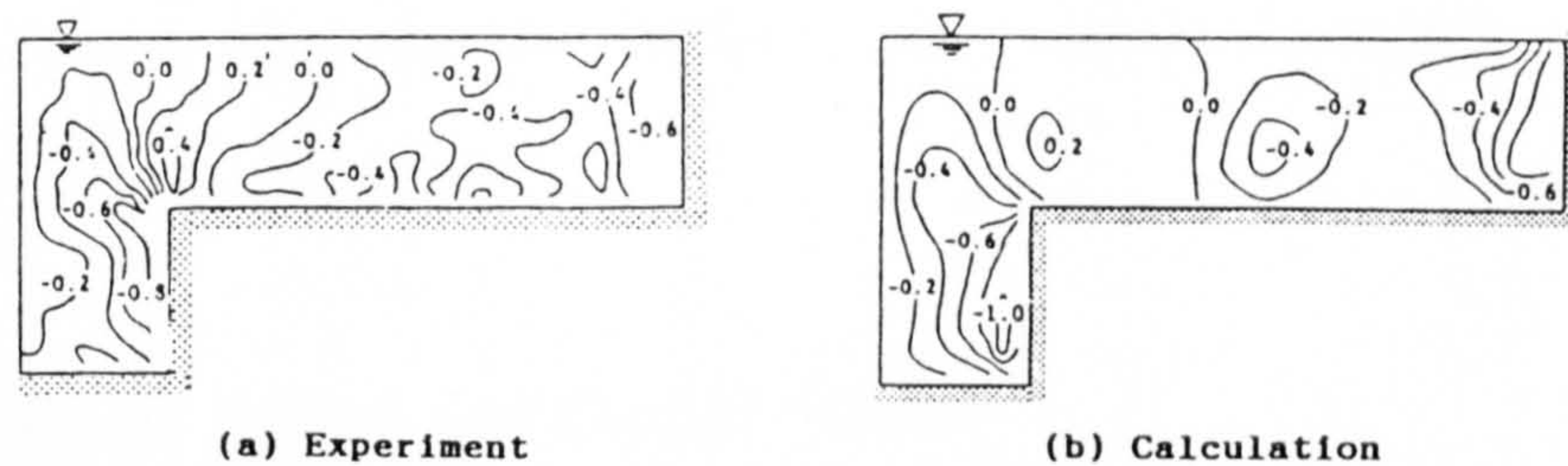


Fig.-4 Turbulent shear stress, $-\overline{u'w'}/U_*^2$.

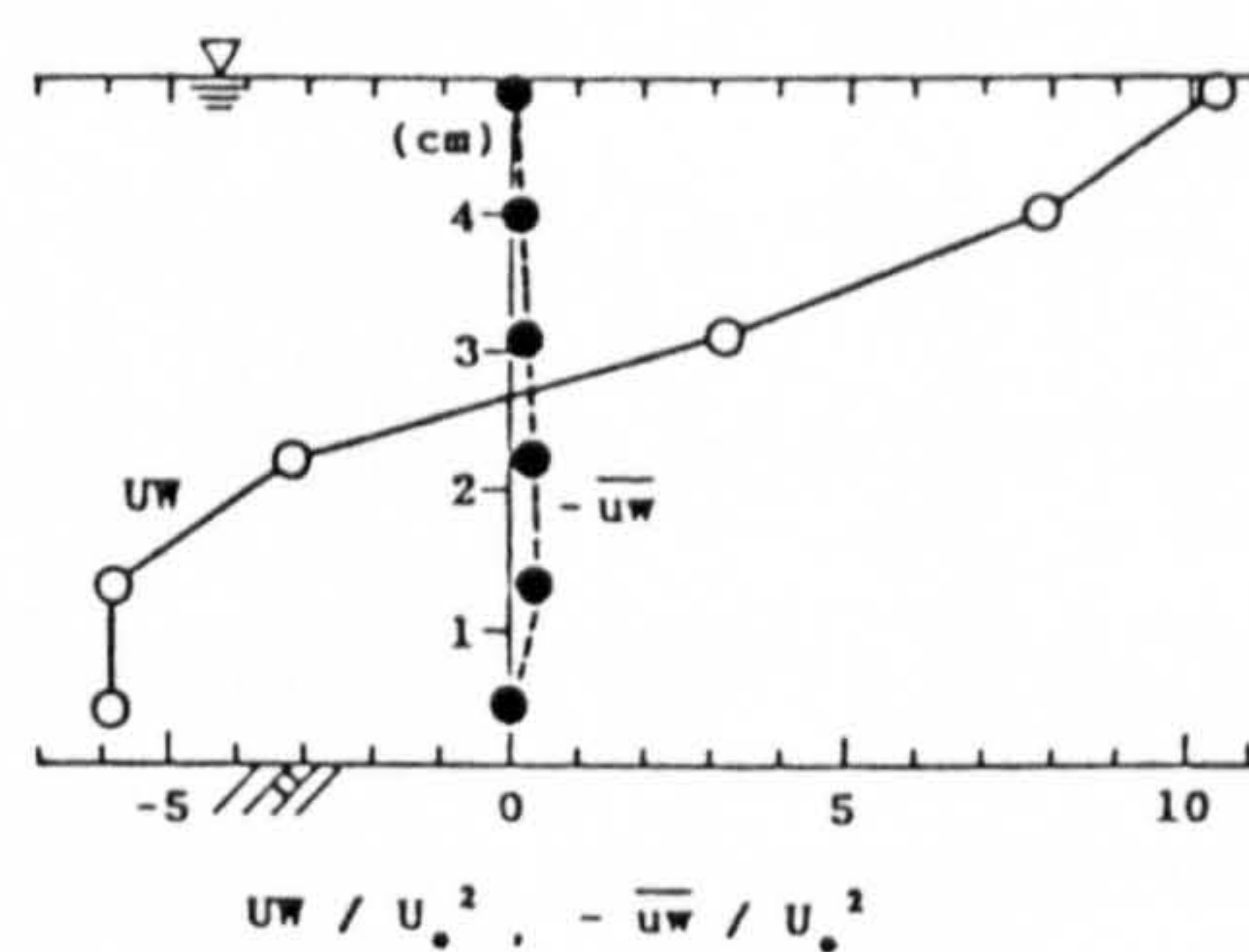


Fig.-5
Momentum transfer rate.

After Kawahara and Tamai (1988)

Figure 7. Typical fully developed three dimensional flow model results

3.0 Chapter 3 Foundations for River Hydraulics

3.1 Physical Laws

To describe three dimensional flows mathematically we require one continuity equation and dynamic equations in each of three orthogonal directions. There follows a brief summary of the derivation of these equations. Firstly, the co-ordinate system is introduced, then the concepts of conservation of mass and momentum are described mathematically. Finally, the relationship between stress and strain in a fluid is outlined.

3.1.1 Coordinate System and Control Volume

The physical laws will be derived in terms of a right handed rectangular Cartesian coordinate system, see figure 8, in which the x axis aligns with the streamwise direction of the river, the y axis takes the lateral direction across the river and z axis aligns with the vertical direction. The coordinates are measured relative to a stationary frame of reference and have corresponding velocity components U, V and W.

There are two approaches to the analysis of fluid mechanics problems. In the Lagrangian approach individual fluid particles are followed and the fluid properties of each particle are determined at any instant in time. In the Eulerian approach interest is fixed on a specific region in space. The fluid properties are

prescribed throughout space and time and information on flow conditions at fixed points is obtained. The Eulerian approach is adopted here. The fixed region is called the control volume and for the following derivation it is an infinitesimally small cube in the fluid. The distinction between the Eulerian and the Lagrangian viewpoint is an important one - some difficulties may be lessened by switching from one viewpoint to another for the purposes of numerical discretisation.

3.1.2 Underlying Assumptions

The following equations are derived for the specific case of water flow in a clear river, i.e. the fluid is assumed incompressible and of constant density, ρ , throughout. It is important to highlight this assumption as the equations (in particular the stress-strain relationships) are often presented in a more general compressible formulation which is then simplified. It is also assumed that the bed of the river remains fixed and the spatial variation of atmospheric pressure can be neglected.

3.1.3 Conservation of Mass

Consider the infinitesimal element in the middle of a river with dimensions δx , δy , and δz . which is shown in figure 9 along with the velocity components. The rate at which mass enters the control volume must equal the rate that mass leaves since the density remains constant in the control volume. Thus,

$$\text{Mass flow rate in} - \text{Mass flow rate out} = 0$$

$$\begin{aligned} & \rho [U\delta y\delta z + V\delta x\delta z + W\delta x\delta y \\ & - (\delta y\delta z(U + \frac{\partial U}{\partial x}\delta x) + \delta x\delta z(V + \end{aligned}$$

$$\frac{\partial V}{\partial y} \delta y) + \delta x \delta y (W + \frac{\partial W}{\partial z} \delta z) / = 0$$

Simplifying and dividing through by the element mass $\rho \delta x \delta y \delta z$ gives,

$$\frac{\partial U}{\partial x} + \frac{\partial V}{\partial y} + \frac{\partial W}{\partial z} = 0 \quad [3.1]$$

This is the equation of continuity for an incompressible fluid of uniform density which may be written in a concise cartesian tensor notation (see Appendix A) as,

$$\frac{\partial U_j}{\partial x_j} = 0 \quad [3.2]$$

The Continuity Equation

3.1.4 Conservation of Momentum

A further analysis based on Newton's Second Law provides the other physical laws. Since momentum is a vector quantity it must be conserved in each of the three orthogonal directions. The following is a derivation of the conservation of momentum equation in the x direction only. The momentum equations for the other directions follow directly.

Newton's Second Law states that 'a body will remain at rest or in a state of uniform motion unless acted upon by some unbalanced force'. For a fluid control volume, see figure 9, this may be stated as

$$\begin{array}{lcl} \text{Rate of change} & & \text{Unbalanced force on} \\ \text{of x momentum} & = & \text{the element in} \\ \text{of a fluid element} & & \text{the x direction} \end{array}$$

Taking each contribution to momentum increase in turn and considering a small time increment δt ,

1.Temporal change in momentum

$$\begin{array}{lcl} \text{Rate of increase in x momentum} & & \\ \text{of a fluid element} & = & \rho \delta x \delta y \delta z \frac{\partial U}{\partial t} \end{array}$$

2.Advective change in momentum

$$\text{Net momentum flux into a fluid element} = (\text{Momentum out} - \text{Momentum in})$$

$$\text{Momentum in} = \rho [\delta y \delta z (UU) + \delta x \delta z (UV) + \delta x \delta y (UW)]$$

$$\text{Momentum out} = \rho [\delta y \delta z ((UU) + \delta x \frac{\partial(UU)}{\partial x}) + \delta x \delta z ((UV) +$$

$$\delta y \frac{\partial(UV)}{\partial y}) + \delta x \delta y ((UW) + \delta z \frac{\partial(UW)}{\partial z})]$$

thus,

$$\text{Net momentum flux into a fluid element} = \rho \delta x \delta y \delta z \left[\frac{\partial UU}{\partial x} + \frac{\partial UV}{\partial y} + \frac{\partial UW}{\partial z} \right]$$

Thus the net rate of increase in x momentum is,

$$\rho \delta x \delta y \delta z \left[\frac{\partial U}{\partial t} + \frac{\partial UU}{\partial x} + \frac{\partial UV}{\partial y} + \frac{\partial UW}{\partial z} \right]$$

Turning now to the unbalanced force on the element as shown in figure 10. There are two kinds of force to be considered: body forces which are distributed throughout the element and surface forces which act on the element surface as a consequence of its interaction with its surroundings.

3.1.4.1 *Body Forces*

For the present only a general body force per unit volume shall be assumed. So for the x direction the body force is $\delta x \delta y \delta z f_x$. This aspect shall be discussed further in section 3.1.4.3.

3.1.4.2 *Surface Forces*

We can express the surface forces in terms of the stresses acting on the faces of the element. To identify the particular stress component a double subscript notation is adopted. The first subscript indicates the direction of the normal to the plane on which the stress acts, and the second subscript indicates the direction of the stress. Thus normal stresses have repeated subscripts, whereas the subscripts for the shearing stresses are always different. Referring to figure 10, the contribution due to normal stresses is given by,

$$\delta y \delta z \left[\left(\sigma_{xx} + \frac{\partial \sigma_{xx}}{\partial x} \delta x \right) - \sigma_{xx} \right]$$

which is,

$$\left(\frac{\partial \sigma_{xx}}{\partial x} \delta x \right) \delta y \delta z$$

The contribution due to shear stresses on an xz plane is given by,

$$\delta x \delta z \left[\left(\sigma_{yx} + \frac{\partial \sigma_{yx}}{\partial y} \delta y \right) - \sigma_{yx} \right]$$

which is,

$$\left(\frac{\partial \sigma_{yx}}{\partial y} \delta y\right) \delta x \delta z$$

The contribution due to shear stresses on a xy plane is given by,

$$\delta x \delta y \left[\left(\sigma_{zx} + \frac{\partial \sigma_{zx}}{\partial z} \delta z \right) - \sigma_{zx} \right]$$

which is,

$$\left(\frac{\partial \sigma_{zx}}{\partial z} \delta z \right) \delta x \delta y$$

Combining these forces gives the total force due to surface stresses,

$$\left(\frac{\partial \sigma_{xx}}{\partial x} + \frac{\partial \sigma_{yx}}{\partial y} + \frac{\partial \sigma_{zx}}{\partial z} \right) \delta x \delta y \delta z$$

Combining this with the rate of increase of momentum expression, the body force component and cancelling δx , δy and δz gives the differential x momentum equation for an incompressible fluid,

$$\frac{\partial \rho U}{\partial t} + \frac{\partial \rho UU}{\partial x} + \frac{\partial \rho UV}{\partial y} + \frac{\partial \rho UW}{\partial z} = \frac{\partial \sigma_{xx}}{\partial x} + \frac{\partial \sigma_{yx}}{\partial y} + \frac{\partial \sigma_{zx}}{\partial z} + f_x$$

The y and z momentum equations follow a similar derivation giving the complete momentum equation set,

$$\frac{\partial \rho U}{\partial t} + \frac{\partial \rho UU}{\partial x} + \frac{\partial \rho UV}{\partial y} + \frac{\partial \rho UW}{\partial z} = \frac{\partial \sigma_{xx}}{\partial x} + \frac{\partial \sigma_{yx}}{\partial y} + \frac{\partial \sigma_{zx}}{\partial z} + f_x$$

$$\frac{\partial \rho V}{\partial t} + \frac{\partial \rho VU}{\partial x} + \frac{\partial \rho VV}{\partial y} + \frac{\partial \rho VW}{\partial z} = \frac{\partial \sigma_{xy}}{\partial x} + \frac{\partial \sigma_{yy}}{\partial y} + \frac{\partial \sigma_{zy}}{\partial z} + f_y$$

$$\frac{\partial \rho W}{\partial t} + \frac{\partial \rho WU}{\partial x} + \frac{\partial \rho WV}{\partial y} + \frac{\partial \rho WW}{\partial z} = \frac{\partial \sigma_{xz}}{\partial x} + \frac{\partial \sigma_{yz}}{\partial y} + \frac{\partial \sigma_{zz}}{\partial z} + f_z$$

The above equations are known as the Navier-Stokes equations.

The equation set may also be

written compactly in tensor notation noting that the stress tensor must be symmetrical, White (1991),

$$\frac{\partial \rho U_i}{\partial t} + \frac{\partial \rho U_j U_i}{\partial x_j} = \frac{\partial \sigma_{ij}}{\partial x_j} + f_i \quad [3.3]$$

The Euler Dynamic Equations

3.1.4.3 The Body Force Vector

In 3.3, f_i is termed the body force vector. It may be written out as a vector of body forces,

$$f_i = \begin{bmatrix} f_x \\ f_y \\ f_z \end{bmatrix} \quad [3.4]$$

This term represents the effect of the environment on the bulk matter of the fluid. Body forces may include gravity, Coriolis and buoyancy forces. In a natural co-ordinate system where the z axis is pointing directly outward from the earth the body force vector due to gravity alone would be,

$$f_i = \begin{bmatrix} 0 \\ 0 \\ -\rho g \end{bmatrix} \quad [3.5]$$

It is often more convenient to work in a different co-ordinate system however when dealing with rivers. In this system the z axis is pointing directly perpendicular to the river bed if the river bed can reasonably be assumed to follow a straight line.

In this case the velocity field is now in the new axis directions. If the river bed makes an angle θ with the horizontal then the body force vector due to gravity is,

$$f_i = \begin{bmatrix} \rho g \sin \theta \\ 0 \\ -\rho g \cos \theta \end{bmatrix} \quad [3.6]$$

To retain generality the body forces in the following are represented by a general gravitational field,

$$f_i = \begin{bmatrix} \rho g_x \\ \rho g_y \\ \rho g_z \end{bmatrix} \quad [3.7]$$

or,

$$f_i = \rho g_i \quad [3.8]$$

3.1.4.4 The Stress Tensor

In 3.3, σ_{ij} is termed the stress tensor. It may be written out as a three by three matrix of stresses,

$$\sigma_{ij} = \begin{bmatrix} \sigma_{xx} & \sigma_{xy} & \sigma_{xz} \\ \sigma_{yx} & \sigma_{yy} & \sigma_{yz} \\ \sigma_{zx} & \sigma_{zy} & \sigma_{zz} \end{bmatrix} \quad [3.9]$$

Depending on the orientation of the axes relative to the river these stresses may be referred to as streamwise, lateral or vertical. This will be clarified in future sections where their relative importance is discussed. The internal stress tensor represents the short range forces exerted on the fluid element boundaries as a result of its interaction with its surroundings.

$$\sigma_{ij} = \begin{bmatrix} \sigma_{xx} & \sigma_{xy} & \sigma_{xz} \\ \sigma_{yx} & \sigma_{yy} & \sigma_{yz} \\ \sigma_{zx} & \sigma_{zy} & \sigma_{zz} \end{bmatrix} \quad [3.10]$$

The stress tensor is made up of normal stresses (σ_{ij} $i=j$) which lie on the main diagonal and tangential or shear stresses which make up the remaining matrix (σ_{ij} $i \neq j$). It is often more difficult to visualise the normal stresses. The effects of the shear stresses are somehow more apparent since they are the most important stresses in many flow situations including simple boundary layers. The normal stresses, however, are also important and civil engineers should be aware of their contribution. Part of the reason for the normal stresses receiving less attention is because often the only normal stress considered important is pressure. It is therefore convenient at this point to separate σ_{ij} into the sum of an isotropic part (pressure) and a deviatoric part (whose components are zero in a motionless fluid).

$$\sigma_{ij} = -P\delta_{ij} + \tau_{ij} \quad [3.11]$$

In the expression above P is the mechanical pressure, δ_{ij} is the Kronecker delta defined as the elements of the identity matrix and τ_{ij} is the deviatoric stress tensor. Substituting equation 3.11 into the Euler equations 3.3 gives Stokes' equations,

$$\frac{\partial \rho U_i}{\partial t} + \frac{\partial \rho U_j U_i}{\partial x_j} + \frac{\partial P}{\partial x_i} = \frac{\partial \tau_{ij}}{\partial x_j} + \rho g_i \quad [3.12]$$

Equation 3.12 is quite general and applicable to any type of fluid, providing the stresses can be estimated.

3.1.5 Viscous Stresses

The equation set 3.12 is indeterminate. Before we can apply these laws to some fluid system we must reduce the number of unknowns by making some assumption about the viscous stresses.

3.1.5.1 The Fluid at Rest

Firstly from the definition of a fluid, the viscous stresses must vanish if the fluid is at rest. Thus all shear stresses are zero and the normal stresses become equal to the hydrostatic pressure,

$$\tau_{ij} = 0 \quad [3.13]$$

Substituting equation 3.13 into equation 3.12 and setting all velocities to zero gives,

$$\frac{1}{\rho} \frac{\partial P}{\partial x_i} = g_i \quad [3.14]$$

Equation 3.14 may be integrated, defining the pressure to be some reference value (say zero) at one unique point, to give a hydrostatic pressure field, denoted by F ,

$$\frac{F}{\rho} = g_x x + g_y y + g_z z = g_i x_i \quad [3.15]$$

It is therefore sometimes convenient to work with an effective pressure,

$$\phi = \frac{P}{\rho} - \frac{F}{\rho} \quad [3.16]$$

$$\phi = \frac{P}{\rho} - g_i x_i \quad [3.17]$$

which is the actual pressure minus the hydrostatic pressure so that,

$$\frac{\partial \phi}{\partial x_i} = \frac{1}{\rho} \frac{\partial P}{\partial x_i} - g_i \quad [3.18]$$

since,

$$\frac{\partial F}{\partial x} = g_x \quad \frac{\partial F}{\partial y} = g_y \quad \frac{\partial F}{\partial z} = g_z \quad [3.19]$$

If this is done it must be remembered that this effective pressure field is now the pressure field minus the hydrostatic pressure field.

In a moving fluid the stress terms are mobilised and must be estimated.

3.1.5.2 Stress - Deformation Laws

A fluid element undergoes deformation in four different ways: translation, rotation, dilatation and shear strain. Referring to figure 11, consider a fluid element with corners ABCD which is initially square and deforms in time δt to the position A'B'C'D'. We are interested in the rate of deformation and will restrict the study to the dilatational and shear strain rates which are the strains which actually distort the element and thus cause a viscous stress. We find that $d\alpha$ and $d\beta$ can be related to the velocity derivatives thus,

$$d\alpha = \lim_{\delta t \rightarrow 0} \left(\tan^{-1} \frac{\frac{\partial V}{\partial x} dx \delta t}{dx + \frac{\partial U}{\partial x} dx \delta t} \right) = \frac{\partial V}{\partial x} dt$$

$$d\beta = \lim_{\delta t \rightarrow 0} \left(\tan^{-1} \frac{\frac{\partial U}{\partial y} dy \delta t}{dy + \frac{\partial V}{\partial y} dy \delta t} \right) = \frac{\partial U}{\partial y} dt$$

Now considering shear strain which is defined as the average decrease of the angle between two lines which are initially perpendicular in the unstrained state then the shear strain increment is $\frac{1}{2}(d\alpha + d\beta)$. The shear strain rate is therefore,

$$\varepsilon_{xy} = \frac{1}{2} \left(\frac{d\alpha}{dt} + \frac{d\beta}{dt} \right) = \frac{1}{2} \left(\frac{\partial V}{\partial x} + \frac{\partial U}{\partial y} \right)$$

Similarly the other shear strain rates may be derived,

$$\epsilon_{yz} = \frac{1}{2} \left(\frac{\partial W}{\partial y} + \frac{\partial V}{\partial z} \right) \quad \epsilon_{zx} = \frac{1}{2} \left(\frac{\partial U}{\partial z} + \frac{\partial W}{\partial x} \right)$$

By analogy with solid mechanics the strain rates are symmetric, i.e. $\epsilon_{ij} = \epsilon_{ji}$.

Considering now dilatational strain which is defined as the fractional increase in length of the horizontal side of the element. This is given by,

$$\epsilon_{xx} dt = \frac{(dx + \frac{\partial U}{\partial x} dx dt) - dx}{dx} = \frac{\partial U}{\partial x} dt$$

with similar expressions for the other two directions. Thus the dilatational strain rates are,

$$\epsilon_{xx} = \frac{\partial U}{\partial x} \quad \epsilon_{yy} = \frac{\partial V}{\partial y} \quad \epsilon_{zz} = \frac{\partial W}{\partial z}$$

Taken together the extensional and shear strain rates may be written as the symmetric tensor,

$$\epsilon_{ij} = \begin{bmatrix} \epsilon_{xx} & \epsilon_{xy} & \epsilon_{xz} \\ \epsilon_{yx} & \epsilon_{yy} & \epsilon_{yz} \\ \epsilon_{zx} & \epsilon_{zy} & \epsilon_{zz} \end{bmatrix} = \frac{1}{2} \left(\frac{\partial U_i}{\partial x_j} + \frac{\partial U_j}{\partial x_i} \right) \quad [3.20]$$

Viscosity is the property of a fluid which relates applied stress to the resulting strain. For most common fluids the applied stress is a unique function of the strain rate,

$$\tau_{xz} = f(\epsilon_{xz}) \quad [3.21]$$

For certain simple fluids, including water, the relationship is linear or Newtonian,

$$\tau_{xz} \propto \epsilon_{xz} \quad \text{or} \quad \tau_{xz} = 2\mu\epsilon_{xz} \quad [3.22]$$

where μ is the constant of proportionality termed the coefficient of viscosity. If the functional relationship is nonlinear then the fluid is termed non-newtonian. A simple but effective approach to non-newtonian behaviour is the power-law approximation of Ostwald and de Waele, White (1991),

$$\tau_{xy} = 2\mu(\epsilon_{xy})^n \quad [3.23]$$

where μ and n are material parameters and, in particular,

$$n < 1 \text{ pseudoplastic}$$

$$n = 1 \text{ Newtonian}$$

$$n > 1 \text{ dilatant}$$

The importance of non-linear stress-strain relationships will become apparent when discussing turbulence modelling. For water, however, the relationship is newtonian with the coefficient of viscosity often taken to be $1.0 \times 10^{-3} \text{kg/m s}^{-1}$ in civil engineering practice. Note however that the coefficient of viscosity is a thermodynamic property and so varies with temperature and pressure.

$$\tau_{ij} = \mu \left(\frac{\partial U_i}{\partial x_j} + \frac{\partial U_j}{\partial x_i} \right) \quad [3.24]$$

Substituting this relationship into the momentum equations, 3.12, assuming constant molecular viscosity and constant density and making use of the continuity constraint gives,

$$\frac{\partial U_i}{\partial t} + \frac{\partial U_j U_i}{\partial x_j} + \frac{1}{\rho} \frac{\partial P}{\partial x_i} = \nu \frac{\partial^2 U_i}{\partial x_j \partial x_j} + g_i \quad [3.25]$$

The Dynamic Equations

where ν is the kinematic viscosity, μ/ρ . Note that 3.25 represents three equations, see Appendix A. Equation 3.25 together with the continuity equation 3.2 describe the motion of many fluids including water in a river. However, they are highly non-linear and tremendous difficulties exist in integrating them in this form. These difficulties will be discussed in chapter 4.

3.1.6 Boundary Conditions

There are basically four boundaries to be considered for a river. These are: inlet, exit, free surface and wall or bed. Normally only a finite portion of a river will be modelled. Whether the portion is several thousands of miles long or only a few metres long it will be a finite portion with a beginning and end. Conditions must therefore be specified at the beginning and end of the reach which allow it to be decoupled from the rest of the river. The inlet and exit boundary conditions are, therefore, computational details which are dealt with in chapter 5.

At the free surface there are two conditions to be satisfied. Firstly, the kinematic condition that any particle on the free surface remains there or the particles upward velocity equals the motion of the free surface. This is expressed mathematically as,

$$W = \frac{Dh}{Dt} = \frac{\partial h}{\partial t} + U \frac{\partial h}{\partial x} + V \frac{\partial h}{\partial y}$$

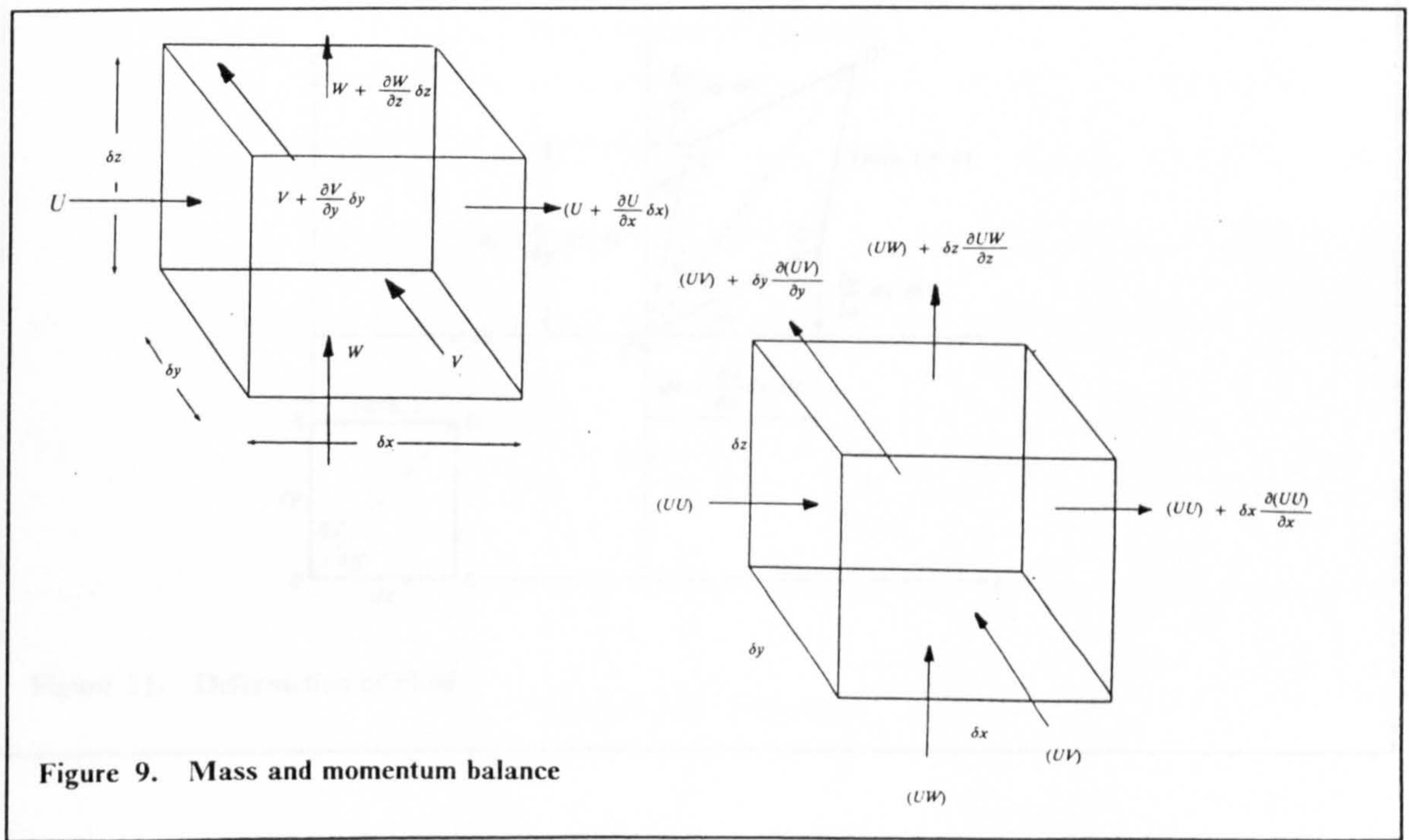
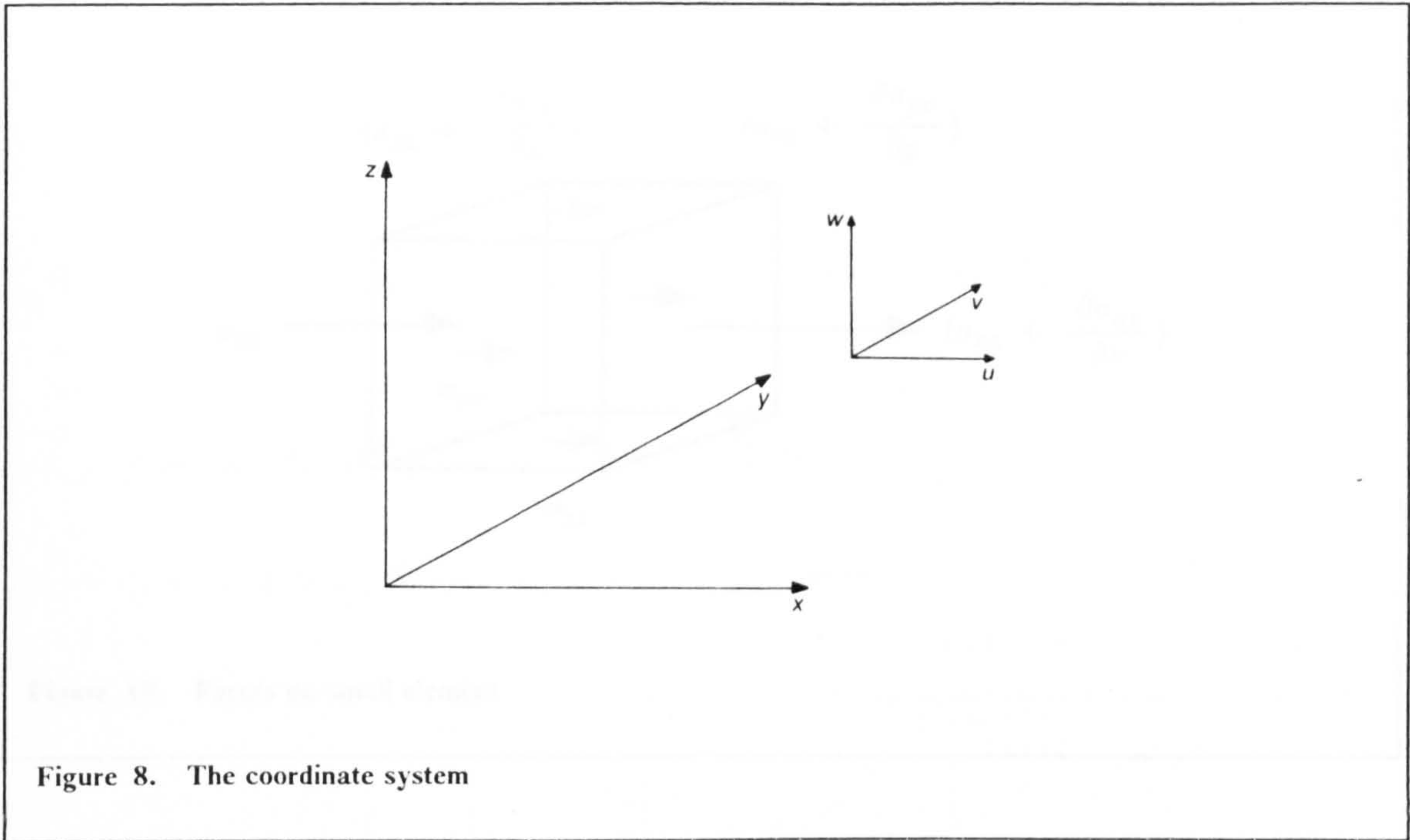
where h is the distance above some reference datum. Secondly, the dynamic condition, that the normal and shear stresses between liquid and air must be in balance. Finally, conditions must be specified at any solid-liquid boundary, i.e. the channel bed and walls. This boundary condition was laid down by Stokes (1845) who suggested that fluid next to a wall stuck to it, i.e. a no slip condition, or,

$$U_{TANGENTIAL} = 0$$

and that the wall is impermeable so,

$$U_{NORMAL} = 0$$

The foregoing physical laws are the foundation for solutions to the problem of river flow prediction. However, as already stated they cannot be applied directly as they stand owing to the phenomenon of turbulence. This is addressed in the following chapter.



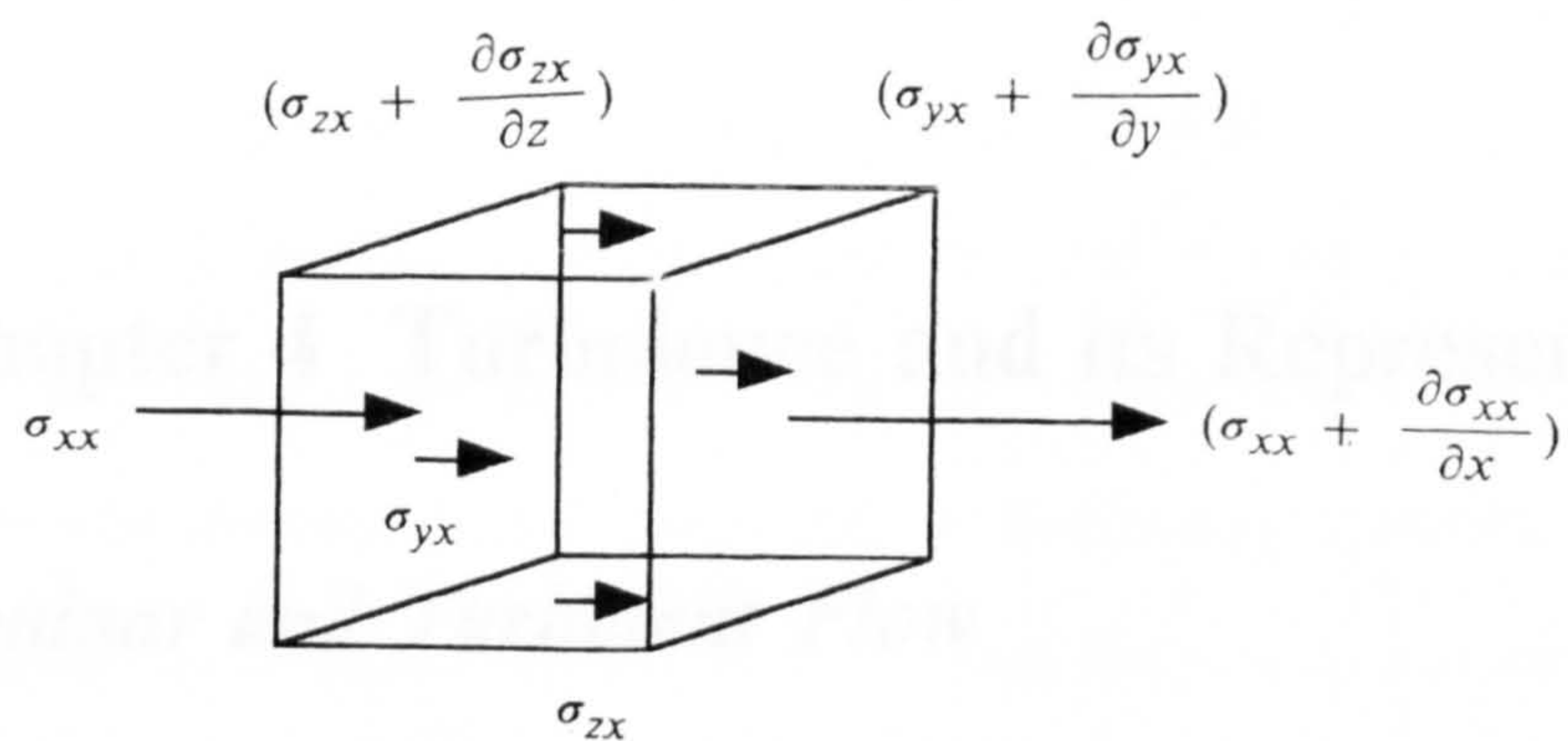


Figure 10. Forces on small element

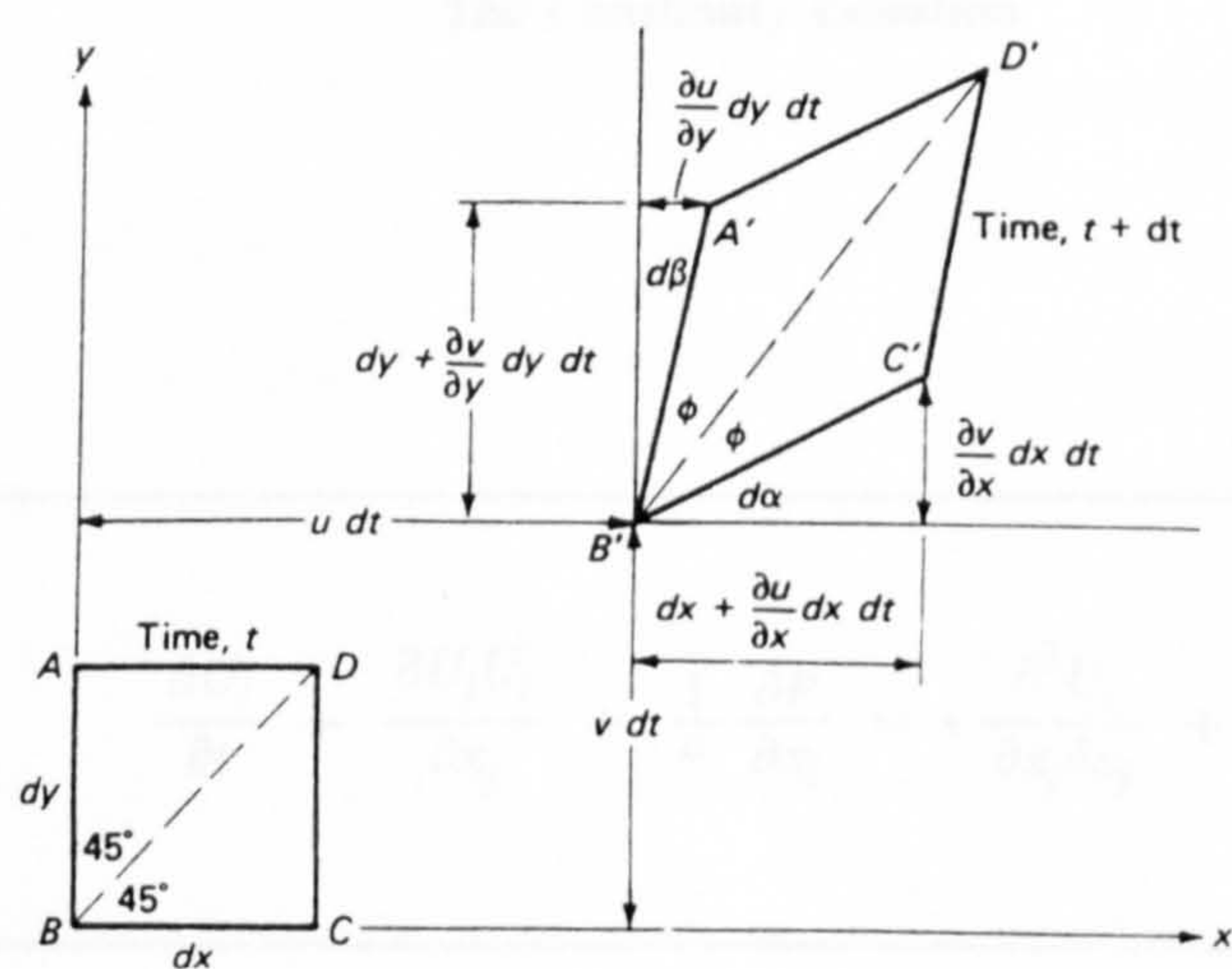


Figure 11. Deformation of Fluid

4.0 Chapter 4 Turbulence and its Representation

4.1 *Laminar and Turbulent Flow*

The equations derived in the previous chapter were,

$$\frac{\partial U_j}{\partial x_j} = 0 \quad [4.1]$$

The Continuity Equation

and

$$\frac{\partial U_i}{\partial t} + \frac{\partial U_j U_i}{\partial x_j} + \frac{1}{\rho} \frac{\partial P}{\partial x_i} = \nu \frac{\partial^2 U_i}{\partial x_j \partial x_j} + g_i \quad [4.2]$$

The Dynamic Equations

As already stated these equations describe flow in a river. However, the equations are highly non-linear and in practice give rise to the phenomena known as turbulence.

Turbulence is a highly irregular motion of fluid particles when the fluid is forced 'too hard'. Of course, hard is a relative term. In practice we categorise how hard a fluid is being forced by the ratio of inertia forces to the stabilising viscous forces. When this ratio is below some critical value the flow is said to be laminar, the name deriving from the fact that the fluid appears to flow in thin laminae which glide over each other. When the ratio is above the critical value the fluid becomes unstable and the laminae break down into a fluctuating random motion. The change between the two flow regimes is not as well defined as described above and in fact there is a transition region. Reynolds (1883) was the first to quantitatively demonstrate this difference between laminar and turbulent flow and demonstrated that this laminar flow becomes unstable when the non-dimensional ratio $\rho UL/\mu$ (which became known as Reynolds number, R_e) is approximately equal to the critical Reynolds number, $R_{e\text{ crit}}$. The flow is in a transition regime (in which the turbulence is not fully developed and thus still depends to a lesser extent on the molecular viscosity) between $R_{e\text{ crit}}$ and $R_{e\text{ FDT}}$, the fully developed turbulence Reynolds number. In the Reynolds number U is a characterising velocity, L is a characterising length scale. The magnitude of $R_{e\text{ crit}}$ varies with the flow configuration studied and thus the choice of the characterising dimensions, however for a river channel, taking L to be the hydraulic radius and U to be the area averaged velocity, $R_{e\text{ crit}}$ is about 500. The flow can usually be considered fully turbulent at about $R_{e\text{ FDT}}$ equal to 12500, French (1985). When the flow is fully turbulent it is disorderly, unsteady and apparently unamenable to deterministic analysis, see figure 12.

4.2 *Representing Turbulent Flow*

If the flow is turbulent then it will consist of eddies of various sizes ranging from the dimensions of the fluid domain (typically say the flow depth in a river) down

to the smallest eddy size which may be of the order of hundredths of a millimetre. This is the so-called Kolmogorov length scale ($L_K = (\nu^3 \delta / U^3)^{1/4}$). In the above expression ν is the kinematic viscosity, which is μ/ρ and δ is the shear layer width. The range widens with Reynolds number so that at higher Reynolds numbers there is a larger spectrum of eddy sizes to be resolved. The eddies are constantly moving. Clearly, the computational discretisation in space and time required to model such a flow and resolve all the detail would have to be fine enough to resolve the smallest eddy but cover a large enough extent to represent the flow structures of engineering importance. The limitations of computing the effects of turbulence can be demonstrated by considering turbulent flow in a river. For a section of river that is 10 kilometres long, 100 metres wide and 5 metres deep with an average velocity of 0.2 m/s, the smallest eddy containing significant energy may be about 0.1 millimetres. There are therefore, $100,000,000 \times 1,000,000 \times 50,000$ significant eddies to be computed. If we further assume that we could get away with 5 computational points in each co-ordinate direction per eddy (which is probably underresolved) then there will be $5^3 \times 5 \times 10^{18}$ computational points in our grid. At each point we would have to store u, v, w and p and compute with one continuity and three momentum equations. Suppose now that we could compute the future values of the variables with no iteration thus we would probably require 100 floating point operations per point per timestep, Emmons (1970). Thus we would have to do about 6×10^{22} computations per timestep. At the time of writing, a fast parallel supercomputer may be able to complete 8,000,000,000 floating point operations per second (FLOPS). Thus to complete one timestep of our calculation would require 250,000 years. Clearly even with highly efficient numerical models this approach is not, at present, an option for practical engineering predictions and is unlikely to become one in the foreseeable future.

4.2.1 Full Simulation

Despite the daunting example given in the previous section this approach which is termed full simulation or direct numerical simulation has been attempted at least for much lower Reynolds numbers over much smaller domains. For example, Spalart (1988) has simulated the turbulent boundary layer on a flat plate with zero pressure gradient for Reynolds numbers (based on the momentum thickness) up to about 1410 by solving the time dependent Navier-Stokes equations with a spectral method. In this simulation 10 million mesh points were used. When the results at these points were correlated over time and space, Spalart was able to verify the following results:

1. Friction factors accurate to within 5%
2. Velocity profiles that verify the logarithmic wall law
3. Accurate estimates of Reynolds stress and rms fluctuations of both velocity and pressure

Although the flows considered were barely turbulent, Spalart's results are very important. It is anticipated that this approach will become an important area of research particularly as computers become ever faster and larger. Its usefulness will probably be for calibrating, validating and even designing simpler turbulence models rather than for actual engineering calculations.

4.2.2 Large Eddy Simulation Models (LES)

A less computationally demanding approach is to use a computational grid that resolves only the 'large' eddies and represents the effect of the 'small' sub grid scale eddies with an empirical model. It is argued that as the eddies under consideration

get smaller they tend towards a more isotropic character allowing a simple sub-grid scale model to be applied. Lesieur (1993) gives a state of the art review of LES. Thomas, Williams and Leslie (1992) seem to be leading advocates of this approach in civil engineering in the United Kingdom. This approach must be three dimensional and unsteady and so requires very large computational resources. It therefore appears to be limited to simple geometries and boundary conditions. Despite these drawbacks, LES has been able to reproduce some of the large transient turbulent eddies that occur at the floodplain interface in compound channels, Williams (1992). Williams (1992) speculates that the ability to compute these motions makes the technique a more effective prediction tool than any other presently used turbulence models. This view is shared by Grass (1992).

4.3 Reynolds Proposal

Consider the section through a typical river shown in figure 13 which includes a representation of some of the tubulent eddies. Figure 14 shows the time trace of the velocity in the x direction at point A at two different resolutions. Different physical processes occur at different timescales. For example, a tidal river in the British Isles may experience flood waves with a period of 24-200 hours and M_2 tidal variations of the seaward water level with a period of about 12.5 hours. The bed, which is usually mobile, may be evolving at a timescale of months or years. The omnipresent turbulent fluctuations may occur with a period of the order of seconds. Other turbulent events, such as turbulent bursting and the large transient eddies mentioned in the previous section which are produced at the interface between a faster flowing main channel and a slower moving flood plain, have a larger time period. However these events should also be considered to be turbulent fluctuations for the present purposes since their period is much smaller than the period of the mean flow quantities. Amsden and Harlow (1968) give further

consideration to the dividing line between the 'large' and 'small' turbulent fluctuations. Fortunately engineers are not usually interested in these fluctuations per se (impinging jets being the notable exception) but rather are interested in their influence on the mean flow quantities.

Reynolds (1895) suggested that any quantity (U,V,W,P) in a fluctuating field may be separated into a mean part and a fluctuating part,

$$U = u + u' \quad V = v + v' \quad [4.3]$$

$$W = w + w' \quad P = p + p'$$

where,

$$q' = \frac{1}{\delta t} \int_{t_0}^{t_0 + \delta t} Q dt \quad [4.4]$$

and δt is large compared to the period of the fluctuations but small with respect to the period of the mean flow quantities (Q). Substituting 4.3 into the Navier-Stokes equations 4.1 and 4.2 and taking the time average of the resulting equations noting the following laws of averaging,

$$\overline{\bar{f}} = 0 \quad \overline{\bar{f}} = 0 \quad \overline{\bar{f}\bar{g}} = \bar{f}\bar{g}$$

$$\overline{\bar{f}\bar{g}} = 0$$

$$\overline{\bar{f} + \bar{g}} = \bar{f} + \bar{g}$$

$$\overline{\frac{\partial \bar{f}}{\partial s}} = \frac{\partial \bar{f}}{\partial s}$$

$$\overline{\bar{f}\bar{g}} = 0 \quad \overline{\bar{f} + \bar{g}} = \bar{f} + \bar{g}$$

$$\overline{\frac{\partial \bar{f}}{\partial s}} = \frac{\partial \bar{f}}{\partial s}$$

we arrive at the Reynolds Averaged Navier-Stokes equations,

$$\frac{\partial u_j}{\partial x_j} = 0 \quad [4.5]$$

The Continuity Equation

and

$$\frac{\partial u_i}{\partial t} + \frac{\partial u_j u_i}{\partial x_j} + \frac{1}{\rho} \frac{\partial p}{\partial x_i} = \nu \frac{\partial^2 u_i}{\partial x_j \partial x_j} + \frac{\partial}{\partial x_j} (-\overline{u'_i u'_j}) + g_i \quad [4.6]$$

The Dynamic Equations

Note now that these equations are written in terms of u_i which is the time averaged quantity. These equations differ from the Navier-Stokes equations in the introduction of the terms $-\overline{u'_i u'_j}$. These terms are due to the fluctuating motion present in turbulent flow. The molecular stress terms are present but they are usually insignificant compared to their turbulent counterparts in civil engineering hydraulics problems. The Reynolds averaged Navier-Stokes equations are a more practical foundation for the simulation of river flows.

4.3.1 Reynolds Stresses

If we compare Reynolds equations with Euler's equations we see that the terms, $\overline{u'_i u'_j}$, are analogous to a stress tensor,

$$-\overline{u'_i u'_j} = \begin{bmatrix} -\overline{u'u'} & -\overline{u'v'} & -\overline{u'w'} \\ -\overline{v'u'} & -\overline{v'v'} & -\overline{v'w'} \\ -\overline{w'u'} & -\overline{w'v'} & -\overline{w'w'} \end{bmatrix} \quad [4.7]$$

Because of this analogy these terms, which are really momentum transferred by the fluctuating motion, are called Reynolds Stresses. There is now a closure problem in the equation set since there are four equations and ten variables (as the stress tensor is seen to be symmetric). To proceed it is necessary to have some way of representing the Reynolds stresses. The choice of representing these stresses is termed turbulence modelling.

4.4 *Turbulence Modelling*

Much of the existing knowledge of turbulence modelling has stemmed from research in the fields of aeronautical and mechanical engineering. Traditionally civil engineering research has adopted much simpler mathematical descriptions of turbulence. This has led to an accessibility problem for civil engineers and civil engineering researchers which has been addressed by the IAHR (1992). Nallasamy (1987) gives an excellent review of turbulence modelling but the terminology and the examples of computations in this report tends to stem from a more mechanical or aeronautical engineering background. Rodi's (1980) report on turbulence modelling certainly has more of a hydraulic flavour but also suffers from a terminology problem with a certain level of knowledge and notation assumed.

In the following sections turbulence modelling is discussed generally, however, differences between depth averaged, quasi and fully three dimensional turbulence modelling will be highlighted.

4.4.1 Zero Reynolds Stress Models ?

The simplest model of the Reynolds stresses would be simply to treat them as zero. Although this seems a rather gross over-simplification in fact this approximation has apparently been used successfully in many applications mostly depth averaged but some fully three dimensional. The success of these applications stems from the fact that for the phenomena being modelled the momentum diffusion was simply not important compared to other terms in the equations although poor numerical treatments of the advection terms introducing an artificial viscosity may have compensated for inadequate (or non-existent turbulence models).

In depth averaged models the success of these 'zero Reynolds stress models' can be attributed, in certain flows, to the relatively small contribution of the lateral momentum diffusion compared to the influence of the strong vertical momentum diffusion promoted by the bed roughness and represented by the bed friction terms. Lean and Weare (1979) demonstrate this and quantify when these terms were important. Subsequently, Babarutsi, Ganoulis and Chu (1989) extended the analysis and introduced a dimensionless number which they suggest distinguishes three flow regimes shallow, intermediate and deep. In shallow flow they suggest that the bed friction dominates whereas in deep flow there is little bed influence therefore lateral turbulent stresses are crucial. In intermediate depths both bed and lateral terms influence the flow. Presumably, therefore, shallow flows would be acceptably modelled using a zero Reynolds stress model while deep flows always require an accurate estimate of the Reynolds stresses. The necessity for representing turbulent shear stresses also depends on the application. Where it is important to predict zones of recirculation (typically pollution or sediment transport problems) then their modelling is important whereas for predicting the

changes in tide propagation or flooding problems then their representation may not be so important.

Depth averaged applications which adopt a 'zero Reynolds stress model' include Townson (1974) for tidal propagation and Townson and Donald (1985) for storm surge prediction. Samuels (1985) has used a zero Reynolds stress model in considering meandering two stage channels. Supercritical flows are often modelled with no turbulence model, Bhallamudi and Chaudhry (1992), as are dam break models, Elliot and Chaudhry (1992). Fully three dimensional applications which contain no turbulence model include Davis and Deutsch (1980).

4.4.2 A Stress-Strain Relationship for Turbulent Flows

Boussinesq (1877) arbitrarily proposed that the Reynolds stress terms may be assumed instantaneously linearly proportional to the mean strain rate tensor in a way analogous to laminar flows.

$$-\overline{u'w'} = \nu_t \frac{\partial u}{\partial z} \quad [4.8]$$

The coefficient of proportionality, ν_t , is termed the eddy viscosity in analogy with the molecular viscosity found in the laminar expression. Boussinesq's proposal was not given in a tensorially invariant form. The general expression is,

$$-\overline{u'_i u'_j} = \nu_t 2D_{ij} - \frac{\overline{u'_k u'_k}}{3} \delta_{ij} \quad [4.9]$$

where

$$D_{ij} = \frac{1}{2} \left(\frac{\partial u_i}{\partial x_j} + \frac{\partial u_j}{\partial x_i} \right) \quad [4.10]$$

is the mean strain rate tensor based now on the time averaged velocity field. The second term on the right hand side of equation 4.9 is necessary so that sum of the normal stresses is always positive in an incompressible flow which is a physical requirement, $(\frac{1}{2} \overline{u'_i u'_i} \geq 0)$. The problem is now one of specifying the value of the eddy viscosity which, it will be apparent, is not a constant like its laminar counterpart. Intuitively, one feels it should be higher where there is stronger turbulent mixing but the problem is to express this quantitatively.

In models of large areal extent which are less influenced by shear layers it may be adequate to assume a constant eddy viscosity throughout the domain of study. Typically this has been used in models of lakes. Falconer, George and Hall (1991) used this approach in modelling shallow lake circulation. It is common in quasi-three dimensional flows to represent the vertical shear stresses with a refined turbulence model while the horizontal stresses are represented in a more phenomenological fashion. Note that for the depth averaged applications the mean strain rate tensor is based on the depth averaged velocity field.

4.4.3 Models Based on Algebraic Formula

In a fully developed infinitely wide open channel the eddy viscosity distribution is given by a parabolic distribution, French (1985) ,

$$\nu_t = \kappa u^* z \left(1 - \frac{z}{h}\right) \quad [4.11]$$

with maximum,

$$v_t^{\max} = \kappa u^* \frac{h}{2} \frac{1}{2} = \kappa u^* \frac{h}{4} \quad [4.12]$$

at mid-depth and average (over the depth)

$$v_t^{\text{avg}} = \frac{2}{3} v_t^{\max} = \kappa u^* \frac{h}{6} = 0.067 u^* h \quad [4.13]$$

where z is the distance above the bed. The friction velocity is given by $u^* = \sqrt{\frac{\tau_b}{\rho}}$ where τ_b is the bottom shear stress and may be calculated by some appropriate empirical friction law. Therefore as a first approximation either constant values of the eddy viscosity based on 4.13 or depth varying values based on 4.11 have been tried even when the flow is not strictly fully developed, Sauvaget and Usseglio-Polatera (1987). Prandtl (1925) proposed a closure for the Reynolds stresses which for fully developed boundary layers does remarkably well in representing the experimental data. He suggested that, in analogy with the kinetic theory of gases, each turbulent fluctuation could be related to a length scale and a velocity gradient,

$$-\overline{u'w'} = (\text{const.}) u'_{rms} w'_{rms} = (\text{const.}) (l \frac{\partial u}{\partial z}) (l \frac{\partial u}{\partial z}) \quad [4.14]$$

The length scale, l , is termed the mixing length and represents some mean eddy size. A comparison of Prandtl's expression 4.14 with the Boussinesq expression 4.8 shows that it may be thought of as a formula for the eddy viscosity,

$$v_t = (\text{const.}) l^2 \left| \frac{\partial u}{\partial z} \right| \quad [4.15]$$

A more general expression is required for non-boundary layer flows,

$$v_t = (\text{const.}) l^2 \sqrt{(D_{ij} D_{ij})} \quad [4.16]$$

The model is completed by relating the mixing length to the gross flow features. By dimensional considerations we may see that the mixing length hypothesis may be thought of as suggesting that,

$$v_t = (\text{const.}) \times \text{length scale} \times \text{velocity scale} \quad [4.17]$$

so that the velocity scale originally taken by Prandtl was the product of the mixing length and the velocity gradient. In hydraulics several alternative suggestions for the mixing length have been tried including Sauvaget and Usseglio-Polatera (1987),

$$l = \min [0.2\kappa h, \kappa z, \kappa h(1 - \frac{z}{h})] \quad [4.18]$$

where $\min[x,y,z]$ means the minimum of x , y and z . Alfrink (1982) suggests an alternative form,

$$l = \kappa z \text{ if } z < 0.25h \quad [4.19]$$

$$l = 0.25\kappa h \text{ otherwise}$$

The advantage of the mixing length proposal is primarily simplicity. The mixing length proposal is disadvantaged through the need to prescribe a priori the length scale throughout the domain of interest. At best this is probably an inexact science, the prescription of the mixing length being relatively reliable for simple boundary layers but near impossible for complex recirculation zones. In addition no account is taken of the history effects, i.e. the fact that stronger eddies generated upstream may be swept with the mean velocity downstream to thus influence mixing there is not accounted for.

4.4.4 Models Based on One Differential Transport Equation

In an effort to somehow take account of history effects in the flow and also to provide more turbulence information for validation and enlightenment, Prandtl (1945), proposed that instead of taking the product of the mixing length and the velocity gradient as the velocity scale a more direct measure of the turbulence should be chosen. The new velocity scale was chosen to be the square root of the turbulent kinetic energy, \sqrt{k} .

$$k = \frac{1}{2}(\overline{u'^2} + \overline{v'^2} + \overline{w'^2}) = \frac{1}{2}\overline{u'_i u'_i} \quad [4.20]$$

The eddy viscosity would thus be given as,

$$\nu_t = c'_\mu \times l \times \sqrt{k} \quad [4.21]$$

where c'_μ is a constant. The advantage of this proposal is that it is possible to theoretically derive an exact transport equation for the turbulent kinetic energy, k , by considering energy relations in turbulent flow. Unfortunately the derivation of this equation introduces new higher order correlations which must be represented as functions of the mean quantities. The modelled form of this equation which has been adopted for use in practical predictions is,

$\frac{Dk}{Dt} = \frac{\partial}{\partial x_j} \left(\frac{\nu_t}{\sigma_k} \frac{\partial k}{\partial x_j} \right) + (-\overline{u'_i u'_j}) \frac{\partial u_i}{\partial x_j} - \epsilon$ <div style="display: flex; justify-content: space-around; margin-top: 5px;"> Advection Diffusion Production Viscous Dissipation </div>	[4.22]
---	--------

The shorthand notation for the advection operator has been adopted,

$$\frac{D\phi}{Dt} = \frac{\partial \phi}{\partial t} + \frac{\partial u\phi}{\partial x} + \frac{\partial v\phi}{\partial y} + \frac{\partial w\phi}{\partial z} \quad [4.23]$$

In order to identify the length scale it is assumed that there is a constant rate of energy transfer from the energy containing eddies to the small scale dissipative flow structures. This is the turbulent energy dissipation rate, ε . With this assumption the dissipative time scale of the large eddies is,

$$T \propto \frac{k}{\varepsilon}$$

The energy transfer from the large structures of the inertial range is a mechanism due to the non-linear advection terms, so that T may be assumed to be proportional to the time scale of the large eddies,

$$T \propto \frac{1}{k^{1/2}}$$

thus,

$$l \propto \frac{k^{3/2}}{\varepsilon}$$

which may be substituted in 4.22 giving,

$$\begin{array}{ccccccc} \frac{Dk}{Dt} & = & \frac{\partial}{\partial x_j} \left(\frac{v_t}{\sigma_k} \frac{\partial k}{\partial x_j} \right) & + & (-\overline{u'_i u'_j}) \frac{\partial u_i}{\partial x_j} & - & c_d \frac{k^{3/2}}{l} \\ \text{Advection} & & \text{Diffusion} & & \text{Production} & & \text{Viscous Dissipation} \end{array} \quad [4.24]$$

The rate of change of k is governed by the advective transport due to the mean velocity, the diffusive transport due to velocity and pressure fluctuations, the production of k by interaction of the Reynolds stresses and the mean velocity

gradients and the dissipation of k by viscous action into heat. This approach has been tried by Koutitas and O'Connor (1980) for computing three dimensional wind induced flows in a coastal bay. They conclude that it has advantages over simpler and more complex models for this particular application.

The advantages of this 'one equation' approach is the limited inclusion of history effects and the firmer base in theory. The disadvantage is that a length scale distribution must still be prescribed throughout the domain a priori.

4.4.5 Models Based on Two Differential Transport Equations

The length scale of the energy containing eddies is subject to transport processes in the same way as the kinetic energy. This fact, combined with the desire to avoid having to prescribe the length scale a priori has encouraged researchers to try to formulate a second differential transport equation for the turbulent length scale. In fact the length scale is rarely used itself but rather a variable proportional to it has been adopted. Several different variables have been suggested for the second differential equation with the most popular being ε , the rate of dissipation of the turbulent kinetic energy. The fact that ε appears as the last term in the k equation, i.e.,

$$\varepsilon = c_d \frac{k^{3/2}}{l} \quad [4.25]$$

has probably contributed to this adoption. Although a theoretical transport equation may be derived for ε , Tennekes and Lumley (1972), it contains complex correlations whose behaviour is little understood and for which fairly drastic modelling assumptions must be introduced to provide a useful form. The equation contains terms representing convection, diffusion, generation of vorticity due to

vortex stretching connected with the energy cascade and a term representing the viscous destruction of vorticity. In its modelled form it is,

$$\underbrace{\frac{D\varepsilon}{Dt}}_{\text{Advection}} = \underbrace{\frac{\partial}{\partial x_j} \left(\frac{\nu_t}{\sigma_\varepsilon} \frac{\partial \varepsilon}{\partial x_j} \right)}_{\text{Diffusion}} + \underbrace{\frac{\varepsilon}{k} \left[c_{1\varepsilon} (-\overline{u'_i u'_j}) \frac{\partial u_i}{\partial x_j} - c_{2\varepsilon} \varepsilon \right]}_{\text{Generation-Destruction}} \quad [4.26]$$

With k and ε computed the eddy viscosity is given by,

$$\nu_t = c'_d c'_\mu \times \frac{k^{3/2}}{\varepsilon} \times \sqrt{k} \quad [4.27]$$

or,

$$\nu_t = c_\mu \frac{k^2}{\varepsilon} \quad [4.28]$$

Equations 4.26 and 4.28 combined with equation 4.22 and the Boussinesq assumption 4.9 represent a k - ε turbulence model. A number of constants are required for the k - ε model. These have been obtained with reference to observed data. They are given below.

c_μ	$c_{1\varepsilon}$	$c_{2\varepsilon}$	σ_k	σ_ε
0.09	1.44	1.92	1.0	1.3

Table 4. Model Constants for Standard Linear Model: Rodi (1980)

This model manages to predict the level of the eddy viscosity, at least to an order of magnitude, in many flows of interest in civil engineering. However, Younis (1992) describes several situations when this model fails to produce the correct flow behaviour which can be traced to inadequacies in the modelled equations. Some of the drawbacks of the standard k- ϵ model (e.g. erroneous prediction of the normal Reynolds stresses) can be attributed to the underlying Boussinesq assumption. For computational reasons modellers have clung tenaciously to the model modifying it in an ad hoc manner to enable better predictions for the particular flow of interest to them. Younis (1992) comments that this type of model is likely to remain one of the most popular for practical applications for some time. It is the simplest model that does not require specification of a length scale throughout the domain.

4.4.5.1 *Considerations for Depth Averaged Modelling*

In depth averaged models it is common to prescribe the depth averaged eddy viscosity from 4.29,

$$\overline{\nu}_t = (const) \times \underbrace{u^*}_{\text{velocity scale}} \times \underbrace{h}_{\text{length scale}} \quad [4.29]$$

where values for the constant has been given by Elder (1959). Alternatively, the constant may be chosen from other data, Fischer et al (1979), or calibrated to fit observed data.

Depth averaged versions of the k- ϵ model are available. They are similar to the equations presented above but include extra terms which account for the bed generated turbulence. On this point it is worth mentioning recent work of Chu and Barbarutsi (1989) and Booji (1989). These investigators have independently suggested that the original depth averaged form of the k- ϵ model, Rastogi and Rodi

(1978), does not predict the correct weighting between production of turbulence due to horizontal velocity gradients and production of turbulence due to the presence of the bottom. They suggest alternate ways to correct for this but seem to have gone unnoticed by the other researchers, Falconer and Li (1992).

4.4.6 Non-Linear Stress-Strain Relationships

The Boussinesq assumption is flawed by the assumption that the stress and strain are in local equilibrium. There have been several attempts to relax this assumption, by analogizing turbulent flow with non-Newtonian laminar flows, Rivlin (1957), by reference to continuum mechanics and invoking invariance constraints and other consistency measures, Speziale (1987), or by reference to statistical theories, Yoshizawa (1993).

The rationale that underlies non-linear models basically says that the Boussinesq assumption 4.9 is really a Taylor expansion restricted to terms of the first order, Baker and Orzechowski (1983). By extending the expression to include higher order terms more accurate predictions may result.

4.4.6.1 Baker and Orzechowski (1983)

In this model the Reynolds stresses are represented as,

$$-\overline{u'_i u'_j} = -\alpha_{ij}k + \nu_t 2D_{ij} + C_2 \nu_t T (2D_{ij})^2 \quad [4.30]$$

$$\alpha_{ij} = \frac{1}{3k} (\overline{u'_i u'_i}) a_i \delta_{ij} \quad [4.31]$$

where $T = \frac{k}{\varepsilon}$, defined earlier. The constants a_i are given as $a_1 = C_1$ and $a_2 = a_3 = C_3$.

C_1	C_2	C_3
0.94	0.067	0.56

Table 5. Non-linear Model Constants: Baker and Orzechowski (1983)

The expression for the Reynolds stresses is seen to be similar to the linear model with a further non-linear addition. In this particular non-linear model there is no isotropic part, i.e. the non-isotropy of the normal Reynolds stresses is taken account of by fixing their level with constants. This may limit its application unless it is modified in some ad-hoc way. This model is relatively simple and numerically robust. It gives plausible results in predicting turbulence driven secondary motions found in uniform channel flows, Baker and Orzechowski (1983), and also results in better predictions for the recirculation zone size at backward facing steps, Benocci and Skovgaard (1988). The treatment of the anisotropy of the normal Reynolds stresses is not completely convincing theoretically, however, and this is perhaps why there are very few applications of it in the literature. This is unfortunate as it is considerably simpler than other non-linear models.

4.4.6.2 *Speziale's Model (1987)*

This model is much more complex than the previous non-linear model however the theoretical development of it is considerably more rigorous.

$$\begin{aligned}
-\overline{u'_i u'_j} = & -\frac{2}{3} k \delta_{ij} + \nu_t 2 D_{ij} + 4C_D c_\mu \nu_t T (D_{im} D_{mj} - D_{mn} D_{mn} \delta_{ij} / 3) \\
& + 4C_E c_\mu \nu_t T (\overset{\circ}{D}_{ij} - \overset{\circ}{D}_{mm} \delta_{ij} / 3)
\end{aligned} \quad [4.32]$$

The constants C_D and C_E are equal and have been assigned the value 1.68. In these expressions, $\overset{\circ}{D}_{ij}$ is the Oldroyd derivative, which is,

$$\overset{\circ}{D}_{ij} = \frac{D}{Dt} (D_{ij}) - \frac{\partial u_i}{\partial x_k} D_{kj} - \frac{\partial u_j}{\partial x_k} D_{ki} \quad [4.33]$$

where,

$$\frac{D}{Dt} (D_{ij}) = \frac{\partial (D_{ij})}{\partial t} + \frac{\partial u_l (D_{ij})}{\partial x_l} \quad [4.34]$$

and T is defined earlier. This model is composed of an isotropic part, the linear model and an additional non-linear part. The anisotropy of the normal Reynolds stresses is taken account of in a more general way than in the previous non-linear model.

This model has been applied by Speziale and Ngo (1988) for the computation of re-circulating flow over a backward facing step and by Basara and Younis (1992) for this and other recirculating flows. Speziale (1987) has considered its use for the

computation of turbulence driven secondary motions in square ducts. Younis and Obdellatif (1989) have also considered its use for computing flows in square ducts and the consequences for sediment transport. Younis (1991) has considered its use for two-stage channels and compared it with a Reynolds Stress Transport Model. Cokljat (1993) has also considered the use of this type of model for computing secondary motions in ducts and channels. Hwang, Zhu, Massoudi and Ekman (1993) have considered its use in predicting swirling flows.

4.4.6.3 Other Non-Linear Models

Pope (1975) suggested a 'more general effective viscosity hypothesis' for two dimensional problems. However Pope (1975) suggested that its extension to three dimensional flows was probably impossible owing to the difficulties in the algebraic manipulation. The model has therefore found little application as yet in practical problems, a notable exception being the work of Schnell (1988). Recently Speziale and Gatski (1993) have extended Pope's analysis using computer aided mathematics software to produce a three dimensional model formula. This will no doubt rekindle an interest in this type of model. Craft, Launder and Suga (1993) have also introduced a non-linear model which retains terms up to the third order in the stress-strain constitutive relation. Despite this being the first stage in the development of the model, promising results are obtained for about a third of the computational time required of a full Reynolds Stress Transport Model.

4.4.7 Discussion of Non-linear Stress-strain Relationships

The use of non-linear turbulent stress-strain relationships is a relatively new development and their usefulness has not yet been fully established. They require slightly more computational work than the linear stress-strain relationship (20-30% depending on the implementation) and whether or not this extra work is

justified is still a matter for debate. The extra computation required, however, is still much less than that required by more complex models and also they may be implemented into a Navier-Stokes solver relatively easily, Speziale and Ngo (1988). In addition they require less storage space which may be important for large computational grids.

Certainly they allow the simulation of certain physical processes that can simply not be achieved with a linear model, in particular the reproduction of turbulent driven secondary motions in non-circular channels, Younis and Obdellatif (1989), and Baker and Orzechowski (1983). They also appear to give better predictions for the separation length in separated recirculating flows, Speziale and Ngo (1988). However, there are also studies which maintain that no clear advantage could be established for non-linear models over linear models, Hwang, Zhu, Massoudi and Ekman (1993). Indeed there are also studies that conclude that slightly erroneous predictions may be forthcoming, Benocci and Skovgaard (1988). The success of these models seems to be problem dependent (or even grid dependent). What can be said with certainty is that these models look promising but many more applications of them are required to establish their usefulness. There is certainly research needed to establish a robust numerical method for handling the Oldroyd derivative terms in Speziale's model as numerical problems have been reported, Speziale and Ngo (1988), Benocci and Skovgaard (1988). One possible strategy for this is suggested in chapter 5 although it is acknowledged that this problem may deter the general adoption of this particular model for practical problems. The extension of Pope's (1975) more general effective viscosity method to three dimensions, Speziale and Gatski (1993), is likely to focus interest in this type of model.

4.4.8 Reynolds Stress Transport Models (RSTM)

A transport equation may be derived for each individual Reynolds stress, and is presented below to demonstrate its complexity,

$$\frac{D}{Dt} (\overline{u'_i u'_j}) = - [\overline{u'_j u'_k} \frac{\partial u_i}{\partial x_k} + \overline{u'_i u'_k} \frac{\partial u_j}{\partial x_k}] - 2\nu \overline{\frac{\partial u'_i}{\partial x_k} \frac{\partial u'_j}{\partial x_k}} \quad [4.35]$$

$$\frac{p'}{\rho} \left(\frac{\partial u'_i}{\partial x_j} + \frac{\partial u'_j}{\partial x_i} \right) - \frac{\partial}{\partial x_k} [\overline{u'_i u'_j u'_k} - \nu \frac{\partial \overline{u'_i u'_j}}{\partial x_k} + \frac{p'}{\rho} (\delta_{jk} u'_i + \delta_{ik} u'_j)]$$

Equation 4.35, which actually requires seven model equations since the stresses are symmetrical, contains higher order correlations which must be replaced by known (or predictable) quantities. This modelling of the terms constitutes a Reynolds Stress Transport Model (RSTM) and is, at the time of writing, the state of the art in turbulence modelling research. This type of model may be difficult to use for complex problems due to convergence difficulties. Younis and Obdellatif (1989) suggest that it is not practical for river engineering problems due to its required computer storage and time requirements. Craft, Launder and Suga (1993) state that there are countless complex problems where the application of these type of models will not be applicable this century.

4.4.8.1 Algebraic Stress Models (ASM)

These models are simplifications of the Reynolds Stress Transport Model. For some years, these have been seen as a lower cost alternative to the RSTM offering a limited amount of the physics of the RSTM at much reduced computation. Despite much research effort and several promising results they have not emerged as a practical alternative to RSTM. While in 2D parabolic flows they have sometimes been successful, in elliptic flows they have led to poor predictive accuracy and a highly stiff equation set which causes severe convergence

difficulties, Craft, Launder and Suga (1993). Younis and Obdellatif (1989) have commented that they are unlikely to be practical for river engineering.

4.5 *Boundary Conditions for Turbulent River Flows*

Boundary conditions are required at the bed and free surface to solve the system. Although, in theory, the same boundary conditions as described in the previous chapter are applicable the mesh required to resolve the steep velocity gradients close to the wall would be far too demanding of computer resources. In addition the flow close to the wall is not fully turbulent and the above turbulence equations are not strictly applicable. For these reasons, it is convenient to terminate computations close to the wall where certain universal wall laws are assumed to be valid.

4.5.1 Near Wall Turbulent Flow Characteristics

The first computing mesh element is within a layer where it can be assumed that the flow follows the logarithmic law of the wall. Therefore, it can be assumed that the fluid shear stress is equivalent to the wall shear stress,

$$\nu_t \frac{\partial u_\tau}{\partial x_n} = u^\star |u^\star| \quad [4.36]$$

where u^\star is the friction velocity ($= \sqrt{\frac{\tau_b}{\rho}}$) and,

$$u_n = 0 \quad [4.37]$$

In the above expressions the subscript n means normal to the wall and τ means tangential to the wall. For the turbulence quantities it is assumed that local equilibrium prevails (Production = ε) giving,

$$k = \frac{u^{\star 2}}{\sqrt{c_\mu}} \quad [4.38]$$

$$\varepsilon = \frac{|u^{\star}|^3}{\kappa Z} \quad [4.39]$$

In order to apply the above a value of the friction velocity, u^{\star} , is required. There are several alternatives for its evaluation. Commonly a logarithmic wall law, equation 4.40, is solved iteratively for u^{\star} by using the velocity at the first internal grid point at the previous timestep or iteration,

$$u^+ = \frac{1}{\kappa} \ln(Ez^+) \text{ if } z^+ > 11.63 \quad [4.40]$$

$$u^+ = z^+ \text{ if } z^+ < 11.63$$

and $u^+ = u_i/u^{\star}$, $z^+ = zu^{\star}/\nu$ and E is set according to the following criteria,

Wall Type	E
Hydraulically Smooth	9.0
Intermediate	$\frac{\exp(\kappa B_s)}{k_s^+}$ where $B_s = (5.5 + 2.5 \ln(k_s^+)) \exp[-0.062(\ln k_s^+)^3]$ $+ 8.5\{1 - 8.5[-0.062(\ln k_s^+)^3]\}$
Hydraulically Rough	$\frac{30}{k_s^+}$

Table 6. Wall Friction Relationships: Smooth to Rough

where $k_s^+ = \frac{k_s u^{\star}}{\nu}$ and κ is the von Karman constant taken here to be 0.4. These wall laws have been proposed by Launder and Spalding (1974). The expression for B_s given above has been obtained by Sajjadi and Aldridge (1993) by best-fitting a curve to the data of Nikuradse (1933) although other suggestions have been given Naot (1984) or Krishnappan and Lau (1986). k_s would have to be estimated with

help from tables with a knowledge of the bed material or calibrated with reference to field data. However, for natural mobile river beds this procedure would be fraught with difficulty.

Bed Material	k , cm.
Brass,copper,glass,perspex	0.0003
Asbestos cement	0.003
Plastic	0.003
Bitumen lined ductile iron	0.003
Galvanised iron	0.015
Slimed concrete sewer	0.6

Table 7. Typical values of Nikuradse's equivalent sand grain size

For field calibration a procedure similar to that described by Krishnappan (1984) may be useful. Presumably, for fully developed rough turbulent flow a friction factor of the following type could also be used,

$$u^{*2} = \frac{f}{2} u^2 \tag{4.41}$$

Indeed, this is commonly used in quasi-three dimensional models, Blumberg and Mellor (1983) although in fully three dimensional computations wall laws appear to be more popular. This may simply be because of the differing applications of these models.

4.5.2 Free Surface Turbulent Flow Characteristics

The rigid lid assumption is adopted in which the free surface is replaced with a fictitious frictionless lid at some equilibrium height. This concept has been used with much success in the past, where the free surface is reasonably flat, Alfrink and Van Rijn (1983). Alfrink and Van Rijn (1983) suggest that the rigid lid approximation is valid as long as the Froude number ($\frac{\bar{U}}{\sqrt{gh}}$) is low. There are many circumstances in river engineering where these assumptions could reasonably be assumed particularly when considering short lengths of channel. A problem may come in its practical application in defining an equilibrium level where the rigid lid is to be placed. In the computational cell closest to the free surface a pressure is computed and the magnitude of this, in some way, represents the height to which the water surface could rise if the surface were free. In any event, the effect of the free surface on the internal flow is taken account of. It is assumed that the fluid shear stress at the surface equals the surface stress which in the absence of wind is zero,

$$\nu_t \frac{\partial u_\tau}{\partial x_n} = 0 \quad [4.42]$$

Zero mass flux is assumed normal to the free surface,

$$u_n = 0 \quad [4.43]$$

For the turbulence quantities symmetry conditions have often been used, Stamou, Adams and Rodi (1989),

$$\frac{\partial k}{\partial x_n} = 0 \quad [4.44]$$

$$\frac{\partial \varepsilon}{\partial x_n} = 0 \quad [4.45]$$

however there is evidence that, at least for simple boundary layer flows, that the length scale of the turbulence is reduced at the free surface as evidenced by the eddy viscosity returning to zero, see figure 14. Krishnappan and Lau (1986) have suggested a formula relating ε at the free surface to k at the free surface (k_f) through an effective length scale (y_f),

$$\varepsilon = \frac{C_f}{\kappa c_\mu^{3/4}} \frac{k_f^{3/2}}{y_f} \quad [4.46]$$

where C_f is a constant and y_f is the distance between the free surface and the nearest internal grid node. Naot (1988) suggests a boundary condition for ε at the free surface which does not rely on an effective length scale,

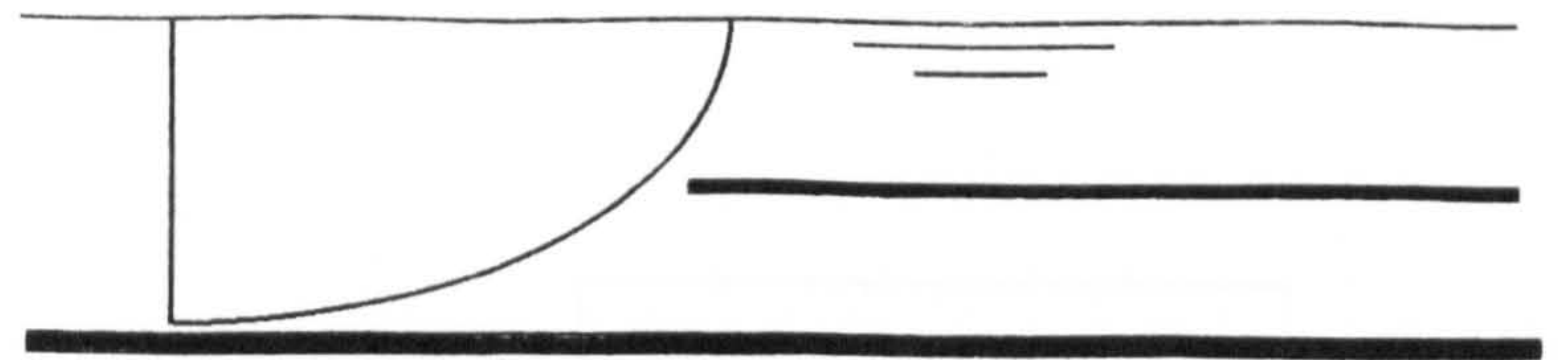
$$\frac{\partial \varepsilon}{\partial x_n} = 3.5 \frac{\varepsilon^2}{k^{3/2}} \quad [4.47]$$

which may be more useful when an effective length scale cannot be defined. Recent experiments, Nelson, McLean and Wolfe (1993), see figure 15 have indicated that for complex bed topographies and lower relative depths the turbulence characteristics are not as simple as for boundary layer type flows and in this circumstance applying a symmetry condition may be no worse than applying one of relations above. In addition, because of the other uncertainties prevalent in civil engineering computations, it may be that the boundary conditions on the free surface turbulence may not be the critical factor in determining accuracy and this may be why the simpler symmetry conditions have often been adopted in geophysical applications, Ushijima, Shimizu, Sasaki and Takizawa (1992) or Finnie and Jepson (1991).

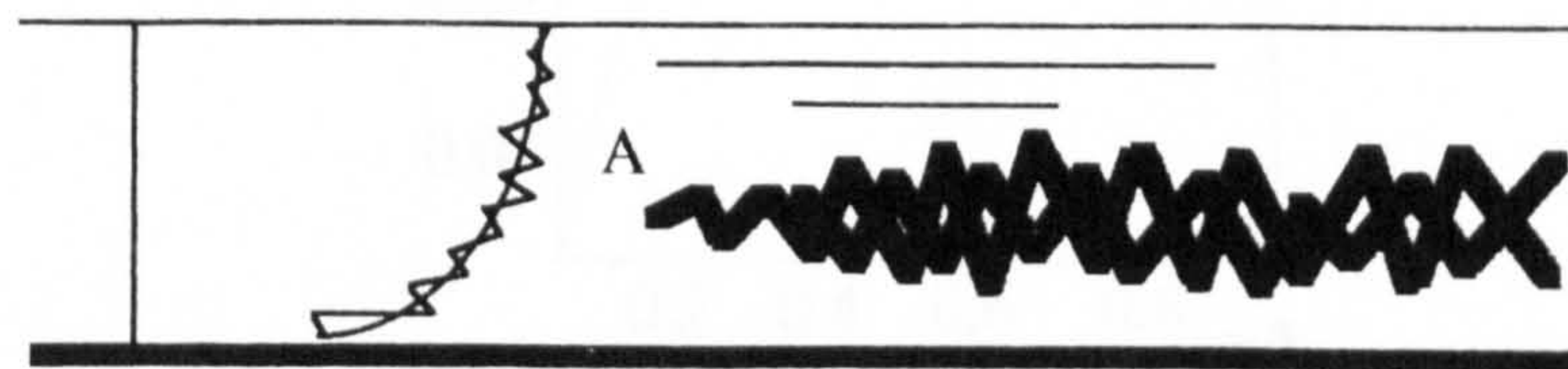
4.6 Strategy for a Three Dimensional River Model

On the basis of the previous chapters a strategy for developing and applying a three dimensional river model has been devised. The strategy focuses on the following points:

1. Model to be based on the fully elliptic three dimensional Reynolds Averaged Navier-Stokes Equations.
2. Turbulence to be represented by a two equation model to avoid the need to prescribe a length scale throughout the domain a priori. Linear stress-strain relationship, 4.9, to be adopted initially but to investigate the possible applications of a non-linear stress-strain relationship, 4.32, by studying representative two dimensional problems.
3. Free surface to be represented by a rigid lid initially although future developments to allow for a relaxation of this restriction.



Laminar Flow



Turbulent Flow

Figure 12. Laminar and Turbulent Flow

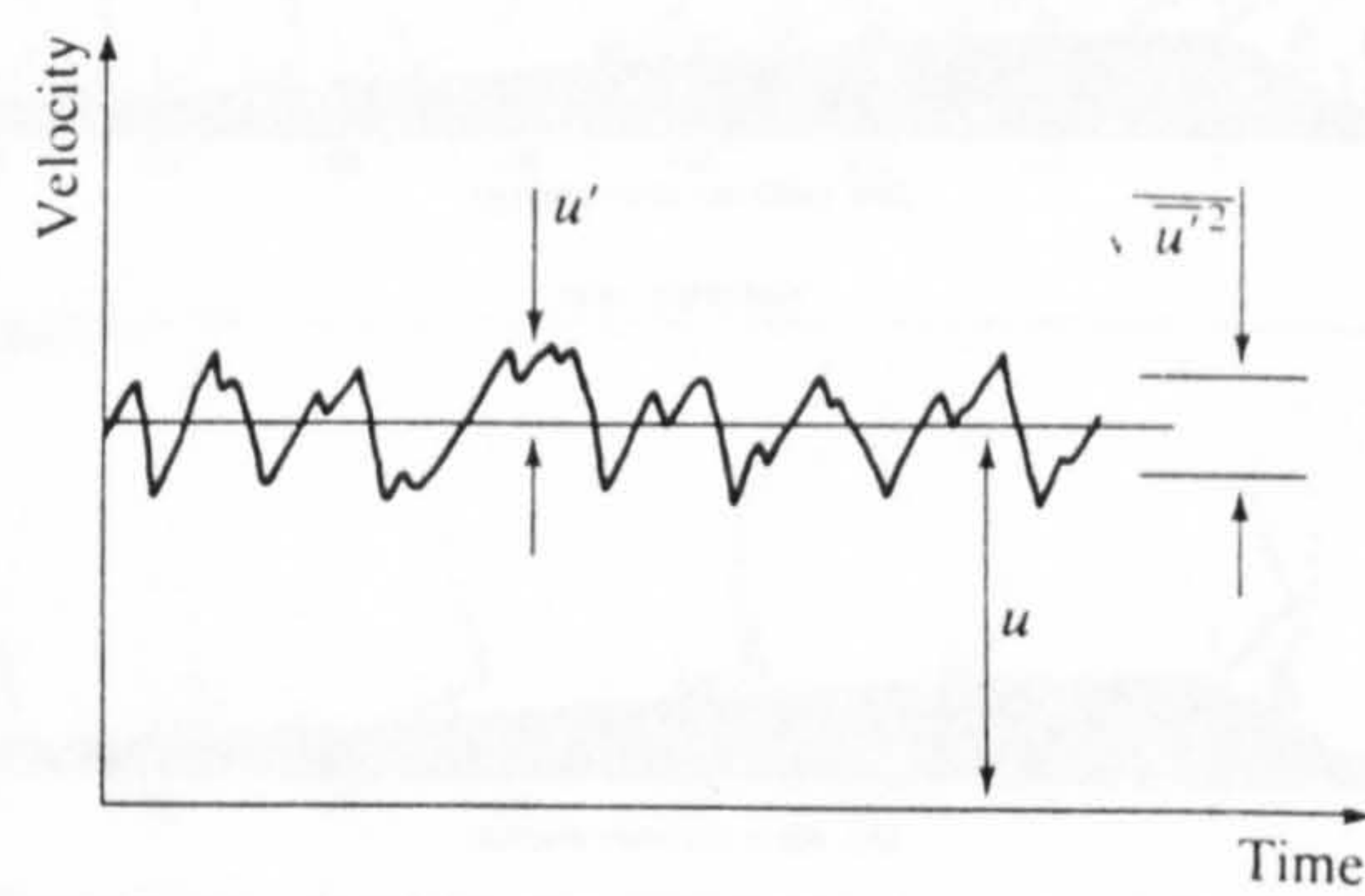


Figure 13. Time Trace of Velocity in a River at Point A

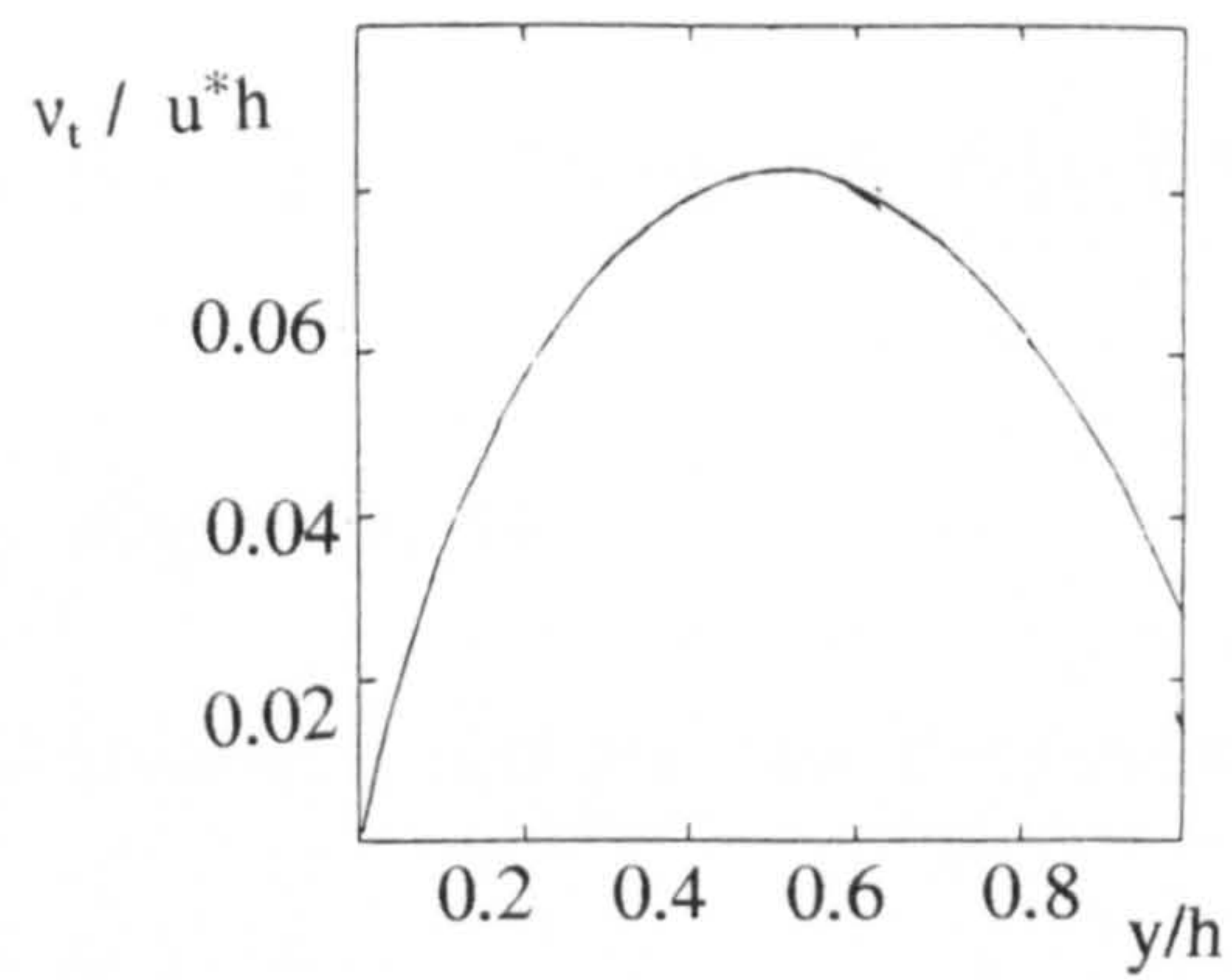


Figure 14. Eddy viscosity in uniform flow

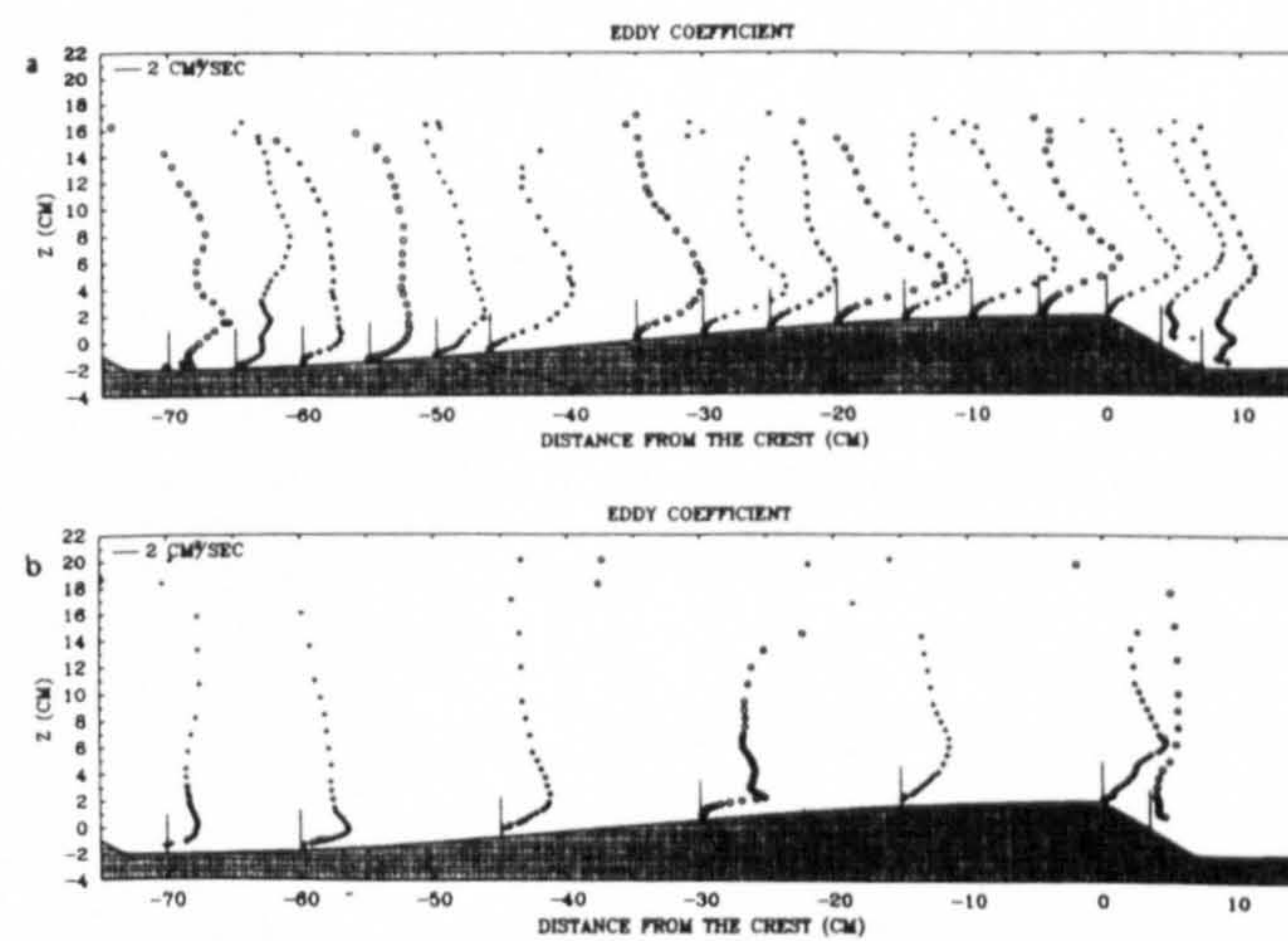


Fig. 9. Eddy coefficients in flow over two-dimensional bed forms for (a) run 1 and (b) run 4. These values were computed from the smoothed measurements of mean velocity and Reynolds shear stress using (16). Small differences in the magnitude of the eddy viscosity in these two cases is attributable to the differences in mean velocity (see Table 1).

Figure 15. Eddy viscosity in localised non-uniform flows

5.0 Chapter 5 The Present Model

5.1 System of Equations

The system of equations describing the flow were derived in preceeding chapters as,

$$\frac{\partial u_j}{\partial x_j} = 0 \quad [5.1]$$

The Continuity Equation

$$\frac{\partial u_i}{\partial t} + \frac{\partial u_j u_i}{\partial x_j} + \frac{1}{\rho} \frac{\partial p}{\partial x_i} = \nu \frac{\partial^2 u_i}{\partial x_j \partial x_j} + \frac{\partial}{\partial x_j} (-\overline{u'_i u'_j}) + g_i \quad [5.2]$$

The Dynamic Equations

$$-\overline{u'_i u'_j} = -\frac{2k}{3} \delta_{ij} + \nu_t \left(\frac{\partial u_i}{\partial x_j} + \frac{\partial u_j}{\partial x_i} \right) \quad [5.3]$$

$$\nu_t = c_\mu \frac{k^2}{\varepsilon}$$

Turbulent Closure Assumption One - Linear stress strain relationship

$$-\overline{u'_i u'_j} = -\frac{2}{3}k\delta_{ij} + \nu_t 2D_{ij} + 4C_D c_\mu \nu_t T(D_{im}D_{mj} - D_{mn}D_{mn}\delta_{ij}/3) \quad [5.4]$$

$$+ 4C_E c_\mu \nu_t T(\overset{\circ}{D}_{ij} - \overset{\circ}{D}_{mm}\delta_{ij}/3)$$

$$\nu_t = c_\mu \frac{k^2}{\varepsilon} \quad T = \frac{k}{\varepsilon}$$

$$\overset{\circ}{D}_{ij} = \frac{D(D_{ij})}{Dt} - \frac{\partial u_i}{\partial x_k} D_{kj} - \frac{\partial u_j}{\partial x_k} D_{ki}$$

Turbulent Closure Assumption Two - Non-Linear stress-strain relationship

$$\frac{\partial k}{\partial t} + \frac{\partial u_j k}{\partial x_j} = \frac{\partial}{\partial x_j} \left(\frac{\nu_t}{\sigma_k} \frac{\partial k}{\partial x_j} \right) + (-\overline{u'_i u'_j}) \frac{\partial u_i}{\partial x_j} - \varepsilon \quad [5.5]$$

Transport Equation for Turbulence Kinetic Energy

$$\frac{\partial \varepsilon}{\partial t} + \frac{\partial u_j \varepsilon}{\partial x_j} = \frac{\partial}{\partial x_j} \left(\frac{\nu_t}{\sigma_\varepsilon} \frac{\partial \varepsilon}{\partial x_j} \right) + \frac{\varepsilon}{k} (c_{1\varepsilon} (-\overline{u'_i u'_j}) \frac{\partial u_i}{\partial x_j} - c_{2\varepsilon} \varepsilon) \quad [5.6]$$

Transport Equation for Turbulence Kinetic Energy Dissipation Rate

5.1.1 Boundary Conditions and Model Constants

The boundary conditions have been defined in chapter 4 and are summarised below.

Boundary Type	Normal Velocity	Tangential Velocity	k	ε
Inlet	Specified	$u_t = 0$	Specified	Specified
Outlet	Computed	Computed	$\frac{\partial k}{\partial x_n} = 0$	$\frac{\partial \varepsilon}{\partial x_n} = 0$
Bed or Wall	$u_n = 0$	$v_t \frac{\partial u_t}{\partial x_n} = u^* u^* $	$k = \frac{u^{*2}}{\sqrt{c_\mu}}$	$\varepsilon = \frac{ u^* ^3}{\kappa x_n}$
Free Surface	$u_n = 0$	$\frac{\partial u_t}{\partial x_n} = 0$	$\frac{\partial k}{\partial x_n} = 0$	$\frac{\partial \varepsilon}{\partial x_n} = 0$

Table 8. Summary of boundary conditions

where u^* is defined in chapter 4.

The model constants are given below.

c_μ	$c_{1\varepsilon}$	$c_{2\varepsilon}$	σ_k	σ_ε	C_D	C_E
0.09	1.44	1.92	1.0	1.3	1.68	1.68

Table 9. Model Constants

5.2 Mathematics of the Equations

Partial differential equations may be categorised as elliptic, parabolic or hyperbolic by considering their form. Typically, elliptic partial differential equations represent an equilibrium problem, parabolic partial differential equations represent a diffusion type problem and hyperbolic differential equations represent a wave

propagation problem. The full Reynolds Averaged Navier-Stokes Equations (5.1-7) do not fall into any of the categories defined above. If certain limiting assumptions are made however it is possible to reduce them to one of these simpler forms. These different forms are usually solved by different numerical methods. That is, a numerical method that works well for solving an elliptic problem will not necessarily work well for solving a parabolic problem and will almost certainly not be the best method for a hyperbolic problem. This fact is crucial to the solution method which is implemented in this research. The present method recognises that different terms in the equations deserve different numerical treatment and so advocates a splitting of the differential operators and solving them in distinct steps using an appropriate method. It is argued that this approach produces more accurate, more robust code.

5.3 Solving the Hydrodynamic Equations

There are two difficulties associated with the solution of the incompressible Navier-Stokes equations which are a recurring theme in the literature. Firstly, the treatment of the advection terms and secondly the pressure-velocity coupling. One of the most well known techniques, the SIMPLE algorithm, has already been mentioned in chapter 2. This algorithm, a traditional finite volume approach, will be shown to be subject to certain limitations particularly for unsteady problems.

In the following the shorthand notation,

$$[\text{Differential Expression}]$$

is used to indicate some kind spatial discretization process (which could be finite difference, finite volume, finite element, etc.). Finite differences are used at all times for the temporal discretisation.

5.3.1 Co-ordinate System and Grid Aspects

The simplest and least computationally demanding solutions are those in cartesian co-ordinates. Of course these solutions are less accurate in the boundary regions where curved boundaries must be approximated by a rectangular 'staircase' of computational cells, McGuirk and Palma (1992), see figure 16. The physical equations may be transformed into another general coordinate system which is chosen to fit the boundary, Viollet, Keramsi and Benque (1981). The code described here uses a cartesian co-ordinate system. It is envisaged that a future development of the present model will involve using a non-orthogonal grid system and this has been borne in mind during the present coding effort. Having chosen a co-ordinate system there now remains the question of the discrete placement of variables on the grid.

This problem has been considered in some detail by Shih et al (1989). Figure 17 shows some alternatives for the placement of variables on a computational grid. Figure 17(a) shows the placement suggested by Harlow and Welch (1965) and later adopted by Patankar and Spalding (1972). Figure 17(b) shows the placement used by Rhie and Chow (1983) and Majumdar, Rodi and Zhu (1992) and figure 17(c) shows the placement used by Pracht (1975), Viollet, Benque, and Goussebaile (1983), Albanese, Grasso and Meola (1984) and Kim and Benson (1992). The advantages and disadvantages of the various grids are summarised in the table below. In particular we note that grid arrangement 17(a) is poor for non-orthogonal grids and also requires an accuracy lowering averaging of velocities when computing the advection terms. The alternative grids however suffer from problems of a pressure-velocity decoupling which manifests itself by producing a chequerboard pressure solution. This will be discussed further in section 5.3.5. The grid arrangement 17(b) (the collocated arrangement) allows for the accurate

treatment for advection and diffusion, it has good properties for non-orthogonal grids, however artificial boundary conditions for the pressure solution may be required, indeed Alfrink (1981) shows how this type of variable arrangement may lead to an inconsistent equation set. The grid arrangement 17(c) has been adopted here because it allows for an accurate treatment for advection and diffusion, it has good properties for non-orthogonal grids, it does not require boundary conditions for pressure, and has easy indexing. The weak possibility of chequerboarding must, however, be dealt with.

Variable arrangement	Advantages	Disadvantages
17(a)	No chequerboarding, no need for pressure boundary conditions.	Poor for non-orthogonal grids, accuracy lower for advection.
17(b)	Good for non-orthogonal grids, useful for computer indexing (ease of development)	Chequer-boarding may occur, Require 'artificial' boundary conditions for pressure.
17(c)	Good for non-orthogonal grids, accurate for advection, ease of computer indexing, no pressure boundary conditions required	Weak possibility of chequer-boarding

Table 10. Summary of grid types: Present model uses 17(c)

5.3.2 Overview of Solution Technique

The method that is advocated here is a fractional step or operator splitting method. The solution proceeds in two steps: the advection-diffusion step and the pressure-velocity coupling step.

Step 1 - Advection-diffusion

$$\frac{u_i^{aux} - u_i^n}{\Delta t} = [- \frac{\partial u_j u_i}{\partial x_j} + \frac{\partial}{\partial x_j} (- \overline{u'_i u'_j})] \quad [5.7]$$

where $[]$ represents a discretisation operator.

Step 1 is discretised in an explicit-implicit manner,

$$\frac{u_i^{aux} - u_i^n}{\Delta t} = [- \frac{\partial u_j u_i}{\partial x_j}]^n + [\frac{\partial}{\partial x_j} (- \overline{u'_i u'_j})]^{aux} \quad [5.8]$$

which may be written as two sub-steps since the advection term is taken explicitly,

$$\frac{\tilde{u}_i - u_i^n}{\Delta t} = [- \frac{\partial u_j u_i}{\partial x_j}]^n \quad [5.9]$$

$$\frac{u_i^{aux} - \tilde{u}_i}{\Delta t} = [\frac{\partial}{\partial x_j} (- \overline{u'_i u'_j})]^{aux} \quad [5.10]$$

This is readily seen by substituting equation 5.9 into 5.10 to return equation 5.8. Thus, the advection terms of the momentum equation are treated explicitly and the diffusion type terms are treated implicitly. The advection terms, equation 5.9, are solved with a third order method of characteristics. A method of characteristics solution appears to be the only way in which accurate unconditional stability can be achieved at low grid resolutions. It will be shown in chapter 6 that at high

courant numbers (greater than 1 or 2) traditional finite volume codes, despite implicit temporal differencing, have tremendous difficulty resolving time dependent problems at low spatial resolutions. Treating the advection terms in this way also means that the matrix that has to be solved for u_i^{aux} is structurally symmetric since the advection terms, which generally must be unsymmetrically differenced (upwinded), have been taken on to the right hand side. This has been noted by Viollet, Benque and Goussebaile (1983). A structurally symmetric matrix is much easier to deal with numerically than an unsymmetrical matrix. The stress terms, equation 5.10, at least for the linear model present no numerical difficulties and are therefore treated with a fully implicit central differencing. The non-linear model introduces some additional complexity and requires special treatment. This is discussed in section 5.3.4.

Step 2 - Pressure-Velocity Coupling

The method which has been adopted here for the pressure-velocity coupling is a projection method which has been used in different forms by a number of researchers including Alfrink and Van Rijn (1982), Viollet, Benque and Goussebaile (1983), Kim and Moin (1985), Peyret (1983), Fortin (1972), Hufenus and Khaletzky (1981) and more recently by Kothe and Mjølness (1992). The method has recently been favourably re-assessed by Perot (1993). The pressure velocity coupling is algorithmically similar to the SMAC method due to Amsden and Harlow (1970).

The velocity field at the auxiliary level does not, in general, satisfy the continuity equation (5.1). This auxiliary velocity field must be corrected, so as to produce a velocity field at the future time level which satisfies continuity.

$$\frac{u_i^{n+1} - u_i^{aux}}{\Delta t} = \left[-\frac{\partial \phi}{\partial x_i} \right]^{n+1} \quad [5.11]$$

where $\phi = p/\rho + 1/3 \overline{u'u'_i} - g_i x_i$. This pressure field at the future time level is computed from the following Poisson equation for the effective pressure at the future time level which may be derived by taking the divergence of equation system 5.11 assuming incompressibility at the future time level.

Pressure Solution

$$\left[\frac{\partial^2 \phi}{\partial x_j \partial x_j} \right]^{n+1} = \frac{1}{\Delta t} \left[\frac{\partial u_j}{\partial x_j} \right]^{aux} \quad [5.12]$$

Equation 5.12 implicitly assumes continuity at the future time level,

$$\left[\frac{\partial u_j}{\partial x_j} \right]^{n+1} = 0 \quad [5.13]$$

This is explained in detail in section 5.3.5. Equation 5.12, which is elliptic in character, is replaced with a standard symmetrical differencing and then solved with a preconditioned conjugate gradient method.

5.3.3 Treatment of the Advection Terms in Step 1

The advection terms are,

$$\frac{\partial u_i}{\partial t} + \frac{\partial u_j u_i}{\partial x_j} = 0 \quad [5.14]$$

which may be written, by virtue of the continuity equation, in a non-conservative form as,

$$\frac{\partial u_i}{\partial t} + u_j \frac{\partial u_i}{\partial x_j} = 0 \quad [5.15]$$

Consider the u velocity only,

$$\frac{\partial u}{\partial t} + u \frac{\partial u}{\partial x} + v \frac{\partial u}{\partial y} + w \frac{\partial u}{\partial z} = 0 \quad [5.16]$$

This partial differential equation may be written as a four ordinary differential equations,

$$\frac{du}{dt} = 0 \quad [5.17]$$

$$\frac{dx}{dt} = u, \quad \frac{dy}{dt} = v, \quad \frac{dz}{dt} = w \quad [5.18]$$

since by the chain rule,

$$\frac{du}{dt} = \frac{\partial u}{\partial t} + \frac{\partial u}{\partial x} \frac{\partial x}{\partial t} + \frac{\partial u}{\partial y} \frac{\partial y}{\partial t} + \frac{\partial u}{\partial z} \frac{\partial z}{\partial t} \quad [5.19]$$

The ordinary differential equation set 5.18 indicates that flow information travels along streamlines or characteristics. Figure 18 shows a typical characteristic curve in one dimension for simplicity. Therefore to compute u at the future time level two steps are involved. For the characteristic curve that passes through the point where we wish to find u:

1. Compute the position of the characteristic foot by solving equations 5.18. In general, this will not be at a grid point.
2. Find the value of u at the characteristic foot by interpolation. This corresponds to the value sought by virtue of equation 5.17.

$$\tilde{u}_{l,m,n} = u_{(x^n, y^n, z^n)} \quad [5.20]$$

The subscripts show that \tilde{u} is being evaluated at grid point l,m,n. In the present code a simple Euler's forward differencing has been used to solve 5.18 for (x^n, y^n, z^n) ,

$$\frac{x^{n+1} - x^n}{\Delta t} = u^n \quad [5.21]$$

$$\frac{y^{n+1} - y^n}{\Delta t} = v^n \quad [5.22]$$

$$\frac{z^{n+1} - z^n}{\Delta t} = w^n \quad [5.23]$$

giving,

$$x^n = x^{n+1} - \Delta t u^n \quad [5.24]$$

$$y^n = y^{n+1} - \Delta t v^n \quad [5.25]$$

$$z^n = z^{n+1} - \Delta t w^n \quad [5.26]$$

where $(x^{n+1}, y^{n+1}, z^{n+1})$ is the co-ordinate position of the point where the u value is required and (x^n, y^n, z^n) is the co-ordinate position of the foot of the characteristic. This method is adequate for problems with smoothly varying velocity fields, Casulli (1990). The advantage of this lagrangian approach is that the backtracking procedure can be extended over many elements allowing simulation at Courant numbers greater than unity. In order to achieve this, accurately, it may be necessary to break the total trajectory from $(x^{n+1}, y^{n+1}, z^{n+1})$ to (x^n, y^n, z^n) into a series of segments each of which is contained within one cell of the computational grid. This backtracking is carried out using the known velocity field (u^n, v^n, w^n) and if a velocity is required at a non grid point then it is interpolated linearly (in space and time).

Having determined the position of the characteristic foot an adequate interpolation is then required to determine $u_{(x^n, y^n, z^n)}$. Various alternatives are possible and will be

discussed further in chapter 6. In the present code a third order polynomial is fitted to the points surrounding the required interpolation point. The coefficients of the polynomial are evaluated by identifying the values of u at surrounding nodes. Close to the boundary the degree of the polynomial is downgraded. Note that this interpolation is required for the three components of velocity.

A stability analysis for this type of scheme is given by Pirroneau (1982). Here the more intuitive reasoning is suggested that upwinding is driven backwards according to the Courant number and thus the point of interpolation is always within the domain of influence. The method is applied to the non-conservative version of the advection terms (equation 5.15) and therefore doubts have been raised over the conservative properties of Lagrangian schemes. Recently, however, Roache (1992) and Garcia-Navarro and Priestley (1994) have independently suggested different ways of constructing characteristic schemes that are conservative and this may render arguments over conservation redundant. The method will be further explained in chapter 6 where its superiority over a traditional finite volume method is demonstrated.

5.3.4 Treatment of the Diffusion Terms in Step 1

The Reynolds stresses are often represented with a Boussinesq eddy viscosity approach. This could be thought of as a Fickian type momentum diffusion model. For that reason, the stress terms are often termed the diffusion terms although, particularly for the non-linear model, they are not the simple diffusion envisaged by Fick (1855). This type of partial differential equation is better treated with a different numerical method from the advection terms since there is no physical or numerical reason to treat this term in an unsymmetrical fashion. As mentioned in chapter 4 the Boussinesq eddy viscosity model is used for many engineering problems despite growing concern over its reliability. One of the main reasons for

its enduring success is that it is numerically well behaved. The discretisation of the stress step is,

$$\frac{u_i^{aux} - \tilde{u}_i}{\Delta t} = \left[\frac{\partial}{\partial x_j} (-\overline{u'_i u'_j}) \right] \quad [5.27]$$

In the present research two stress-strain relationships have been tried. Ignoring the isotropic part $\frac{2}{3}k$ which may be absorbed into the effective pressure variable, the $-\overline{u'_i u'_j}^{deviatoric}$ term may be written,

$$-\overline{u'_i u'_j}^{deviatoric} = \nu_t 2 D_{ij}$$

or

$$-\overline{u'_i u'_j}^{deviatoric} = \nu_t 2 D_{ij} + 4C_D c_\mu \nu_t T (D_{im} D_{mj} - D_{mn} D_{mn} \delta_{ij}/3) + 4C_E c_\mu \nu_t T (\dot{D}_{ij} - \dot{D}_{mm} \delta_{ij}/3)$$

When these relationships are substituted into equation 5.27 the following general expression is produced,

$$\frac{u_i^{aux} - \tilde{u}_i}{\Delta t} = \left[\frac{\partial}{\partial x_j} (\nu_t \frac{\partial u_i}{\partial x_j}) \right] + [S] \quad [5.28]$$

where the stress expression is separated into momentum diffusion like terms and other terms which will be termed source terms, S. Note that for a constant eddy viscosity model, when ν_t does not vary in space, the source term is zero by virtue of continuity.

Relationship for $-\overline{u'_i u'_j}$ deviatoric.	S in diffusion equation
Linear	$\frac{\partial}{\partial x_j} (v_i \frac{\partial u_j}{\partial x_i})$
Non-Linear	$\frac{\partial}{\partial x_j} (v_i \frac{\partial u_j}{\partial x_i} + 4C_D c_\mu v_i T (D_{im} D_{mj} - D_{mn} D_{mn} \delta_{ij}/3) + 4C_E c_\mu v_i T (\dot{D}_{ij} - \dot{D}_{mn} \delta_{ij}/3))$

Table 11. Source terms due to stress terms: $T = \frac{k}{\varepsilon}$

These source terms introduce some difficulties into the numerical method of solution which will be addressed shortly. An implicit treatment of this step is recommended to avoid the stability restriction,

$$\frac{u_i^{aux} - \tilde{u}_i}{\Delta t} = [\frac{\partial}{\partial x_j} (v_i \frac{\partial u_j}{\partial x_i})]^{aux} + [S]^{aux} \quad [5.29]$$

Spatially discretising the diffusion terms on a uniform grid, figure 19, and for the moment considering only the u_1 velocity, denoted by u ,

$$[\frac{\partial}{\partial x_j} (v_i \frac{\partial u}{\partial x_j})]^{aux} = \quad [5.30]$$

$$\begin{aligned} & \frac{1}{\Delta x} (v_i^n (\frac{u_{l+1,m,n}^{aux} - u_{l,m,n}^{aux}}{\Delta x}) - v_i^n (\frac{u_{l,m,n}^{aux} - u_{l-1,m,n}^{aux}}{\Delta x})) \\ & + \frac{1}{\Delta y} (v_i^n (\frac{u_{l,m+1,n}^{aux} - u_{l,m,n}^{aux}}{\Delta y}) - v_i^n (\frac{u_{l,m,n}^{aux} - u_{l,m-1,n}^{aux}}{\Delta y})) \\ & + \frac{1}{\Delta z} (v_i^n (\frac{u_{l,m,n+1}^{aux} - u_{l,m,n}^{aux}}{\Delta z}) - v_i^n (\frac{u_{l,m,n}^{aux} - u_{l,m,n-1}^{aux}}{\Delta z})) \end{aligned}$$

where l,m,n represent the grid point indices. Substituting this into equation 5.29 and gathering all terms at the future auxiliary level,

$$(1 + a_{l+1} + a_{l-1} + b_{m+1} + b_{m-1} + c_{n+1} + c_{n-1}) u_{l,m,n}^{aux} \quad [5.31]$$

$$\begin{aligned}
& -a_{l+1}u_{l+1,m,n}^{aux} - a_{l-1}u_{l-1,m,n}^{aux} \\
& -b_{m+1}u_{l,m+1,n}^{aux} - b_{m-1}u_{l,m-1,n}^{aux} \\
& -c_{n+1}u_{l,m,n+1}^{aux} - c_{n-1}u_{l,m,n-1}^{aux} = \tilde{u}_{l,m,n} + [S]^{aux}
\end{aligned}$$

where,

$$\begin{aligned}
a_{l+1} &= \frac{v_l^n \Delta t}{\Delta x^2} & a_{l-1} &= \frac{v_l^n \Delta t}{\Delta x^2} \\
b_{m+1} &= \frac{v_l^n \Delta t}{\Delta y^2} & b_{m-1} &= \frac{v_l^n \Delta t}{\Delta y^2} \\
c_{n+1} &= \frac{v_l^n \Delta t}{\Delta z^2} & c_{n-1} &= \frac{v_l^n \Delta t}{\Delta z^2}
\end{aligned}$$

In the above expression v_l is evaluated at appropriate points using the known value at the present time. Unfortunately, this implicit treatment links all values at the future time level in a matrix which must be solved to furnish the answer. However, because the advection terms have been dealt with explicitly and are now part of the right hand side the matrix is sparse, symmetric and positive definite. This considerably improves the chances of obtaining a solution. There are basically two alternatives for solving this equation: direct or iterative methods. A direct method would mean solving the simultaneous equations by Gaussian elimination however standard Gaussian elimination would be highly inefficient since most of the matrix contains zeros.

Therefore, a point iterative method has been implemented here because:

1. Iteration is necessary because of the non-linearity
2. Iterative methods take complete account of the sparsity pattern

3. Point iterative methods are more efficient for irregular regions
4. The method is relatively easy to extend to boundary fitted co-ordinates

The method employed to solve is a straightforward Gauss-Seidel relaxation method. This is represented below with the superscript $k+1$ meaning the present iteration and the superscript k meaning the previous iteration.

$$\begin{aligned}
 (u_{l,m,n}^{aux})^{k+1} = & \frac{1}{D} [\tilde{u}_{l,m,n} + [S^{aux}]^k \\
 & + a_{l+1}(u_{l+1,m,n}^{aux})^k + a_{l-1}(u_{l-1,m,n}^{aux})^{k+1} \\
 & + b_{m+1}(u_{l,m+1,n}^{aux})^k + b_{m-1}(u_{l,m-1,n}^{aux})^{k+1} \\
 & + c_{n+1}(u_{l,m,n+1}^{aux})^k + c_{n-1}(u_{l,m,n-1}^{aux})^{k+1}]
 \end{aligned} \tag{5.32}$$

where,

$$D = 1 + a_{l+1} + a_{l-1} + b_{m+1} + b_{m-1} + c_{n+1} + c_{n-1}$$

Using this formula repeated sweeps through the computational mesh are carried out until convergence is achieved. Convergence is assumed when the normalised residual,

$$\text{Normalised Residual} = \frac{\max |u^{k+1} - u^k|_{\text{Domain}}}{u_o}$$

falls below some stopping criteria, where u_o is some typical value. A typical convergence curve is depicted in figure 20. Hageman and Young (1981) suggest that this is an acceptable iterative method for this type of problem because,

1. For many cases a stopping criteria of 10^{-4} or 10^{-5} is adequate for reasonable accuracy.

2. If the dependent variable is not changing rapidly with time then the result from the previous time-step is a good initial condition for starting iteration.
3. The convergence rate is a function of the chosen timestep, Δt , so this becomes an adjustable parameter to aid convergence.

A relaxation parameter has been introduced,

$$(u_i^{aux})_{actual}^{k+1} = (u_i^{aux})^k + \Omega \{ (u_i^{aux})^{k+1} - (u_i^{aux})^k \} \quad [5.33]$$

where,

$$0.0 < \Omega < 1.0$$

$$1.0 < \Omega < 2.0$$

Ω may be set to values less than one when convergence difficulties are encountered.

The source terms were estimated with the most recent estimate of the auxiliary velocity field at the previous iteration. The complete expression for the Reynolds stresses according to the non-linear model are given in appendix B after Speziale and Ngo (1988) in which use was made of the continuity equation to simplify them. The Oldroyd derivatives are numerically troublesome. Some insight into their behaviour may be obtained, however, by noting that they contain advective terms describing the advection with the mean velocity of the mean strain rate tensor. This means that the Reynolds stresses depend not only on the strain at the point in the fluid where the stress is being evaluated but also on the strain upstream of this point. The Oldroyd derivative terms contain the expression,

$$\frac{D(D_{ij})}{Dt} = \frac{\partial(D_{ij})}{\partial t} + \frac{\partial u_l(D_{ij})}{\partial x_l}$$

which describes advection of the mean strain rate tensor, D_{ij} . Where these terms have been retained in numerical models the treatment of these terms have all been attempted with symmetrical numerical discretisations of greater or lesser order, Speziale and Ngo (1988), and Benocci and Skovgaard (1988). Symmetrical discretisations are not appropriate for advection terms and some form of upwinding should be employed. In the present work a simple first order upwinding was employed in the discretisation of these terms which is physically more correct. Of course a higher order treatment would be better (e.g. third order) but this would involve a larger computational molecule and therefore was not adopted here.

5.3.5 Treatment of the Pressure Terms and Continuity in Step 2

The basic principle of this step was described in an earlier section. Here a more detailed description of this step is presented. Although described in two dimensions for ease of notation the same principles have been used for the three dimensional implementation.

The auxiliary velocity field obtained from the advection and diffusion steps does not satisfy continuity. We still have to apply the pressure gradient correction,

$$\frac{u_i^{n+1} - u_i^{aux}}{\Delta t} = \left[-\frac{\partial \phi}{\partial x_i} \right]^{n+1} \quad [5.34]$$

in order that continuity at the future time level is satisfied,

$$\left[\frac{\partial u_j}{\partial x_j} \right]^{n+1} = 0 \quad [5.35]$$

In two dimensions (see figure 21) the discrete approximation for continuity at the future time level is given by,

$$\left[\frac{\partial u_j}{\partial x_j} \right]_e^{n+1} = \frac{1}{\Delta x} \left[\frac{1}{2} (u_\beta^{n+1} + u_\delta^{n+1}) - \frac{1}{2} (u_\alpha^{n+1} + u_\gamma^{n+1}) \right] \quad [5.36]$$

$$+ \frac{1}{\Delta z} \left[\frac{1}{2} (w_\alpha^{n+1} + w_\beta^{n+1}) - \frac{1}{2} (w_\gamma^{n+1} + w_\delta^{n+1}) \right]$$

Now,

$$u_\beta^{n+1} = u_\beta^{aux} - \frac{\Delta t}{\Delta x} \left(\frac{1}{2} (\phi_c^{n+1} + \phi_f^{n+1}) - \frac{1}{2} (\phi_b^{n+1} + \phi_e^{n+1}) \right)$$

$$u_\delta^{n+1} = u_\delta^{aux} - \frac{\Delta t}{\Delta x} \left(\frac{1}{2} (\phi_f^{n+1} + \phi_i^{n+1}) - \frac{1}{2} (\phi_e^{n+1} + \phi_h^{n+1}) \right)$$

$$u_\alpha^{n+1} = u_\alpha^{aux} - \frac{\Delta t}{\Delta x} \left(\frac{1}{2} (\phi_b^{n+1} + \phi_e^{n+1}) - \frac{1}{2} (\phi_a^{n+1} + \phi_d^{n+1}) \right)$$

$$u_\gamma^{n+1} = u_\gamma^{aux} - \frac{\Delta t}{\Delta x} \left(\frac{1}{2} (\phi_e^{n+1} + \phi_h^{n+1}) - \frac{1}{2} (\phi_d^{n+1} + \phi_g^{n+1}) \right)$$

and,

$$w_\beta^{n+1} = w_\beta^{aux} - \frac{\Delta t}{\Delta z} \left(\frac{1}{2} (\phi_b^{n+1} + \phi_c^{n+1}) - \frac{1}{2} (\phi_e^{n+1} + \phi_f^{n+1}) \right)$$

$$w_\delta^{n+1} = w_\delta^{aux} - \frac{\Delta t}{\Delta z} \left(\frac{1}{2} (\phi_e^{n+1} + \phi_f^{n+1}) - \frac{1}{2} (\phi_h^{n+1} + \phi_i^{n+1}) \right)$$

$$w_\alpha^{n+1} = w_\alpha^{aux} - \frac{\Delta t}{\Delta z} \left(\frac{1}{2} (\phi_a^{n+1} + \phi_b^{n+1}) - \frac{1}{2} (\phi_d^{n+1} + \phi_e^{n+1}) \right)$$

$$w_\gamma^{n+1} = w_\gamma^{aux} - \frac{\Delta t}{\Delta z} \left(\frac{1}{2} (\phi_d^{n+1} + \phi_e^{n+1}) - \frac{1}{2} (\phi_g^{n+1} + \phi_h^{n+1}) \right)$$

Substituting the above expressions into the discrete continuity equation and re-arranging gives a discrete Poisson equation for pressure at the future time level,

$$k_1 \phi_a^{n+1} + k_2 \phi_b^{n+1} + k_1 \phi_c^{n+1} - k_2 \phi_d^{n+1} - \quad [5.37]$$

$$4k_1 \phi_e^{n+1} - k_2 \phi_f^{n+1} + k_1 \phi_g^{n+1} + k_2 \phi_h^{n+1}$$

$$+ k_1 \phi_i^{n+1} = \frac{1}{\Delta t} D_e^{aux}$$

where,

$$k_1 = \frac{1}{4\Delta x^2} + \frac{1}{4\Delta z^2} \quad k_2 = \frac{1}{2\Delta z^2} - \frac{1}{2\Delta x^2}$$

The above represents a nine point discrete operator approximation to the Poisson equation sometimes called the diagonal square discretization. In fact, what has been done here is the discrete analog of the pressure-velocity coupling described in differential terms in section 5.3.2. Here the nine point discrete operator approximation shall be termed $\Delta_2\phi^{n+1}$. The alternative (and more commonly used) five point operator will be denoted $\Delta_1\phi^{n+1}$,

$$\Delta_1\phi^{n+1} = \frac{1}{\Delta z^2}\phi_b^{n+1} + \frac{1}{\Delta x^2}\phi_d^{n+1} + \quad [5.38]$$

$$\frac{1}{\Delta x^2}\phi_f^{n+1} + \frac{1}{\Delta z^2}\phi_h^{n+1}$$

$$- \left(\frac{2}{\Delta x^2} + \frac{2}{\Delta z^2} \right) \phi_e^{n+1}$$

Since the Δ_2 operator is derived by rigorously satisfying the continuity equation at the future time level it follows that using this operator would be strictly mass conserving in the finite difference sense. Indeed this is the case and the Δ_2 operator is preferred for this reason. However the Δ_2 operator has a problem associated with it in that for certain cases ($\Delta x = \Delta z$) the nine point operator reduces to the five point diagonal square shown in figure 22, The five point diagonal square operator has no direct coupling between adjacent pressure cells (e.g e and f). This can lead to an uncoupling and the pressure solution developing in to two distinct solutions when Neumann boundary conditions like,

$$\frac{\partial \phi}{\partial n} = 0$$

are used for the pressure, Viollet, Benque and Goussebaille (1983). There is no possibility of this 'chequerboarding' occurring if the usual Δ_1 discrete Poisson operator is used since a direct coupling exists between adjacent pressure cells, see figure 22. However the Δ_1 operator does not result from a consideration of conservation of mass. We therefore choose to approximate the Poisson operator by a weighted average of the Δ_1 and the Δ_2 operators with the weighting factor chosen so that if there is a danger of pressure uncoupling occurring then we weight the Poisson approximation towards the Δ_1 operator.

$$\bar{\Delta}\phi = \lambda\Delta_1\phi + (1-\lambda)\Delta_2\phi \quad [5.39]$$

If λ is equal to 0 then the Poisson approximation is equal to the Δ_2 operator and if λ is equal to 1 then the Δ_1 operator results. In practice λ is set as close to 0 as is possible without inducing chequerboarding. Generally, it cannot be predicted a priori whether or not uncoupling may occur and therefore the weighting factor must be determined by numerical trials. The use of the λ factor would be more significant if a boundary fitted grid transformation is used. This λ -approach has also been advocated by Viollet, Benque and Goussebaille (1983) and may be seen to be in the same spirit as the momentum interpolation of Rhie and Chow (1983) commonly used in collocated grid finite volume approaches.

The resulting pressure matrix is symmetric and positive semi-definite and is therefore efficiently solved by a preconditioned conjugate gradient method. If the pressure equation is represented thus,

$$A\vec{x} = b$$

then the conjugate gradient algorithm is,

- Let $k=0$, $r_0 = b - Ax_0$ and $p_0 = r_0$

- For $k=0,1,2,3,\dots$ until convergence. Compute the vectors x_k , r_k and p_k from

$$x_{k+1} = x_k + \alpha_k p_k \text{ where } \alpha_k = r_k^T r_k / p_k^T A p_k$$

$$r_{k+1} = r_k - \alpha_k A p_k$$

$$p_{k+1} = r_{k+1} + \beta_k p_k \text{ where } \beta_k = r_{k+1}^T r_{k+1} / r_k^T r_k$$

This is a standard numerical algorithm and may be found in most reference texts on numerical methods, e.g. Mitchell and Griffiths (1980). A relatively simple preconditioning has been adopted, namely preconditioning by diagonal scaling. Therefore the actual system solved is,

$$M^{-1} A \bar{x} = M^{-1} b$$

where M^{-1} is the preconditioning matrix and here is the diagonal of A . Other preconditionings are possible and may in certain cases prove more efficient. In particular, Kershaw (1978), demonstrates the usefulness of an Incomplete Cholesky Preconditioning and suggests it results in a 200 times faster convergence than a block iterative method. However concerns over the stability of the Incomplete Cholesky Preconditioning have encouraged the simpler and more robust diagonal scaling to be used here. The convergence is monitored by examining the residual,

$$Res2 = r_{k+1}^T r_{k+1}$$

and the maximum normalised change in pressure at each iteration,

$$Pdel = \max\left(\frac{\alpha_k p_k}{x_k}\right)$$

These are both plotted in figure 23. Interestingly convergence is often tested by checking whether $\text{Res2} < \text{tol}$, where tol is some prescribed tolerance e.g. 10^{-8} or some other form, Larabi and De Smedt (1994). As can be seen from figure 23 this may not be the best parameter to monitor since the Res2 convergence curve is not monotonic exhibiting a rise after decreasing steadily, at least for this type of preconditioning. Convergence can only be concluded once this rise has been passed. This characteristic of the curve has also been observed by Kightley and Jones (1985). It can be noted from figure 23 that until this rise has been passed Pdel will not decrease monotonically. Therefore a more suitable convergence criteria would be $\text{Pdel} < \text{tol}$. This type of convergence criteria is thus recommended for preconditioned conjugate gradient solvers.

The velocity correction for pressure (i.e. application of equation 5.11) completes the calculation of the hydrodynamic variables.

The same analysis may be carried out for the three dimensional case however the working becomes rather tedious and so this has not been detailed here. The logic is identical however.

5.4 Solving the Turbulence Equations

In solving the turbulence equations we note that they are of a similar form to the momentum equations, i.e. they contain advection, diffusion and other differential operators. For the advection and diffusion parts we use the same methods as used for the momentum equations. For the source and sink terms a more appropriate treatment is required.

5.4.1 Treatment of Advection and Diffusion

The method used is identical to that used in solving the momentum equations. An exception is adopted following the suggestion Leschziner and Rodi (1981) who point out that the accuracy with which we treat the advection terms in the turbulence equations is not generally crucial, since the source terms are usually more important. A spurious negative value for the turbulence variables due to advection error is strictly unacceptable, leading to instability. This may occur with the cubic interpolation therefore the lower order but strictly bounded linear interpolation for the advection of the turbulence variables is adopted.

5.4.2 Treatment of Turbulence Source and Sink Terms

Source terms in a differential transport equation represent a mechanism that increases the amount of a dependent variable whereas sink terms represent a mechanism that decreases the amount of a dependent variable. The source and sink terms in the turbulence equations are,

$$\frac{\partial k}{\partial t} = \underset{\text{Source}}{Prod} - \underset{\text{Sink}}{\varepsilon} \quad [5.40]$$

Source and sink terms for Turbulence Kinetic Energy

$$\frac{\partial \varepsilon}{\partial t} = c_{1\varepsilon} \frac{\varepsilon}{k} \underset{\text{Source-Sink}}{Prod} - c_{2\varepsilon} \frac{\varepsilon}{k} \varepsilon \quad [5.41]$$

Source and sink terms for Turbulence Kinetic Energy Dissipation Rate

where

$$Prod = (-\overline{u'_i u'_j}) \frac{\partial u_i}{\partial x_j}$$

and $-\overline{u'u'_j}$ is given by the expressions 5.3 or 5.5. Numerically, these terms are treated between the advection and diffusion stages. The sink terms, i.e the negative ones, can be troublesome. Consider the following simpler equation,

$$\frac{\partial T}{\partial t} = -aT$$

where a is positive. If this equation is discretised explicitly,

$$\frac{T^{n+1} - T^n}{\Delta t} = -aT^n$$

Re-arranging this gives,

$$T^{n+1} = T^n(1 - \Delta ta)$$

Taking T^0 as the initial value of T the future values are given by,

$$T^1 = T^0(1 - \Delta ta)$$

$$T^2 = T^1(1 - \Delta ta) = T^0(1 - \Delta ta)^2$$

Giving for the general case,

$$T^N = T^0(1 - a\Delta t)^N$$

The analytical solution is,

$$T(t) = T^0 e^{-at}$$

i.e. an exponential decay. The numerical solution only behaves like the analytical solution when $a\Delta t$ is small ($\ll 1$) and in fact becomes unstable if $a\Delta t > 2$. This stability condition has led to this type of equation being termed 'stiff'. To achieve unconditional stability, implicit formulations are generally recommended for 'stiff' equations. Consider an implicit formulation,

$$\frac{T^{n+1} - T^n}{\Delta t} = -aT^{n+1}$$

Re-arranging and taking T^0 as the initial condition means that,

$$T^1 = \frac{T^0}{(1 + \Delta t a)}$$

$$T^2 = \frac{T^1}{(1 + \Delta t a)} = \frac{T^0}{(1 + \Delta t a)^2}$$

Giving for the general case,

$$T^N = \frac{T^0}{(1 + \Delta t a)^N}$$

Note that with this formulation instability cannot occur since the denominator is always greater than 1 so that an exponential decay occurs as in the analytical solution. The same problem does not occur for source terms and they may be represented explicitly. So the turbulent source terms have been treated explicitly and the sink terms implicitly,

$$\frac{k^{n+1} - k^n}{\Delta t} = [Prod]^n - \left[\frac{\varepsilon}{k}\right]^n k^{n+1} \quad [5.42]$$

$$\frac{\varepsilon^{n+1} - \varepsilon^n}{\Delta t} = c_{1\varepsilon} \left[\frac{\varepsilon}{k} Prod\right]^n - c_{2\varepsilon} \left[\frac{\varepsilon}{k}\right]^n \varepsilon^{n+1} \quad [5.43]$$

These equations may be re-arranged to give,

$$k^{n+1} = \left(\frac{1}{1 + \Delta t \left[\frac{\varepsilon}{k}\right]^n}\right)(k^n + \Delta t [Prod]^n) \quad [5.44]$$

$$\varepsilon^{n+1} = \left(\frac{1}{1 + \Delta t c_{2\varepsilon} \left[\frac{\varepsilon}{k}\right]^n}\right)(\varepsilon^n + \Delta t [c_{1\varepsilon} \frac{\varepsilon}{k} Prod]^n) \quad [5.45]$$

Notice that k and ε can never become negative (which is a physical requirement) since the denominator is always positive. This treatment of the turbulent sink terms is also recommended by Amsden and Harlow (1968), Lemos (1992) and Lee (1992).

5.5 Boundary Conditions

The boundary conditions for the Navier-Stokes equations are very important and have been the source of some controversy in the literature, Gresho and Sani (1987). The boundary conditions are summarised in table 8. Velocity boundary conditions may be specified directly where the velocity is known or indirectly by specifying the velocity gradient which is related to the shear stress at the boundary. This is conveniently done during the diffusion step by setting the appropriate coefficient ($a_{l+1}, a_{l-1}, b_{m+1}, b_{m-1}, c_{n+1}, c_{n-1}$) to zero and introducing the known bed stress value on the right hand side.

The operator splitting, however, means that boundary conditions are required for the intermediate variables at the auxiliary level. The relationship of these boundary conditions to the boundary conditions at the $n+1$ level must be addressed. Equation 5.11 advances the auxiliary velocity field, u_i^{aux} to the final velocity field, u_i^{n+1} . It is possible therefore at boundaries to use this relation working backwards to determine u_i^{aux} in terms of u_i^{n+1} , Perot (1993),

$$u_i^{aux} = u_i^{n+1} + \Delta t \left[\frac{\partial \phi}{\partial x_i} \right]^{n+1} \quad [5.46]$$

The required pressure gradient may be derived from theoretical considerations, Alfrink (1981). However investigators have found from many numerical experiments that for the component normal to the boundary the use of a homogeneous pressure gradient boundary condition is also often acceptable, Alfrink (1981), Hufenus and Khaletsky (1984). This may be thought of as a computational boundary condition rather than a physical one. The use of a homogeneous pressure boundary condition makes computational if not physical sense since if the normal velocity is specified at a boundary then a pressure boundary is not actually required, Patankar (1980). Therefore the neutral

homogeneous boundary condition is acceptable, Patankar (1980). In this way boundary conditions may be derived that satisfy the pressure solution and the velocity solution. So it is assumed, arbitrarily, that the normal velocity boundary conditions for the auxiliary field to be equal to the final normal velocity,

$$u_n^{aux} = u_n^{n+1}$$

giving, from 5.11, a homogeneous pressure boundary condition for the pressure solution,

$$\frac{\partial \phi^{n+1}}{\partial n} = 0$$

Equation 5.11 suggests that for the tangential velocity,

$$u_\tau^{n+1} - u_\tau^{aux} = \Delta t \left[-\frac{\partial \phi}{\partial x_\tau} \right]^{n+1} \quad [5.47]$$

Differentiating to define in terms of velocity gradients,

$$\frac{\partial u_\tau^{n+1}}{\partial x_n} - \frac{\partial u_\tau^{aux}}{\partial x_n} = \Delta t \frac{\partial}{\partial x_n} \left[-\frac{\partial \phi}{\partial x_\tau} \right]^{n+1} = \Delta t \frac{\partial}{\partial x_\tau} \left[-\frac{\partial \phi}{\partial x_n} \right]^{n+1} = 0 \quad [5.48]$$

assuming the normal homogenous pressure boundary condition. So that a velocity gradient (or stress) boundary condition may be applied at the auxiliary level equivalently as for the whole step, Baron, Benque and Coefe (1981).

Additionally, at one point in the solution domain a reference pressure must be specified.

The turbulence boundary conditions are simpler than the hydrodynamic. Either Dirichlet or Neumann conditions are applied during the diffusion step.

5.6 Accuracy

The way the numerical method is formulated is of first order temporal accuracy overall although second and higher order methods can be derived, Schutt (1989) or Perot (1993). First order temporal accuracy is apparently acceptable for hydraulic engineering problems, there being many examples in the literature of its use, McGuirk and Islam (1987), Benque, Cunge, Feuillet, Hauguel and Holly (1982) or Falconer (1985). In the present application the method has been used with boundary conditions fixed in time and the solution is thus advanced to a steady state. The transient solution is therefore of no interest here and the temporal accuracy is not important. It is interesting to note a serious misunderstanding in designing numerical models based on theoretical accuracy. It is important to make sure the numerical method produces physically realistic solutions which are also accurate. Trying to achieve a certain order of theoretical accuracy often leads to unphysical solutions. This has been realised to our cost in the past. Leonard and Niknafs (1991) show how a spatially fourth order accurate scheme results in a worse solution than a third order scheme for an advection problem. Likewise, for depth averaged two dimensional models it is probably more crucial to avoid the 'A.D.I. Effect' than to achieve (in theory) higher order temporal accuracy to improve solutions at large timesteps, Wilders, van Stijn, Stelling and Fokkema (1988).

Defining when the steady-state solution has been achieved is a rather subjective matter, Roache (1972). A normalised residual was defined for a variable η ,

$$\text{Normalised Residual} = \frac{\max |\eta^{n+1} - \eta^n|_{\text{Domain}}}{\eta_o}$$

where η_o is a typical value of the variable. A prudent practice is always to monitor convergence curves of which examples are given in figure 24. Convergence can be

concluded if this normalised residual becomes less than a prescribed tolerance which, rather worryingly, ranges in the literature from 10^{-3} to 10^{-8} . In this study it was taken to be 10^{-5} for the two dimensional applications and 10^{-3} for the three dimensional applications which was the best that could be achieved within a reasonable computer time. For all runs the grid was constructed in a trial and error fashion. Thus, the grid refinement and the placement of boundaries was systematically changed to check that the grid was adequate. Fortunately, some guidance was available from previous studies. Where a similar problem had been tackled by other researchers it was checked that the grid used in the present study was of a comparable refinement to that used in the previous studies. It will be demonstrated in chapter 6, however, that the present numerical treatment of the advection terms results in very low numerical errors in comparison to other schemes particularly for low grid resolutions which adds further confidence to the numerical results.

5.7 *Stability*

As explained earlier the present numerical method is not restricted on grounds of formal stability to a certain time step value. This is demonstrated in chapter 6 with reference to a simple one dimensional analogue. However, for accuracy in the complete Reynolds Averaged Navier-Stokes applications it was decided to set the timestep to the value suggested by the courant condition,

$$\Delta t < \left[\frac{u}{\Delta x} + \frac{w}{\Delta z} \right]^{-1} \text{ Two Dimensional} \quad [5.49]$$

or

$$\Delta t < \left[\frac{u}{\Delta x} + \frac{v}{\Delta y} + \frac{w}{\Delta z} \right]^{-1} \text{ Three Dimensional} \quad [5.50]$$

because of the non-linearity of the problems. Hauguel (1987) suggests that for the accurate treatment of strong non-linearities courant numbers close to unity are preferred. The treatment of the non-linear model source terms may require that a limit is imposed on the timestep since advective terms are involved. Further work is required, however, to confirm this.

5.8 Computer Aspects

At the outset of this research project, an IBM 3090-VF mainframe was available and all development and computer runs took place on this machine. Runs were carried out as CPU limited batch jobs which meant that in some cases it was necessary to run the job to the CPU limit and then take the results of this run as initial conditions to a further run. For the three dimensional model this process had to be repeated several times. This tactic was useful for the two dimensional runs also. In particular, when a problem was approached initially it could be run with the linear model and a more robust linear interpolation for the advective terms. The results of this run although of low accuracy served as smooth initial conditions for the future high accuracy runs.

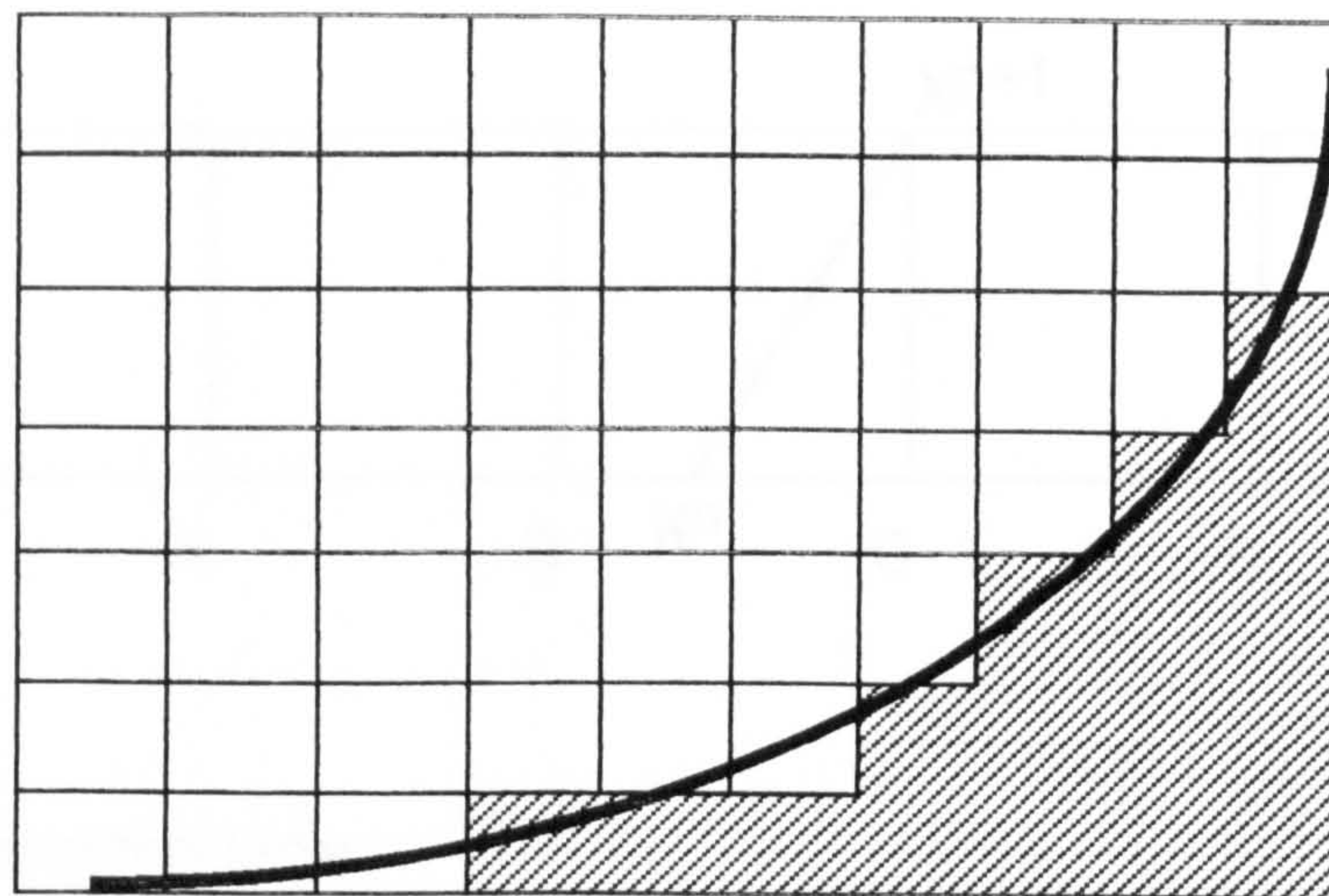


Figure 16. The 'staircase' approximation

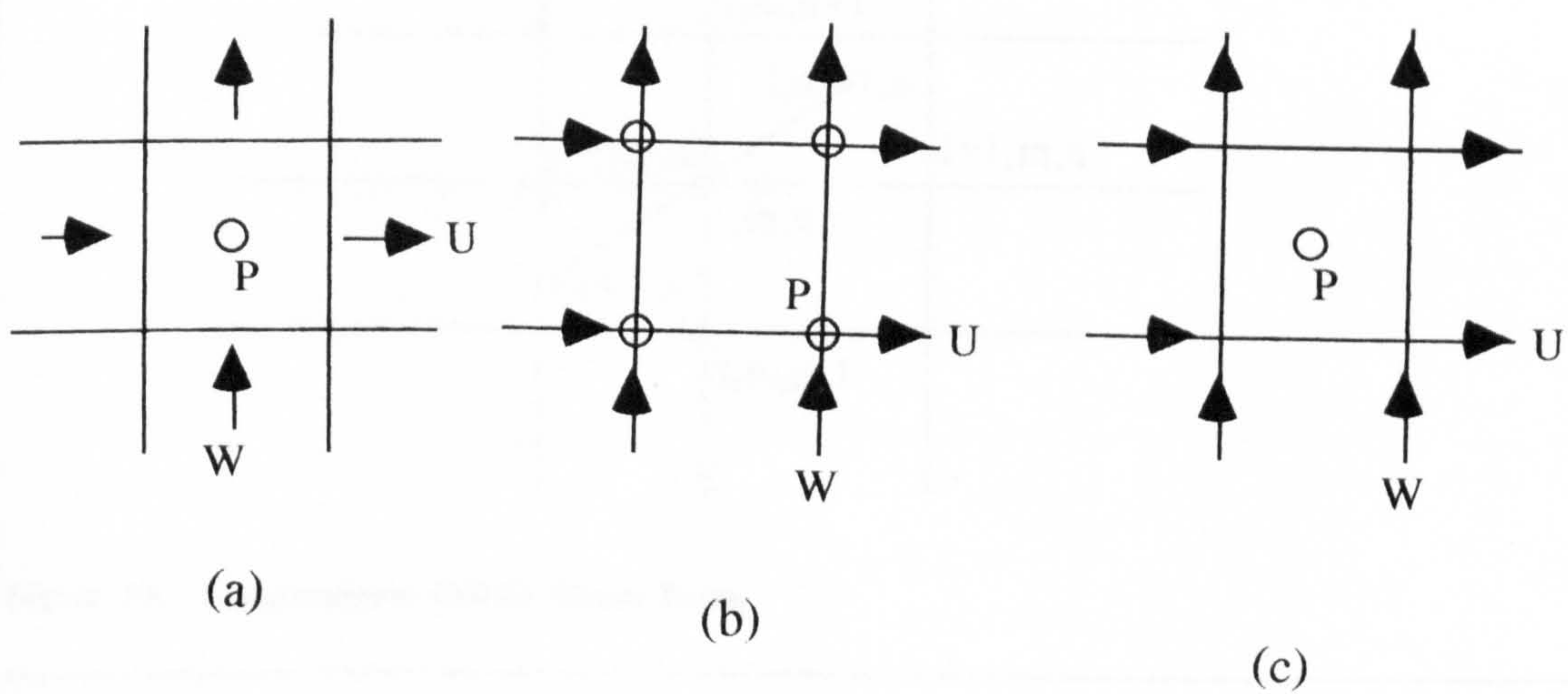


Figure 17. Alternative grids and variable placement

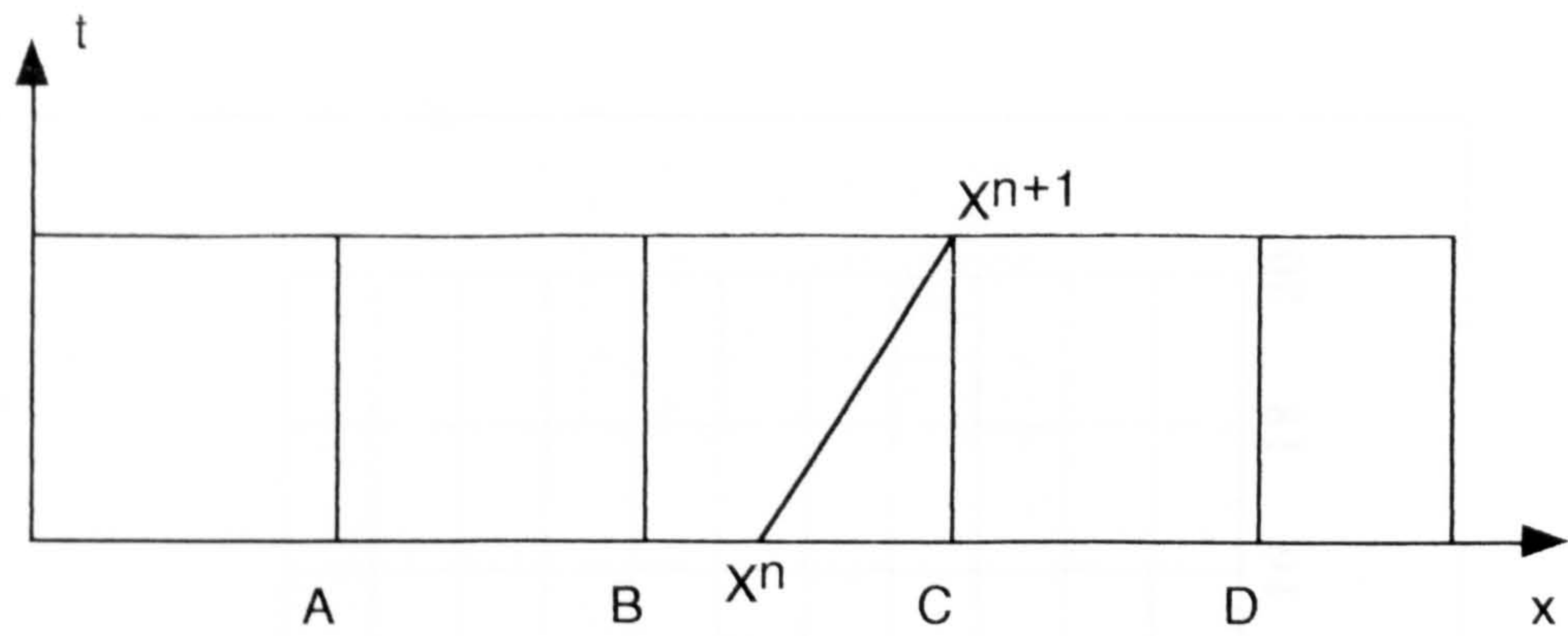


Figure 18. Characteristic Curves

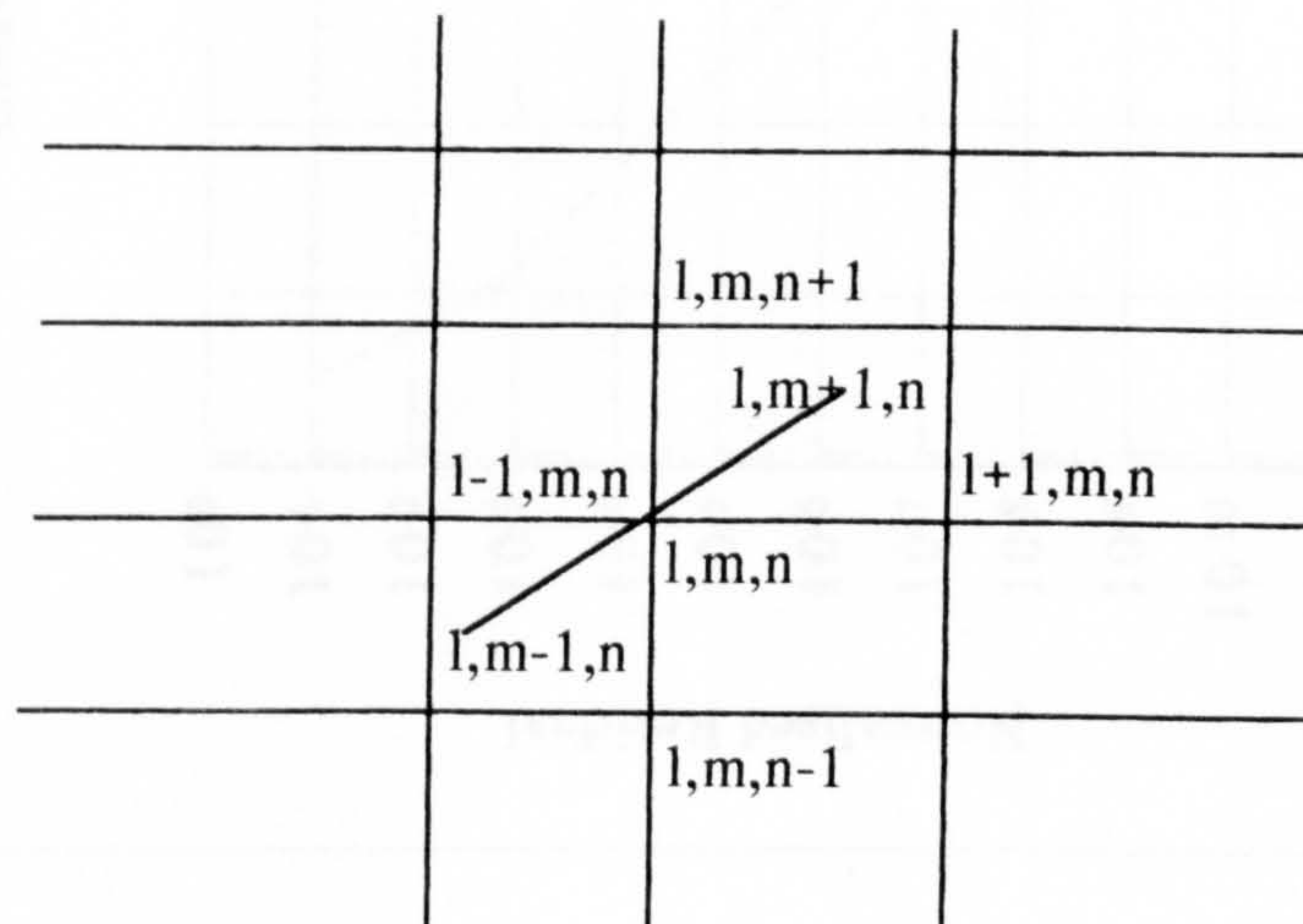


Figure 19. Computational Cell for Stress Terms

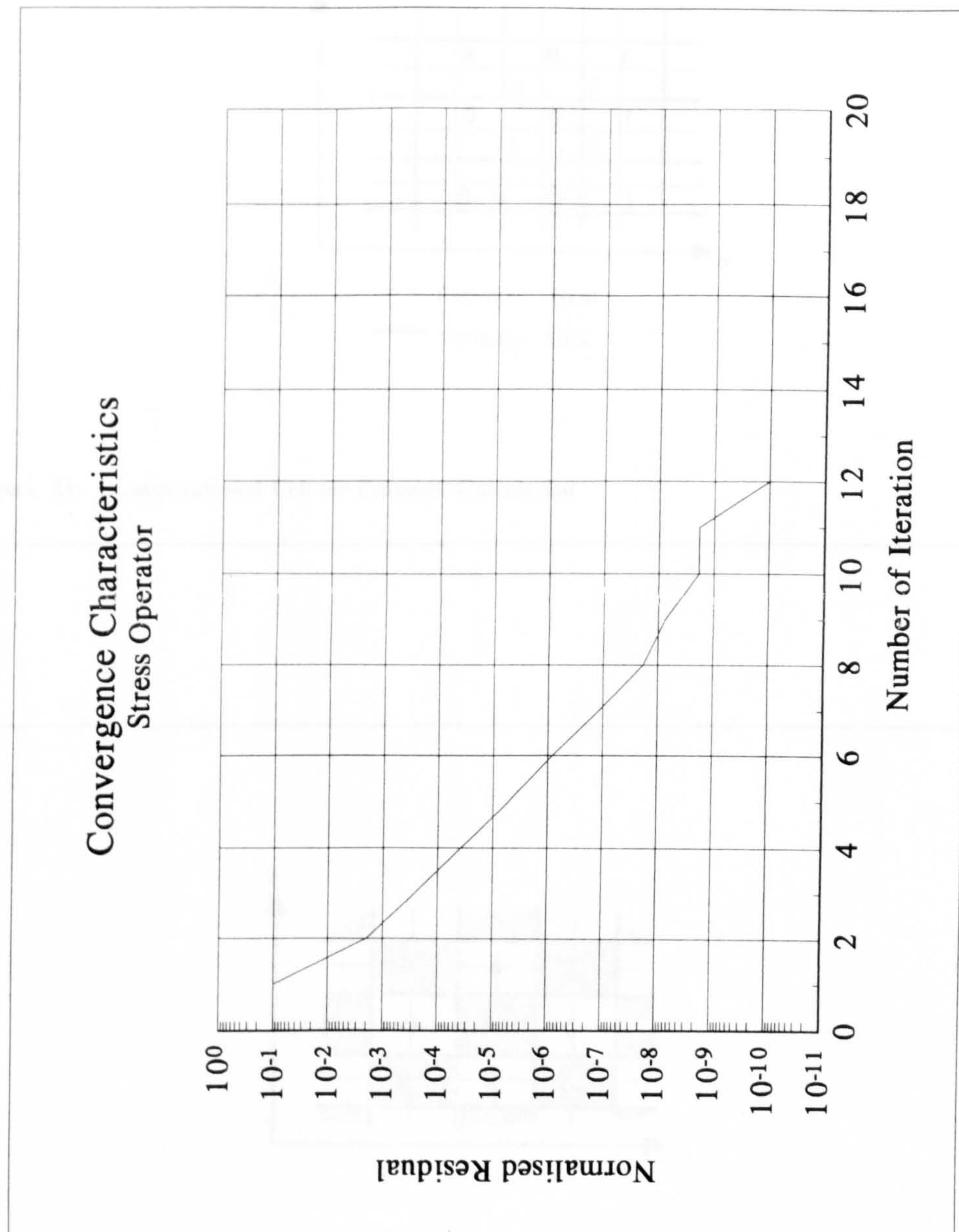


Figure 20. Convergence Curve for Gauss-Seidel Operator for Stress

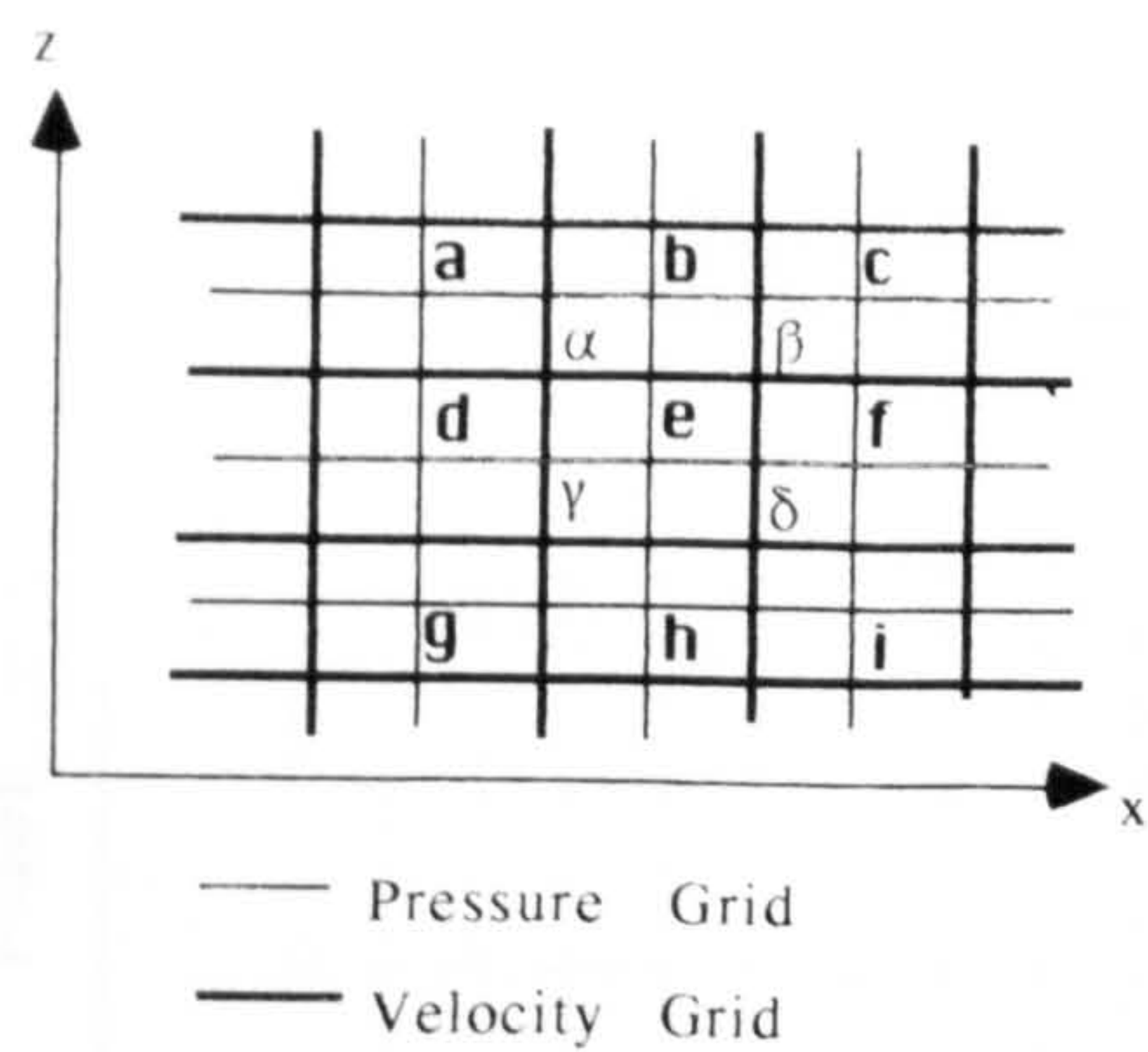


Figure 21. Computational Cell for Pressure Calculation

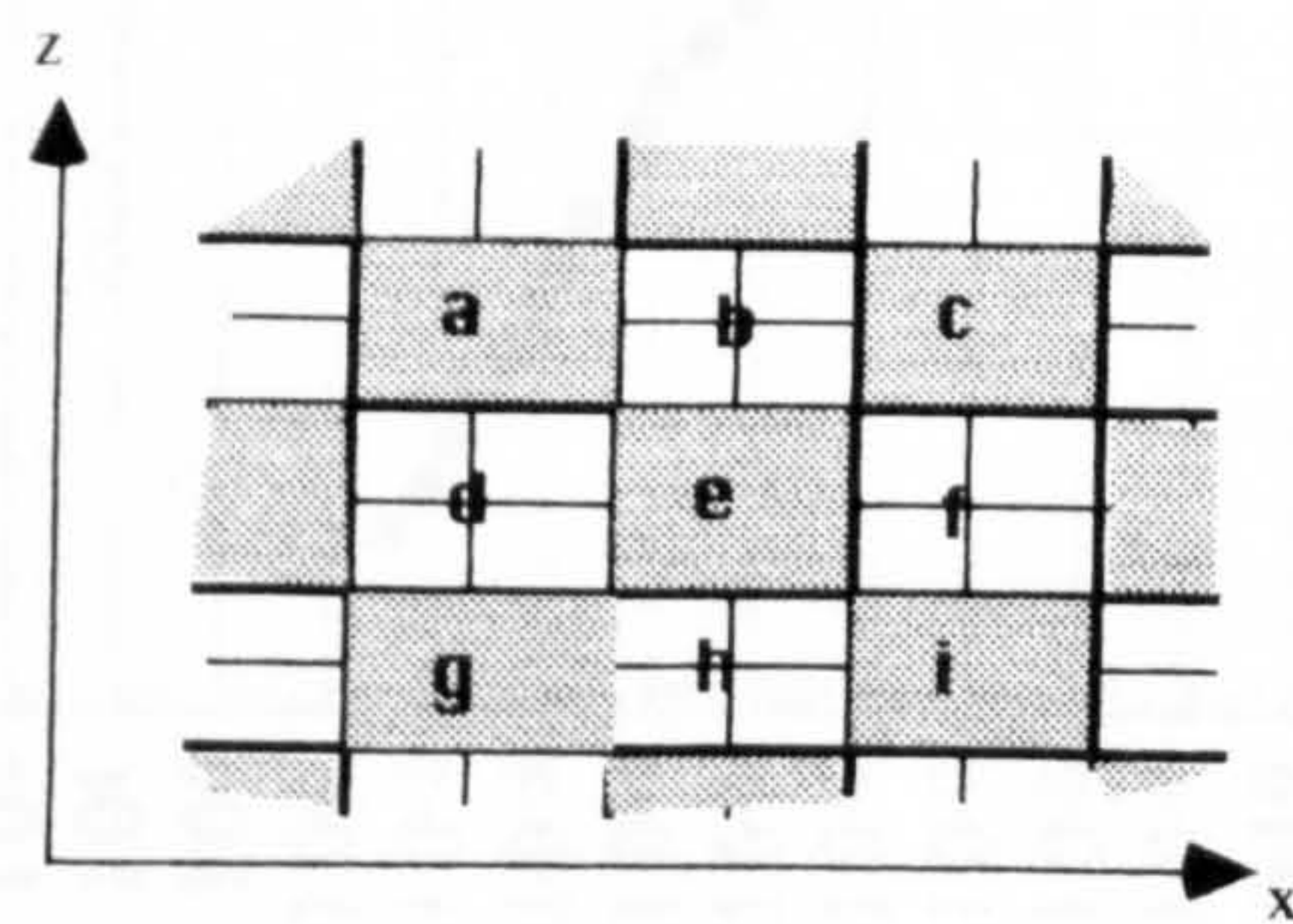


Figure 22. Five point diagonal square and associated uncoupling problem

Convergence Characteristics
Conjugate Gradient Algorithm for Pressure

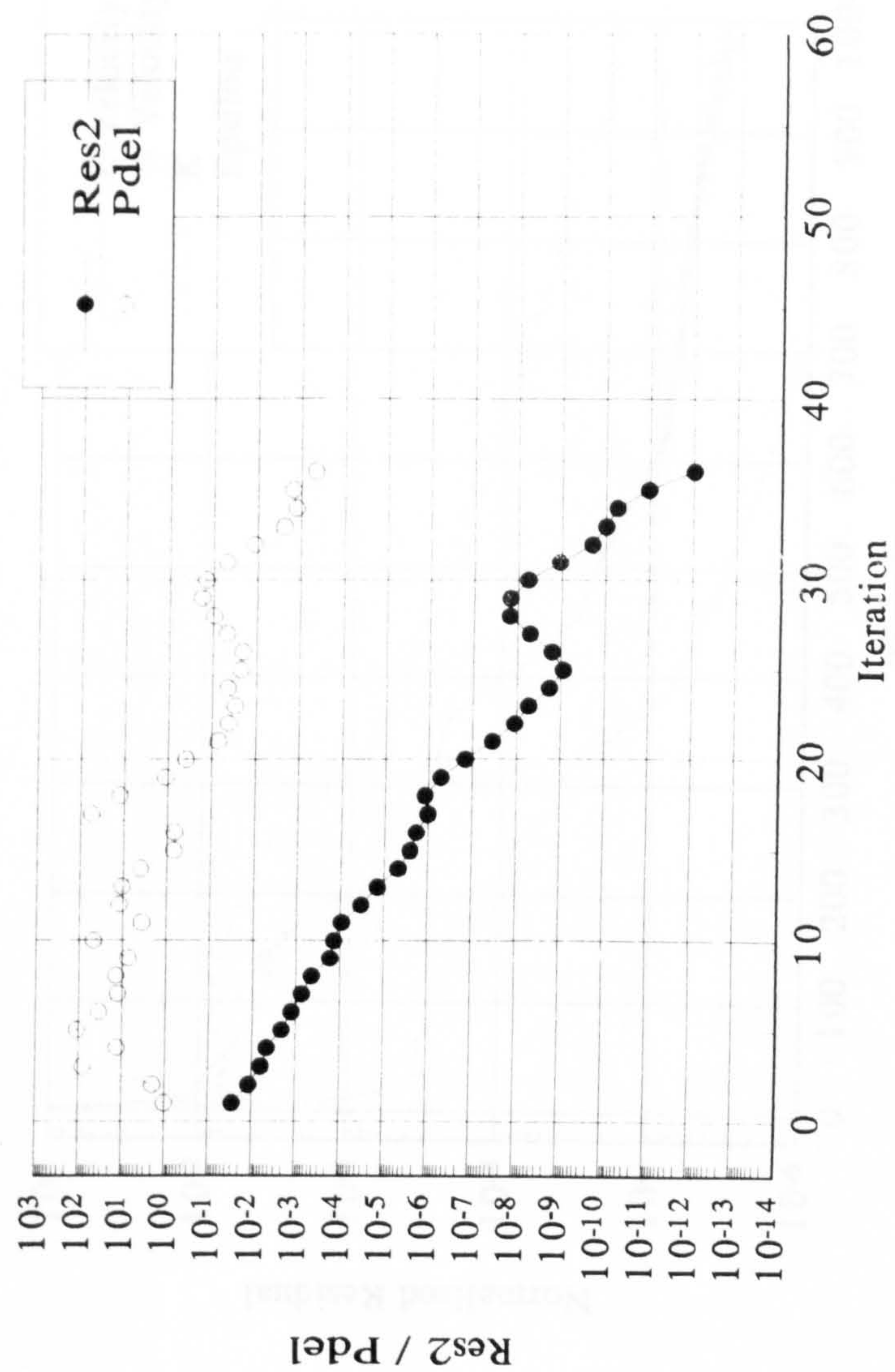


Figure 23. Convergence Curve for PCGM for Pressure Solution (Res2, Pdel)

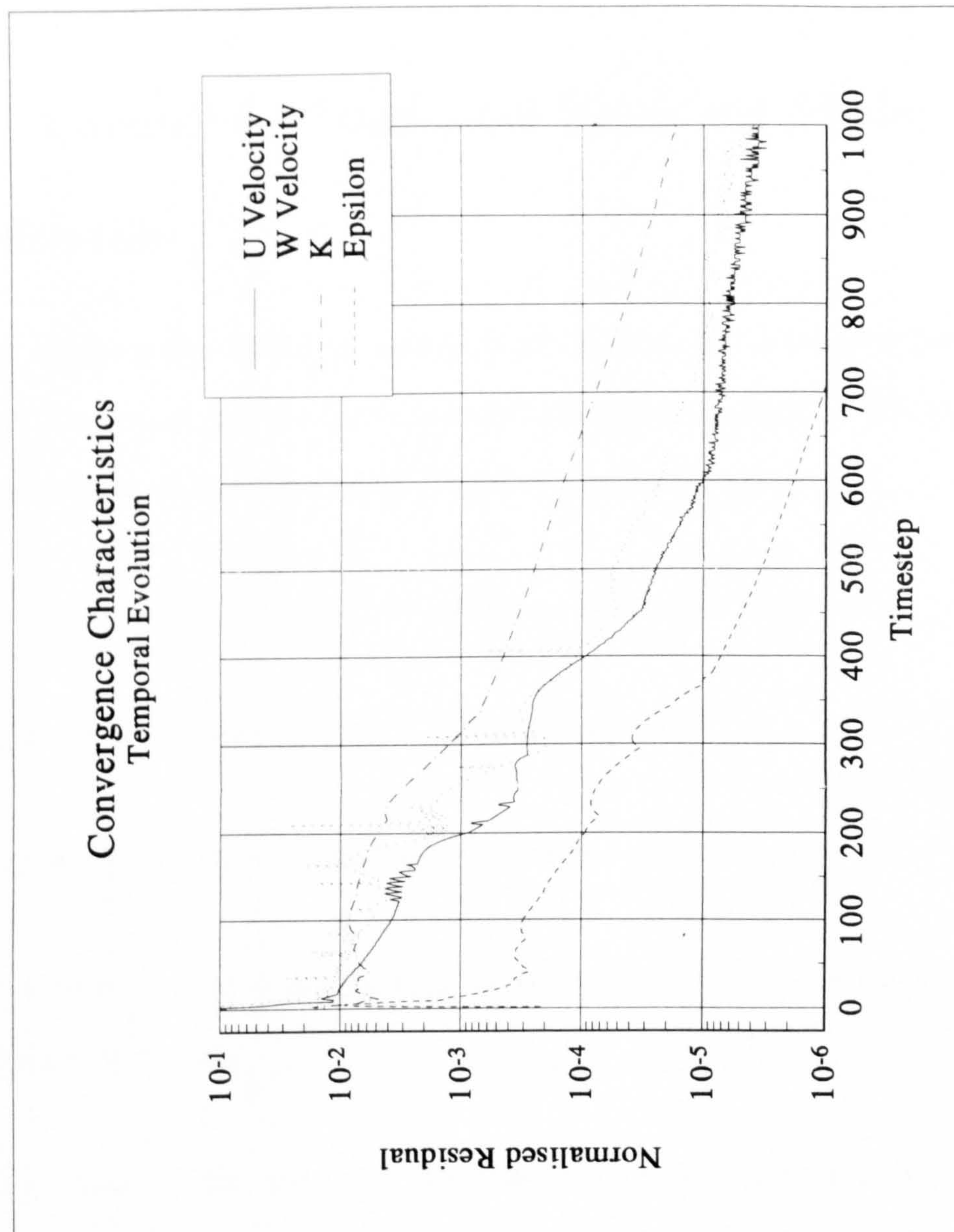


Figure 24. Curves Depicting Attainment of Steady State

6.0 Chapter 6 Numerical Tests and Model Verification

Before applying the model to a fully three dimensional flow phenomenon it was thought prudent to test the numerical method against simpler problems that were less demanding of computer time. This served several purposes:

1. It allowed an evaluation of the treatment of the advection terms.
2. It tested the validity of the Navier-Stokes solver.
3. The linear turbulence model implementation could be verified.
4. It allowed for an understanding to be built up about the behaviour of the numerical method.
5. The value of the non-linear turbulence stress-strain relationship could be assessed.
6. The flow mechanisms in these simpler problems could be studied.

Firstly, the treatment of the advection terms were examined with reference to a simple one dimensional analogue. Next, four two dimensional test cases were chosen for evaluation of the code. The first comes from the field of nuclear

engineering and has served as a test case for many codes. The other three are problems relating to civil engineering. The final problem, flow over a slot, is a simplified sub-system of the cross-over region in a meandering two stage channel.

6.1 *Pure Advection Tests*

The numerical treatment of the advection terms has been found to be highly important and is, therefore, a recurring theme in the literature. In this section, therefore, it has been decided to compare the present method of discretisation with traditional finite volume methods for the simple but challenging case of one dimensional pure advection. A numerical method which performs poorly for this simple test case must be used with caution for the full equation set. Advection terms appear in the momentum equations, the turbulence transport equations and also in any equation describing the transport of a quantity by the mean velocity field. It is not the intention to describe in detail the various alternatives for discretisation here but rather to provide a brief, up to date summary of the numerical problem, to view the problem from a different perspective and consequently to advocate the approach adopted in the present model. Reference will be made to other work where full details may be found of the other numerical treatments.

The advection terms describe mathematically the transport by the mean velocity field of some physical property (momentum, concentration of chemical or biological species, turbulence quantity etc). The advection term looks something like,

$$\frac{\partial c}{\partial t} + \frac{\partial u_j c}{\partial x_j} = 0 \quad [6.1]$$

where c may be velocity (u_i), turbulence quantity (k or ε), concentration of chemical or heat etc. In one dimension it may be re-written, dropping the tensor notation and assuming a constant uniform positive velocity,

$$\frac{\partial c}{\partial t} + u \frac{\partial c}{\partial x} = 0 \quad [6.2]$$

It is paradoxical that such an apparently simple equation (which has an easily found analytical solution for many problems) gives rise to extreme difficulties when its solution is approached numerically. In this section this equation will be examined by numerical experiment so that the treatment of advection may be examined in isolation. In this way the analysis will not be clouded by other terms as would be the case if the full equations were examined. In addition note that it is the linear advection that is examined here where c is some scalar value.

There are essentially two methodologies in the discretisation of this problem although they may, in certain limiting circumstances, produce the same algebraic formula for the unknown variable at the computer coding stage.

6.1.1 Eulerian Methodology

The Eulerian methodology, favoured in finite volume and finite element codes, has been popular in the past since all physical processes can be dealt with at the same sweep of the computational mesh. The Eulerian methodology may proceed to replace the advection equation 6.2 with a finite difference or finite volume discretization without a full consideration of the physical meaning of the advection equation,

$$\frac{c_i^{n+1} - c_i^n}{\Delta t} + u\theta\left(\frac{c_R^{n+1} - c_L^{n+1}}{\Delta x}\right) + u(1-\theta)\left(\frac{c_R^n - c_L^n}{\Delta x}\right) = 0 \quad [6.3]$$

where the notation refers to figure 25. The superscript represents the time index, and the subscript represents the spatial index. For this particular case the time dependent finite volume discretizations and time dependent finite difference discretizations amount to the same final formula, Roache (1972). θ is a temporal weighting factor. Common values for θ are 0 which results in a fully explicit method, and 1 which results in a fully implicit method. It may be shown that θ must be greater than or equal to 0.5 to produce unconditionally stable forms, Vreugdenhil (1989). The main difference in these methods comes in the calculation of the face values, (c_L, c_R) . Some of common differencing schemes are given below,

Scheme	Formula for Right Face Value, c_R	Reference
Central	$\frac{1}{2}(c_i + c_{i+1})$	Patankar (1980) Roache (1972)
Upwind	c_i	Patankar (1980) Roache (1972)
QUICK	$\frac{1}{2}(c_i + c_{i+1}) - \frac{1}{8}(c_{i+1} - 2c_i + c_{i-1})$	Falconer and Chen (1992)
SMART	$\frac{1}{2}(c_i + c_{i+1}) - CF(c_{i+1} - 2c_i + c_{i-1})$ CF given by non-linear formula	Gaskell and Lau (1988)

Table 12. Implicit Schemes: See figure 25

Upwind and central differencing are sometimes termed first generation methods since they have been around the longest. They are plagued however by numerical errors which result in either an artificial diffusion or unphysical oscillations which destroy the solution when either the advection is strong and/or there are steep

gradients in the dependent variable distribution. There have been several suggestions of ways to avoid these errors, however they have not been universally successful. Leonard (1979) suggested an alternative discretisation, Quadratic Upstream Interpolation for Convective Kinematics, for the face values. This so called QUICK differencing has been greeted favourably by computational fluid dynamics researchers, however for unsteady formulations there are some concern that in certain circumstances it fails to produce converged results, Fletcher (1988). A possible reason for this is suggested in section 6.1.3.2. If these schemes are implemented fully implicitly, that is, if all terms at the new time level are actually taken at the new time level then these schemes are unconditionally stable. For the QUICK and SMART schemes this results in a pentadiagonal matrix structure for the general case, whereas for the central and upwind (or hybrid schemes) a tridiagonal matrix results. The tridiagonal matrix involves less computation and therefore some researchers have (for QUICK and SMART) taken the curvature terms $(c_{l+1} - 2c_l + c_{l-1})$ explicitly in order to preserve the tridiagonal matrix structure. This is sometimes described in finite volume applications as transferring the curvature terms into the source term. In this approach however the scheme is then only conditionally stable, Falconer and Chen (1992). This option appears to be favoured despite the stability limitation.

Among the explicit schemes (which can be demonstrated to be conditionally stable) the QUICKEST scheme proposed by Leonard, (1979), and the scheme described by Takacs (1985) are to be recommended. Indeed for Courant numbers less than one they are markedly more accurate than implicit schemes. These two schemes may under certain circumstances be shown to be equivalent. Explicit schemes are more physically suited to the pure advection problem since they do not require downstream boundary conditions for pure advection which is a physical and mathematical requirement. Some explicit schemes are outlined in table 13.

Scheme	Reference
Linear Upwind	Roache (1972)
Leiths Method	Roache (1972)
QUICKEST	Leonard (1979)
Third Order Lax-Wendroff	Takacs (1985)

Table 13. Explicit Schemes: Theoretical Stability Analyses Suggests Conditional Stability - Courant numbers less than 1

6.1.2 Lagrangian Methodology

The Lagrangian methodology, in contrast, takes account of the physical nature of the advection equation before numerical discretisation and therefore, it is argued, is intrinsically unconditionally stable. The partial differential equation,

$$\frac{\partial c}{\partial t} + u \frac{\partial c}{\partial x} = 0 \quad [6.4]$$

may be re-written as two ordinary differential equations,

$$\frac{dc}{dt} = 0 \quad [6.5]$$

and

$$\frac{dx}{dt} = u \quad [6.6]$$

since, by the chain rule,

$$\frac{dc}{dt} = \frac{\partial c}{\partial t} + \frac{\partial c}{\partial x} \frac{\partial x}{\partial t} \quad [6.7]$$

This expresses the fact that c remains constant along characteristic curves which have slope, $1/u$, and is shown graphically in figure 26. Therefore to compute c at the new time level two steps are involved. For the characteristic curve that passes through the point where we wish to find c , i.e. (x^{n+1}) :

1. Compute the position of the characteristic foot by solving equation 6.6
2. Find the value of c at the characteristic foot by interpolation which equals the value at the characteristic head by virtue of equation 6.5.

$$\frac{c_{x^{n+1}}^{n+1} - c_{x^n}^n}{\Delta t} = 0 \quad [6.8]$$

$$c_{x^{n+1}}^{n+1} = c_{x^n}^n \quad [6.9]$$

Equation 6.6 may be solved by any method suitable for ordinary differential equations. For the linear problem described here the characteristics are straight lines and the step is trivial. The extension of the method to non-linear problems (i.e. the Navier-Stokes equations) means that the characteristics will not be straight lines, Benque, Ibler and Labadie (1980). In the present code a simple Euler's forward differencing has been used taking u from the present value at time, t^n ,

$$\frac{x^{n+1} - x^n}{\Delta t} = u^n \quad [6.10]$$

giving,

$$x^n = x^{n+1} - \Delta t u^n \quad [6.11]$$

where x^{n+1} is the x co-ordinate of the point where the c value is required and x^n is the x co-ordinate of the foot of the characteristic. This method is adequate for problems with smoothly varying velocity fields, Casulli (1990). The advantage of this lagrangian approach is that this backtracking procedure can be extended over

many elements thus allowing simulation at Courant numbers greater than unity. Having determined x^n an adequate interpolation is then required to determine c_{x^n} . The simplest approach is a linear interpolation, see figure 26, given by,

$$c_{x^n} = \alpha c_C^n + (1 - \alpha) c_B^n \quad [6.12]$$

where,

$$\alpha = \frac{x^n - x_B}{x_C - x_B} \quad [6.13]$$

and $x_{B,C}$ are the x co-ordinates of the grid nodes around the point of interest. Unfortunately this approach, although strictly bounded, introduces an error something like artificial diffusion. Greater accuracy can be achieved by utilising cubic interpolation over four grid points. This is achieved by fitting a cubic equation over the four grid points surrounding x^n ,

$$c(x) = a_3 x^3 + a_2 x^2 + a_1 x + a_0 \quad [6.14]$$

The coefficients (a_i) are evaluated by identifying the values of c at the four nodes A, B, C and D. If during the backtracking procedure an inflow boundary is reached then backtracking is terminated and the inflow value is required to set c_{x^n} . The extension to two dimensions is straightforward, indeed this lagrangian approach is genuinely multi-dimensional. Firstly, the backtracking requires the solution of two ordinary differential equations,

$$\frac{dx}{dt} = u \quad [6.15]$$

$$\frac{dz}{dt} = w \quad [6.16]$$

Once the point (x^n, z^n) is established an interpolation is again required. For two dimensions a incomplete bi-cubic surface over 12 points (see figure 27) is fitted.

$$c(x,z) = a_{00} + a_{01}x + a_{02}x^2 + a_{03}x^3 \quad [6.17]$$

$$+ a_{10}z + a_{20}z^2 + a_{30}z^3 + a_{11}xz$$

$$+ a_{12}xz^2 + a_{13}xz^3 + a_{31}x^3z + a_{21}x^2z$$

The coefficients (a_{ij}) are evaluated by identifying the values of c at the twelve nodes shown in figure 27. Close to the boundary the degree of the polynomial is downgraded. The analysis can be extended to three dimensions in a straightforward manner.

The Lagrangian approach consists of two very simple computations which are highly suited to implementation on vector or parallel computer architectures.

For the complete Navier-Stokes solver three such advection equations must be solved for the three components of velocity however it will be appreciated that each has the same characteristic curve so the backtracking to find the foot of the characteristic need only be done once. If transport equations are solved for turbulence or other scalars then these will likewise follow the same characteristics.

6.1.3 Results of Different Schemes

To demonstrate the advantage of the present approach in contrast to the traditional finite difference/volume approach a simple one dimensional analogue is used. In this example problem some scalar quantity, c , which will be termed the concentration, with a narrow Gaussian distribution is advected in a uniform positive velocity field, u , with no stabilising diffusion. This process is described by equation 6.4 which may be thought of as some scalar travelling through a channel reach with mean velocity u . The Gaussian distribution is given by,

$$c(x) = c_{\max} e^{(-\frac{(x-x_c)^2}{\sigma^2})} \quad [6.18]$$

where c_{\max} is the maximum value of the concentration, x_c is the position of the centroid of the distribution and σ^2 is the variance of the Gaussian distribution. The analytical solution is easily obtained since the initial distribution simply moves in the x direction with the mean fluid velocity, u , unchanging in shape. Thus equation 6.18 may be used with the x_c suitably translated. In the test case chosen here the distribution has a standard deviation, $\sigma = 1.94\Delta x$. This is a very severe test case with the difference between the maximum and zero discretised over about 4 grid spaces.

The simulation time was chosen to allow the distribution to move $45\Delta x$. The velocity was the same for all runs 0.45 m/s. The space step, Δx , was also kept constant 200m. The Courant number was set therefore by altering the timestep. Thus to achieve the same simulation time less time steps were required as the Courant number increased.

Equation 6.4 was solved by six Eulerian schemes (four implicit and two explicit) and by a Lagrangian scheme with two different interpolations (linear and cubic). The Eulerian schemes used are the implicit central scheme, Fletcher (1988), the implicit upwind scheme, Fletcher (1988), the implicit QUICK scheme, Falconer and Chen (1992), and an implicit SMART scheme, which is similar to the QUICK scheme except the curvature factor is evaluated with a non-linear formula due to Gaskell and Lau (1988) instead of being set to $\frac{1}{8}$ as in the QUICK scheme. These schemes have been tried with θ equal to 0.5 and also with θ equal to 1 which is more common practice in finite volume codes. Two explicit schemes are also used QUICKEST which is described by Leonard (1979) and a third order Lax-Wendroff method described by Takacs (1985). The characteristic method,

advocated in the present research, is also tried with both linear and cubic interpolation.

6.1.3.1 Courant Number Less Than One

Figures 28(a) and 28(b) and figures 29(a) and 29(b) show the results obtained using the implicit schemes with θ equal to 0.5. for a Courant number of 0.45. These results show the problems with the simple upwind and central differencing schemes. Notably, the upwind scheme results in an artificial diffusion and the central scheme results in spurious unphysical oscillations. Note that the hybrid method which is described by Patankar (1980) is a hybrid of these two schemes. Leonard's QUICK interpolation leads to an improvement in the prediction of the peak value but incurs a phase error which manifests itself in producing a spurious unsymmetrical undershoot. The SMART scheme corrects this undershoot producing a bounded solution however the solution is slightly unsymmetric. Patankar (1980) recommends that θ be set to 1. This practice is common in finite volume applications and therefore simulations were undertaken with θ equal to 1. These results are shown in figures 30(a) and 30(b) and in figures 31(a) and 31(b). These results show that setting θ to 1 leads to a severe damping of the solution. Although QUICK and SMART are slightly better than upwind and central even they produce unacceptable solutions to this particular problem. A similar conclusion has been drawn by Falconer and Chen (1992) for Courant numbers less than one.

Computations with the explicit QUICKEST scheme and the explicit Takacs scheme are shown, in figures 32(a) and 32(b). These results show a considerable improvement in accuracy and physical realism over the implicit schemes. Both the amplitude and more noticeably the phase errors are smaller. Symmetrical solutions are obtained however a small undershoot is observed.

The lagrangian methods perform as well as the explicit schemes for Courant numbers less than one resulting in low amplitude and phase errors, see figure 33(a) and 33(b). Note that with linear interpolation a bounded solution is obtained however a rather large false diffusion is evident. With cubic interpolation, although boundedness cannot be guaranteed, much more accurate solutions are evident. In fact for this particular case the QUICKEST scheme, the third order Lax-Wendroff scheme and the lagrangian scheme with cubic interpolation gave identical results. This is interesting since it suggests that QUICKEST somehow has some lagrangian traits.

6.1.3.2 Courant Number Greater Than One

The real benefits of the lagrangian approach, however, become apparent when simulations are attempted at Courant numbers greater than 1. Note that the QUICKEST scheme and the Takacs scheme could not be applied to these situations since these schemes are only stable for Courant numbers less than one.

The unconditionally stable implicit schemes (upwind,central,QUICK,SMART) give very inaccurate results whether with θ equal to 0.5 or 1. When θ equals 0.5 unphysical oscillations again appear (figures 34(a) and (b) and figures 35(a) and (b)) and when θ is equal to 1 a large numerical diffusion is evident (figures 36(a) and (b) and figures 37(a) and (b)). In fact, as the Courant number is increased the artificial diffusion grows proportionally. Interestingly, the traditional finite volume formulation with the QUICK scheme was also used for further tests which included a significant diffusion term and a higher grid resolution. These runs indicated that when the Courant number was greater than one then these serious errors persisted.

In contrast, the lagrangian schemes (figure 38) give even better results for larger timesteps. This is because for a given simulation time larger timesteps means fewer timesteps and this means fewer interpolations for a given simulation. At each interpolation solution accuracy degrades and so fewer interpolations means greater accuracy.

6.2 *Flow in a Plenum Chamber - Boyle and Golay (1983)*

In this and the following sections the complete Reynolds Averaged Navier-Stokes solver is applied and tested for two dimensional problems.

At the 9th meeting of the I.A.H.R. Working Group on Refined Flow Modelling of Flows held at Cadarache (24-25 January, 1985) a test case for turbulent cavity flows was proposed for which research groups could submit numerical solutions. The test case was based on the experiments of Boyle and Golay (1983). Seventeen contributions were forthcoming based on a variety of numerical methods and turbulence models. Because of the previous research on this problem it was decided that this would serve as a useful test of the present code.

The principal flow mechanisms are described by Boyle and Golay (1983). The flow field is dominated by a large recirculation zone occupying most of the model domain. Experimental LDA measurements were taken by Boyle and Golay (1983).

6.2.1 Geometry, Grid and Boundary Conditions

The geometry is shown in figure 39. The results presented here have been obtained with a uniform grid of 35 x 49 with $\Delta x = \Delta z = 0.5$ cm.. This has been shown in figure 39 also. The inlet boundary conditions for the test case are suggested by Bouffinier and Grandotto (1987) and are summarised below.

$$u = 0 \text{ cm/s}$$

$$w = 80.0 \text{ cm/s.}$$

$$k = 250 \text{ cm}^2/\text{s}^2$$

$$\varepsilon = 1250 \text{ cm}^2/\text{s}^3$$

The material of the chamber was perspex and therefore walls were assumed to be hydraulically smooth.

6.2.2 Results

The linear turbulence model was used first to compare the code's performance against other codes which also used a linear model. Figures 40 and 41 show the results of the present model and the results of another research group who tackled the benchmarking exercise, Goussebaile, Jacomy, Hauguel and Gregoire (1987). The present model's k values have been normalised with respect to U_0^2 . The velocity vectors show an encouraging agreement, both models predicting the center of recirculation at about $(x=11.5, z=8.1)$. This prediction is also in line with other contributors to the benchmarking exercise, Bouffinier and Grandotto (1987). The trends in the turbulent kinetic energy fields are also very similar, predicting four areas of local maximum.

The model predictions have also been compared with the experimental results of Boyle and Golay (1983) at the three levels A, B and C which are depicted in figure 41. In figure 42 a satisfactory agreement can be observed for the velocities however in figure 43 the model predictions for the turbulent kinetic energy are seen to be well in excess of the observed values. However, this was also observed by other research groups using the standard k - ε model, Bouffinier and Grandotto (1987). The problem appears not to be numerical in origin but rather a fundamental problem of the physics of the standard k - ε model. Specifically, in regions of flow curvature, turbulence shear stress and intensity are reduced by the curvature when the angular momentum of the flow increases in the direction of the

radius of curvature. They are increased when the angular momentum decreases with radius, Gibson, Jones and Younis (1981). The standard k-ε model is incapable of reproducing this phenomena.

In an effort to improve the predictions the non-linear model has also been tried for this problem. The results with the non-linear stress-strain relationship appear to be an improvement on the linear relationship in some respects. In figure 45 the level of turbulence kinetic energy (computed as the average of the normal Reynolds stresses) appears to be in much closer agreement with the observed level although no actual agreement in the trend could be claimed. The improvement in level is encouraging none-the-less. Computations of this flow with an algebraic stress model and with a Reynolds stress transport model also predict a lower level of turbulent kinetic energy in better agreement with the experiment, Huang (1986). There are no other computations of this flow in the literature with Speziale's non-linear stress-strain relationship to confirm or disqualify this result. However in a study of backward facing step computation, in which the recirculation zone is very highly resolved, Thangam and Speziale (1992) demonstrate that within the recirculation zone a lower turbulence intensity is predicted by using a non-linear model in contrast to a linear model. In fact they predict that within the closed streamlines of a recirculation zone the square root of the normalised normal Reynolds stress predicted by the non-linear model may be about three-quarters the value predicted by the linear model,

$$\left[\sqrt{\frac{\overline{u'^2}}{U_o^2}} \right]_{Non-Linear} \approx 0.75 \left[\sqrt{\frac{\overline{u'^2}}{U_o^2}} \right]_{Linear}$$

Very roughly this implies that,

$$\left[\frac{\overline{u'^2}}{U_o^2} \right]_{Non-Linear} \approx 0.56 \left[\frac{\overline{u'^2}}{U_o^2} \right]_{Linear} \approx 0.56 \left[\frac{k}{U_o^2} \right]_{Linear}$$

within the closed streamlines of a recirculation zone. Of course, this is an approximate analysis (assuming that $\overline{u'^2} = \overline{w'^2}$) but none-the-less it adds confidence to the present predictions which show a similar improvement. Further study is, however, required.

6.3 Open Channel Flow over a Backward Facing Step - Nakagawa and Nezu (1987)

This problem represents an application of the model to a flow of civil engineering interest. Although there have been many computational studies of closed channel flow over a backward facing step there have been very few of the corresponding open channel case. The L.D.A. experimental measurements are detailed by Nakagawa and Nezu (1987) who present 5 sets of experimental data referenced ST1 to ST5. In each experiment flow was subcritical. The case examined here is ST3. The experimental conditions are given in table 14.

U_{max} cm./s	U_{m2} cm./s	R_e	F_r	X_r/H_r
29.2	22.1	23400	0.22	5.2

Table 14. Hydraulic Parameters for experiment ST3 after Nakagawa and Nezu (1987):

6.3.1 Geometry, Grid and Boundary Conditions

The geometry is shown in figure 46. A uniform grid of 100 x 51 has been used with $\Delta x = 0.4$ cm. and $\Delta z = 0.2$ cm. and this has been shown in figure 46 also. The inlet conditions are assumed to be fully developed channel flow,

$$u = \frac{u^*}{\kappa} \ln\left(\frac{z}{z_o}\right)$$

$$w = 0$$

$$k = \frac{u^{*2}}{\sqrt{c_\mu}} \left(1 - \frac{z}{h}\right)$$

$$u^* = 1.692 \text{ cm/s}$$

$$z_o = 0.0082 \text{ cm}$$

$$\varepsilon = \frac{|u^*|^3}{\kappa z} \left(1 - \frac{z}{h}\right)$$

with u^* and z_0 chosen to reproduce the experimental inlet velocity profile as closely as possible. Smooth wall laws are adopted at wall boundaries and the free surface is treated as a symmetry plane.

6.3.2 Model Results and Discussion

Figure 47 shows the velocity vectors within the recirculation zone predicted by both the linear and non-linear models. The velocity field predicted by the linear stress-strain model indicates a reattachment point at about 4.4 step lengths, resulting in a underprediction by about 16%. This is perhaps slightly better than similar predictions for the corresponding closed channel flow case. Figure 48, 49 and 50 show the linear model predictions for turbulent intensity defined as the square root of the normalised normal Reynolds stress in the x direction. Within the recirculation zone at less than about 3 step heights, agreement with experiment is generally poor. Nakagawa and Nezu (1987) show that their measurements are less accurate within this region and this may partly contribute to this discrepancy. Outside of the recirculation zone beyond about 5 step heights downstream the turbulence intensity predictions show a better agreement but a general underprediction. These trends agree with Basara and Younis (1992) who examined the closed channel case. Figure 51, 52 and 53 show the non-linear model predictions for the normalised Reynolds stress. Again these show a general underprediction in this region. These results are again consistent with predictions for the closed channel case e.g. Speziale and Ngo (1988) or Basara and Younis (1992).

Figure 47 shows that the non-linear model predicts a velocity field with a reattachment point at about 5.2 step lengths, which is indistinguishable from the experimental measure. It would be wrong to conclude from this one case that the non-linear model gives exact results. However, it is reasonable to conclude that the non-linear model results in an increased prediction for the recirculation region. Figures 54, 55 and 56 show the predicted turbulence intensities with the non-linear model. These are a marked improvement on the predictions with the linear model beyond about 3 step heights. The normalised Reynolds stresses, figures 57, 58 and 59 show a similar improvement. These results are again consistent with predictions for the closed channel case e.g. Speziale and Ngo (1988) or Basara and Younis (1992). They suggest that, as in the closed channel case, the improvement in predicting the turbulence intensities contributes to an improved prediction of the mean flow field.

The following table summarises some previous attempts at predicting recirculating flows (closed channel flow over a backward facing step) with both linear and non-linear models. The experimental measurements of this case are due to Kim, Kline and Johnston (1980). They observed a recirculation length of 7.0 step heights.

Investigator(s)	Advection Differencing	Grid	Linear Model	Non-Linear Model
Speziale and Ngo (1988)	Central	166 x 73 (Cartesian, non-uniform)	5.5	6.4
Basara and Younis (1992)	Upwind and Power Law	76 x 32 (Cartesian, non-uniform)	5.5	6.3
Benocci and Skovgaard (1988)	2nd Order Hybrid	61 x 41 (Cartesian)	5.7	7.4
Thangam and Speziale (1992)	Not specified	200 x 100 (Cartesian, non-uniform)	6.4	6.9

Table 15. Predictions for the recirculation length in step heights: Experimental results from Kim, Kline and Johnston (1980)

As can be seen from previous studies there is still some uncertainty over the application of both linear and non-linear models. Indeed, Lee (1992) using a finite element method and a linear model of turbulence predicted the recirculation length to be 7.1 step heights as compared to the measured value 7.0. The prevailing uncertainties appear to be related to grid refinement or numerical discretisation.

Despite these discrepancies the present results add weight to the argument that predictions for the mean velocity field and the turbulence quantities can be improved upon for flow over a backward facing step by adopting a non-linear stress-strain relationship rather than a linear stress-strain relationship. The

non-linear relationship results in a better prediction for the recirculation length probably because it results in a better prediction of the Reynolds stresses (both normal and shear). There is uncertainty over the predictions close to the step and within the recirculation zone however these may be because of inadequate experimental measurements and inadequate grid resolution within the recirculating zone.

6.4 Flow in a Settling Tank - Iman and McCorquodale (1983)

In Europe and North America most water and wastewater treatment plants involve at least one stage of sedimentation. The design of sedimentation tanks has traditionally relied on empirical equations derived from physical experiments. These physical experiments are greatly simplified from reality where surface wind effects, solar heating, variable influent temperature and unsteady loading conditions may prevail. Computational fluid dynamics has therefore been seen as useful tool for examining such systems to aid in real designs. There have been several applications of Reynolds Averaged Navier-Stokes Solvers to this problem, Zhou and McCorquodale (1992), Lyn, Stamou and Rodi (1992) and Lyn and Zhang (1989) among others. This research, however, appears to be concerned with refining steady state simulations despite the fact that the loading on such water and wastewater plant is often unsteady. There is a growing concern, Wallis (1993), that for obtaining discharge consents treatment plant operators will have to satisfy discharge consents that require an accurate estimate of the time varying effluent quality. Perhaps therefore efforts could be concentrated on obtaining long unsteady simulations over a typical plant operating cycle rather than on obtaining more accurate steady results. The present numerical method is more readily extendable to the long time unsteady simulations than the others proposed in the literature since it allows the accurate simulation of steep concentration gradients at large timesteps.

However, before going on to study such long term unsteady simulations the present code must be verified against available steady flows in settling tank geometries. Therefore, the code has been applied to the problem studied experimentally by Iman and McCorquodale (1983). Unfortunately, only the longitudinal velocities

were measured and therefore with no turbulence data to test against it was decided to only consider the linear turbulence model.

6.4.1 Geometry, Grid and Boundary Conditions

Figure 60 shows the experimental geometry. The experimental tank was 73 cm long and 11.95 cm deep. The inlet height was 5 cm. The flow through rate was $109.4 \frac{\text{cm}^3}{\text{s}}$ per cm. width. A uniform grid of 101 x 51 was used with $\Delta x = 0.73$ cm. and $\Delta z = 0.239$ cm. This is also show in figure 60. The inlet boundary conditions have been suggested by Celik, Rodi and Stamou (1986) who studied this problem with a finite volume code.

$$u_{\text{inlet}} = 21.88 \text{ cm/s}$$

$$w_{\text{inlet}} = 0 \text{ cm/s.}$$

$$k_{\text{inlet}} = 0.2 u_{\text{inlet}}^2 = 95.75 \text{ cm}^2/\text{s}^2$$

$$l_{\text{inlet}} = c_{\mu}(0.5h_i) = 0.225 \text{ cm}$$

giving

$$\varepsilon_{\text{inlet}} = c \frac{3}{4} \frac{k^{\frac{3}{2}}}{l} = 684.2 \text{ cm}^2/\text{s}^3$$

Smooth walls were assumed which is reasonable since the low velocities observed in such tanks mean that roughness elements rarely protrude beyond the laminar sub-layer. The free surface is treated as a rigid lid symmetry plane following Stamou, Adams and Rodi (1989).

6.4.2 Model Results and Discussion

Figure 61(a) shows the velocity vectors predicted by the model. The model predicts the length of the primary recirculation zone to be 41 cm. which is in excellent agreement with the measured length of 42 cm. Encouragingly the model also computes the presence of a much smaller secondary recirculation zone at the tank base outlet wall. The ability to capture this detail is no doubt important in calculating accurately the 'dead zone' effects of the tank. The normalised turbulent kinetic energy field is shown in figure 61(b) and, as may be expected, shows turbulence generated at the shear layer at the inlet and a further region of high turbulence at the outlet. It also predicts, however, a large region of lower turbulence beyond the recirculation zone and before the outlet. This area of lower turbulence will allow settling to take place. The normalised eddy viscosity field is shown in figure 62(a) and is similar to the one predicted by Stamou, Adams and Rodi (1989) in that a region of high viscosity occurs in the primary recirculation zone and also close to the outlet. The average value of the normalised eddy viscosity ($\frac{\nu_t}{L_o U_o}$) is about 0.01 which is in reasonable agreement with Stamou, Adams and Rodi (1989) and is the same order of magnitude as that calculated by Schamber and Larock (1980) despite their geometry being slightly different. The variation in the eddy viscosity shown in figure 62(a) again highlights the danger of using simpler models which take the eddy viscosity to be constant. The turbulent length scale is also shown in figure 62(b).

The model has also been compared quantitatively with the experimental velocity measurements. These are shown in figures 63, 64 and 65. A good agreement is observed in particular the model appears to resolve the steeper velocity gradients at inlet and outlet very well.

The results of the model application to steady flow in a settling chamber are very encouraging and suggest that the extension of the method to long term unsteady simulations is to be recommended.

6.5 *Open Channel Flow over a Slot*

Sometimes, in river modification works a trench is dredged across the main flow direction either for laying pipelines or as a sediment trap. A knowledge of how flows in the trench will behave is therefore required in order that the trench may be adequately designed or so that its effect on the rest of the river may be predicted. The study of slot flows is therefore important in its own right, however, Jasem (1990) highlights the similarities between the mechanisms in an open channel flow over a slot and the flow in the cross-over region in a two stage meandering channel. For this reason Jasem (1990) chose to study open channel flow over a slot experimentally. Unfortunately, only a mini-propellor was available for velocity measurements and no turbulence data was collected. Never-the-less, Jasem (1990) was able to show some of the main trends in slot flows and, in particular, to demonstrate significant differences depending on the aspect ratio of the slot. Jasem's (1990) water elevation profiles at varying aspect ratios are shown in figure 66. Fujita, Michiue and Hinokidani (1991), Fujita, Komura and Kanda (1993) and Fujita, Kanda, Komura, Yano and Morita (1993) have studied open channel flow over a slot using a flow visualisation technique combined with a correlation method. Their results have further indicated a significant dependence of the flow structure on the aspect ratio of the slot. Some of their observed velocity fields are shown in figure 67. There is very little high quality data available for this problem despite, as will be demonstrated, our current lack of understanding of this flow phenomenon. Alfrink and Van Rijn (1982) have considered numerically the flow over a trench with sloping sides which is similar to slot flows.

6.5.1 Geometry, Grid and Boundary Conditions

The inlet conditions are,

$$u_{in} = \frac{u^*}{\kappa} \ln\left(\frac{z}{z_o}\right)$$

$$w_{in} = 0$$

$$k_{in} = \frac{u^{*2}}{\sqrt{c_\mu}} \left(1 - \frac{z}{h}\right)$$

$$\varepsilon_{in} = \frac{|u^*|^3}{\kappa z} \left(1 - \frac{z}{h}\right) \quad \begin{array}{l} u^* = 1.48 \text{ cm/s} \\ z_o = 0.00075 \text{ cm} \end{array}$$

where u^* was estimated from $\sqrt{g S_o h}$ since a channel slope is defined and z_o chosen to reproduce the experimental inlet velocity profile as closely as possible. The depth of flow on the shallow regions is 1.6 cm. S_o was 0.0014 giving an average friction velocity of 1.48 cm/s. The free surface is treated as a symmetry plane.

Three geometries were considered representing three different slot aspect ratios (5, 10 and 20). These are shown in figure 68. For the smallest aspect ratio a grid of 101 x 29 was used with $\Delta x = 0.5 \text{ cm}$. and $\Delta z = 0.2 \text{ cm}$. A grid of 101 x 19 was used for both the aspect ratio of 10 and 20, with $\Delta x = 0.5 \text{ cm}$. and $\Delta z = 0.2 \text{ cm}$. for the aspect ratio of 10 and $\Delta x = 0.5 \text{ cm}$. and $\Delta z = 0.1 \text{ cm}$. for the aspect ratio of 20.

6.5.2 Model Results and Discussion

Predicted velocity vectors are shown in figures 69(a)-(c). The velocity vector plots concur qualitatively with the experiments of Fujita, Michiue and Hinokidani (1991). Importantly they demonstrate that it is not correct to assume that if the

forward facing step satisfies $\frac{X}{H_s} > 5$ then one can assume that the re-attachment will occur within the slot. In fact, reattachment does not occur even at an aspect ratio of 10. This is on one hand surprising since if the forward facing step is at infinity, i.e. the backward facing step problem, then reattachment has been shown to occur at between 5 to 7 step heights downstream from the step. The effect of the forward facing step may be to promote flow acceleration close to it and thus to drag forward the recirculation zone. This is an important conclusion and contradicts earlier suggestions by Jasem (1990). It has become obvious that more experimental and numerical studies of free surface flow over slots are required. Predicted turbulence quantities (turbulent kinetic energy, turbulent viscosity and turbulent length scale) are shown in figures 70 to 72. In particular note the wake effect, i.e. for small aspect ratios turbulence generated at the slot shear layer is carried forward onto the shallow zone. Although an exact comparison with free surface elevations is not obvious the pressure in the surface cell suitably normalised has been plotted in figure 73. This in some way represents the trends expected in the free surface if the surface were free. The trends are similar in particular at larger aspect ratios the jump in the free surface at the forward facing step is more pronounced and the rise over the slot more elongated.

The ramifications for two-stage meandering channels are worth mentioning. Slot flows are very similar to the cross-over region in such systems. All experimental studies of meandering two stage channels have been with main channel aspect ratios less than 10, Wark (1993). These values are typical of British rivers although natural river bathymetries are quite different from the slot case. None-the-less, understanding of the expansion/contraction flow at a slot will greatly aid in understanding the flows in two-stage meandering channels. It is likely that the main channel aspect ratio will play a crucial role. Further, experimental and

numerical studies of slot flows are therefore encouraged. The present results may act as a starting reference for such studies.

6.6 Conclusions from Initial Numerical Trials

The pure advection tests may suggest why traditional finite volume codes e.g. the SIMPLE algorithm with QUICK differencing, may fail or produce highly inaccurate solutions at large timesteps (Courant numbers greater than 1) if used for unsteady computations or used in unsteady mode with steady boundary conditions to produce steady state results. Of course, this depends on the importance of the advection terms for the particular application. If the advection terms are small then their errors are correspondingly small however if they are significant then their errors are also likely to be significant. In the full Navier-Stokes equations errors in the momentum advection terms may be obscured by the other terms also present (e.g. the pressure gradient terms) however these terms may adjust erroneously to compensate for errors in advection.

There is still a great deal of uncertainty as regards accurate advection computation in CFD applications. The present treatment or a method similar to it is recommended for use in unsteady applications. Researchers using variants of the SIMPLE algorithm for unsteady simulations are encouraged to try implementing a lagrangian type algorithm for computing the advection terms.

The two dimensional simulations have been very valuable for assessing the adequacy of the numerical model. The results are encouraging and have shed new light on these problems. All these two dimensional studies could be extended. The non-linear stress-strain relationship has been demonstrated to be a useful one although further testing is recommended. In particular:

1. The present model is at least as good as other models when used with a linear stress-strain relationship.
2. In strongly recirculating flows non-linear stress-strain relationships may provide better predictions for the level of turbulence than linear relationships.
3. As for the closed channel case, open channel flow over a backward facing step can be better modelled using a non-linear stress strain relationship. Longer recirculation lengths are predicted because more accurate predictions for the turbulent stresses are forthcoming.
4. The present model provides excellent predictions for steady flow in settling tanks. It is recommended to extend its use to the unsteady case.
5. The model has shed some new light on flows in slots. Clearly more experimental and computational work can be done in this regard.

Results for Pure Advection Tests

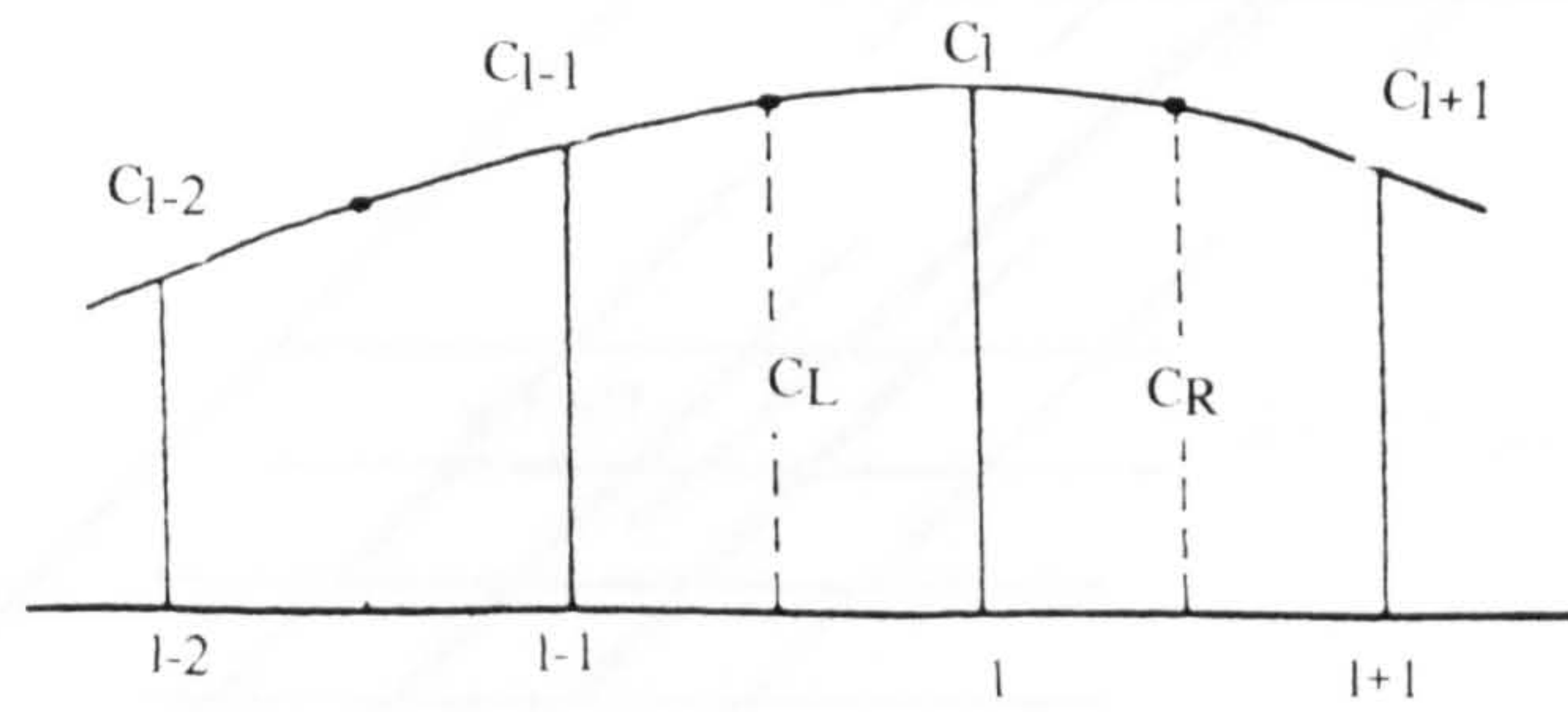


Figure 25. Eulerian Grid

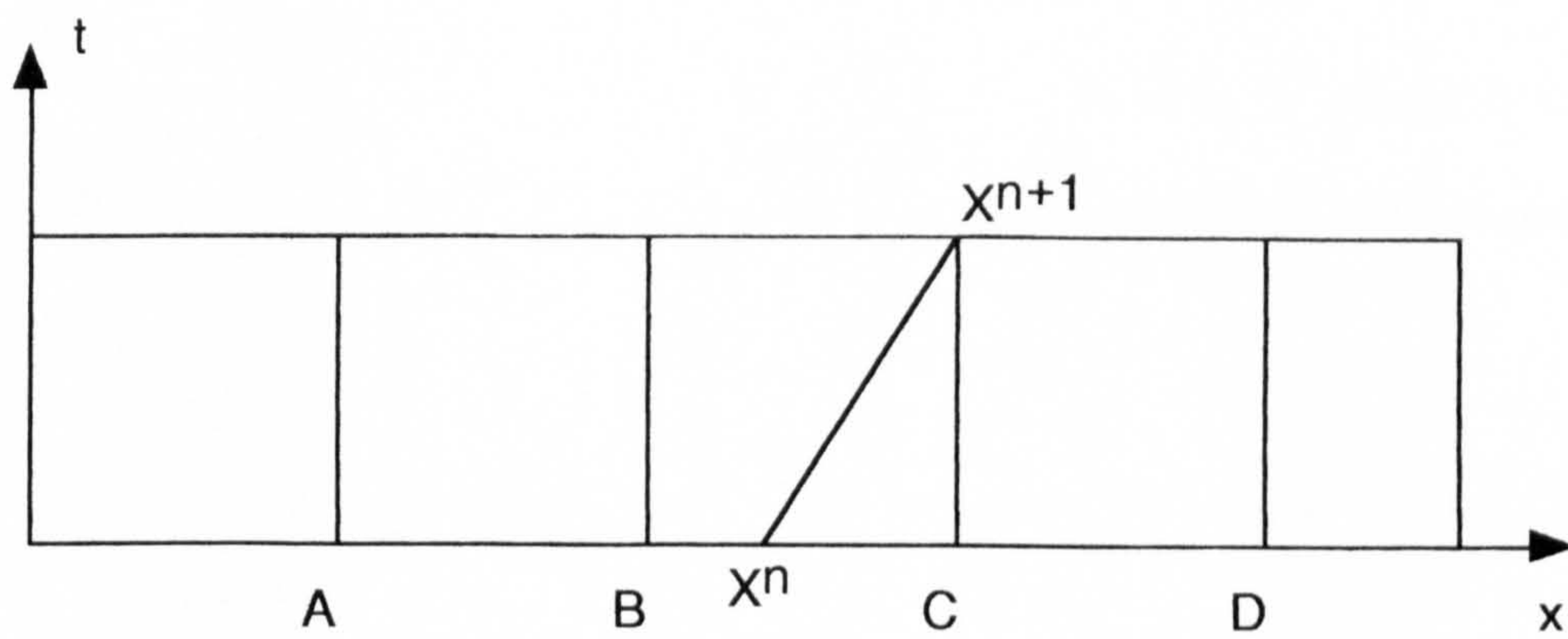
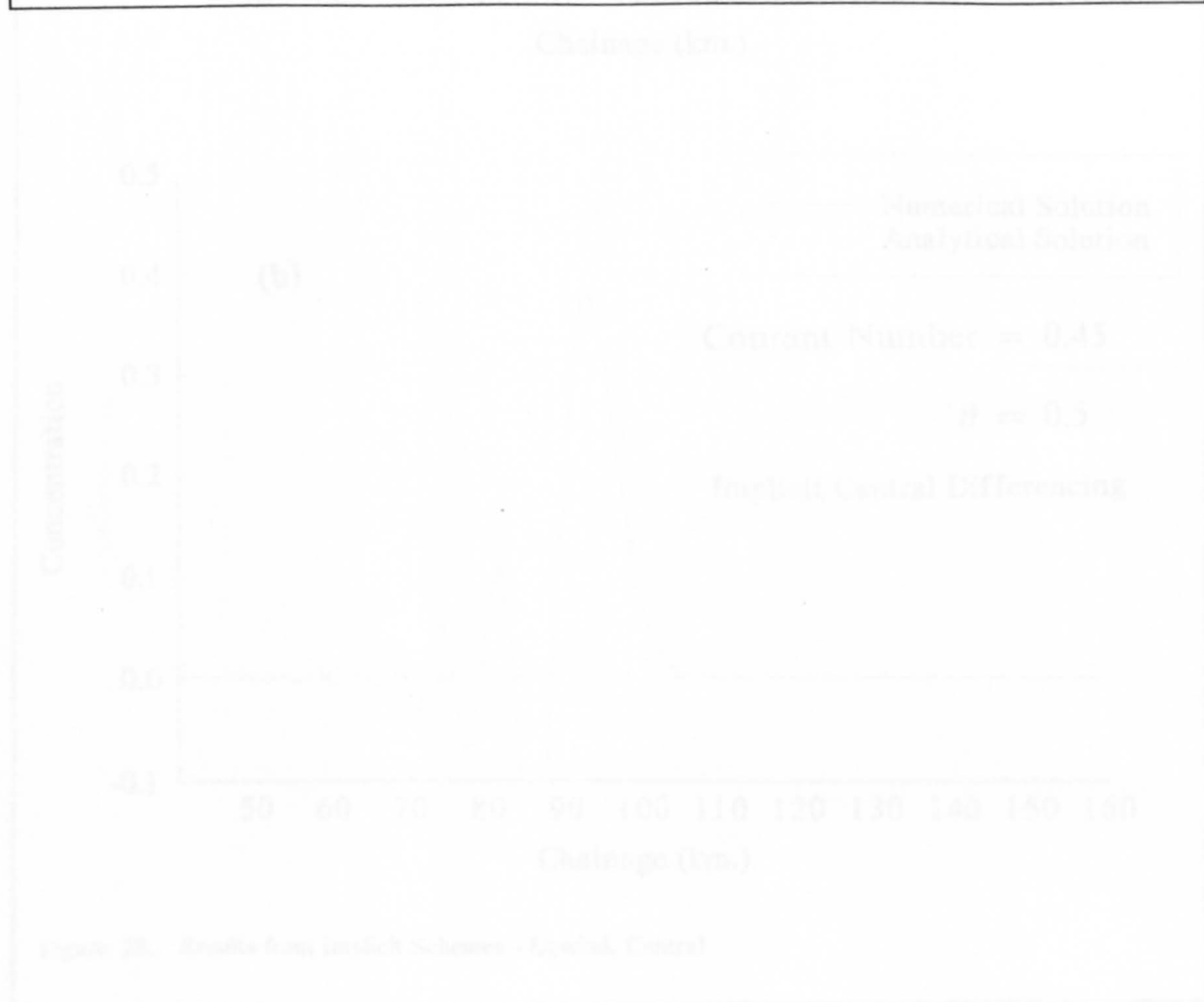
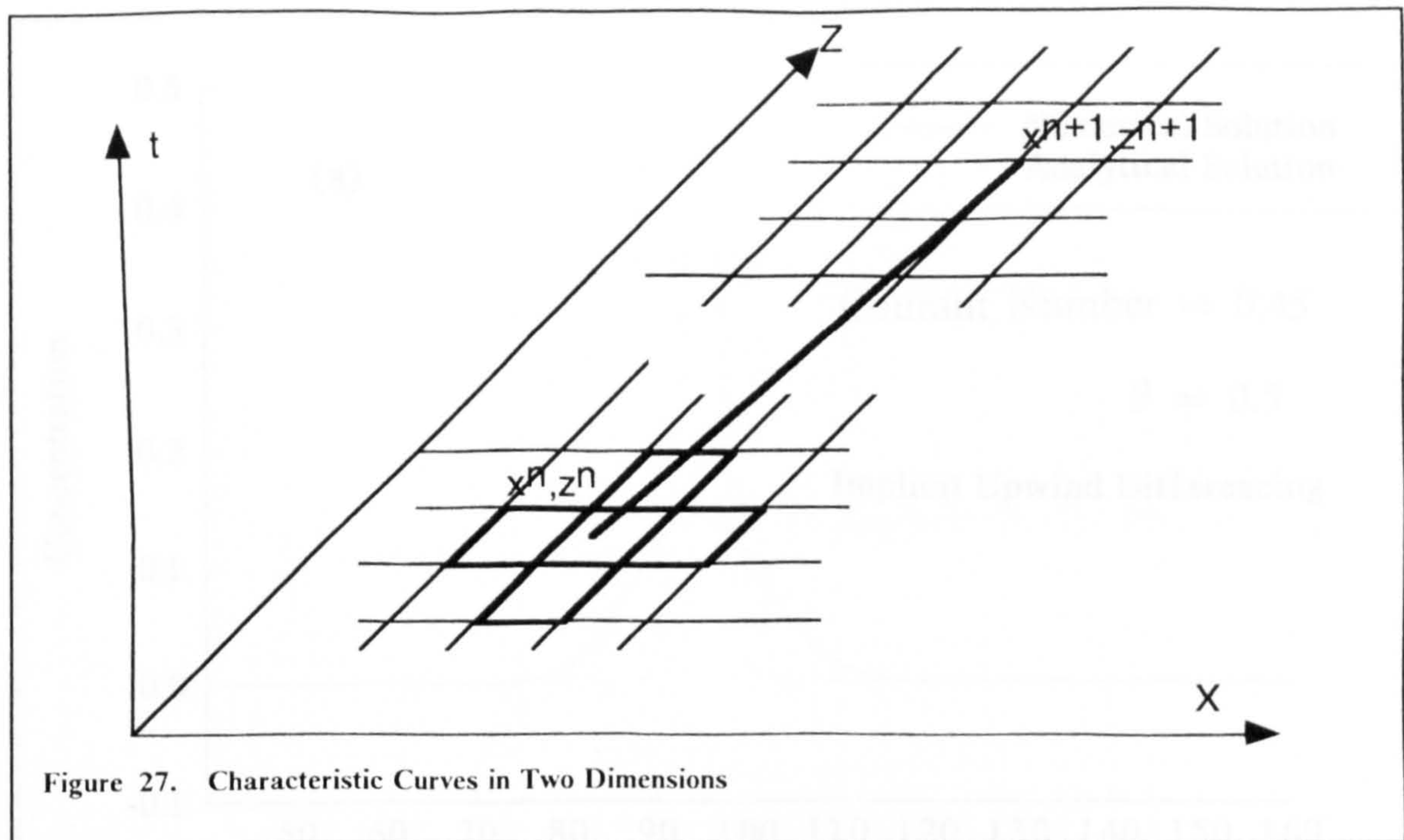
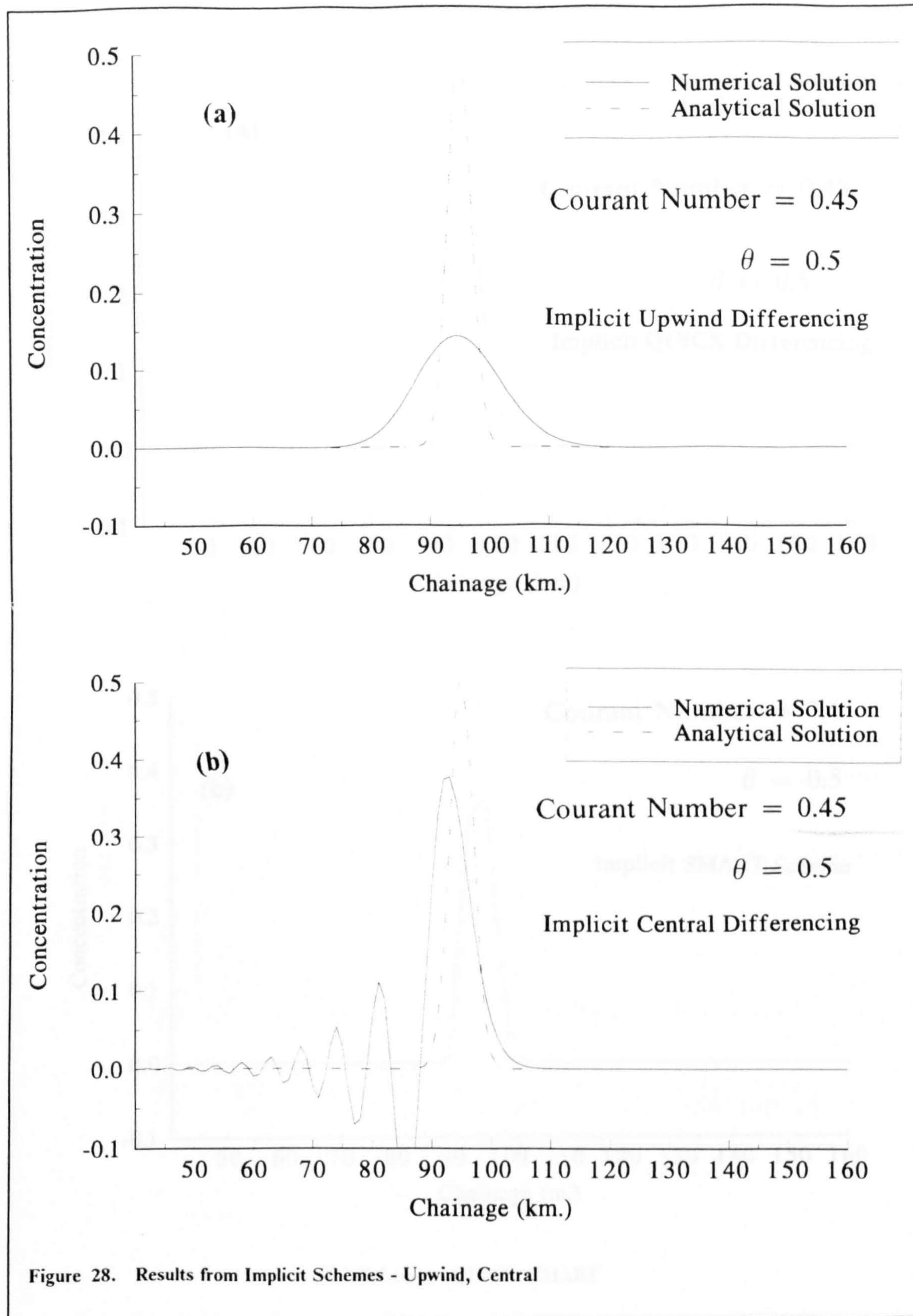


Figure 26. Characteristic Curves in One Dimension





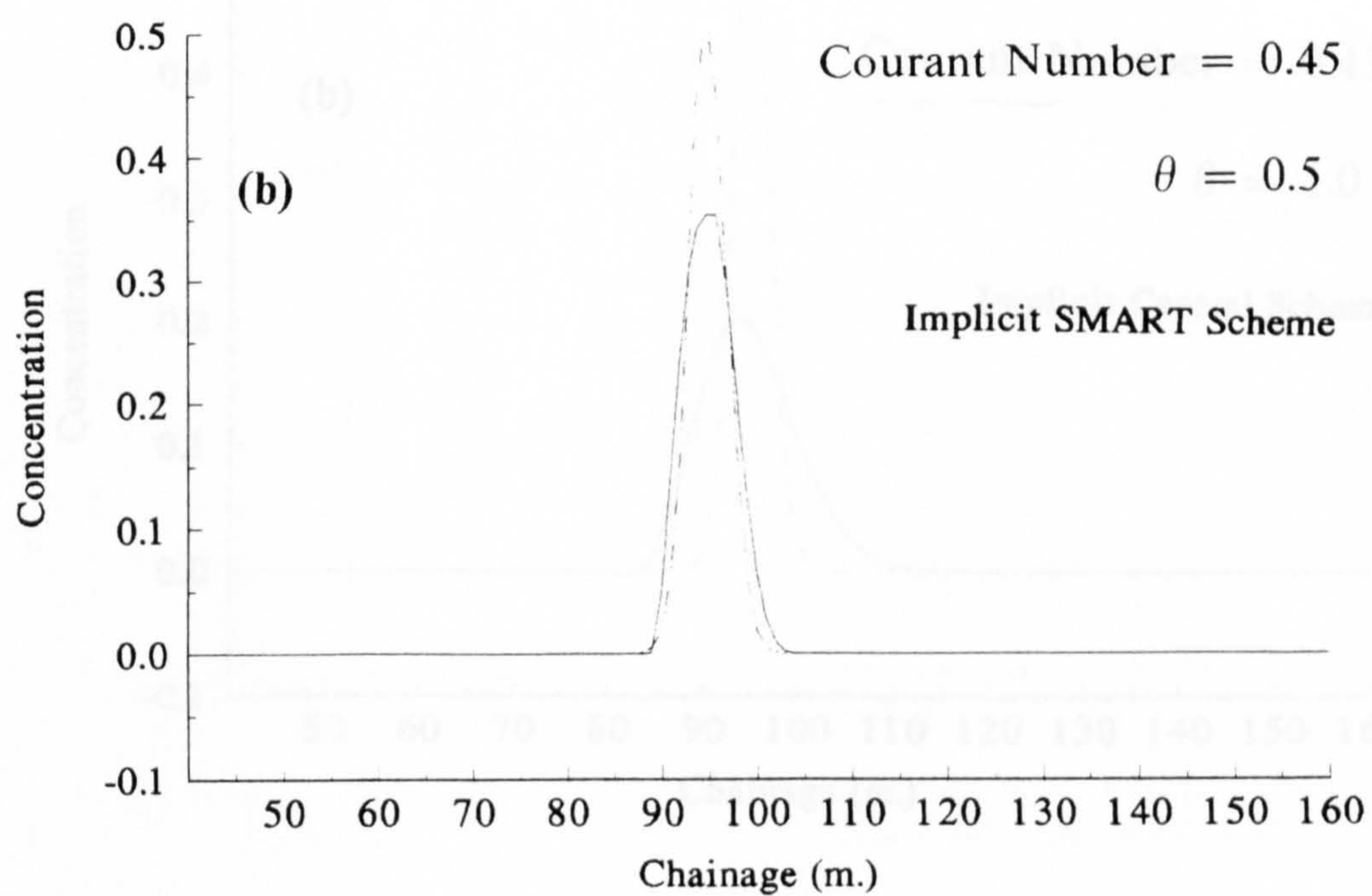
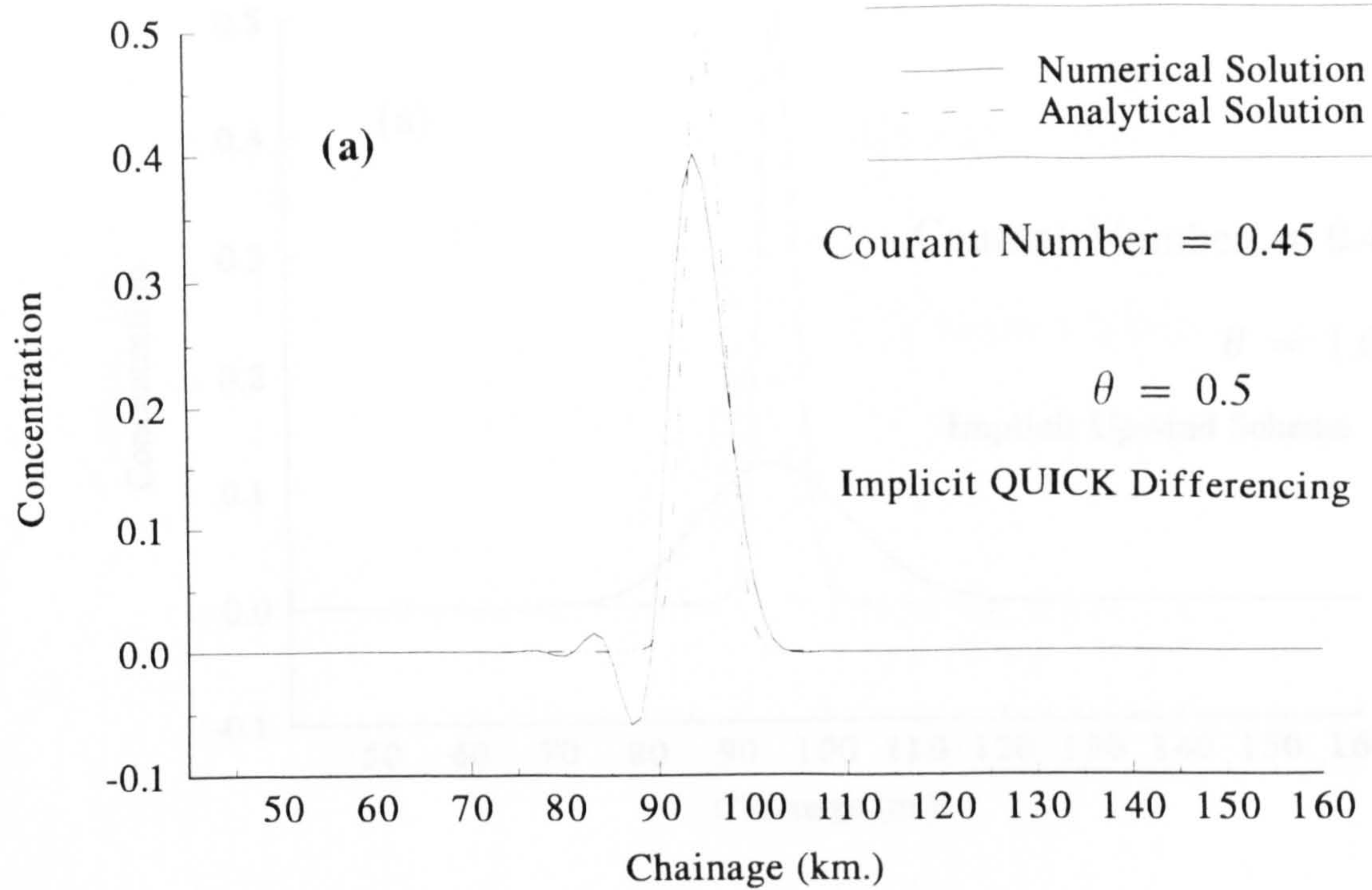


Figure 29. Results from more Implicit Schemes - QUICK, SMART

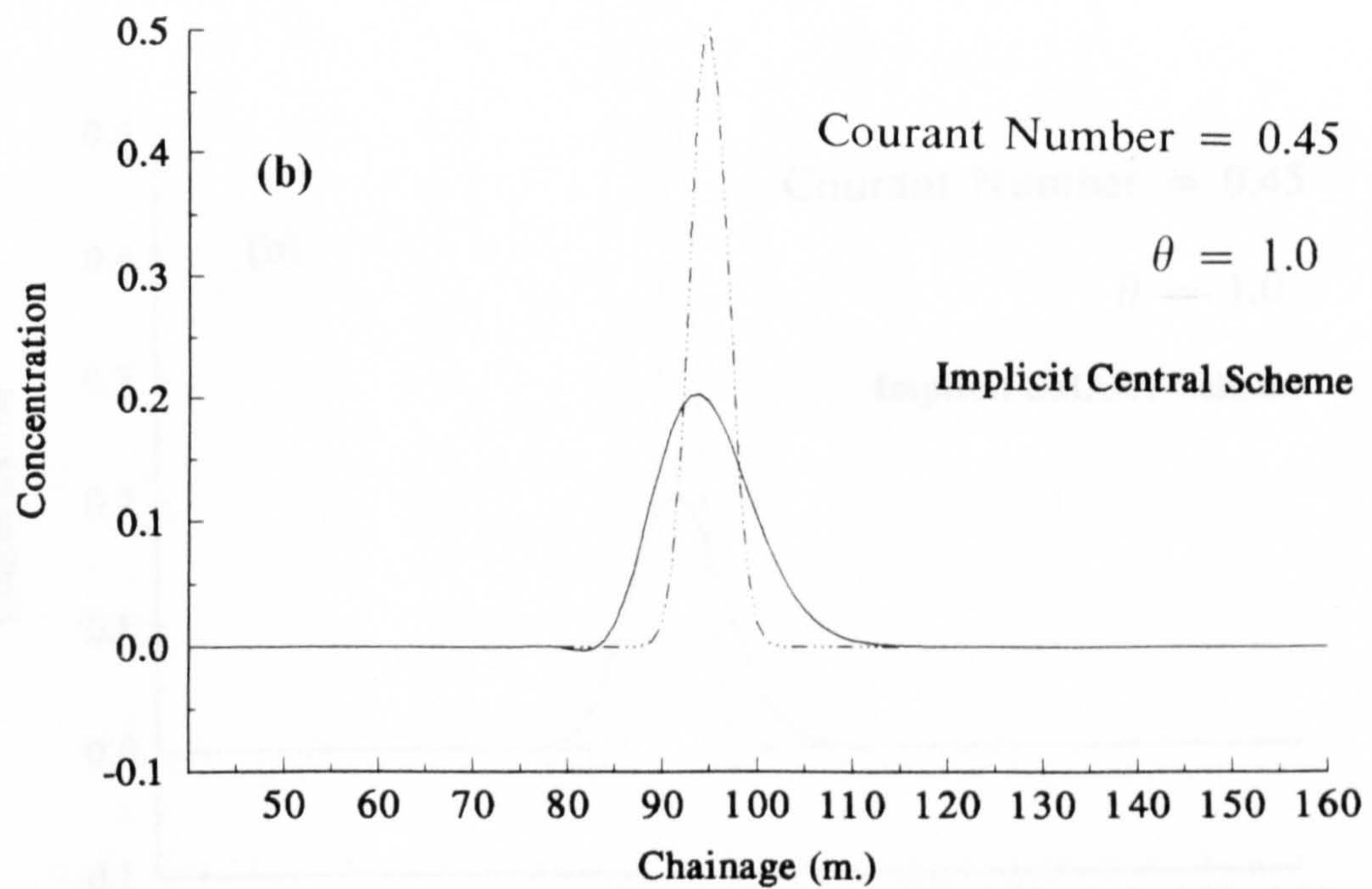
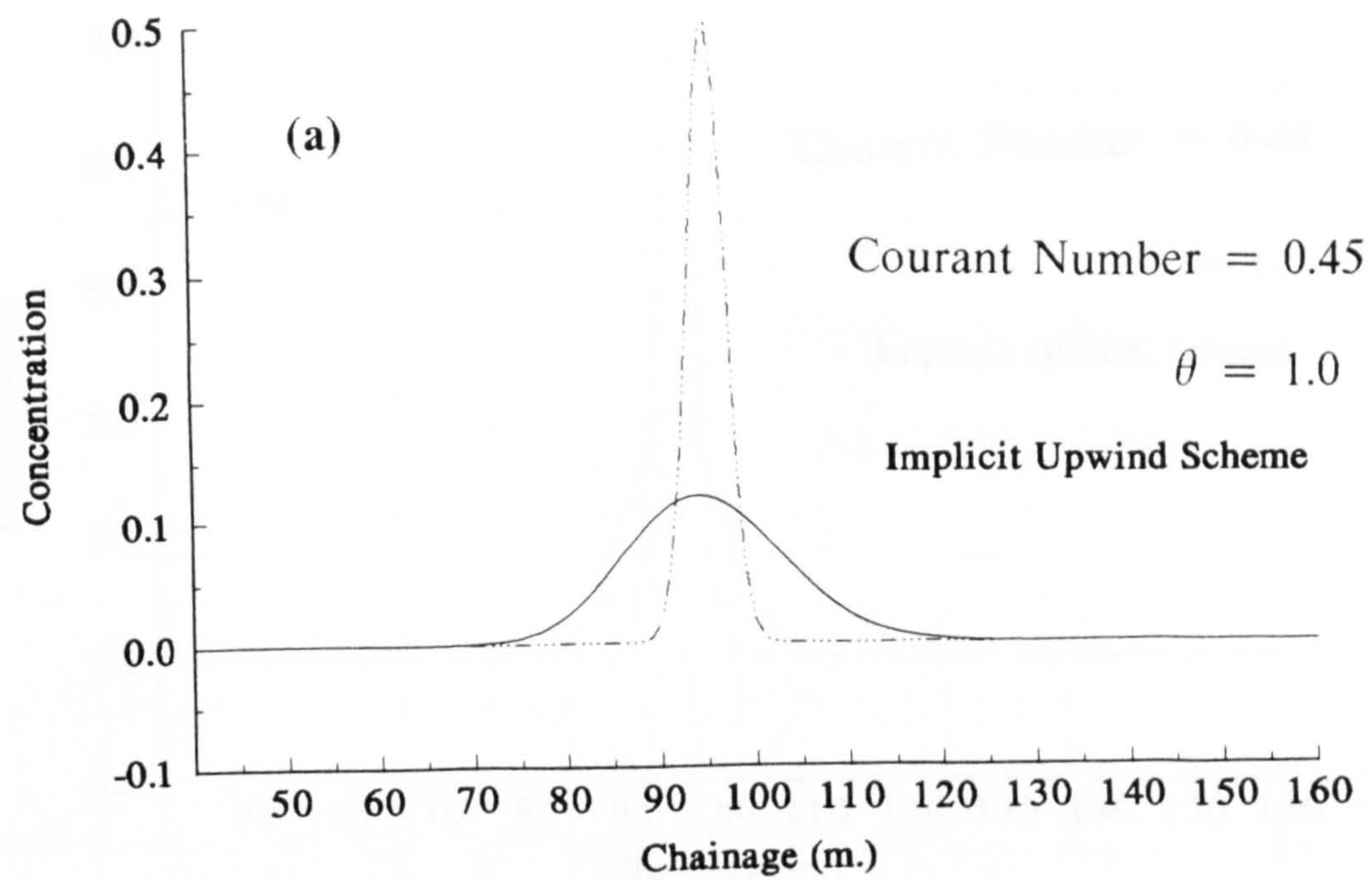


Figure 30. Results from Implicit Schemes - Upwind, Central

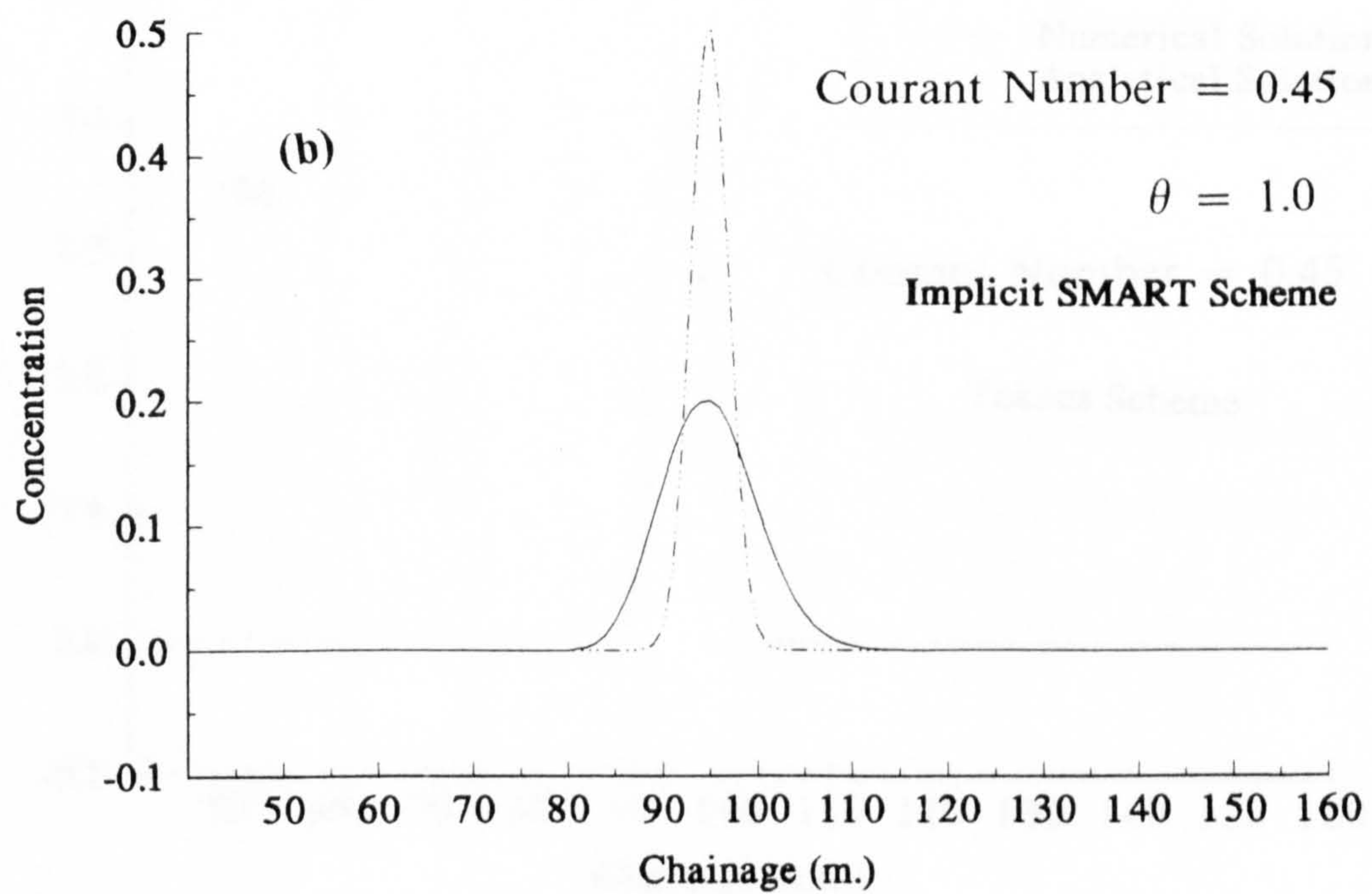
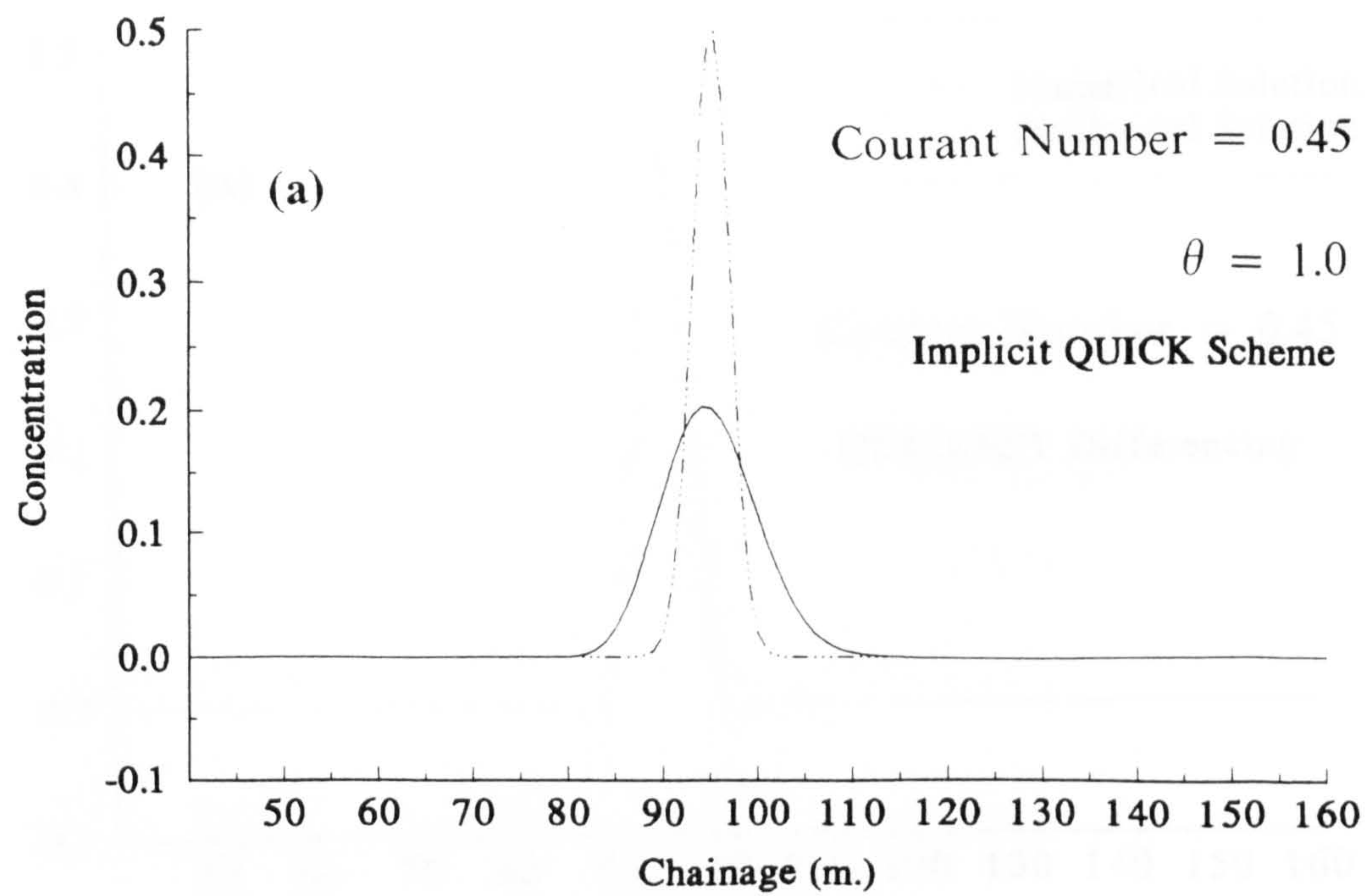


Figure 31. Results from Implicit Schemes - QUICK, SMART

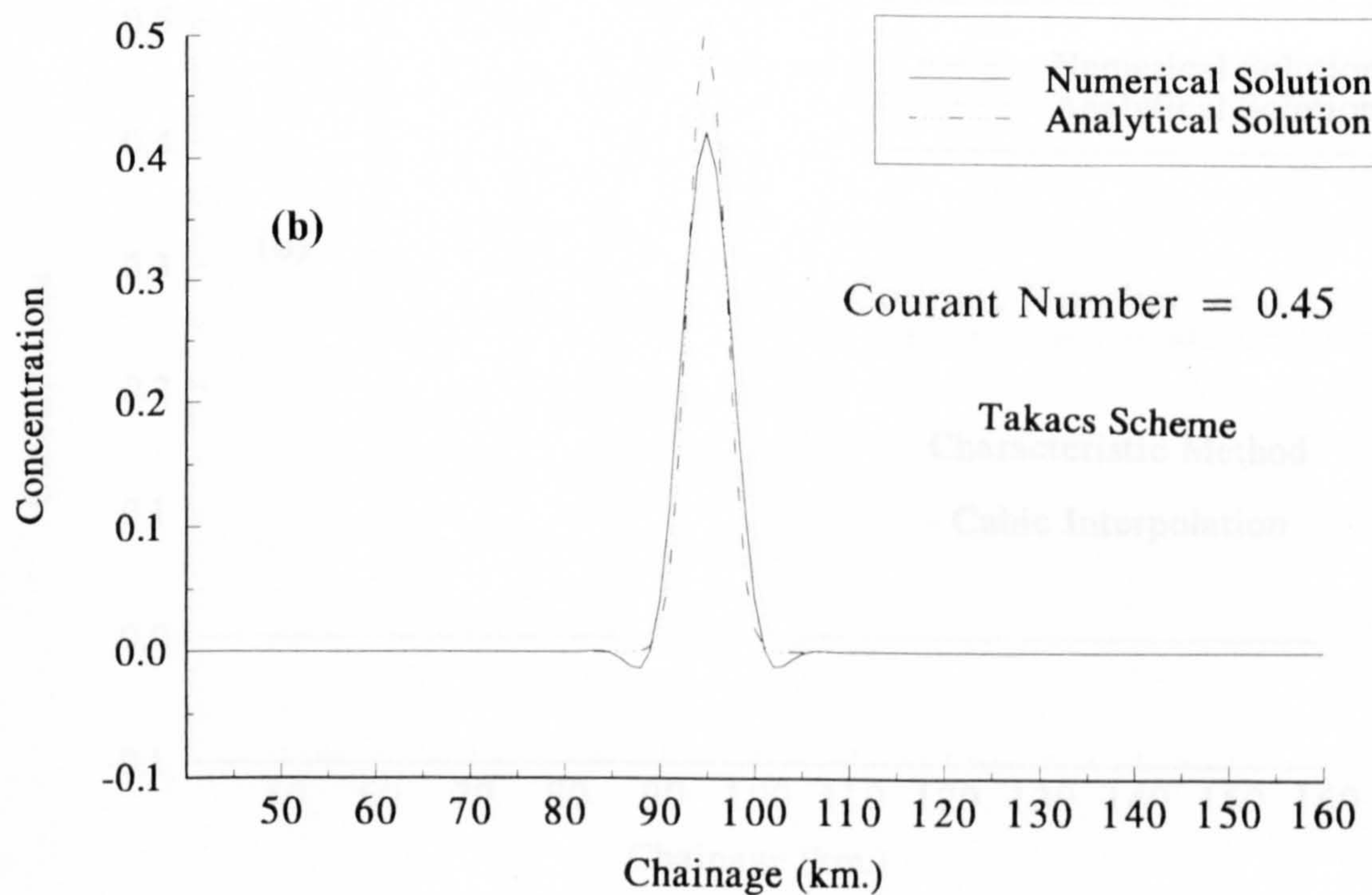
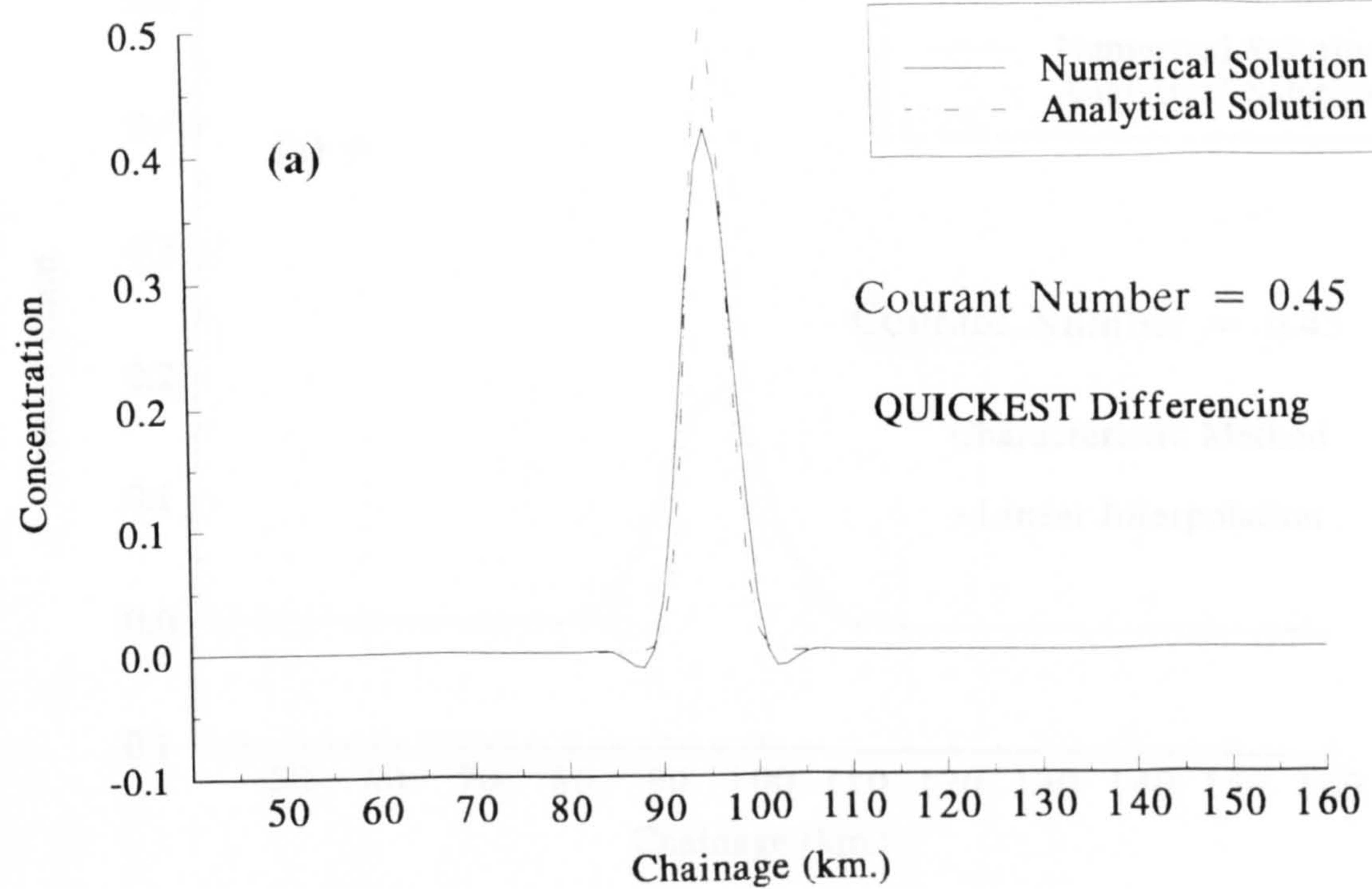
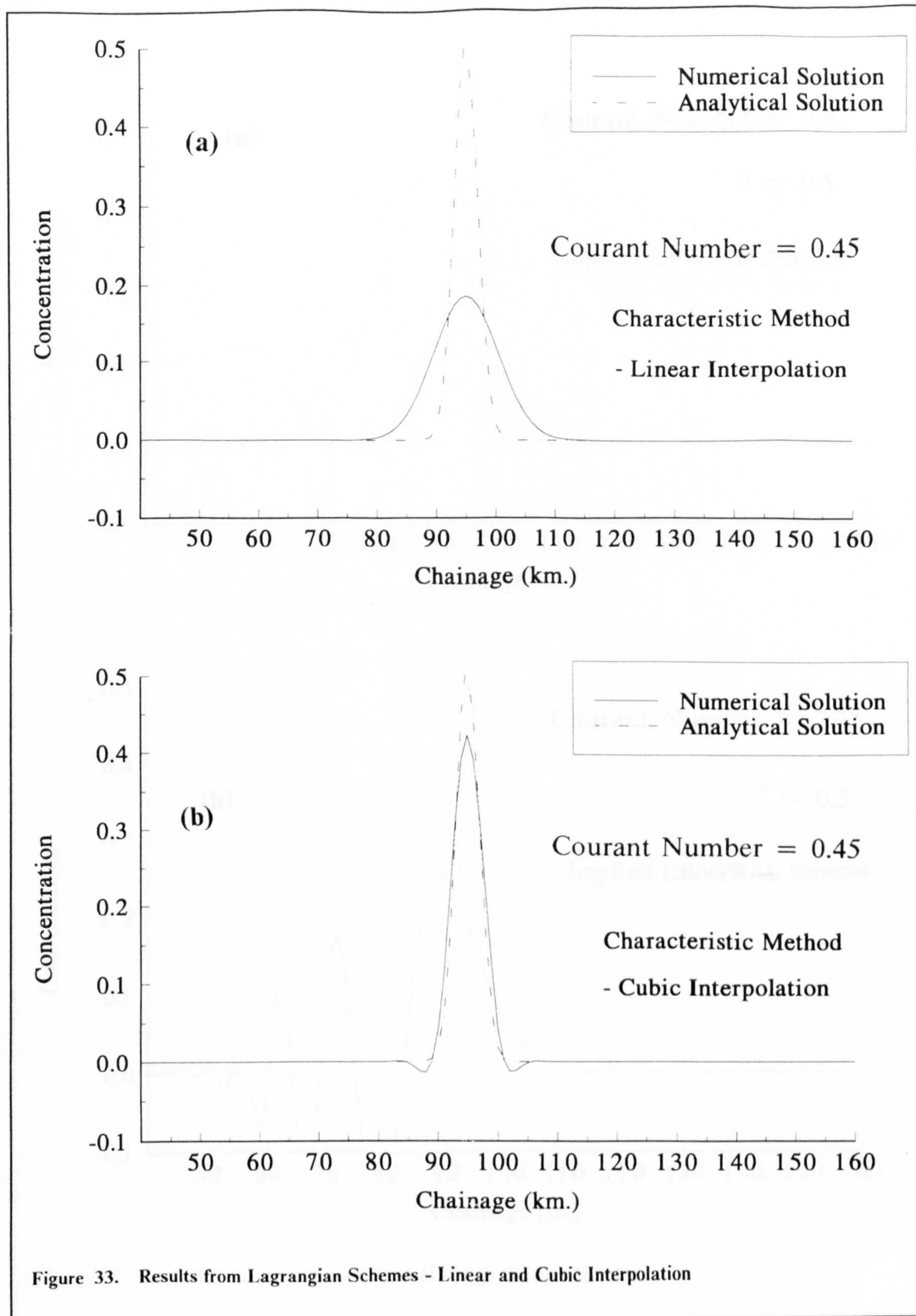


Figure 32. Results from Explicit schemes - QUICKEST, TAKACS



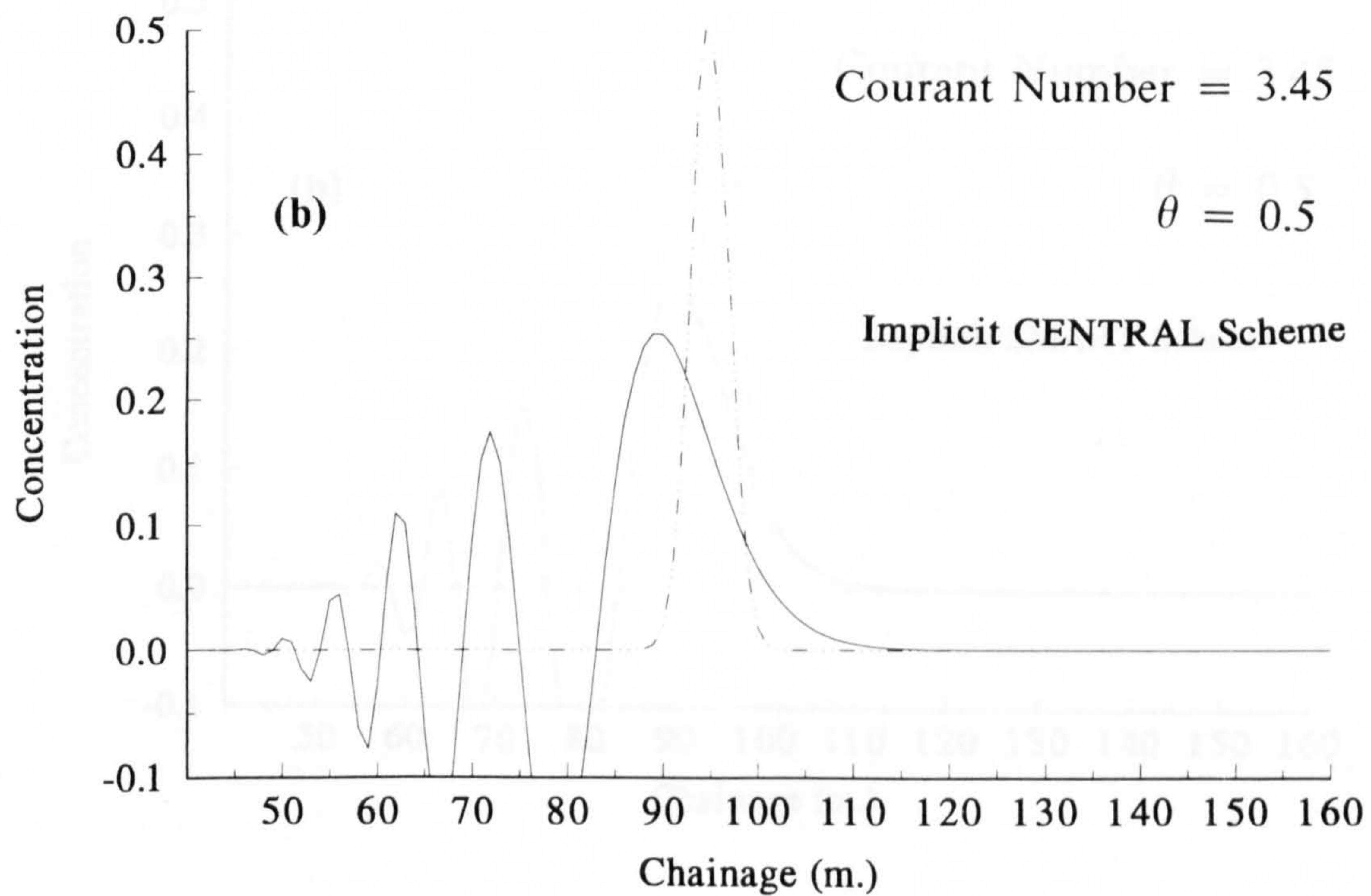
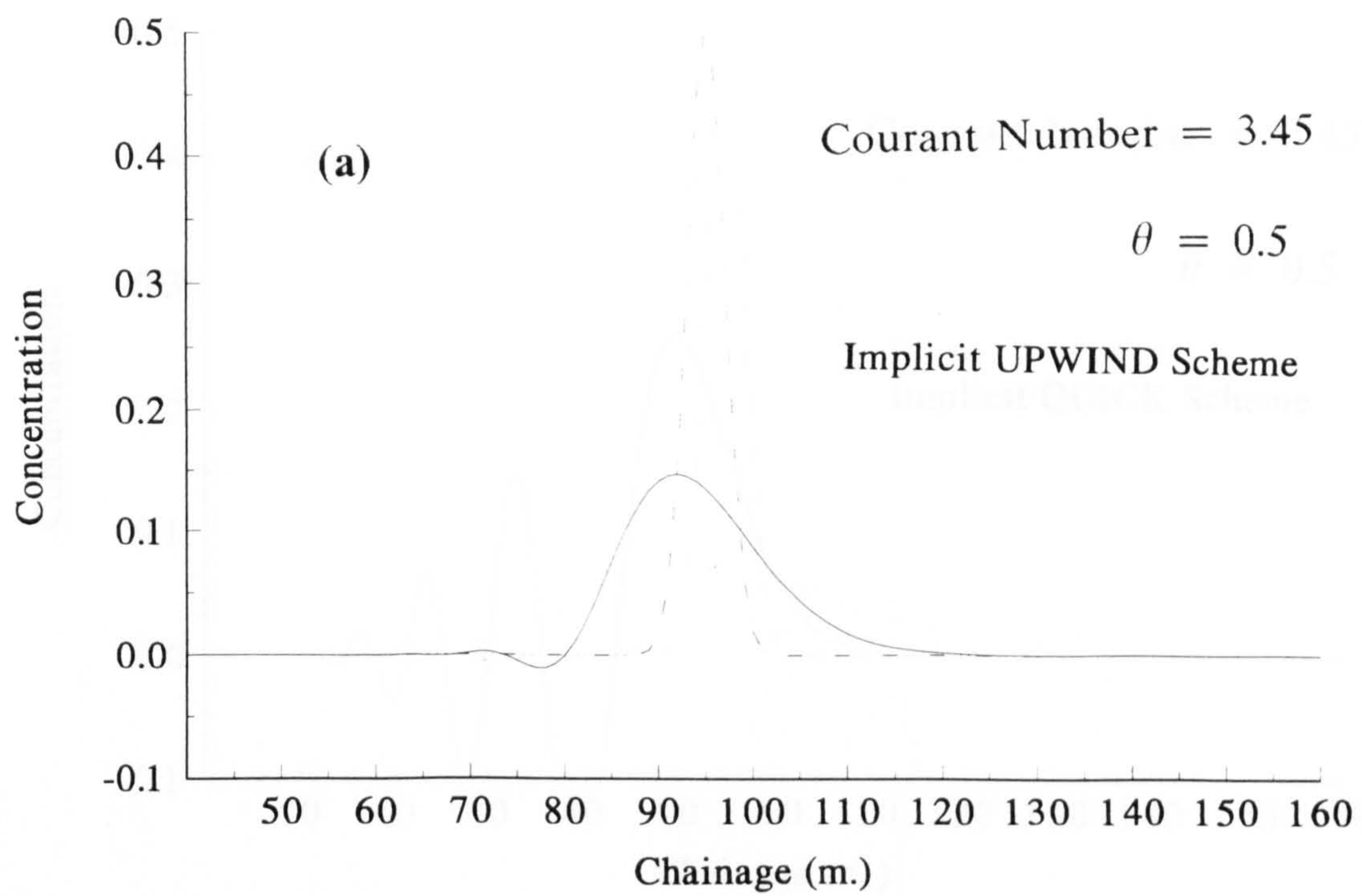


Figure 34. Implicit Schemes - Upwind, Central - High Courant Number

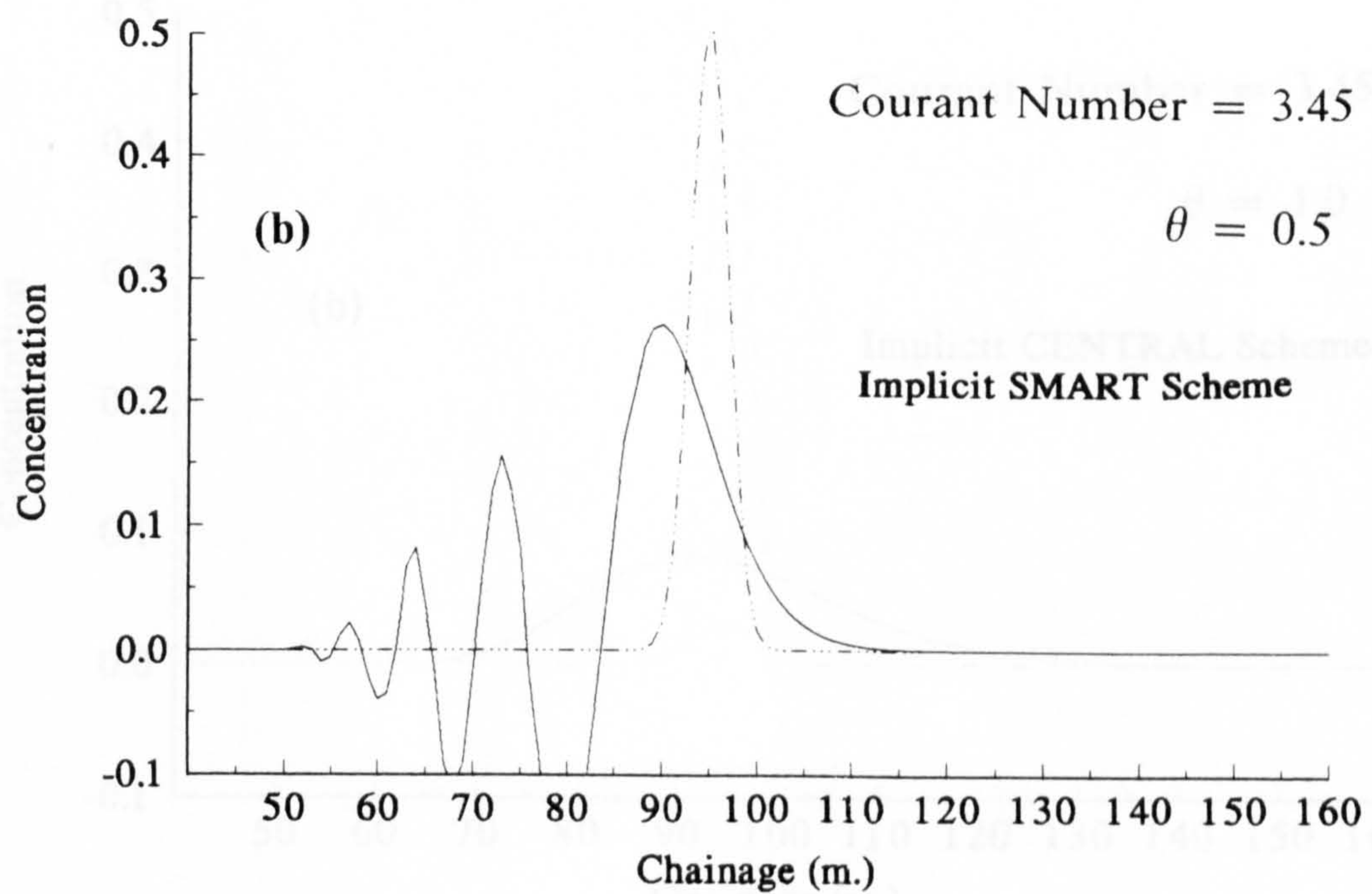
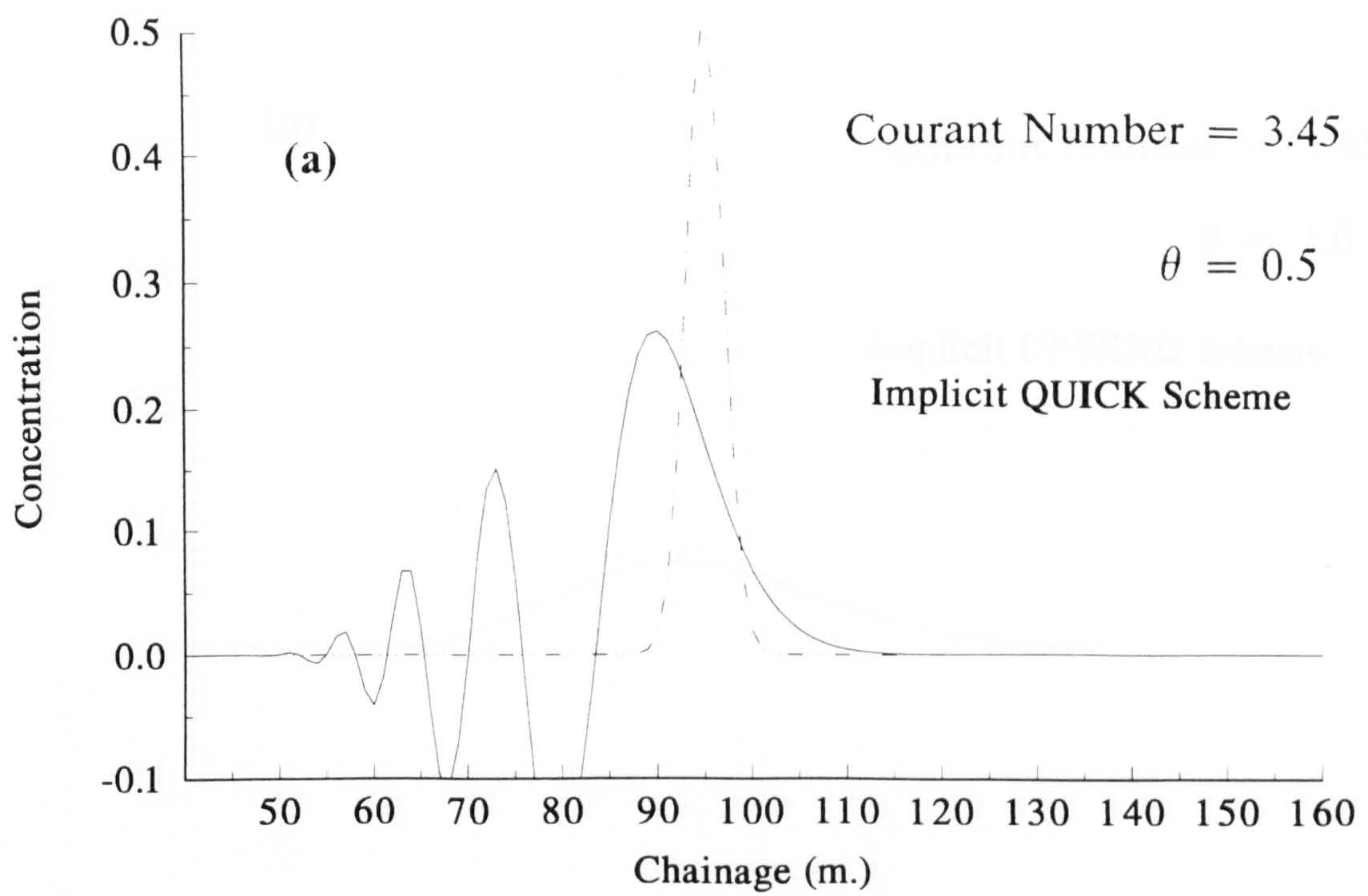


Figure 35. Implicit Schemes - QUICK, SMART - High Courant Number

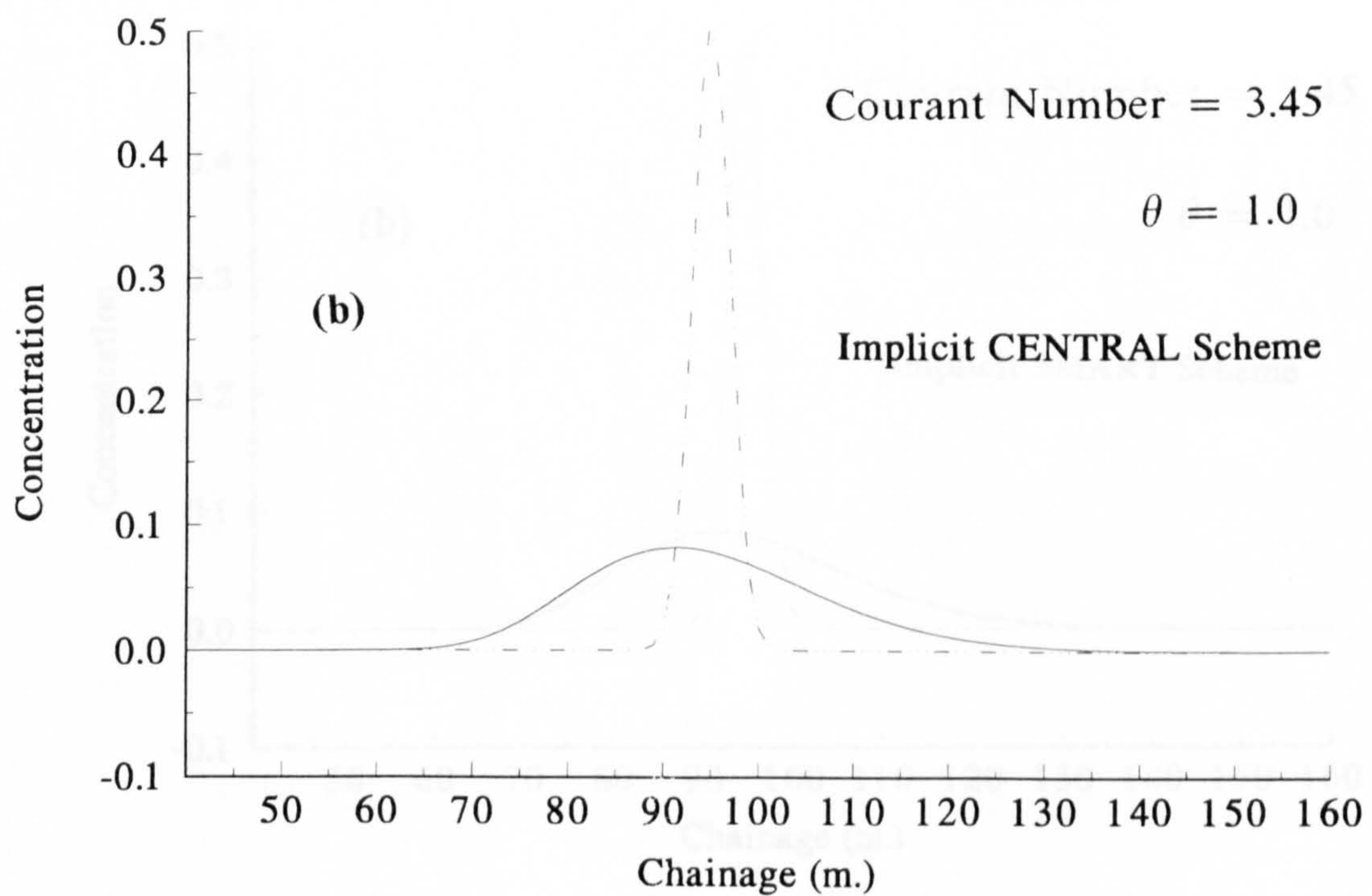
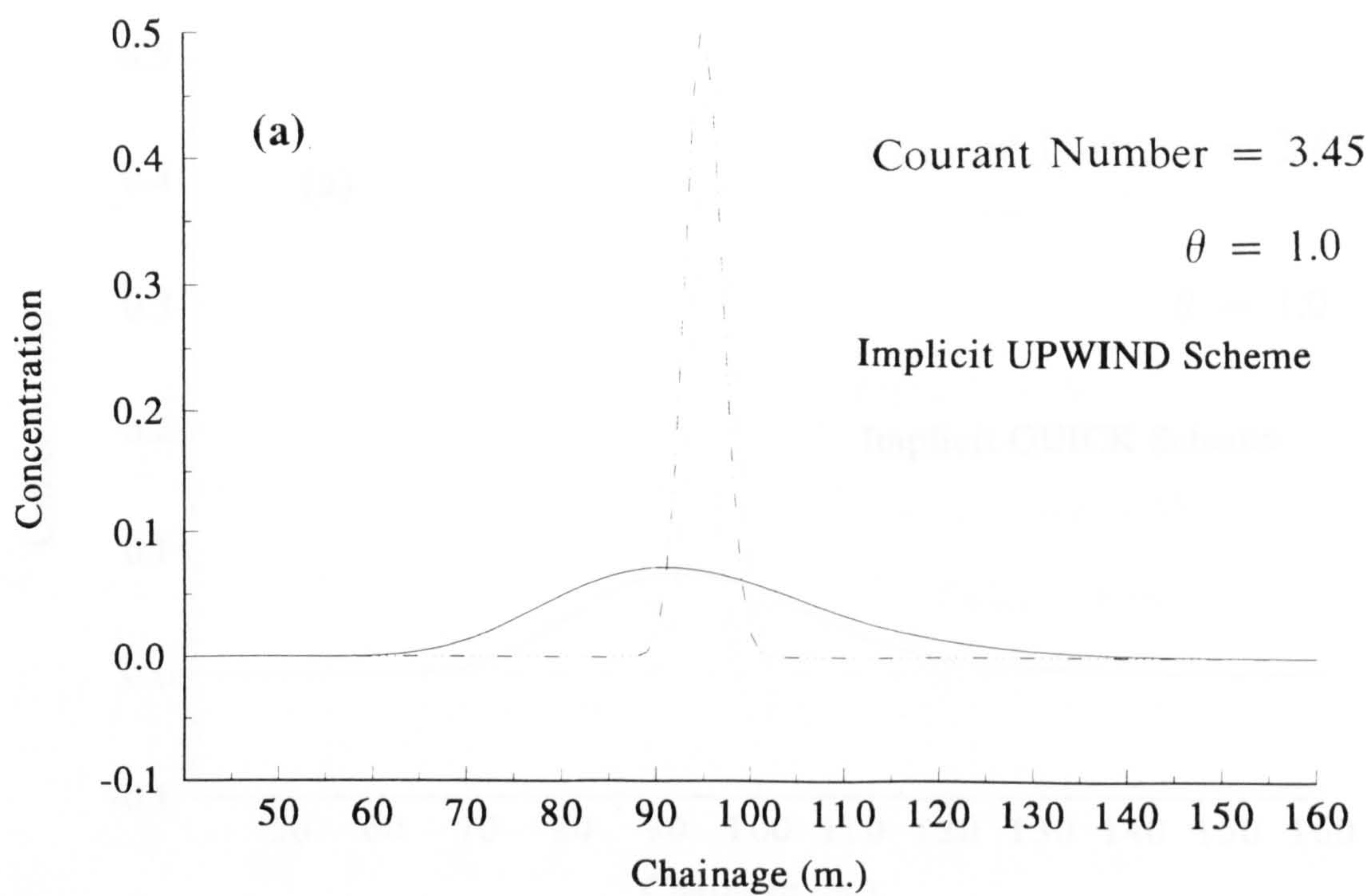


Figure 36. Implicit Schemes - Upwind, Central - High Courant Number

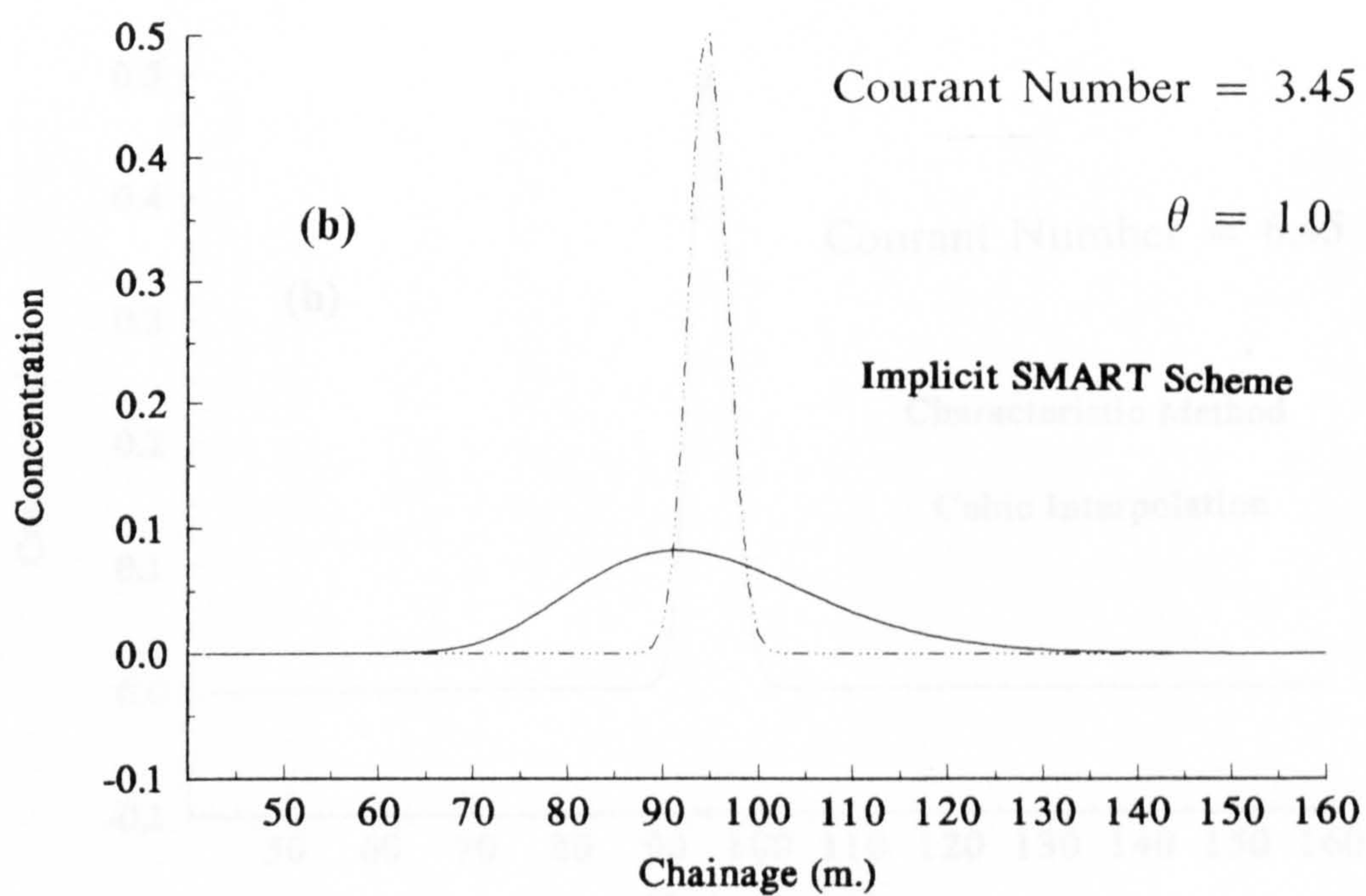
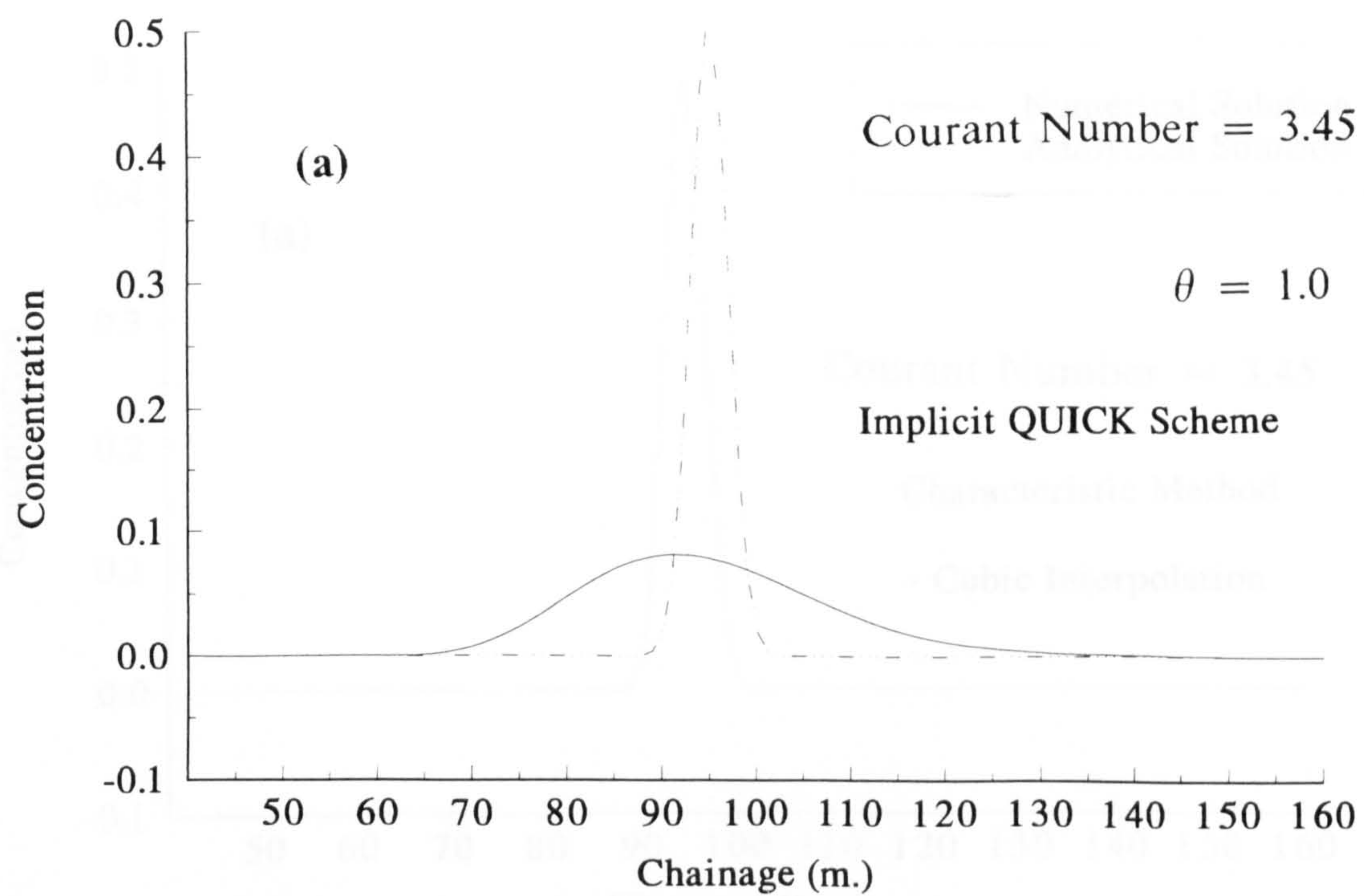


Figure 37. Implicit Schemes - QUICK, SMART - High Courant Number

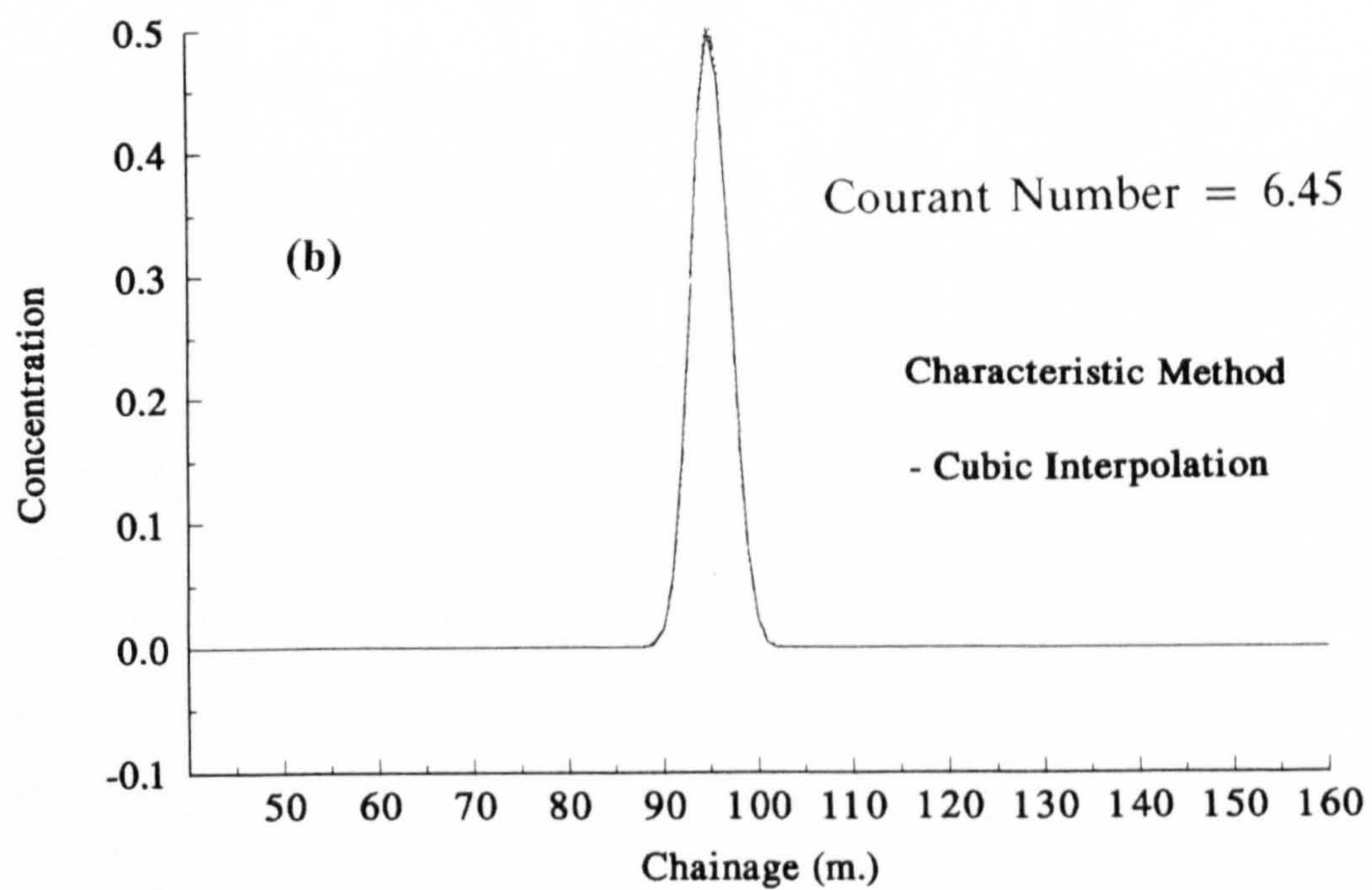
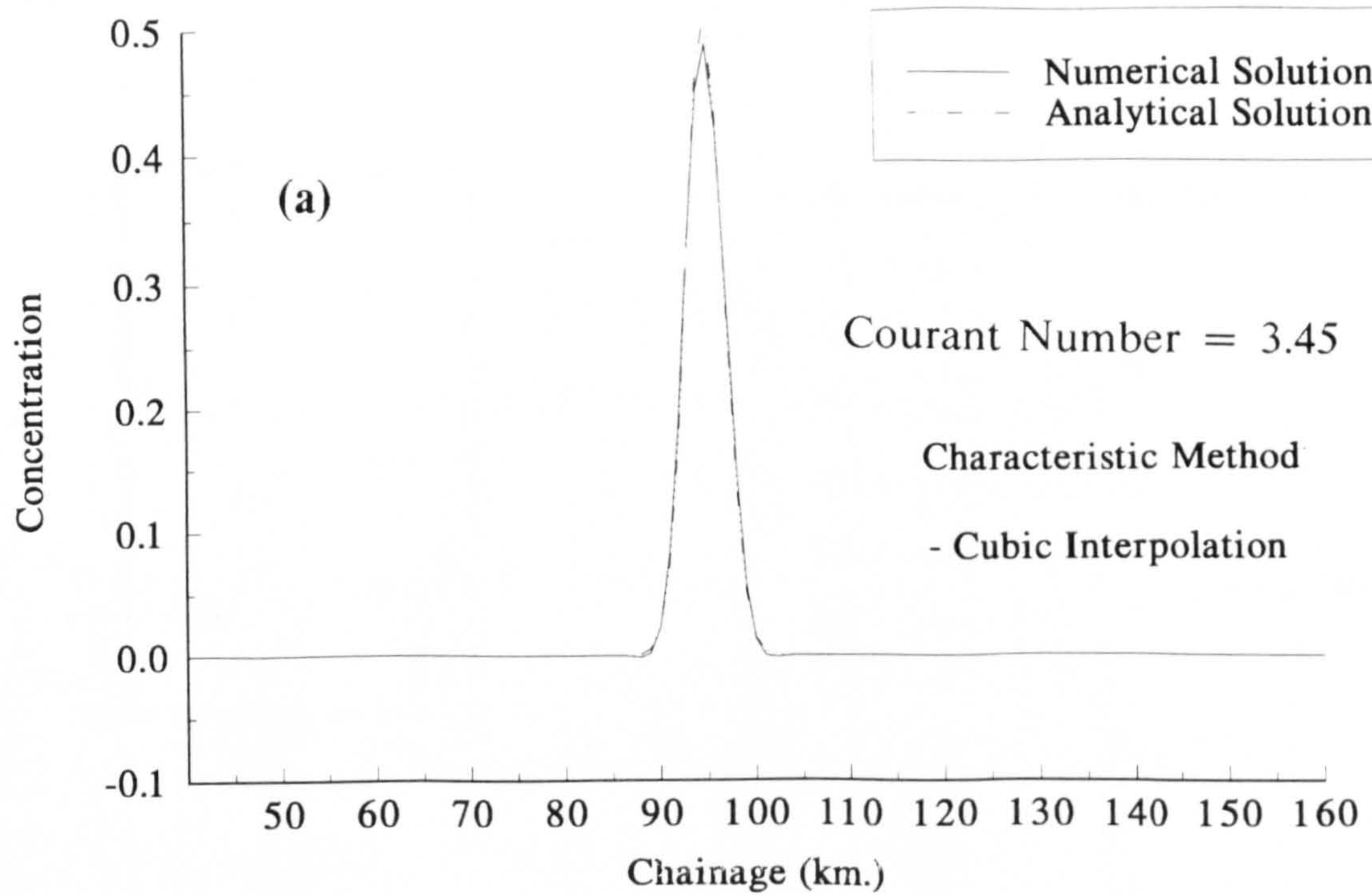
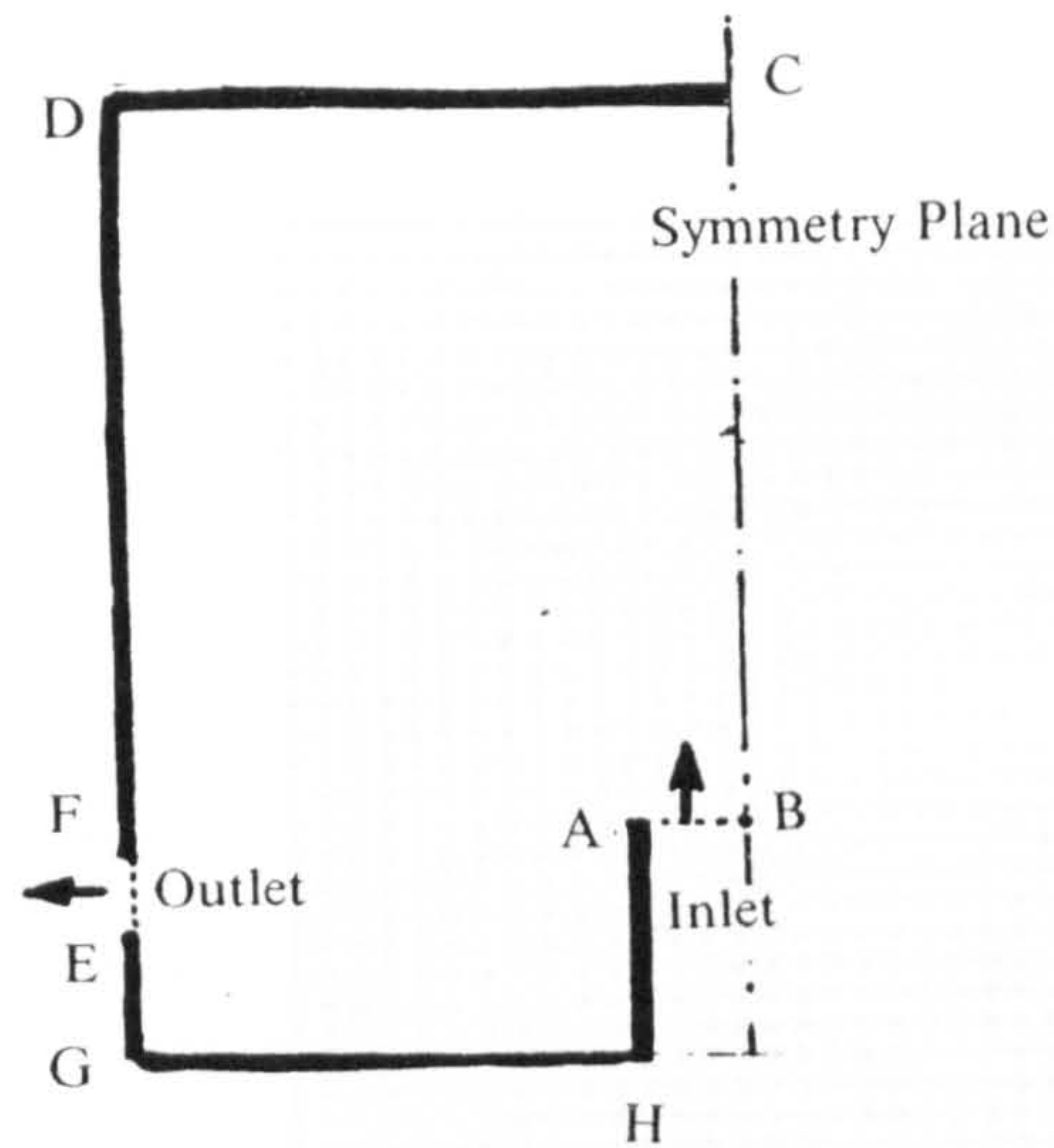


Figure 38. Lagrangian Schemes - Cubic Interpolation - High Courant Number

Results for Cavity Flow - Boyle and Golay (1983)

Geometry of Boyle and Golay (1983)



Dimensions

$$GD = 24 \text{ cm.}$$

$$GE = 3 \text{ cm.}$$

$$EF = 2 \text{ cm.}$$

$$DC = 16 \text{ cm.}$$

$$HA = 6 \text{ cm.}$$

$$AB = 3 \text{ cm.}$$

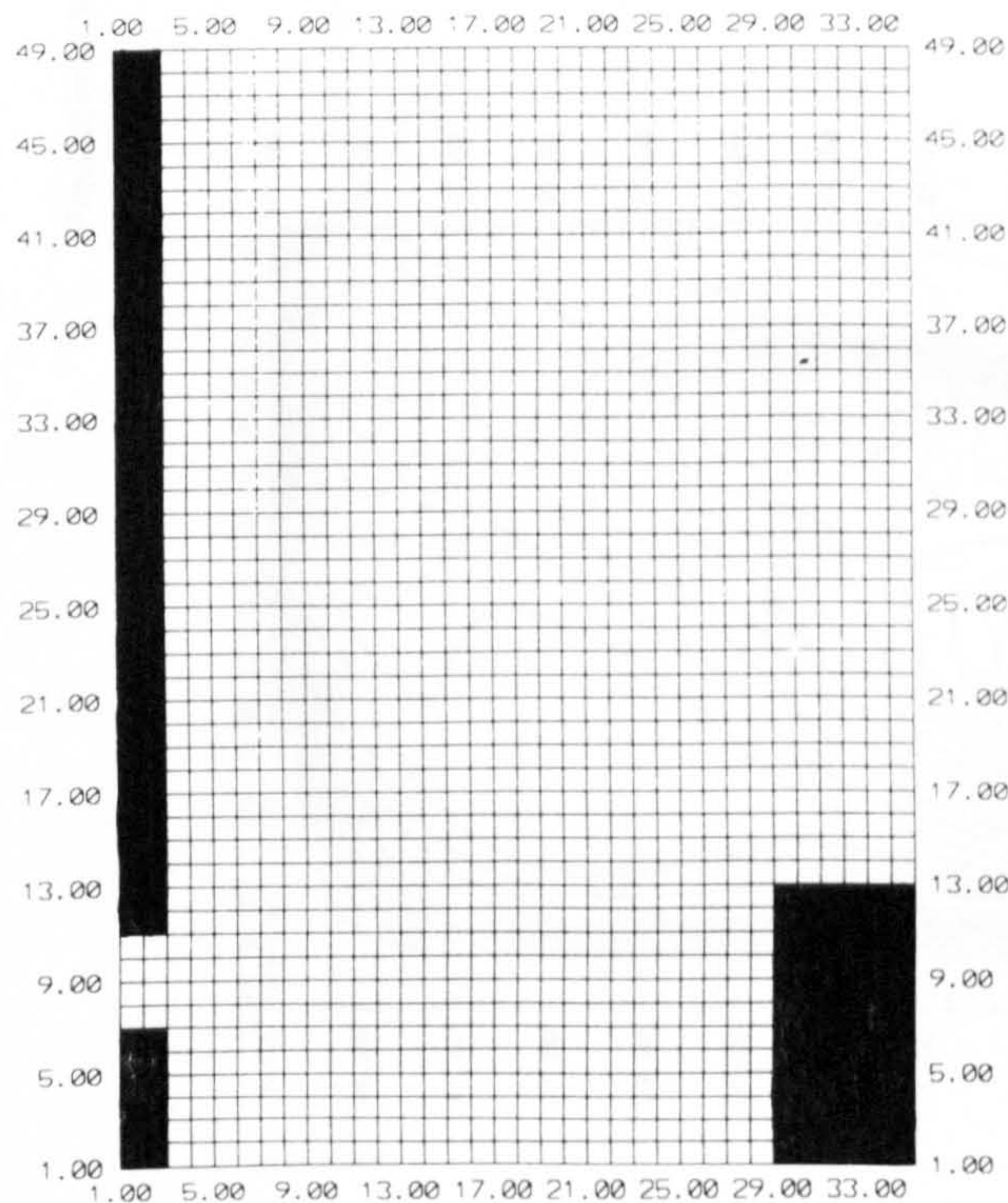
Inlet Conditions

$$u_{inlet} = 0.0 \text{ cm/s}$$

$$w_{inlet} = 80.0 \text{ cm/s}$$

$$k_{inlet} = 250.0 \frac{\text{cm}^2}{\text{s}^2}$$

$$\varepsilon_{inlet} = 1250.0 \frac{\text{cm}^2}{\text{s}^3}$$



Computational Grid 35 x 49

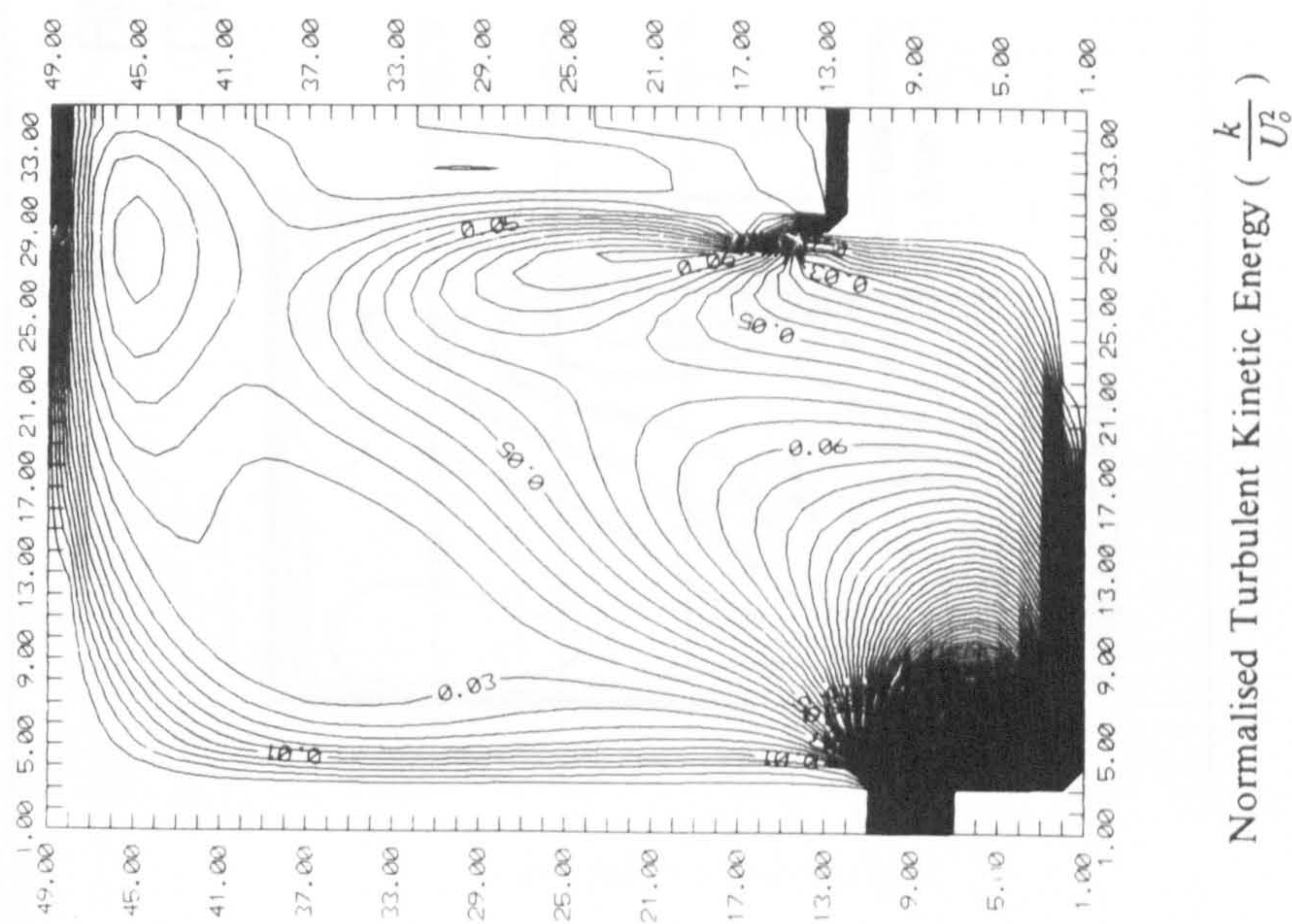
$$\Delta x = 0.5 \text{ cm.}$$

$$\Delta z = 0.5 \text{ cm.}$$

$$U_o = 80.0 \text{ cm/s} \quad L_o = 2.0 \text{ cm.}$$

Figure 39. Geometry and Computational Details

Predictions with Linear Model



Velocity Field

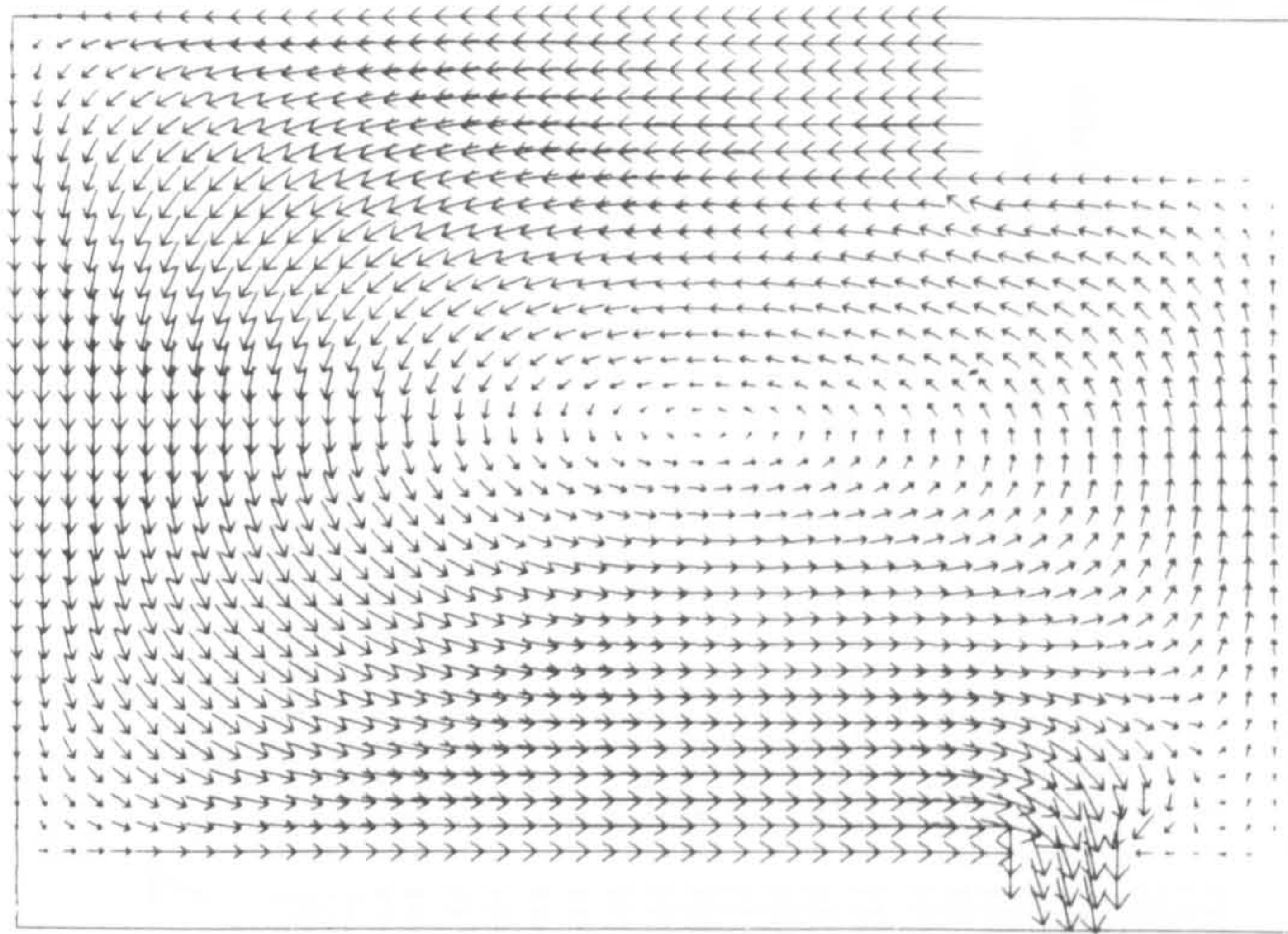


Figure 40. Predicted By Linear Model - Vectors and Contours of normalised k

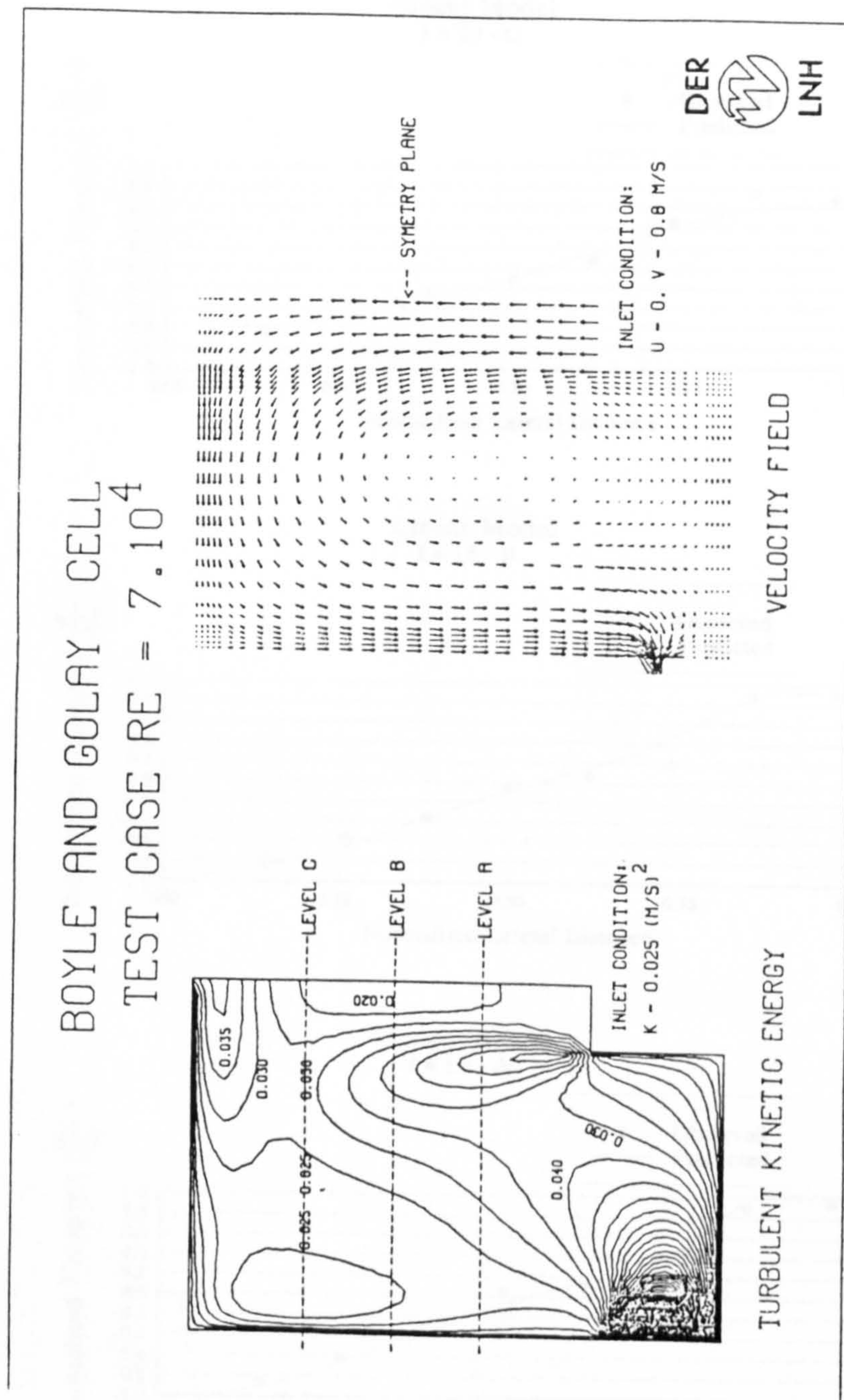


Figure 41. Predicted By Other Research Group - Vectors and Contours of k

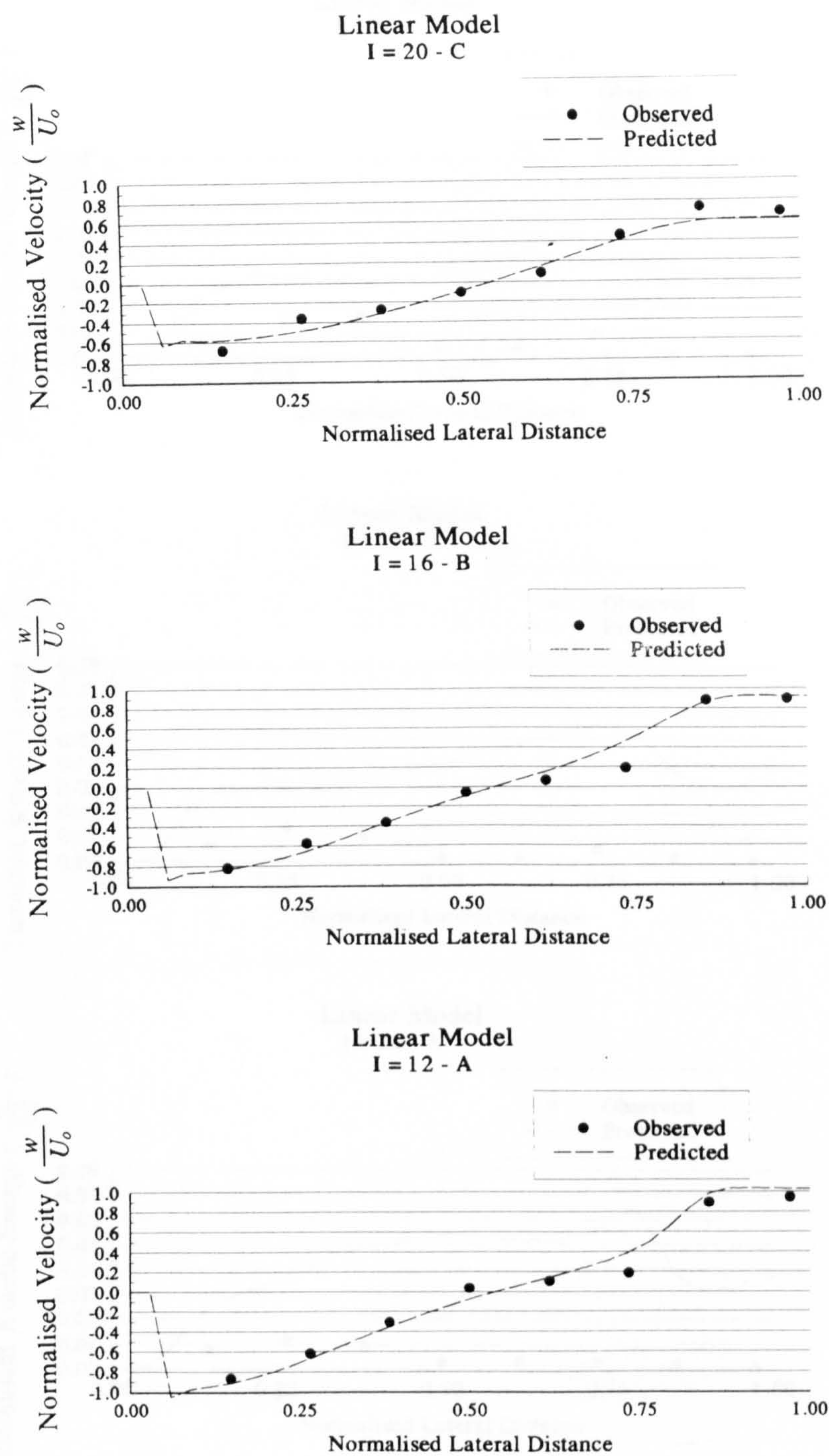
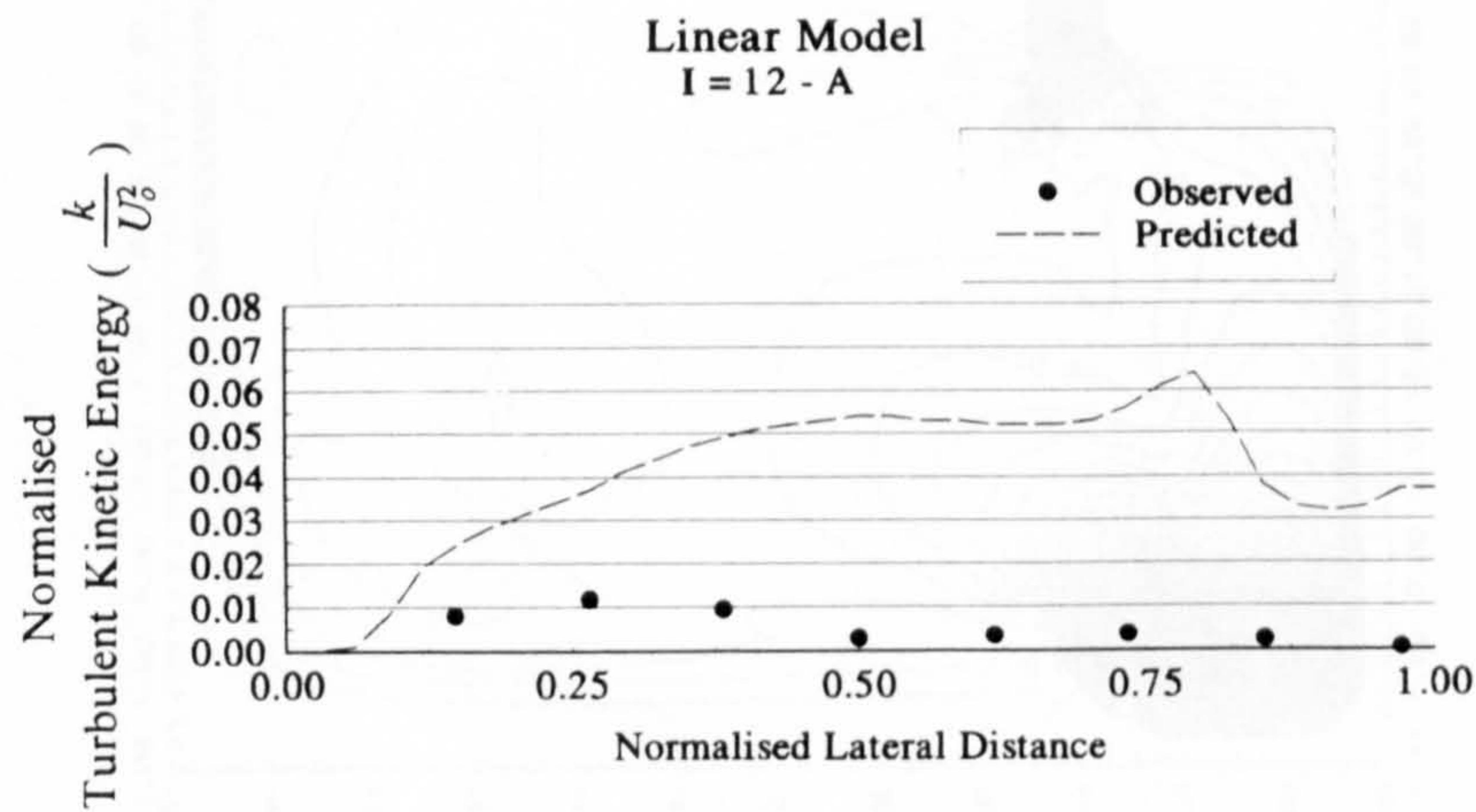
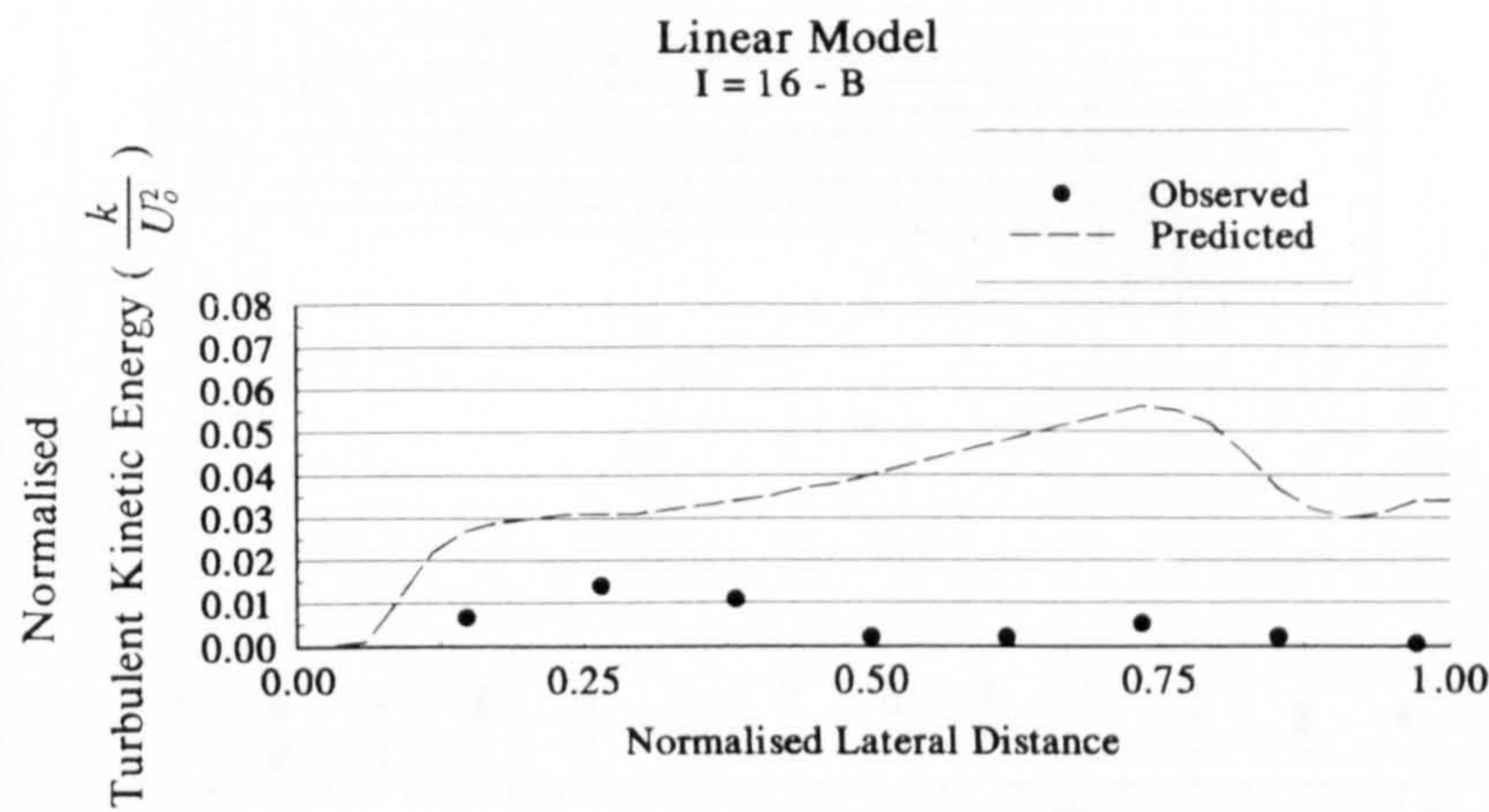
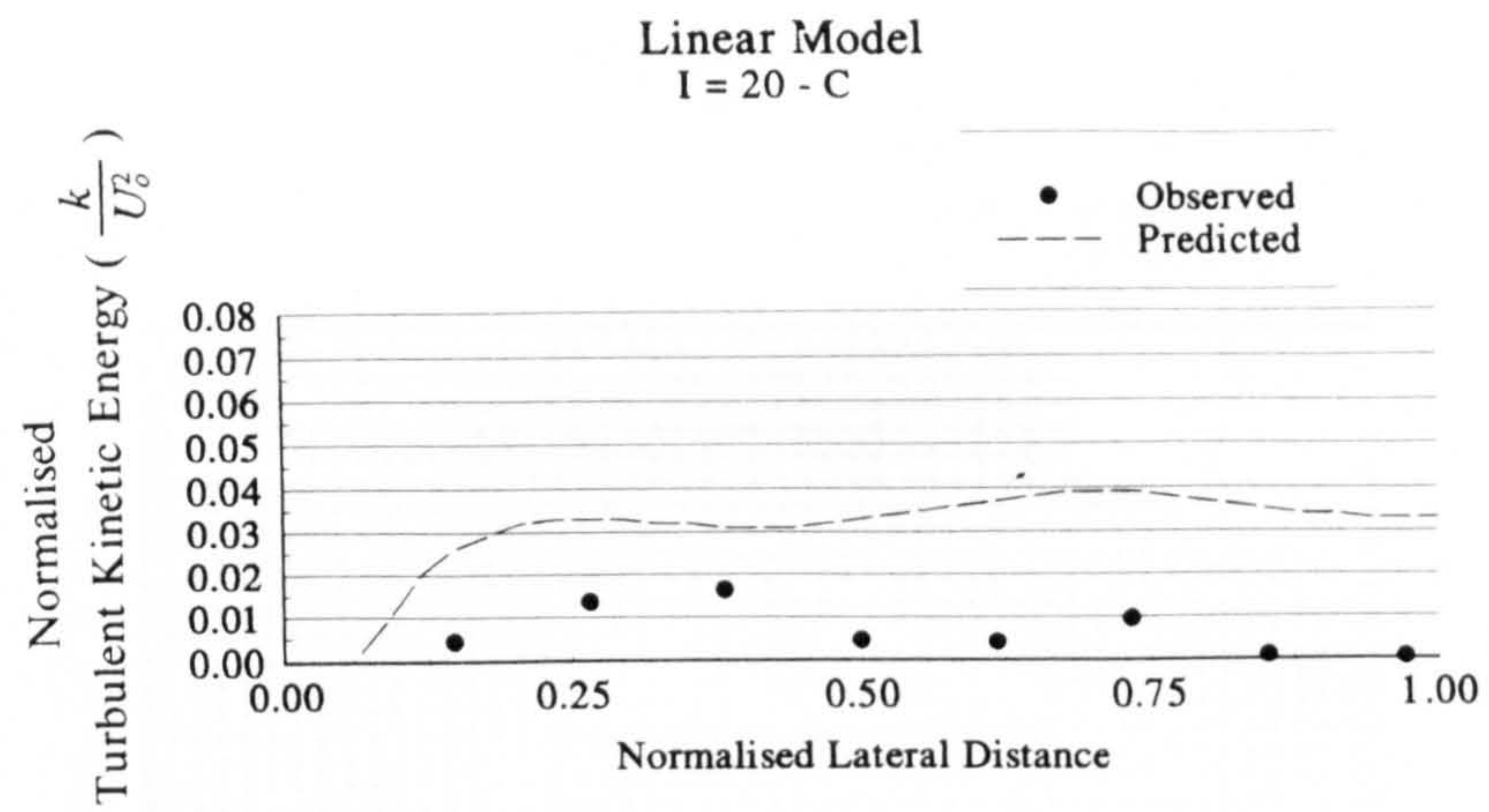


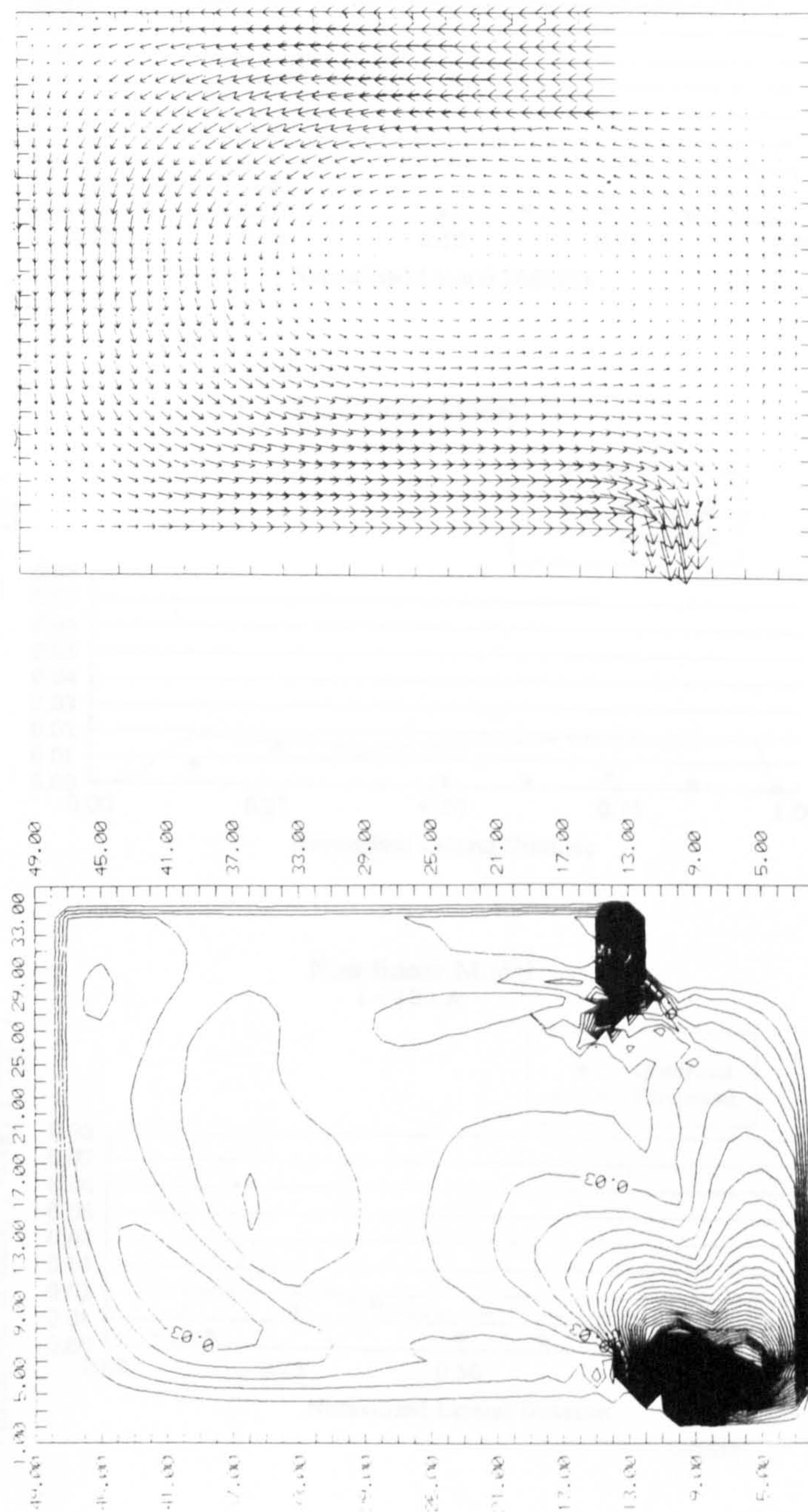
Figure 42. Comparison with experimental data - Velocity Profiles



where $k = \frac{1}{2} (\overline{u'^2} + \overline{w'^2})$

Figure 43. Comparison with experimental data - Normalised k Profiles

Predictions with Non-Linear Model



Velocity Field

Normalised Turbulent Kinetic Energy ($\frac{k}{U_0^2}$)

Figure 44. Predicted By Non-Linear Model - Vectors and Contours of normalised k

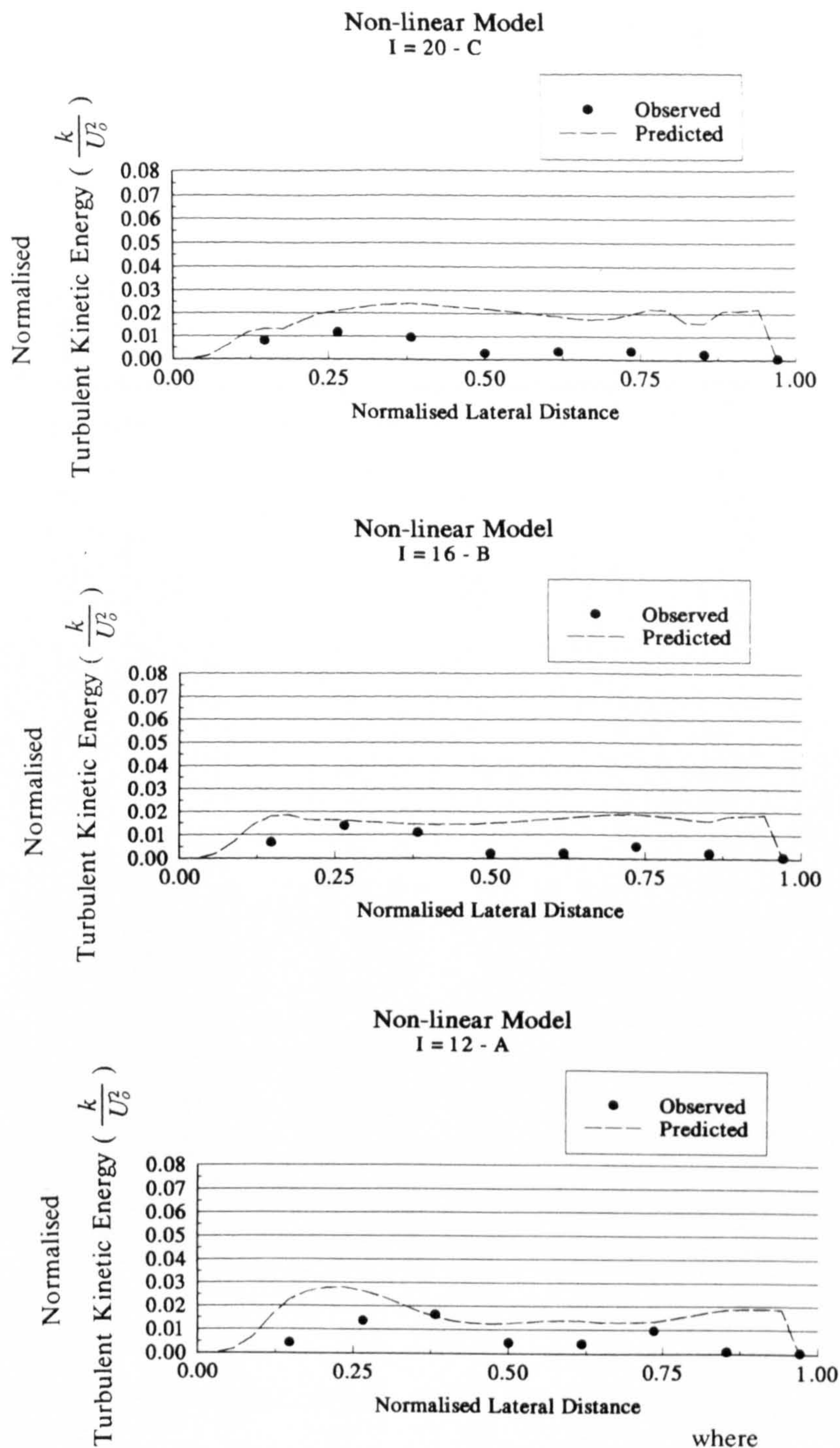
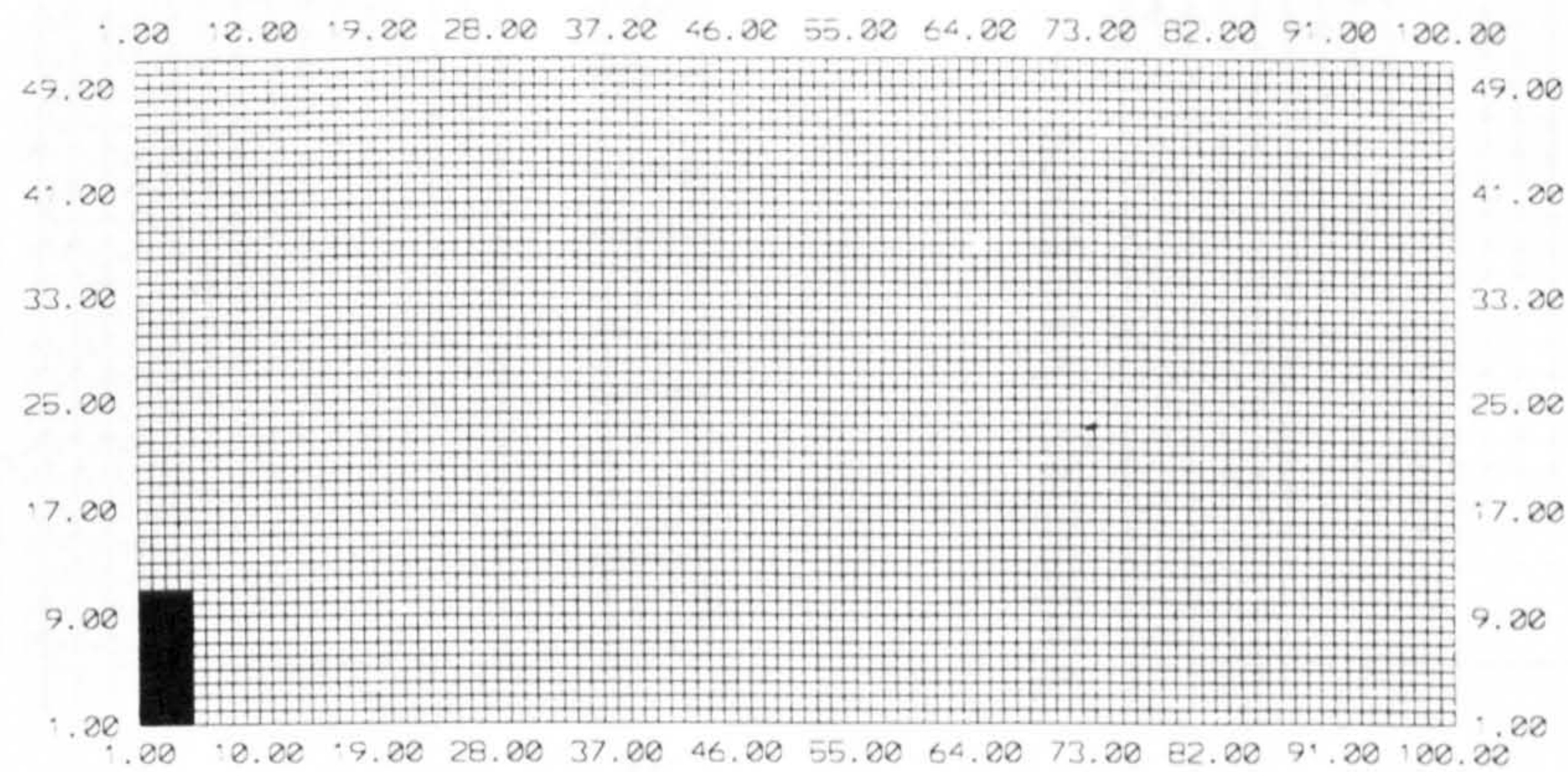
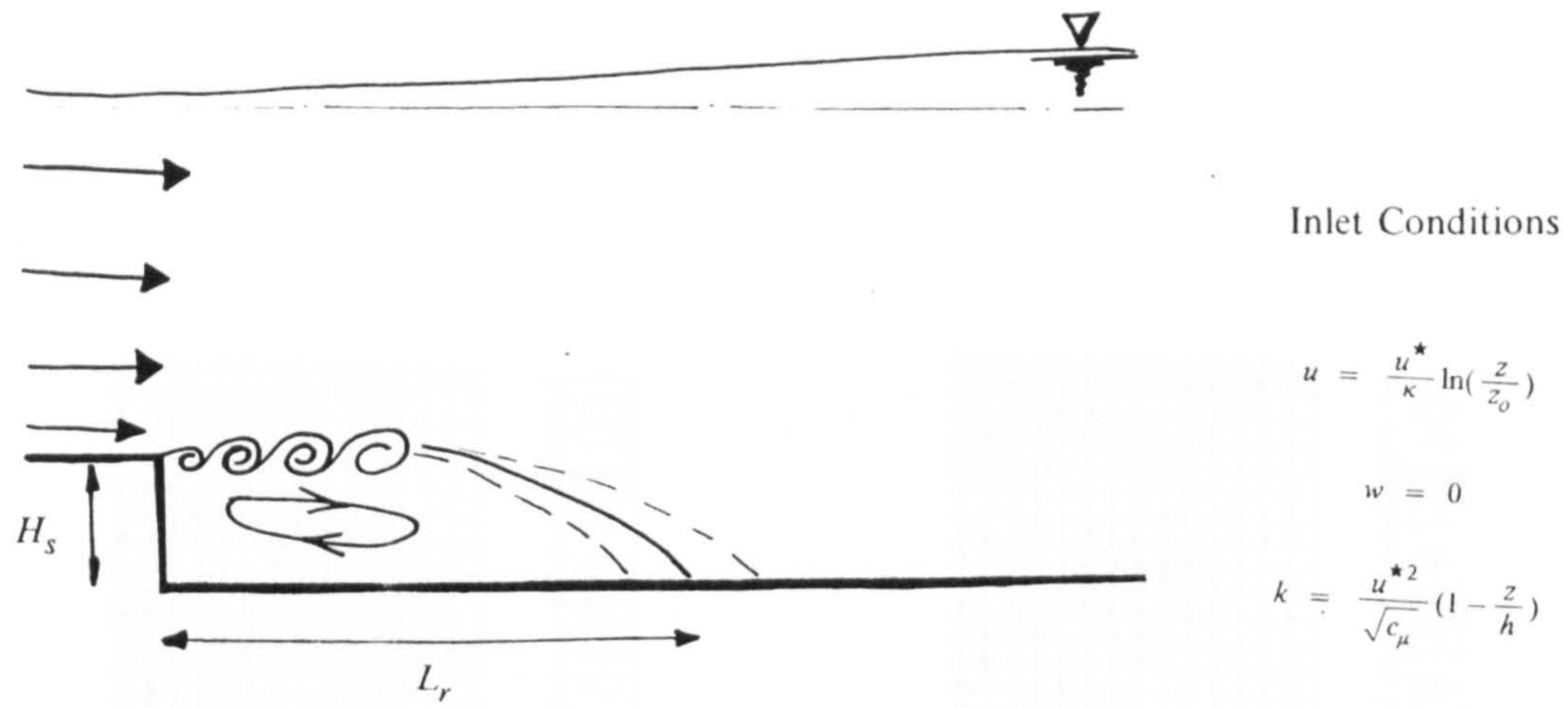


Figure 45. Comparison with experimental data - Normalised k Profiles

Open Channel Flow over a Step - Nezu



Computational Grid 100 x 51

$U_o = 29.2 \text{ cm/s}$ $L_o = H_s = 2.0 \text{ cm}$.

$\Delta x = 0.4 \text{ cm}$.

$\Delta z = 0.2 \text{ cm}$.

Figure 46. Geometry and Computational Details

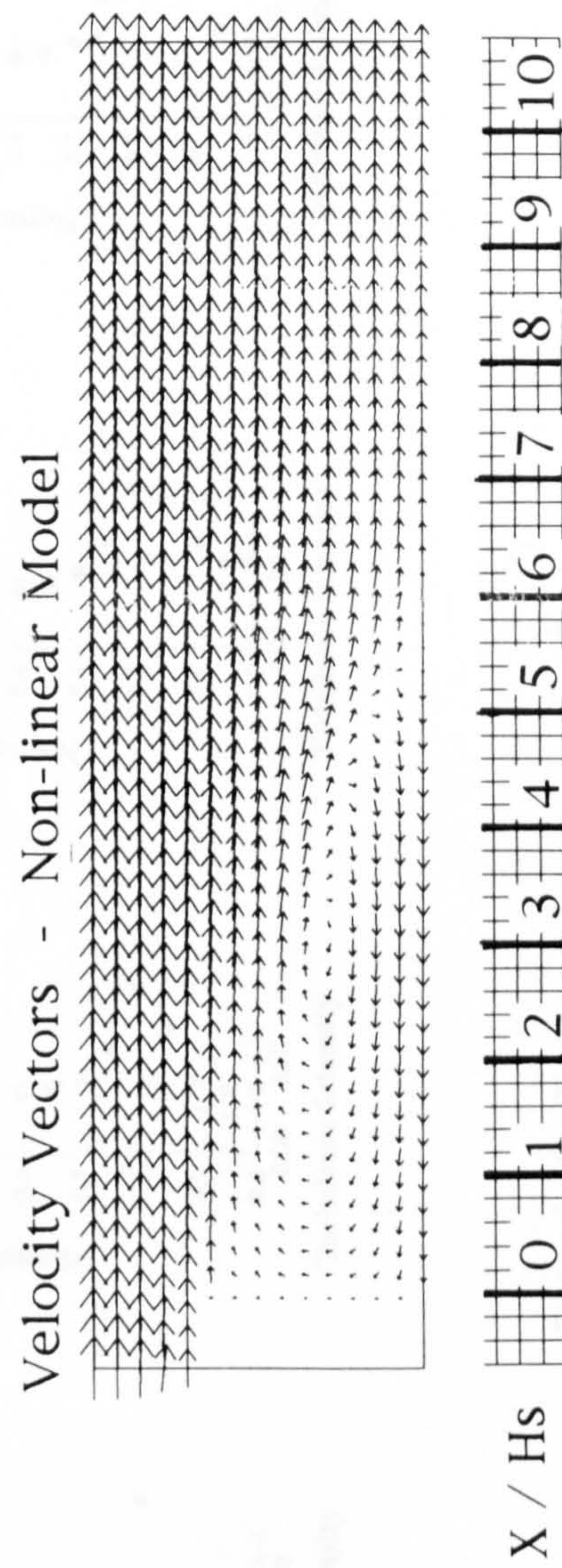
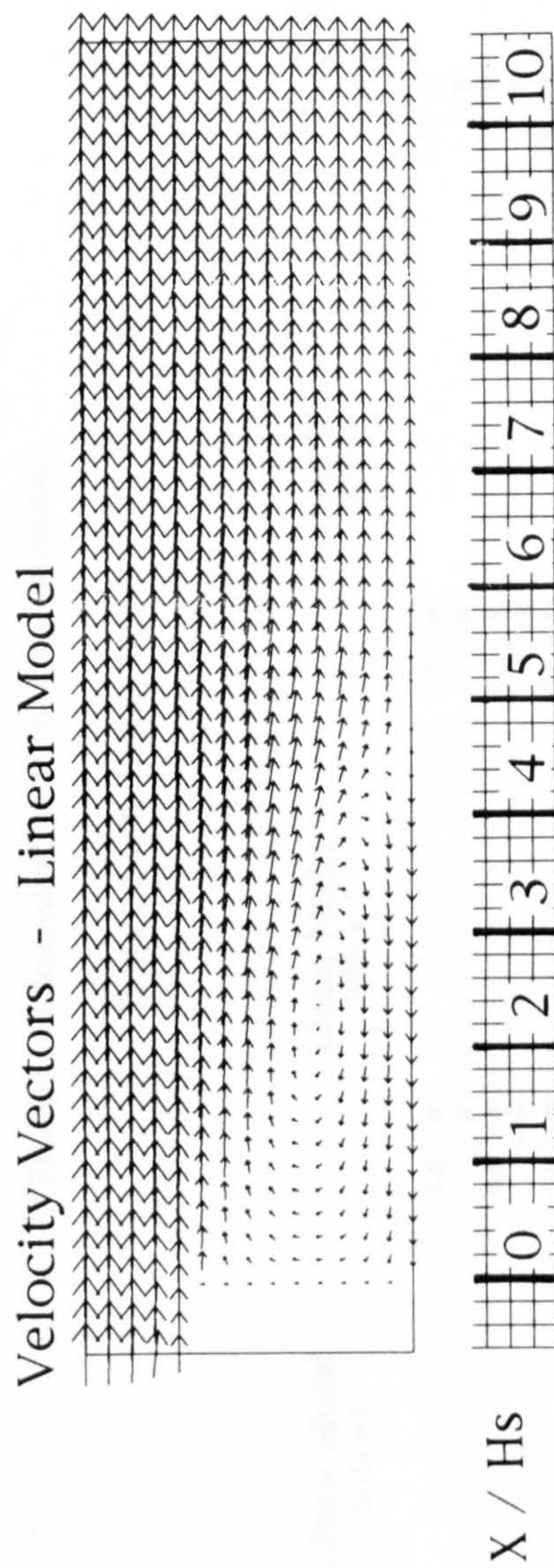
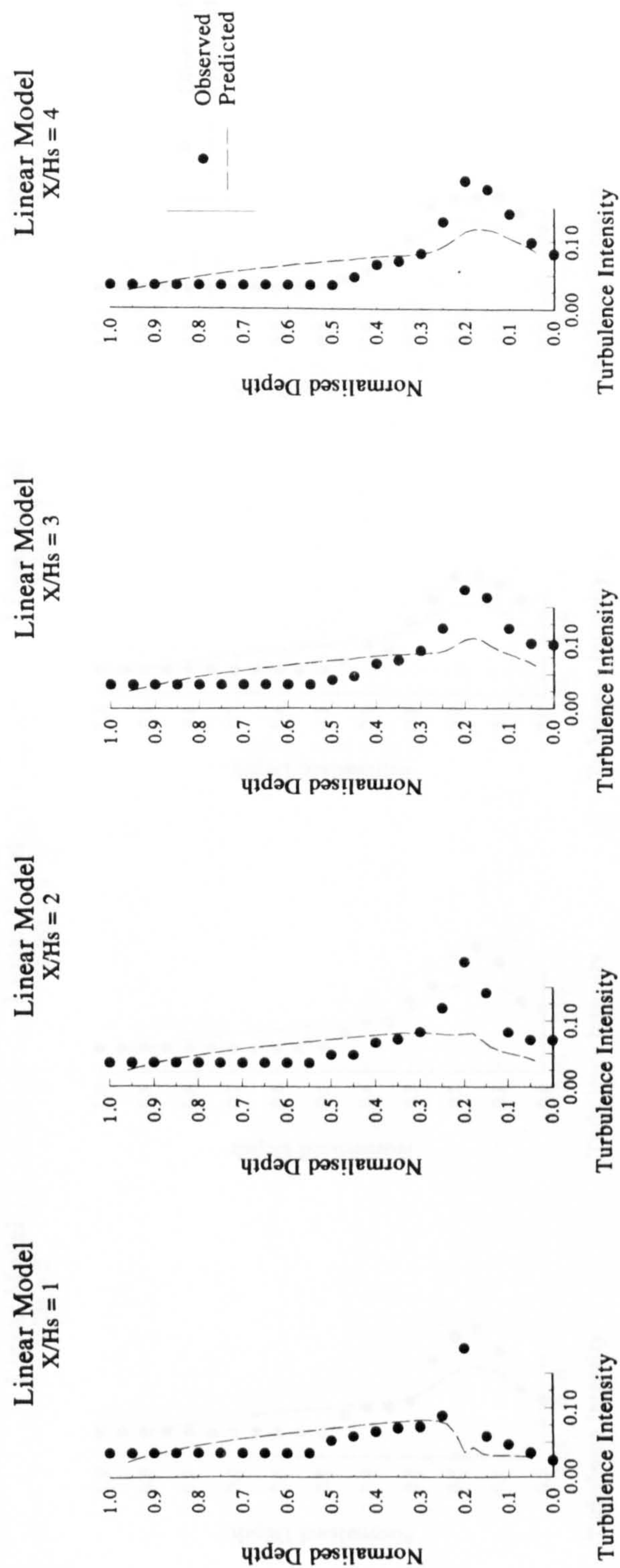


Figure 47. Velocity vectors within the recirculation zone

Profiles of Dimensionless Turbulence Intensities

Predicted with Linear Model



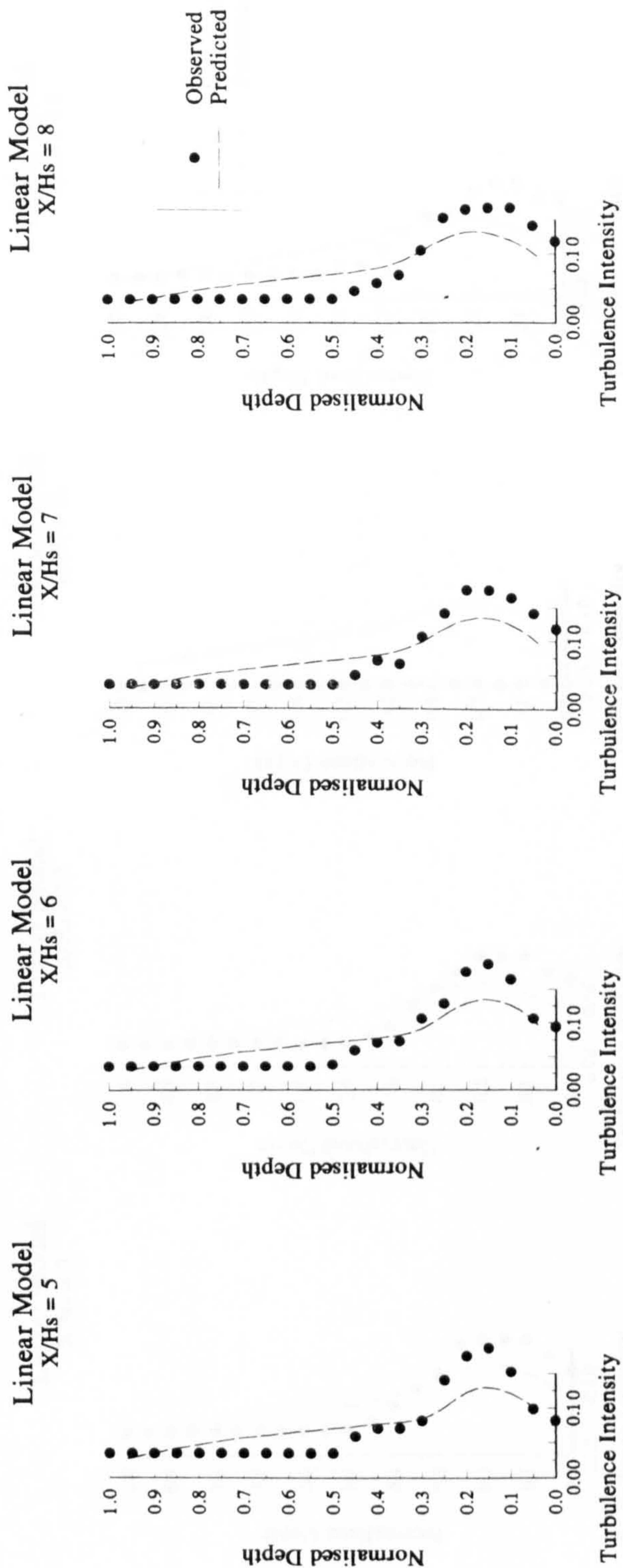
$$\frac{1}{2} \left(\frac{u'^2}{U_o^2} \right)$$

Dimensionless Turbulence Intensities

Figure 48. Comparison of Linear Model with experiment - Turbulence Intensity

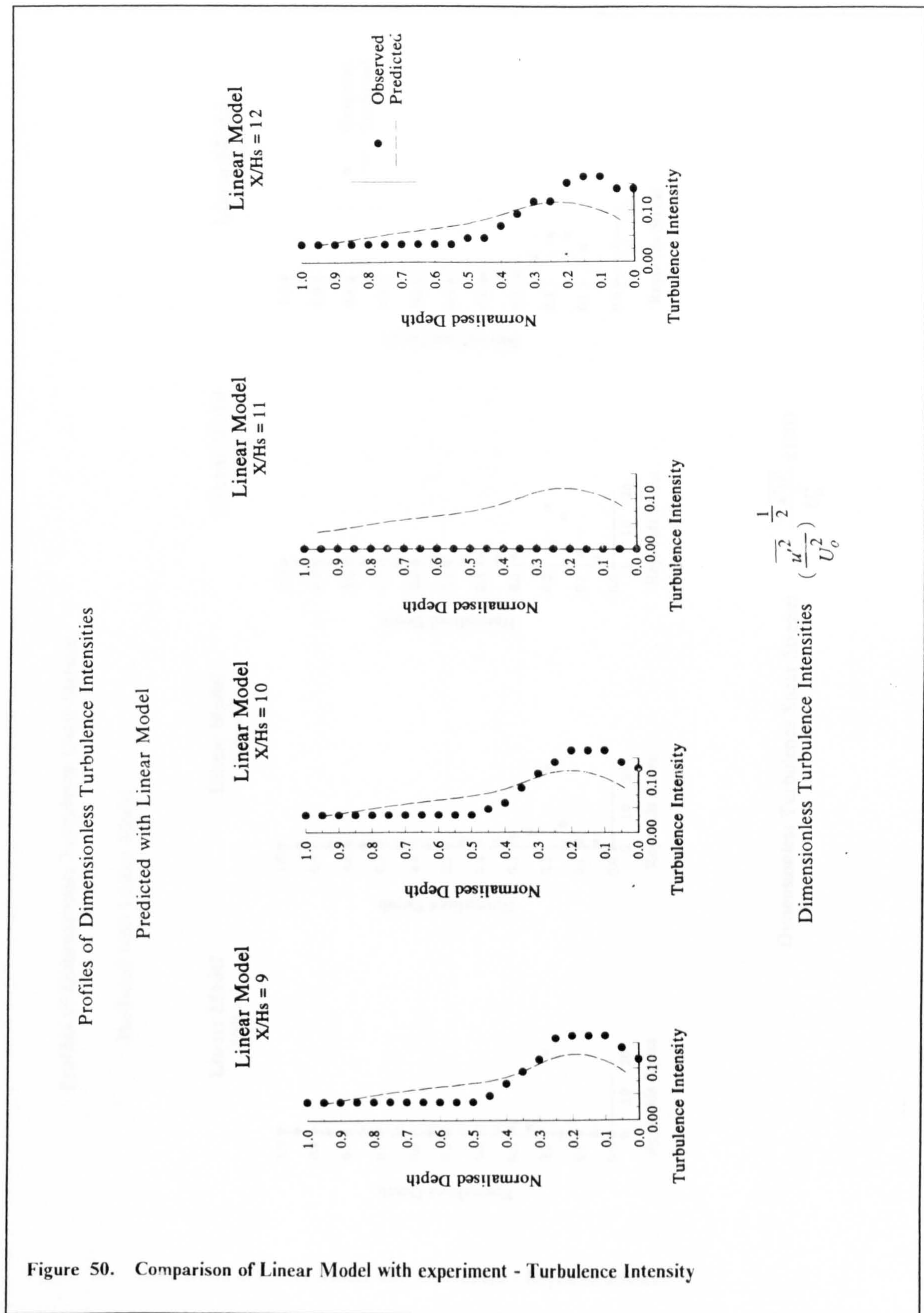
Profiles of Dimensionless Turbulence Intensities

Predicted with Linear Model



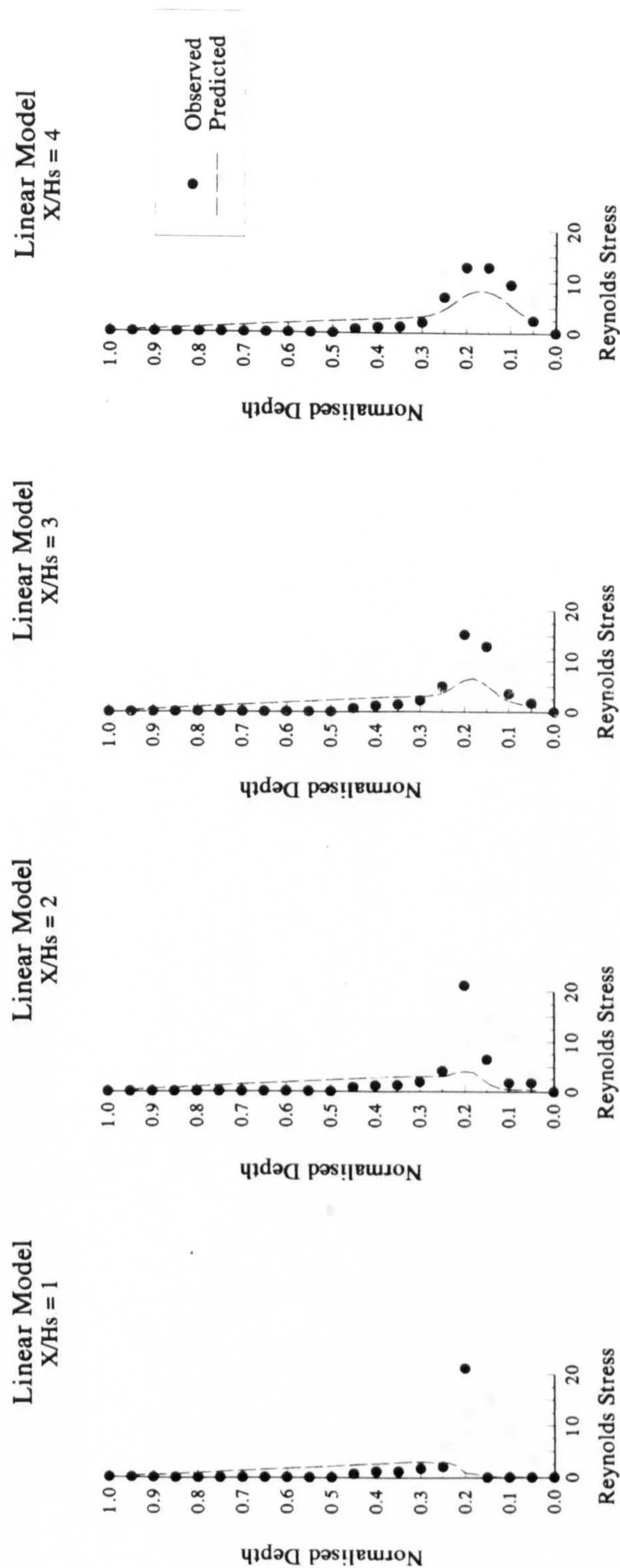
$$\frac{1}{2} \left(\frac{\overline{u'^2}}{U_o^2} \right)$$

Figure 49. Comparison of Linear Model with experiment - Turbulence Intensity



Profiles of Dimensionless Turbulence Shear Stresses

Predicted with Linear Model



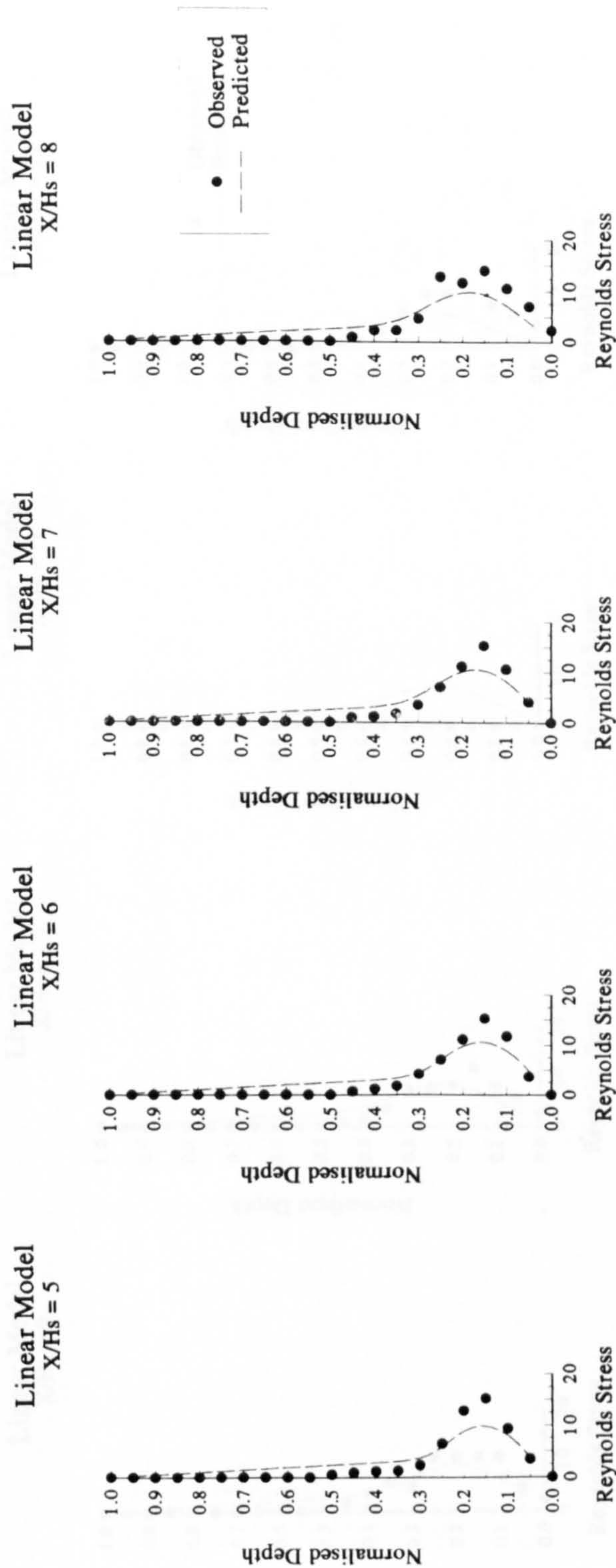
$$\frac{-\overline{u'w'}}{U_o^2} \times 1000$$

Dimensionless Turbulence Shear Stresses

Figure 51. Comparison of Linear Model with experiment - Reynolds stresses

Profiles of Dimensionless Turbulence Shear Stresses

Predicted with Linear Model



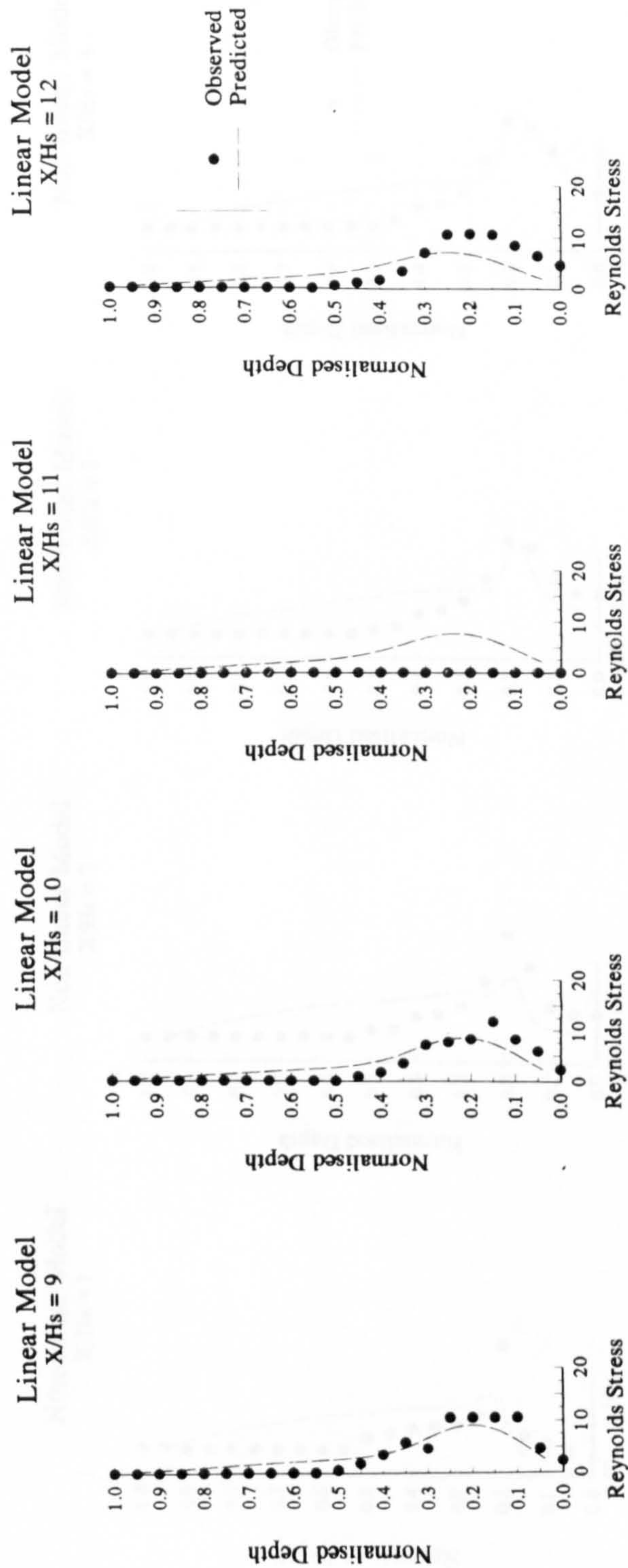
$$\frac{-\overline{u'w'}}{U_o^2} \times 1000$$

Dimensionless Turbulence Shear Stresses

Figure 52. Comparison of Linear Model with experiment - Reynolds stresses

Profiles of Dimensionless Turbulence Shear Stresses

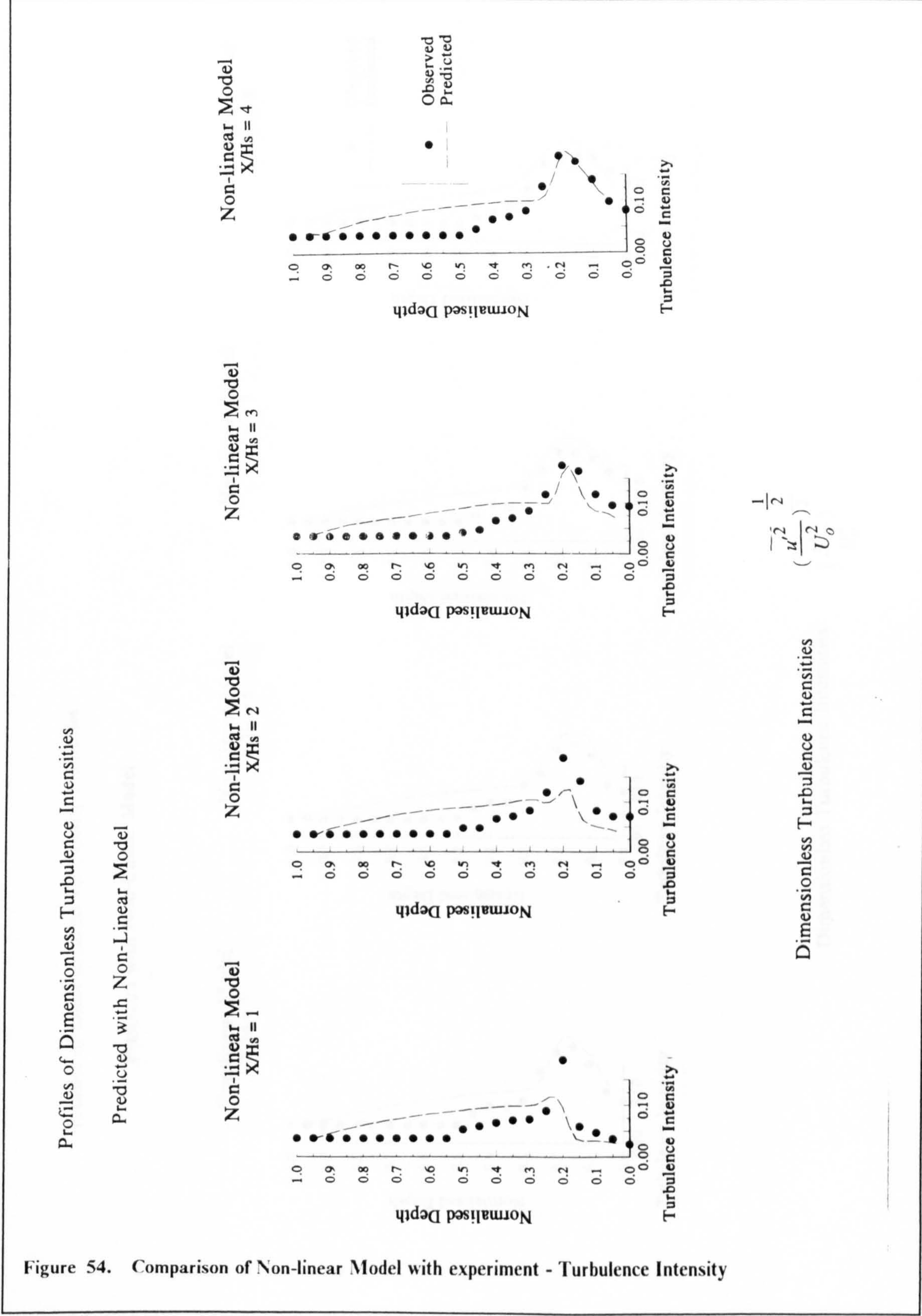
Predicted with Linear Model



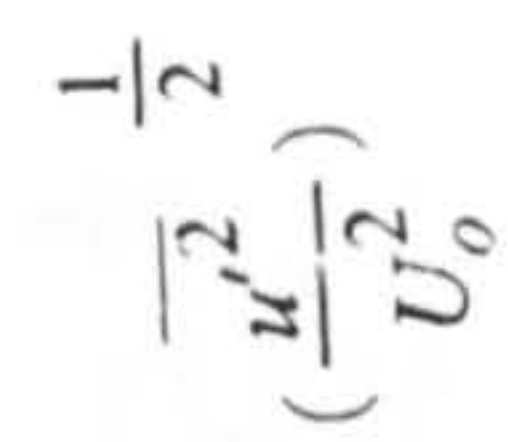
Dimensionless Turbulence Shear Stresses

$$-\frac{\overline{u'w'}}{U_o^2} \times 1000$$

Figure 53. Comparison of Linear Model with experiment - Reynolds stresses



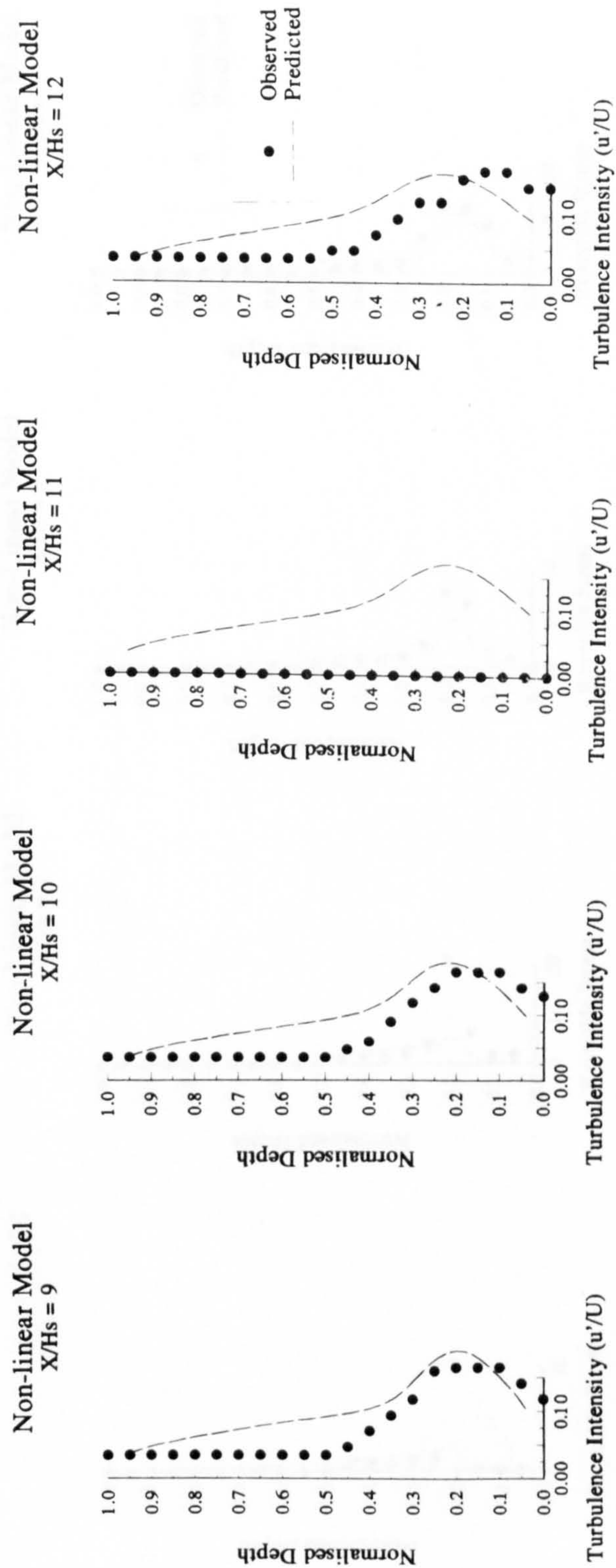
Predicted with Non-Linear Model



Dimensionless Turbulence Intensities

Profiles of Dimensionless Turbulence Intensities

Predicted with Non-Linear Model



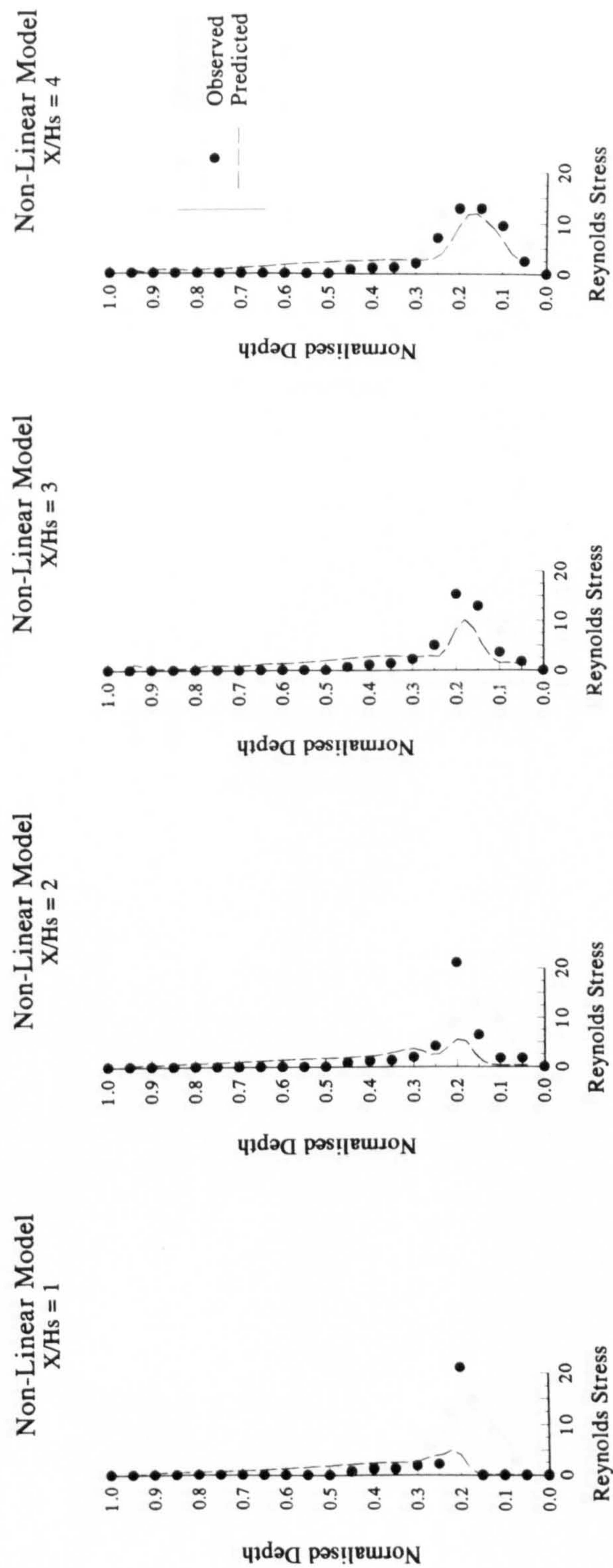
$$\frac{1}{2} \left(\frac{u'^2}{U_o^2} \right)$$

Dimensionless Turbulence Intensities

Figure 56. Comparison of Non-linear Model with experiment - Turbulence Intensity

Profiles of Dimensionless Turbulence Shear Stresses

Predicted with Non-Linear Model



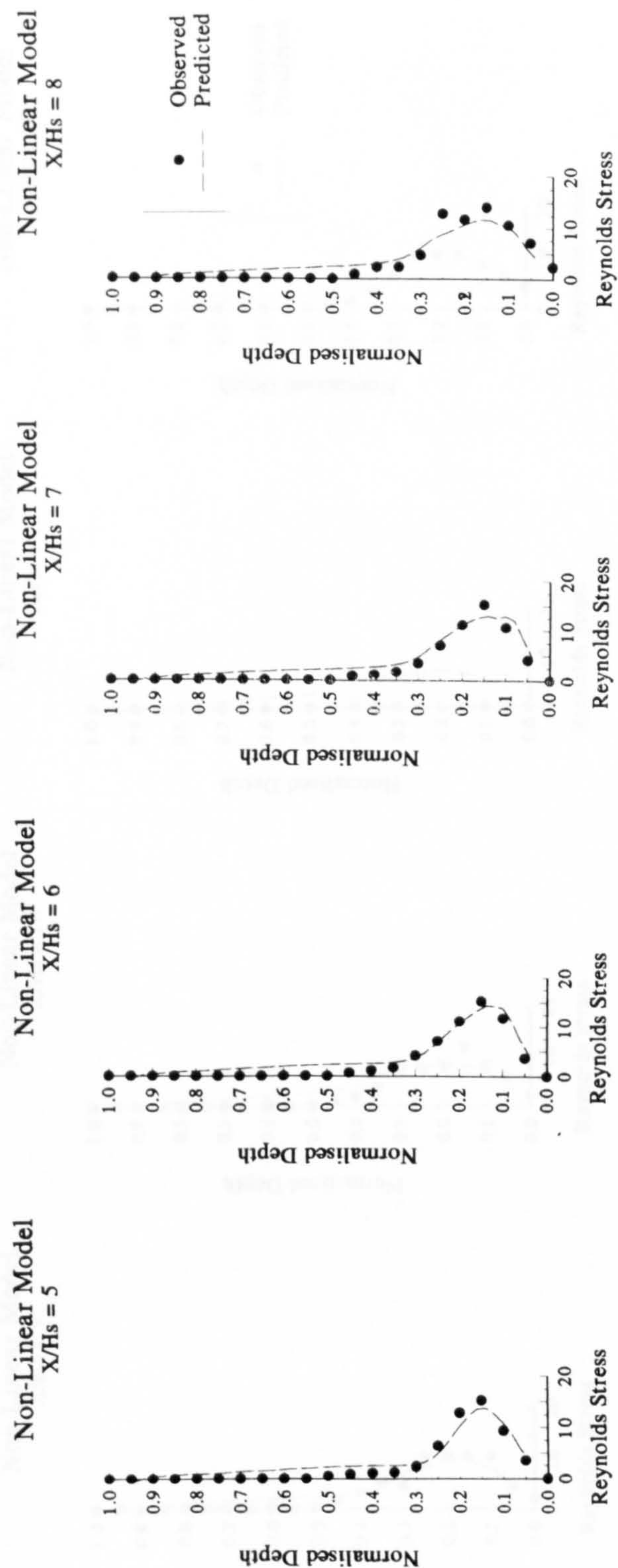
$$\frac{-\overline{u'w'}}{U_o^2} \times 1000$$

Dimensionless Turbulence Shear Stresses

Figure 57. Comparison of Non-linear Model with experiment - Reynolds Stresses

Profiles of Dimensionless Turbulence Shear Stresses

Predicted with Non-Linear Model



$$\text{Dimensionless Turbulence Shear Stresses} \quad -\frac{\overline{u'w'}}{U_o^2} \times 1000$$

Figure 58. Comparison of Non-linear Model with experiment - Reynolds Stresses

Profiles of Dimensionless Turbulence Shear Stresses
Predicted with Non-Linear Model

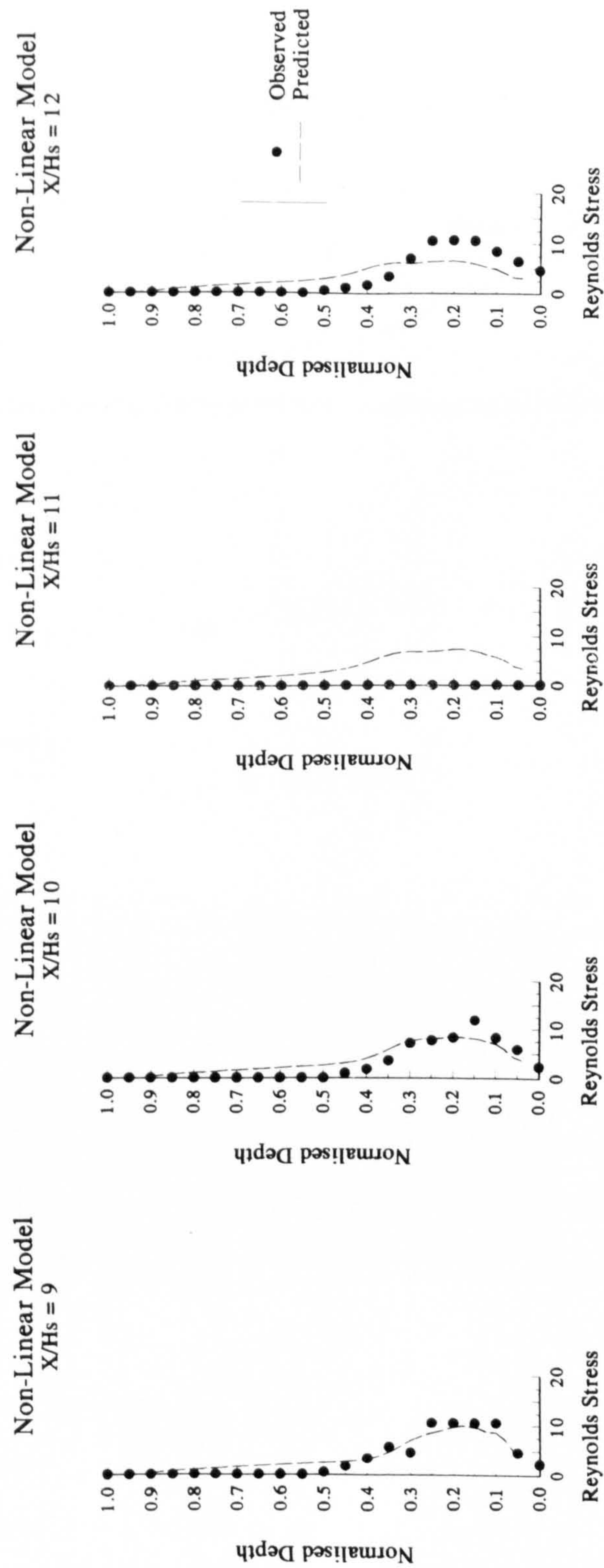
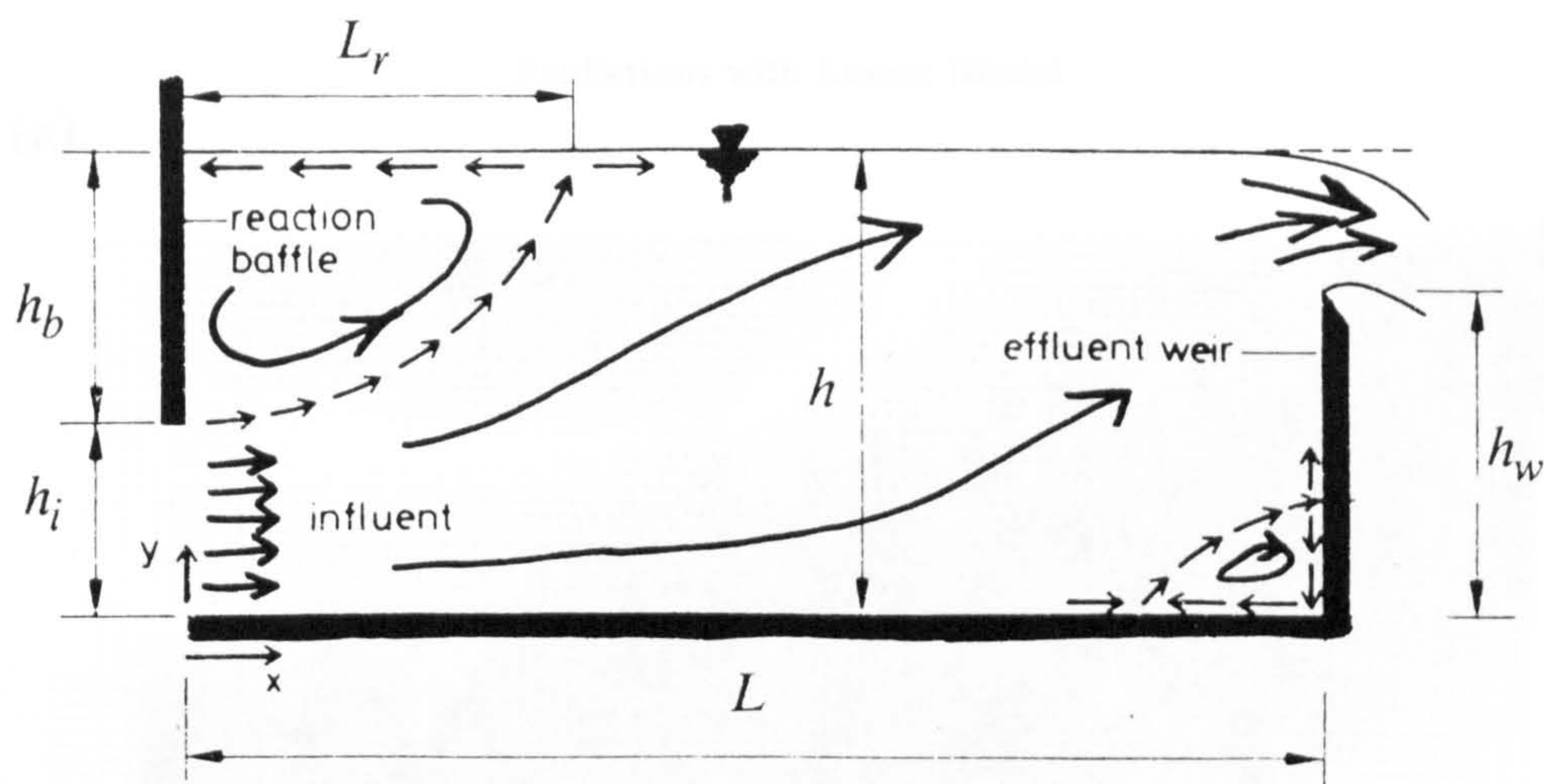


Figure 59. Comparison of Non-linear Model with experiment - Reynolds Stresses

$$\frac{-\overline{u'w'}}{U_o^2} \times 1000$$

Dimensionless Turbulence Shear Stresses

Flow in a Settling Tank - Iman and McCorquodale



Inlet Conditions

$$u_{inlet} = 21.88 \text{ cm/s} \quad k_{inlet} = 95.75 \frac{\text{cm}^2}{\text{s}^2}$$

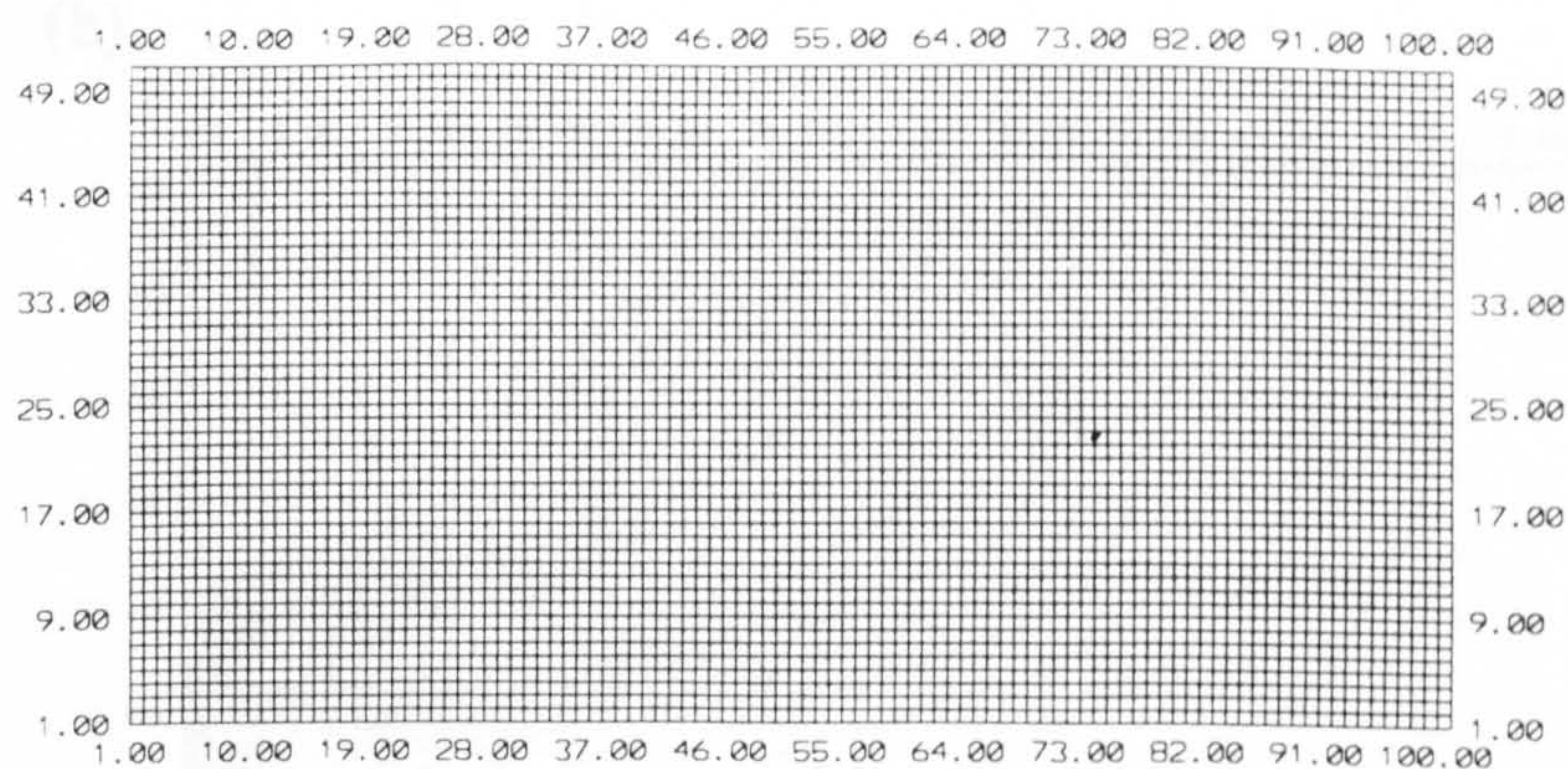
$$h_i = 5.0 \text{ cm.}$$

$$w_{inlet} = 0.0 \text{ cm/s}$$

$$\varepsilon_{inlet} = 682.9 \frac{\text{cm}^2}{\text{s}^3}$$

$$h = 11.95 \text{ cm}$$

$$h_b = 6.95 \text{ cm.}$$



$$L = 73.0 \text{ cm.}$$

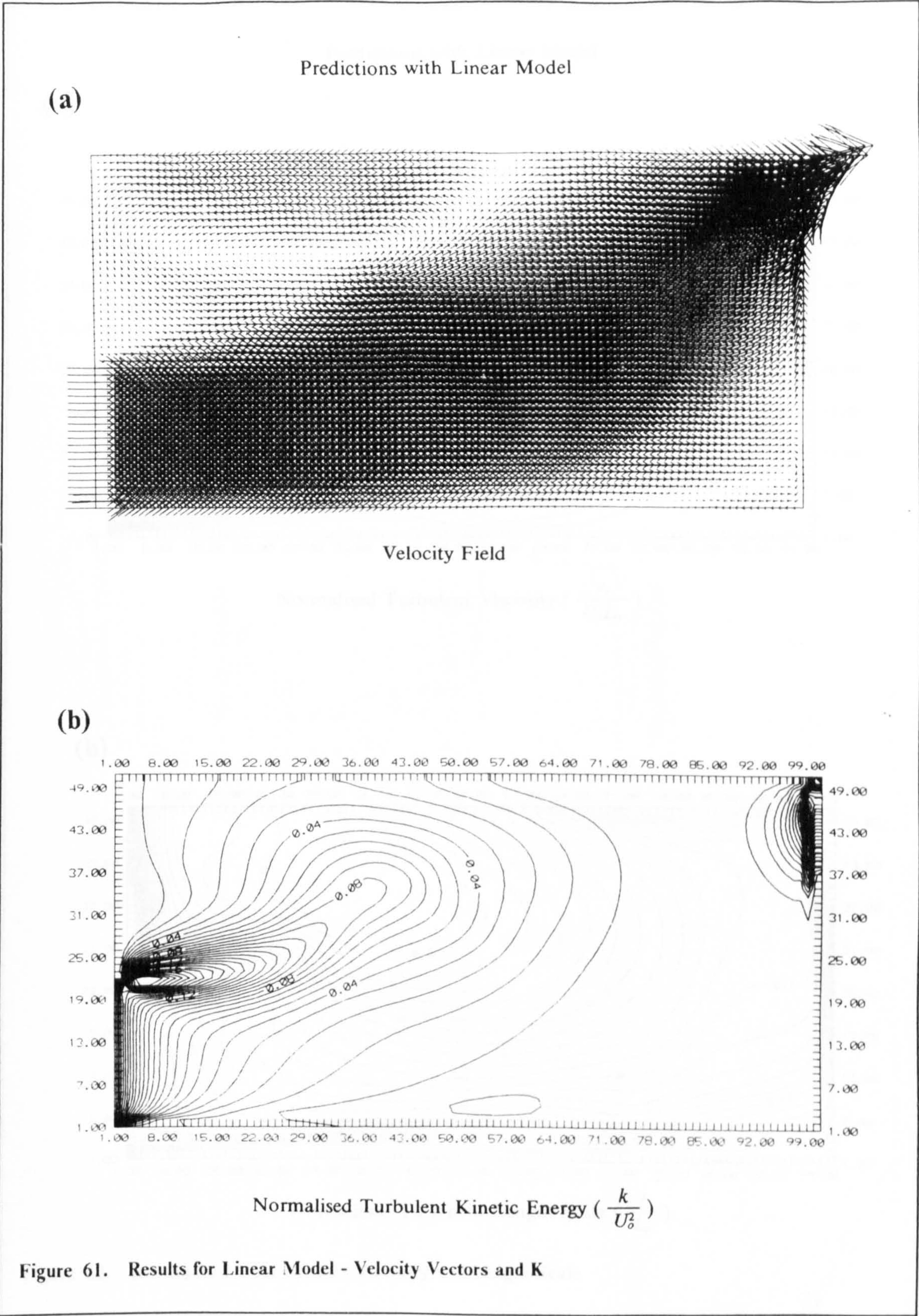
Computational Grid 101 x 51

$$\Delta x = 0.73 \text{ cm.}$$

$$\Delta z = 0.239 \text{ cm.}$$

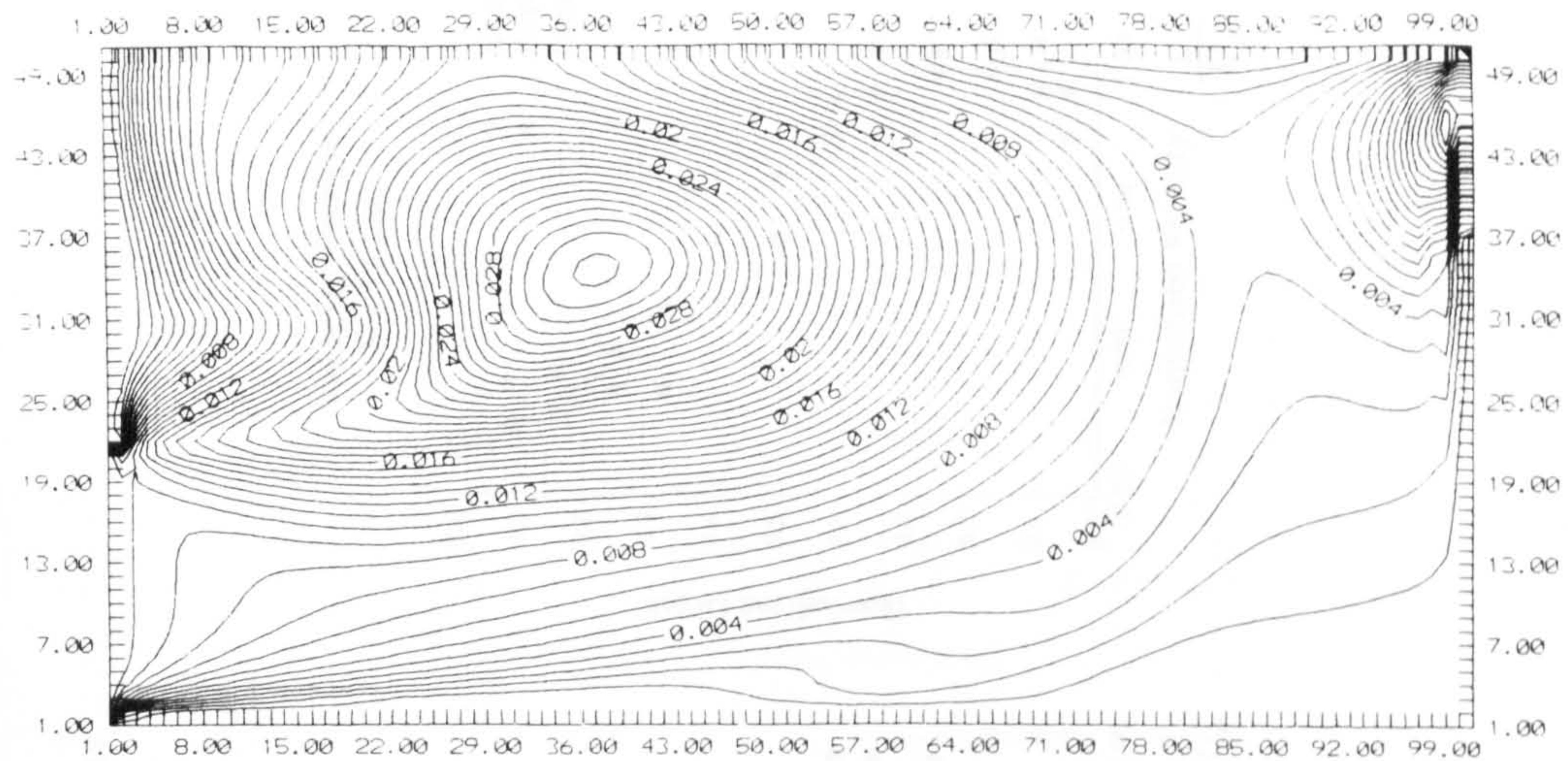
$$U_o = 21.88 \text{ cm/s} \quad L_o = h_i = 5.0 \text{ cm.}$$

Figure 60. Geometry and Computational Details



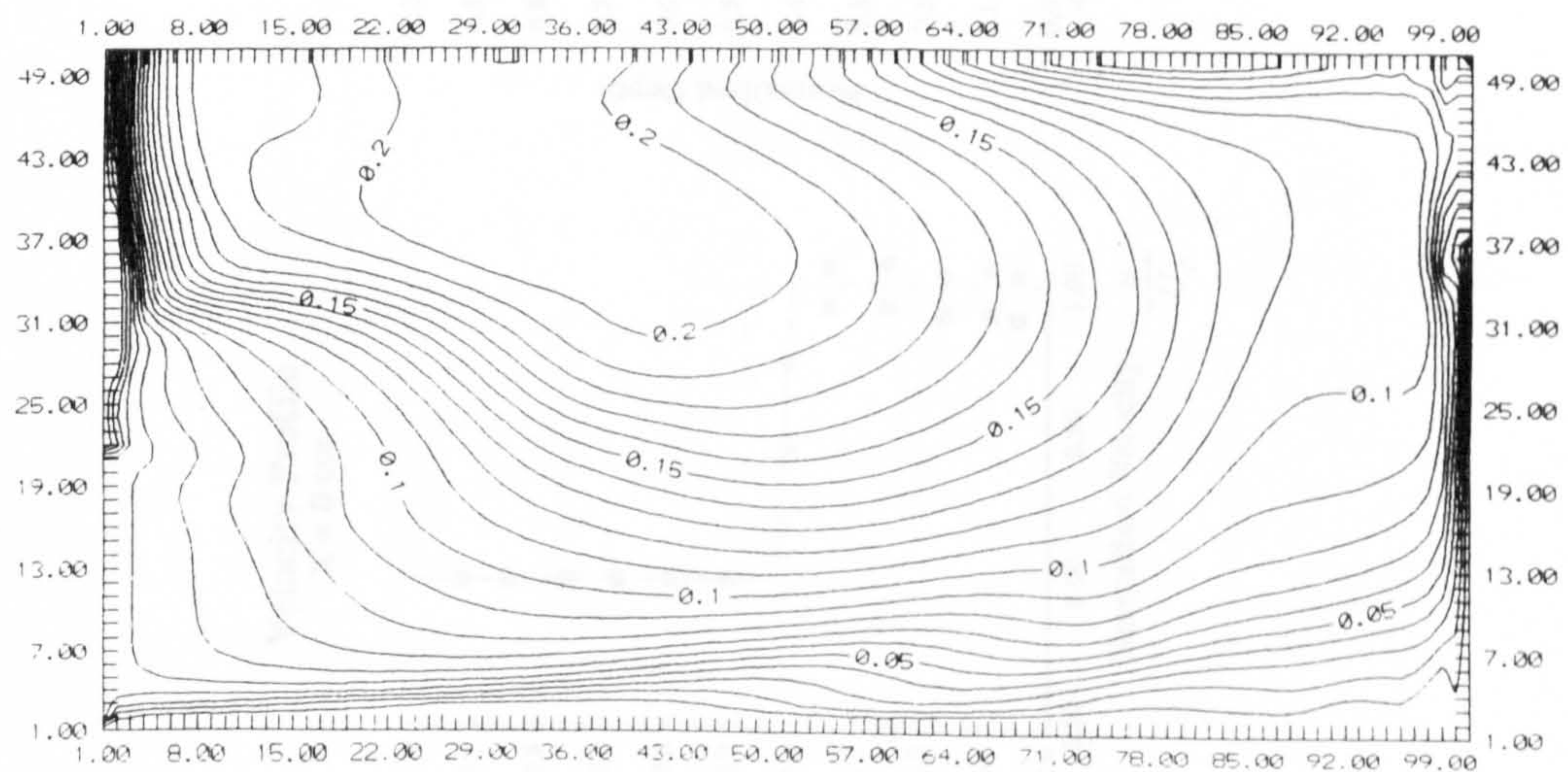
Predictions with Linear Model

(a)



Normalised Turbulent Viscosity ($\frac{\nu_t}{U_o L_o}$)

(b)



Normalised Turbulent Length Scale ($\frac{l}{L_o}$)

Figure 62. Results for Linear Model - Viscosity and Length Scale

Profiles of
Normalised Velocity

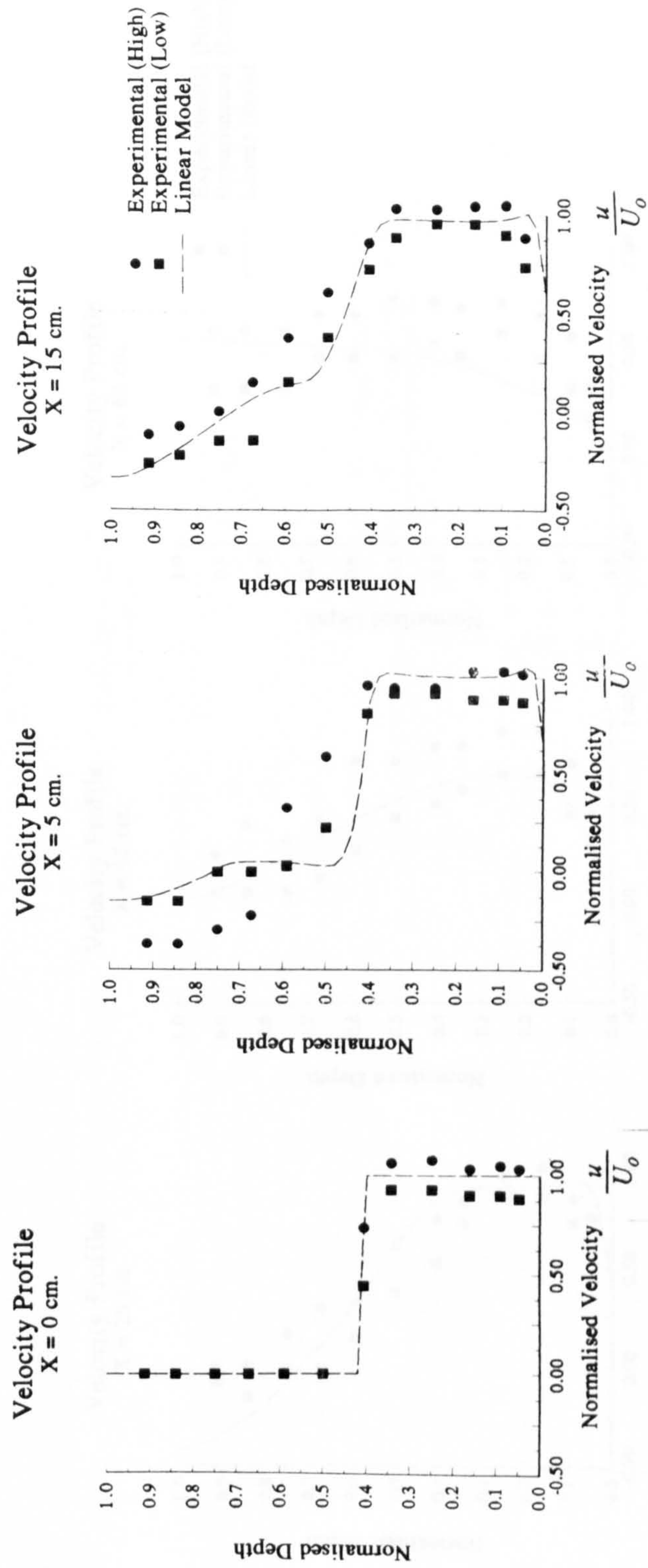


Figure 63. Comparison with experimental data - U Profiles

Profiles of
Normalised Velocity

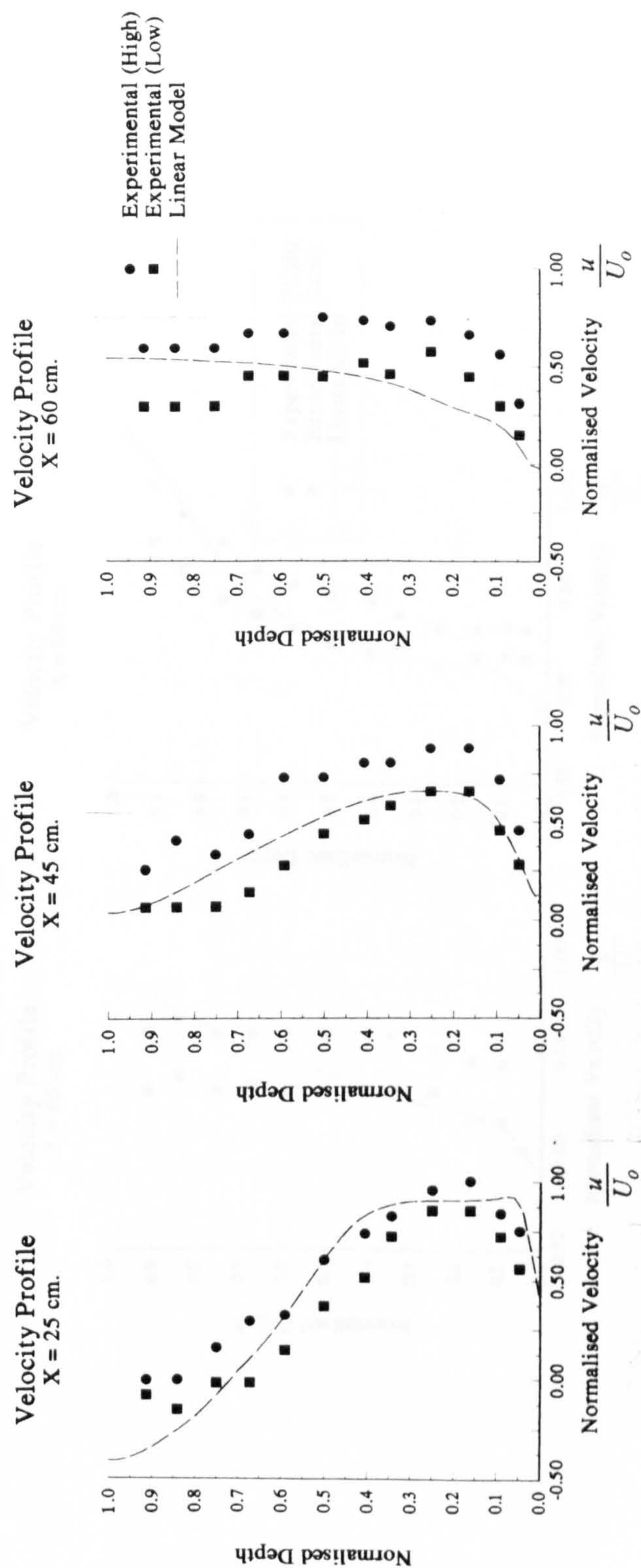


Figure 64. Comparison with experimental data - U Profiles

Profiles of
Normalised Velocity

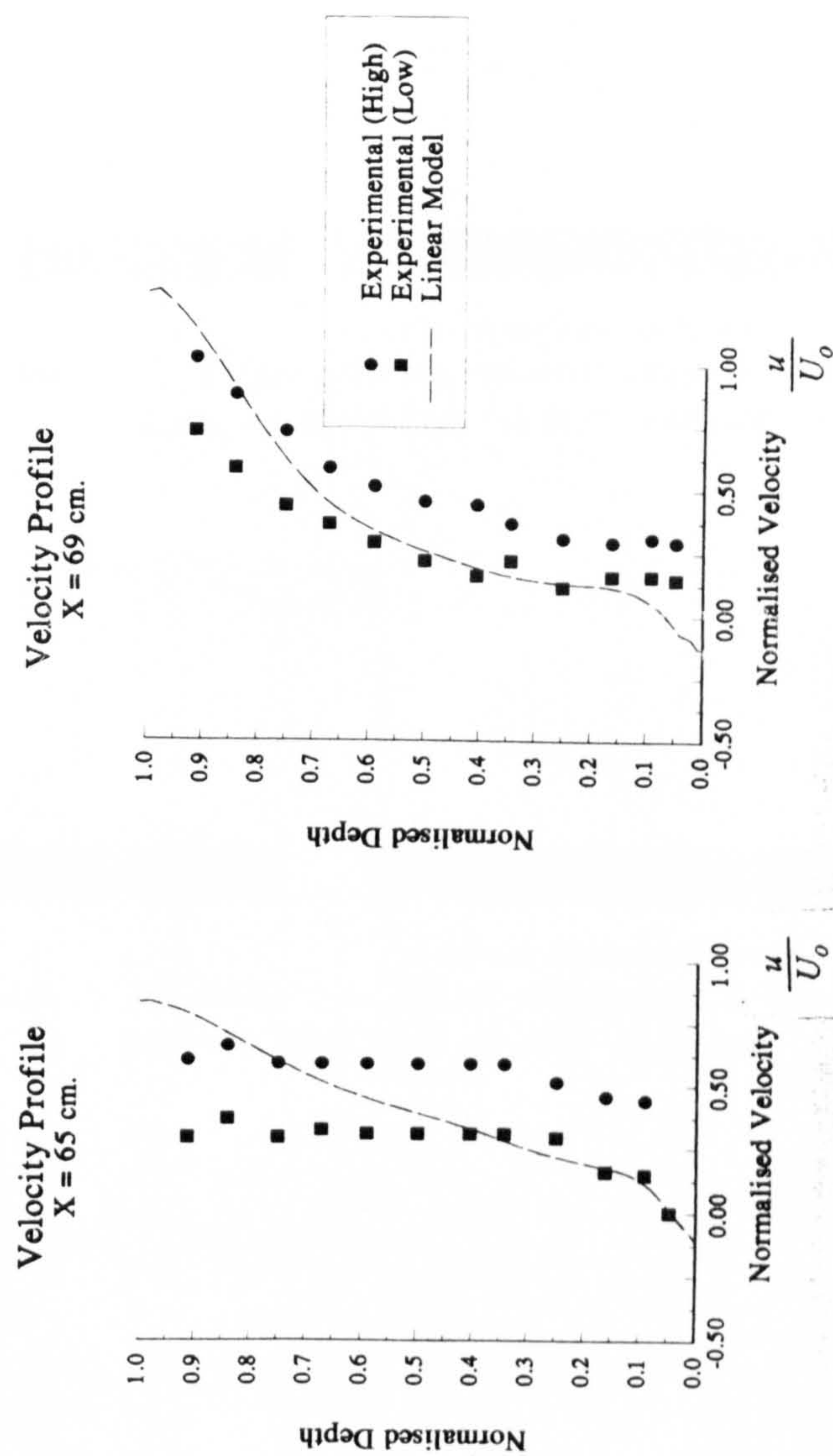


Figure 65. Comparison with experimental data - U Profiles

Open Channel Flow Over Slots of Varying Aspect Ratio

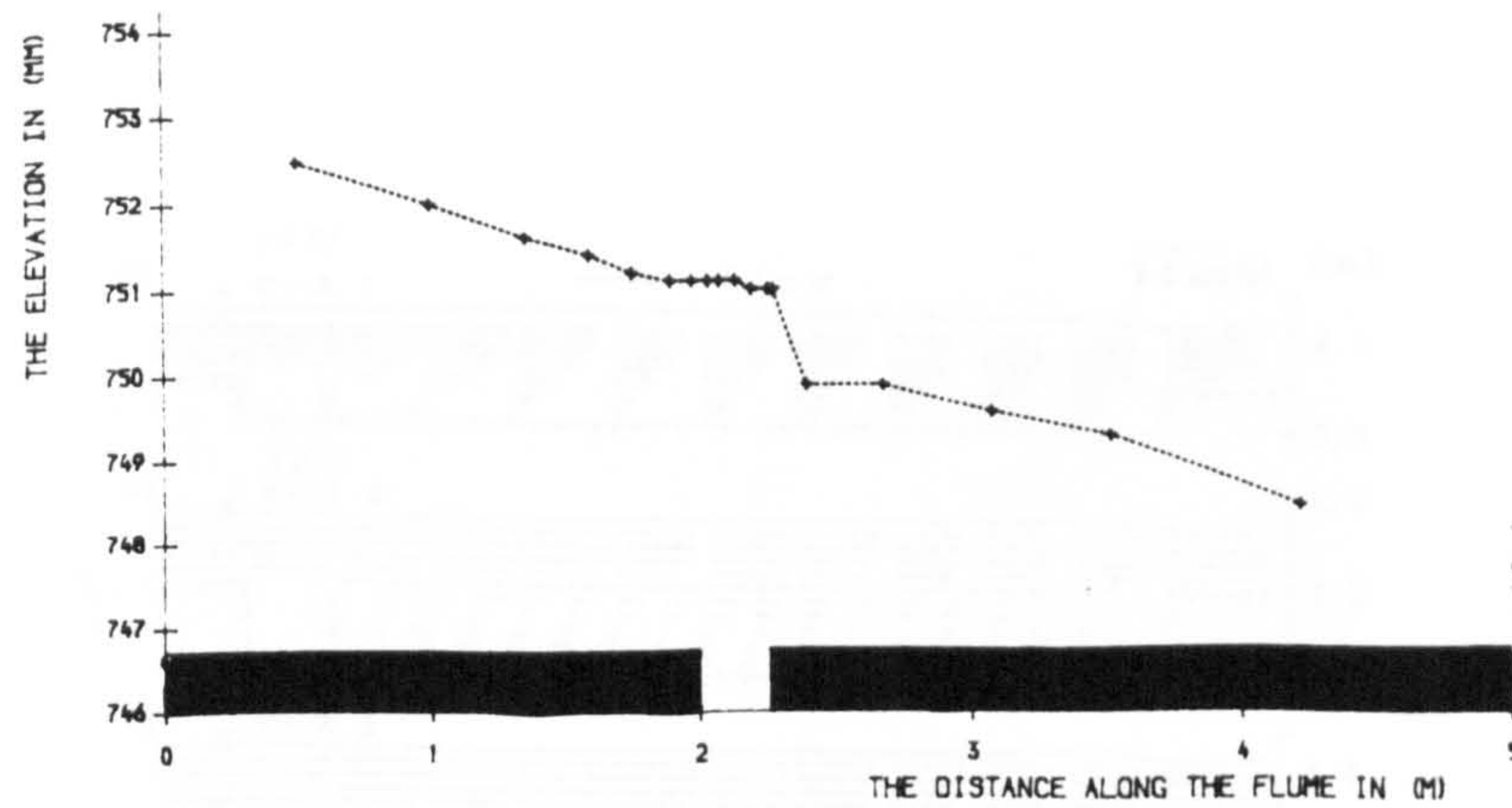


FIG (6.17) THE ENERGY LINE AND THE WATER-LEVEL IN (MM) ALONG THE FLUME WITH THE SLOT ($Bs/hg=5$).

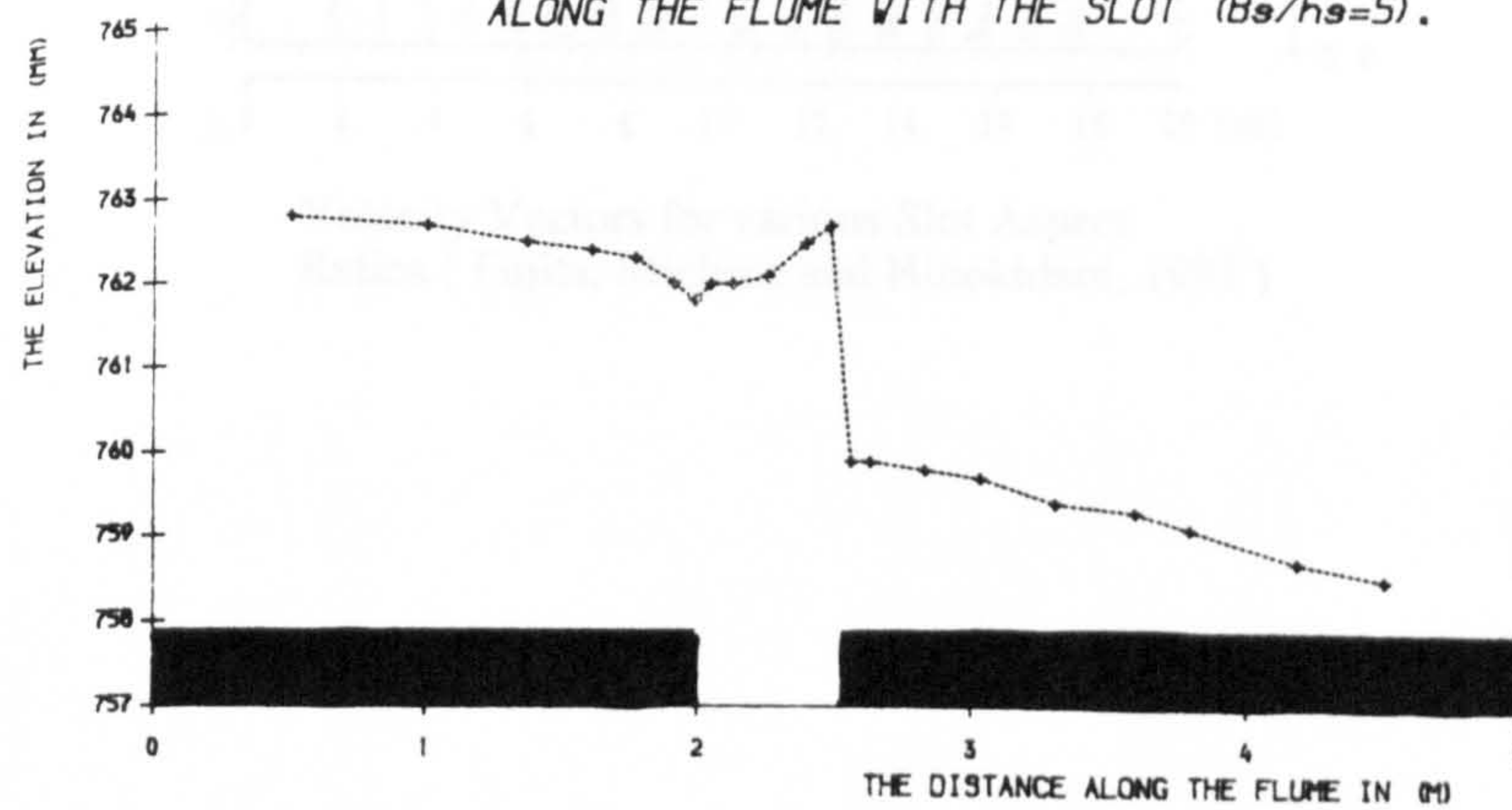


FIG (6.13) THE ENERGY LINE AND THE WATER-LEVEL IN (MM) ALONG THE FLUME WITH THE SLOT ($Bs/hg=10$).

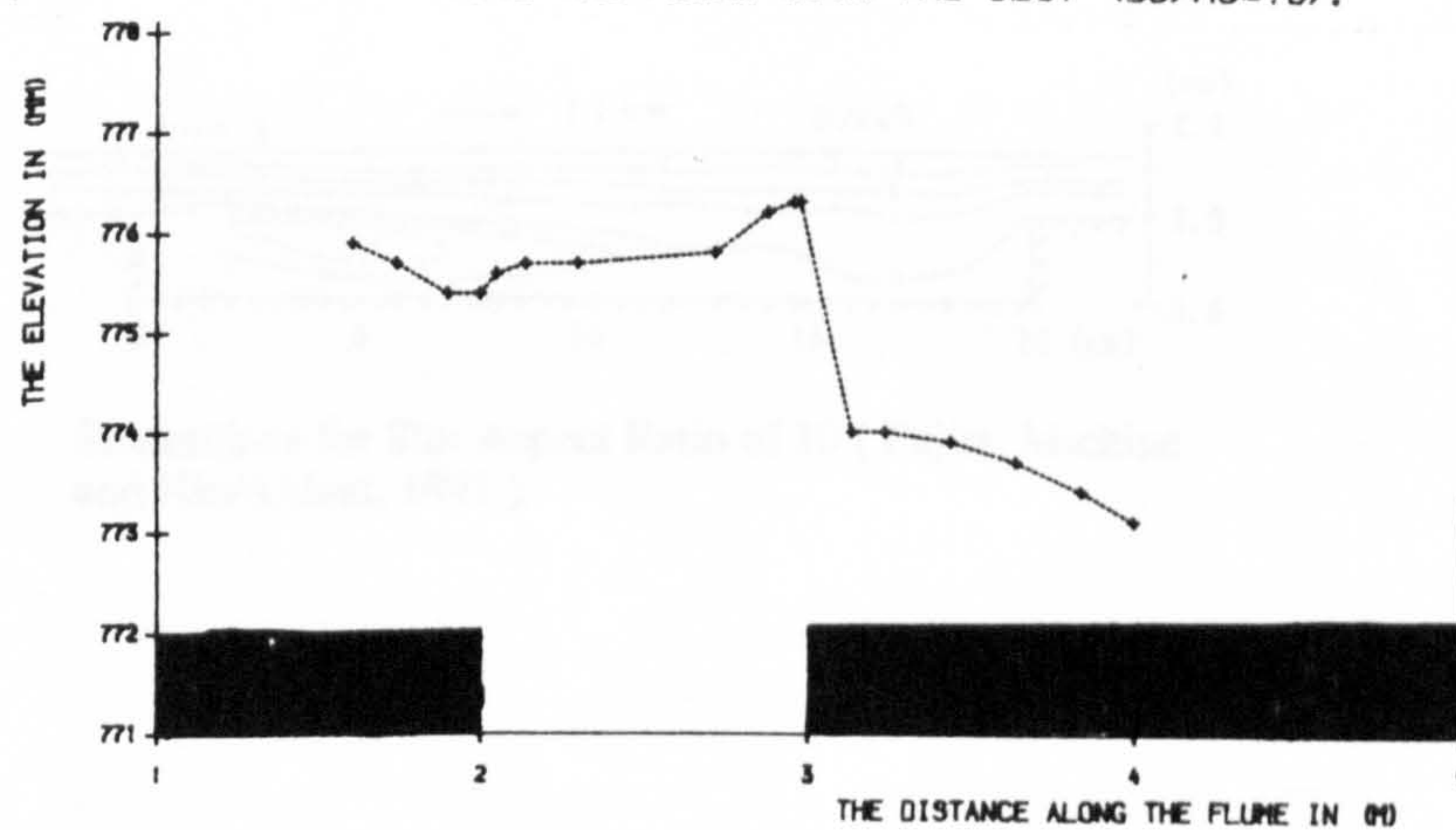
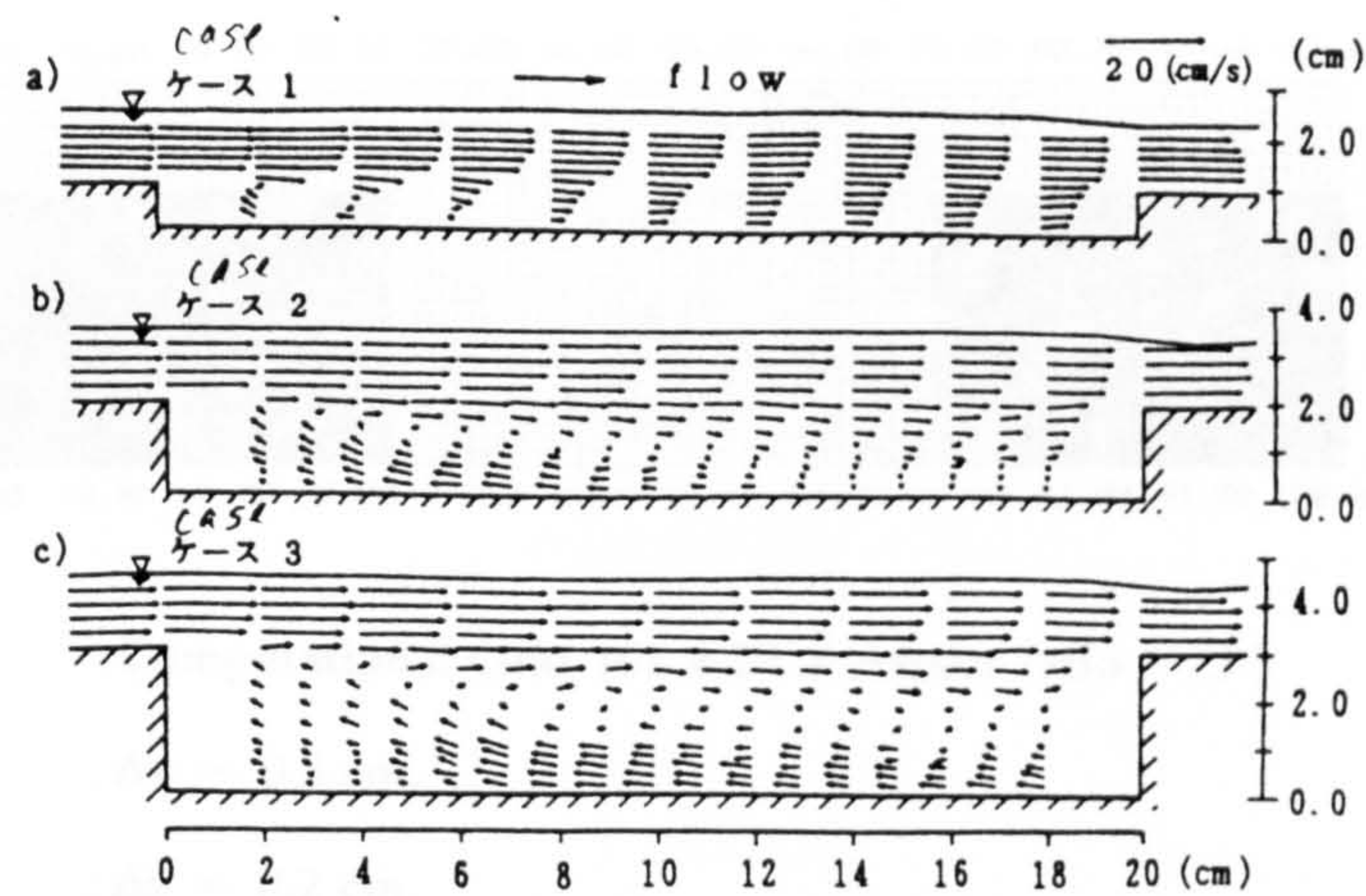
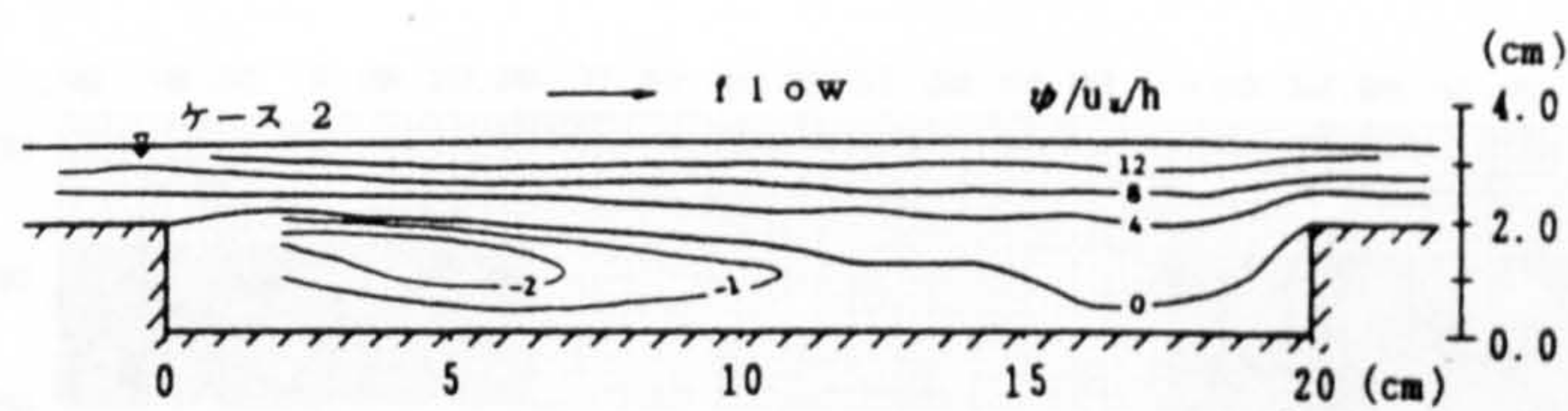


FIG (6.9) THE ENERGY LINE AND THE WATER-LEVEL IN (MM) ALONG THE FLUME WITH THE SLOT ($Bs/hg=20$).

Figure 66. Water Surface Profile Results of Jasem (1990)

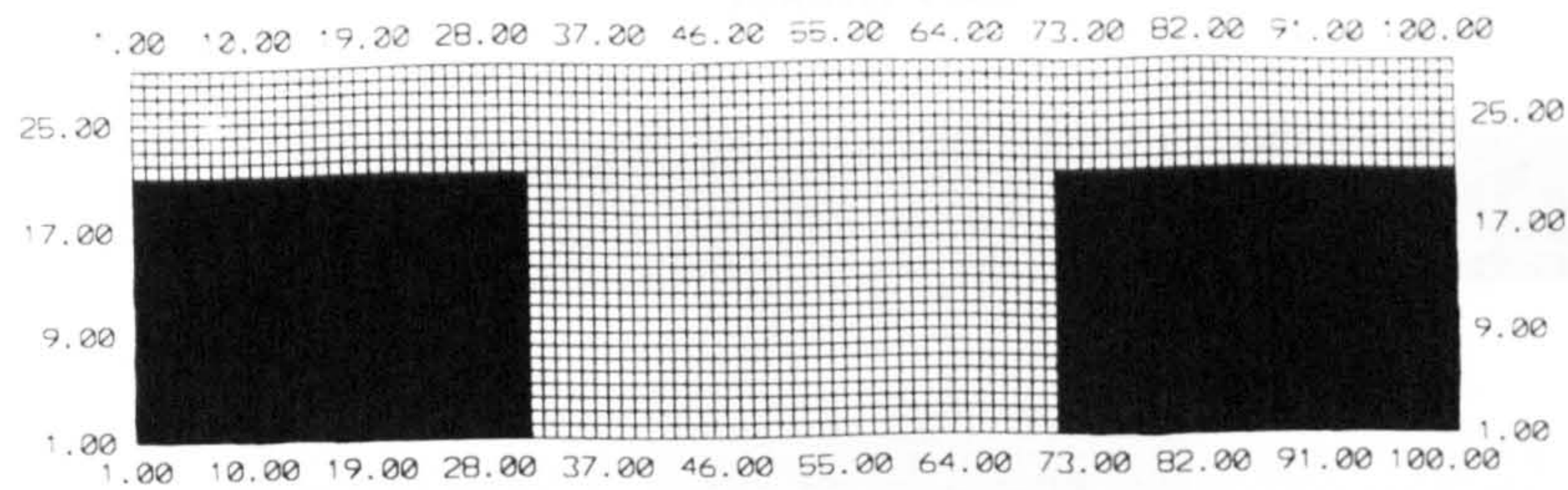


Velocity Vectors for various Slot Aspect Ratios (Fujita, Michiue and Hinokidani, 1991)



Streamlines for Slot Aspect Ratio of 10 (Fujita, Michiue and Hinokidani, 1991)

Figure 67. Flow Results of Fujita et al (1991)

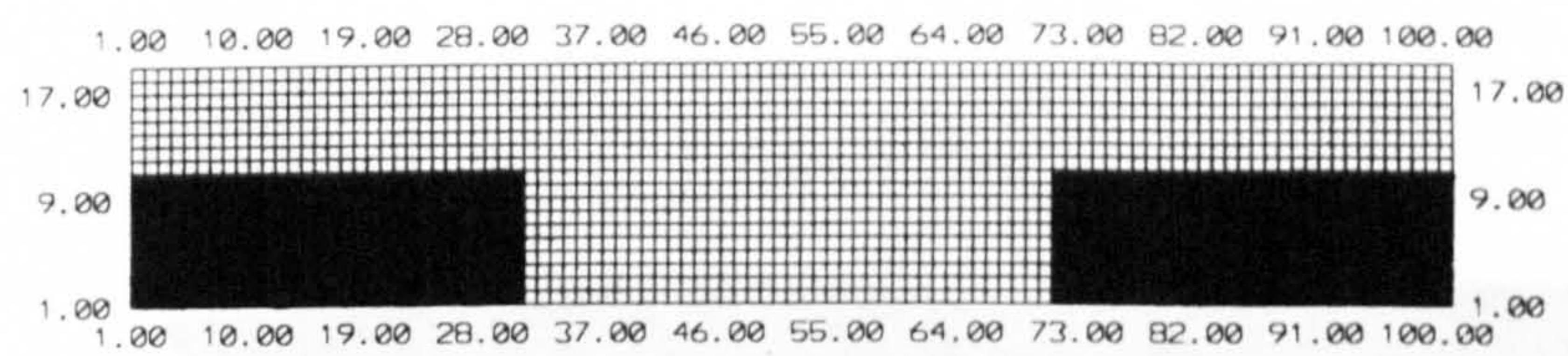


Computational Grid 101 x 29 (Aspect ratio = 5)

$$\Delta x = 0.5 \text{ cm.}$$

$$\Delta z = 0.2 \text{ cm.}$$

$$U_o = 28.35 \text{ cm/s} \quad L_o = 2.0 \text{ cm.}$$



Computational Grid 101 x 19

$$\Delta x = 0.5 \text{ cm.}$$

$$\Delta z = 0.2 \text{ cm. (Aspect ratio = 10)}$$

$$\Delta z = 0.1 \text{ cm. (Aspect ratio = 20)}$$

$$U_o = 28.35 \text{ cm/s} \quad L_o = 2.0 \text{ cm.}$$

Figure 68. Computational Grids

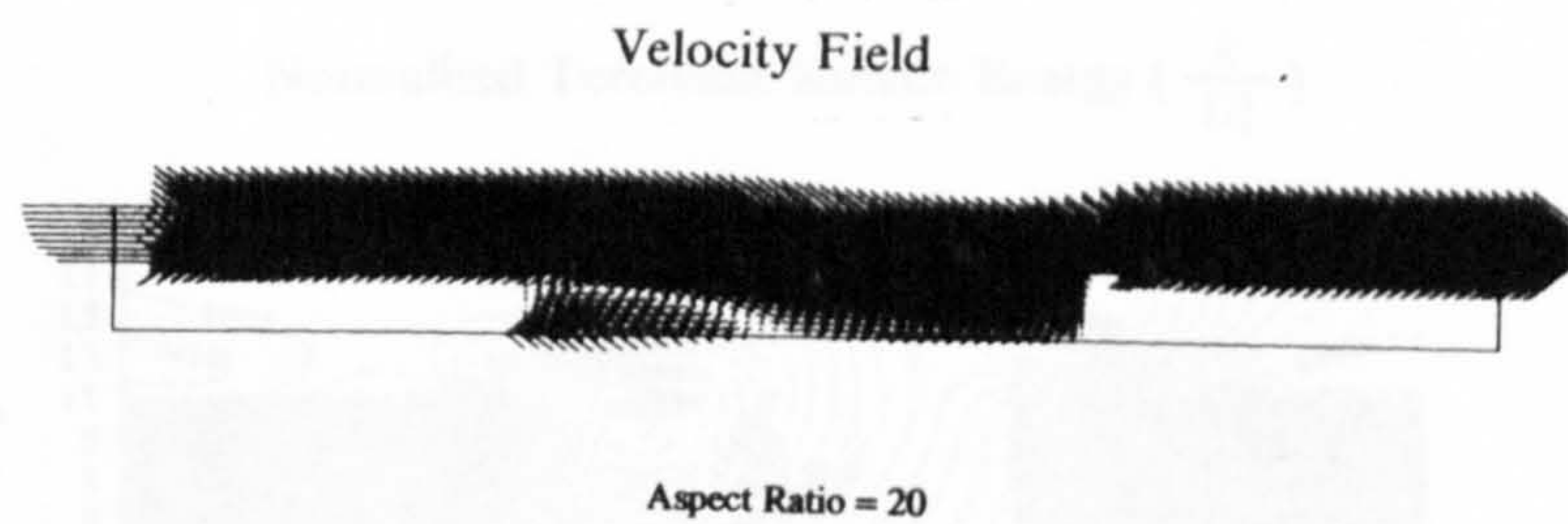
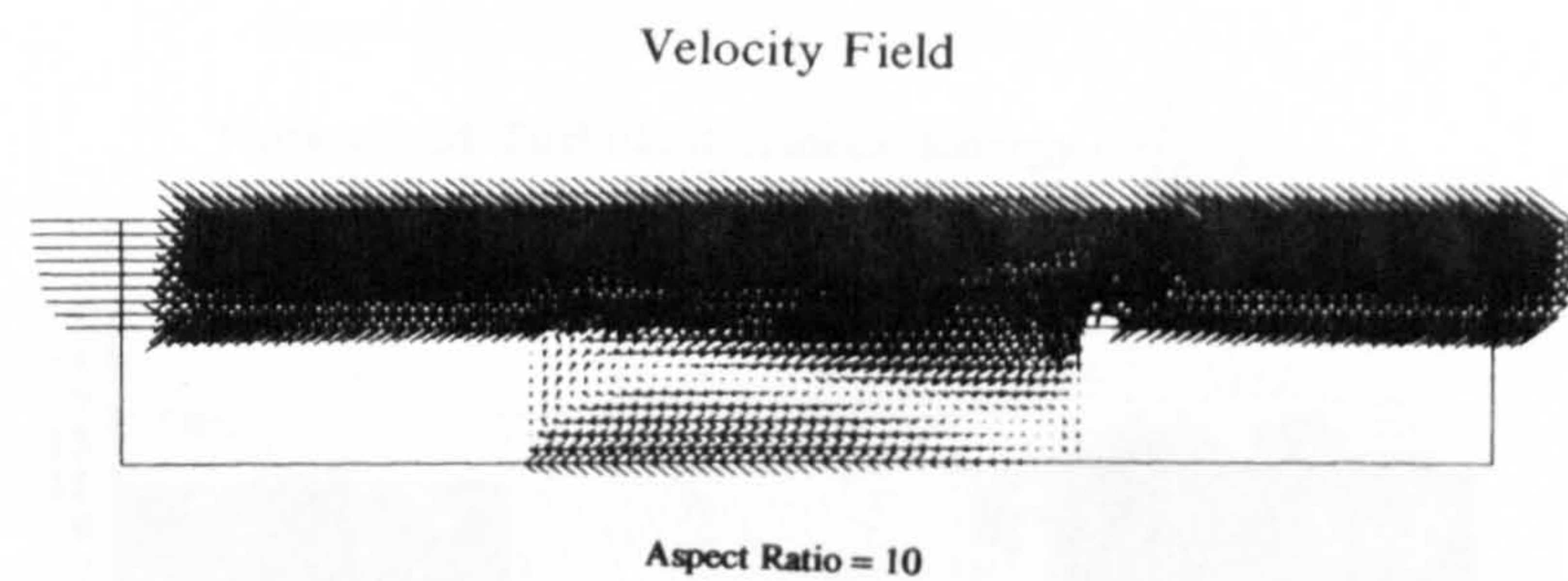
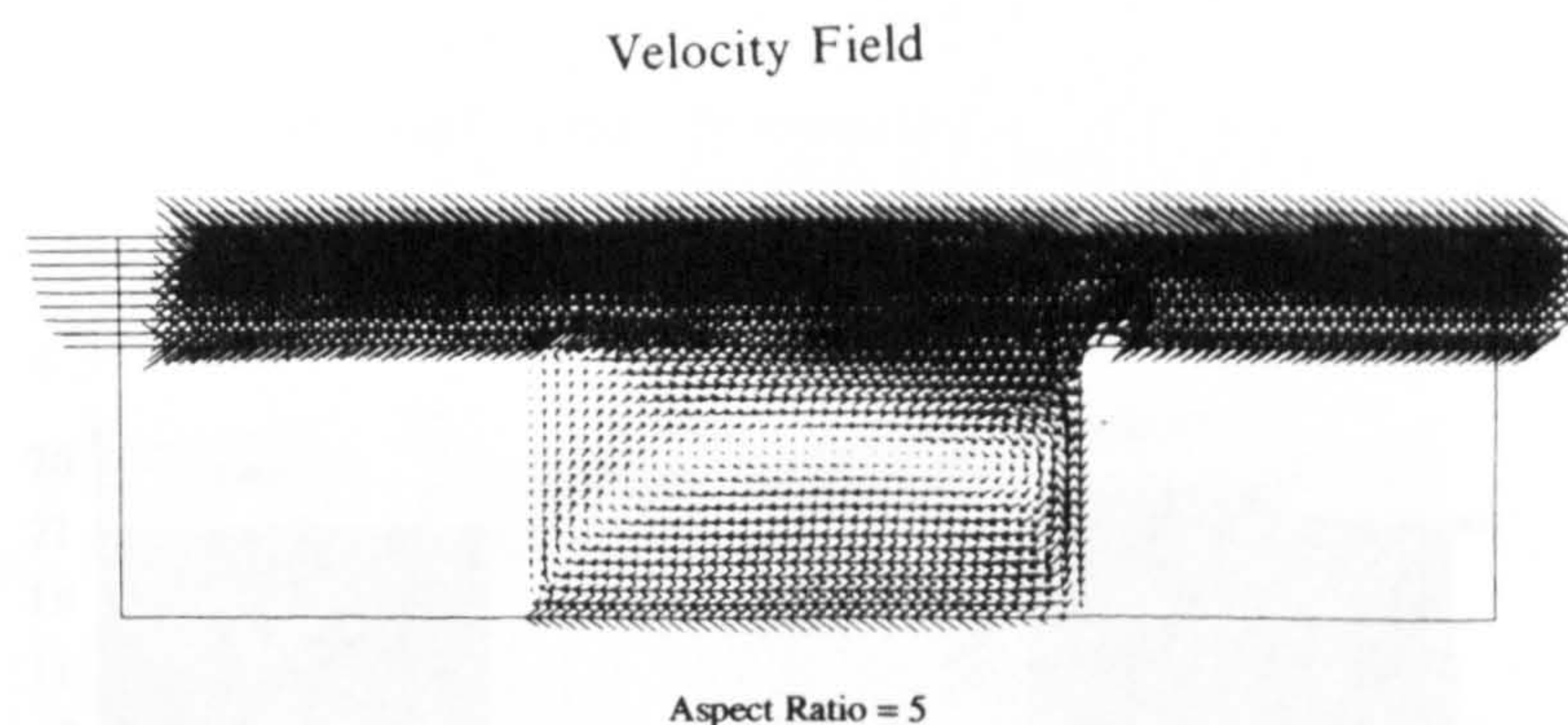


Figure 69. Velocity Vectors at Differing Aspect Ratios

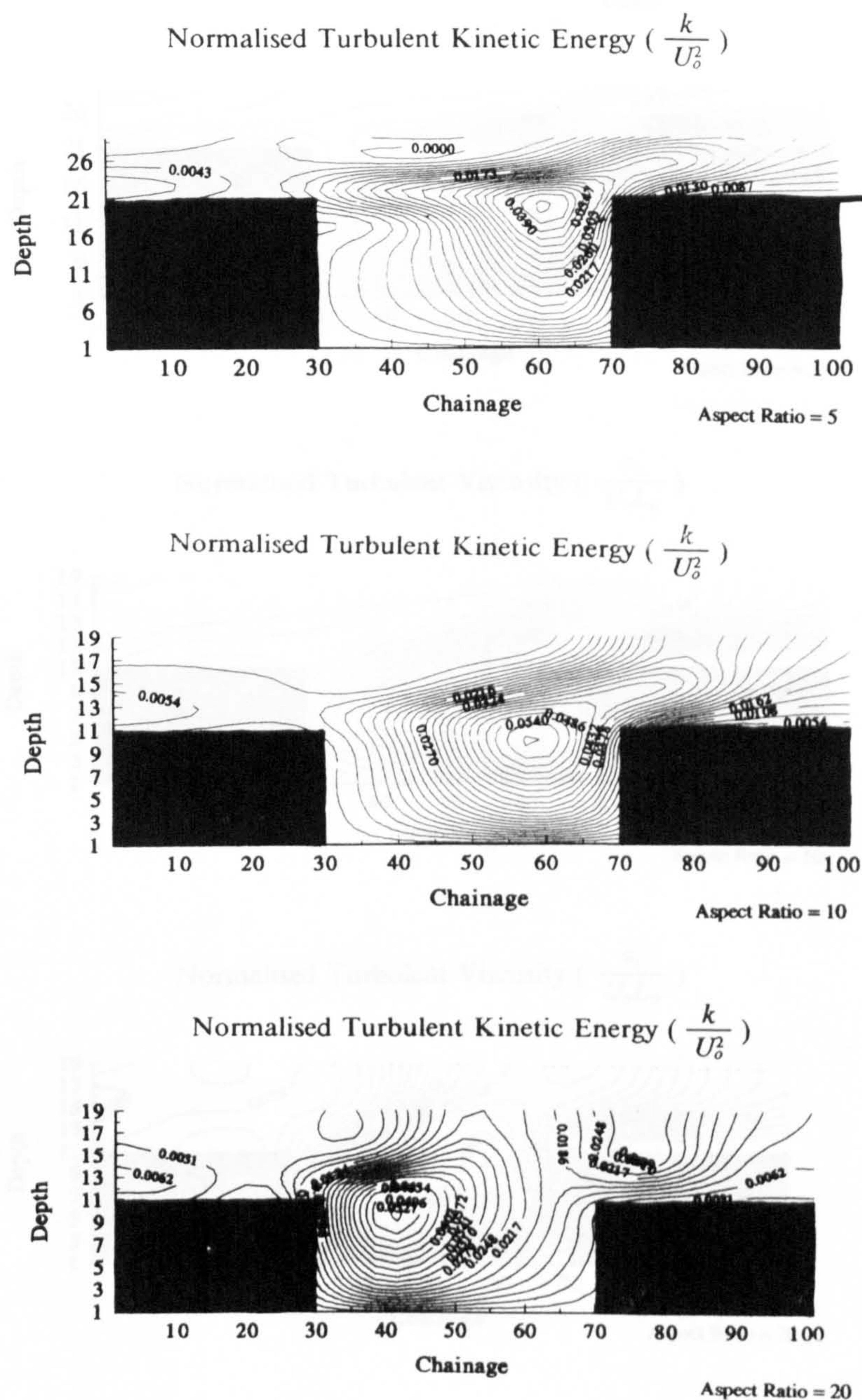


Figure 70. K Values at differing Aspects Ratios

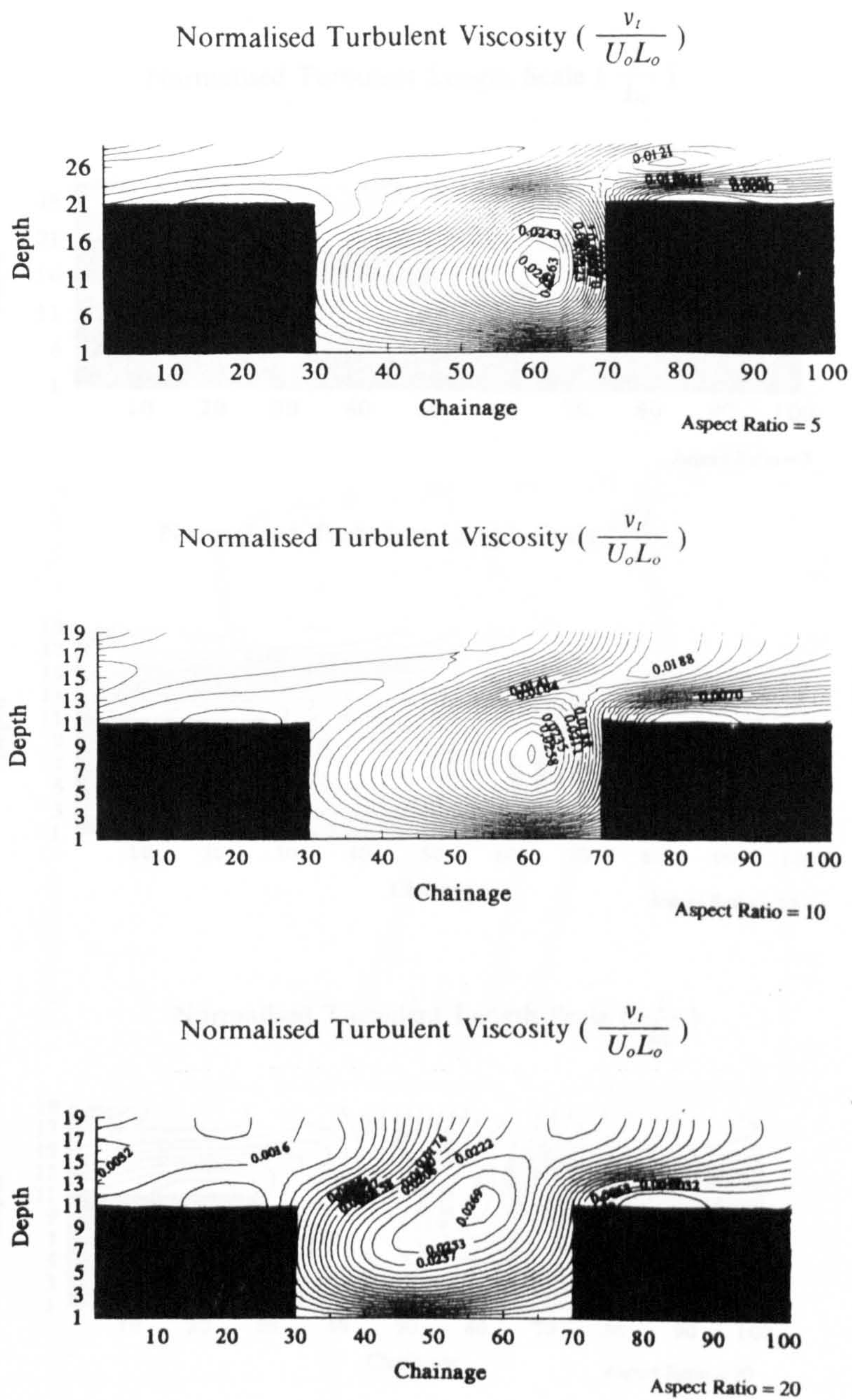


Figure 71. Eddy Viscosity Values at differing Aspects Ratios

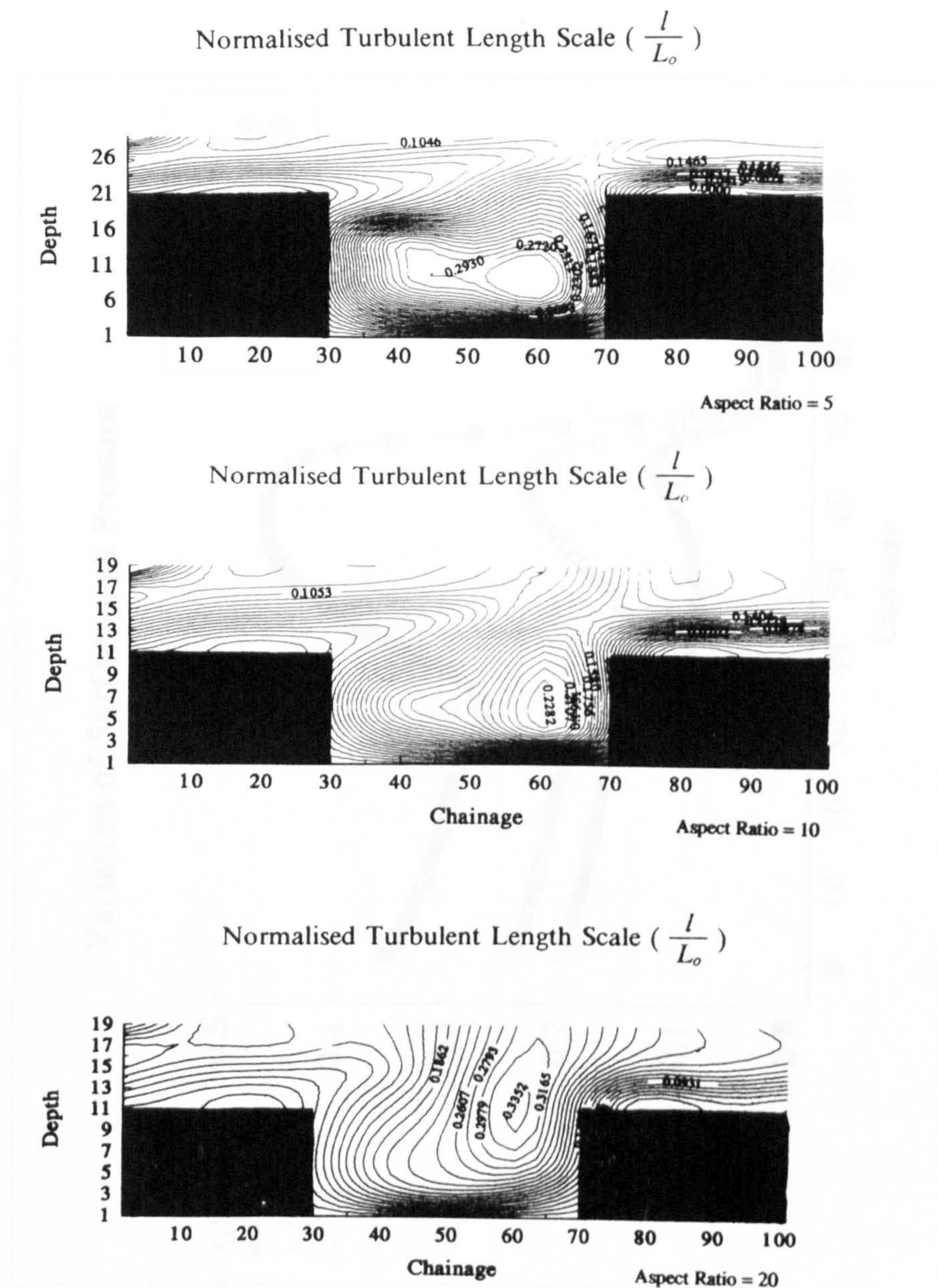


Figure 72. Turbulent Length Scale Values at differing Aspects Ratios

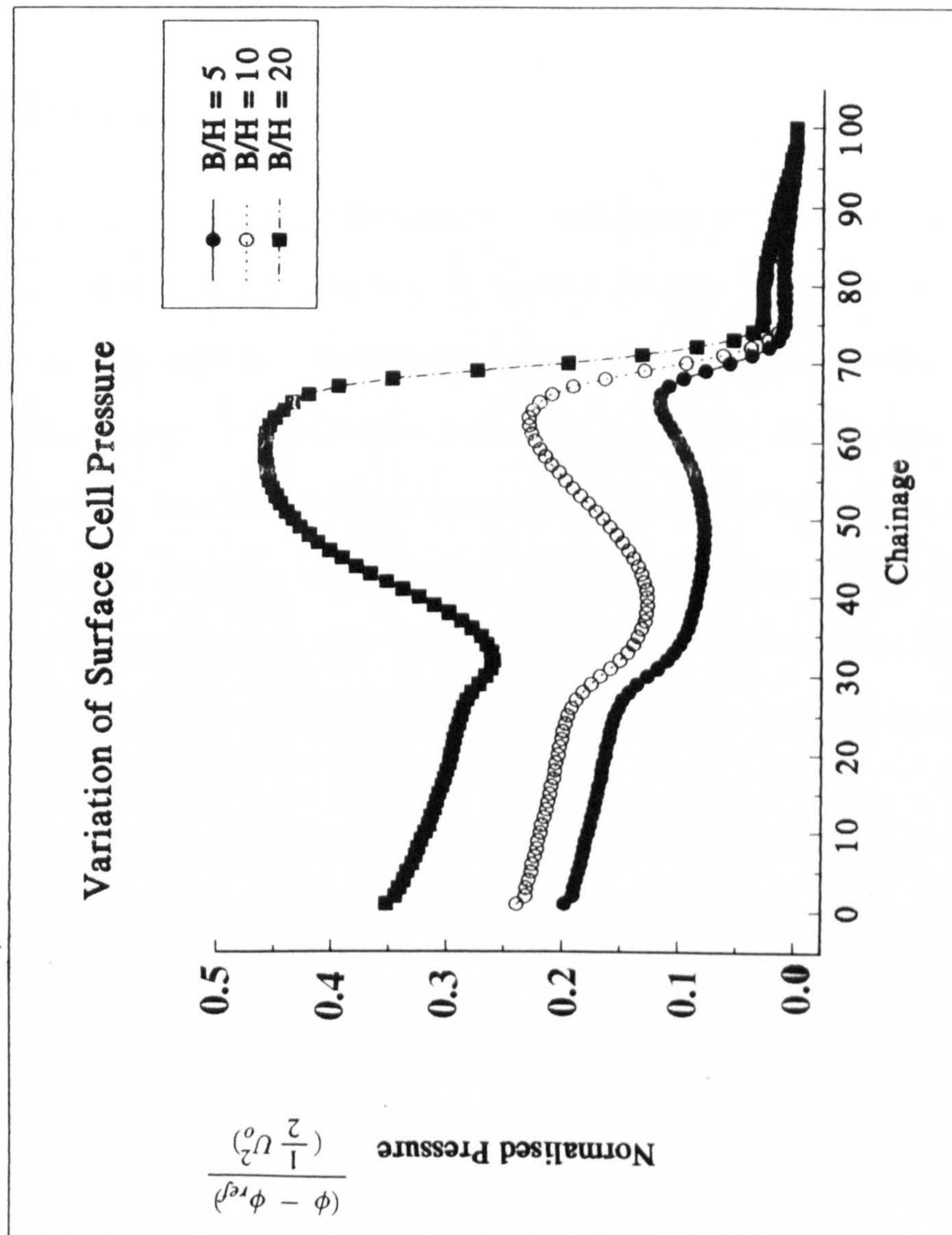


Figure 73. Normalised Surface Pressure Profiles

7.0 Chapter 7 Three Dimensional Applications

7.1 Overview

In this chapter a fully three dimensional application of the model is attempted. It is anticipated that the results will be limited because of the treatment of curved boundaries with the staircase approximation. Exactly how this effects the solution is not obvious and this simulation may shed some light on this type of boundary approximation. In addition limitations of computer time and storage mean that a relatively coarse grid has been adopted. Despite the higher order treatment of the advection terms it was felt that this grid may not be sufficiently refined to capture all of the flow features. None-the-less this exercise is important because:

- The experience of attempting this simulation will identify deficiencies in the present model and in particular may suggest suitable grid requirements for future computations.
- The results will demonstrate some of the main flow features known to occur in such systems and therefore it is believed that the present model, with further development, will be able to be used in a predictive mode.

It is interesting to get an idea of the computational requirements of fully three dimensional models. Table 16 shows some other recent studies.

Investigator(s)	Grid Details	Computer CPU Time	Computer Type
McGuirk and Palma (1992)	70 x 40 x 25	40 hours CPU over a period of a month	AMDHAL 470/V8
Henry, Collins and Ciofalo (1991)	24 x 24 x 24	Over 7 hours CPU (rough estimate)	IBM 3090 Mainframe
Henry, Collins and Ciofalo (1991)	24 x 24 x 24	Over 0.5 hours CPU	Cray 2

Table 16. Summary of some other fully three dimensional model applications: k-ε model for turbulence and traditional finite volume method

The present study uses a grid 61 x 49 x 17.

7.2 *Flow Mechanisms in Meandering Two-Stage Channels*

Certain flow mechanisms have been identified as important in meandering two-stage channels, Sellin, Ervine and Willetts, (1993).

1. There is a very strong interaction between the the flow in a meandering main channel and the over-bank flow on the floodplains. This interaction is characterised by net mass transfer between the main channel and the floodplains. The lateral shear stress (zero net mass transfer), so vitally

important in the straight channel case is insignificant in the meandering main channel case even for relatively low sinuositities. The mechanisms arising from the cross-over flow region driven by horizontal shear are much more important. This has consequences for the success of certain turbulence models. In particular, it may not be necessary to have such a refined treatment of the normal Reynolds stresses since clearly the pressure gradients may be so influential.

2. A consequence of the horizontal shear in the cross-over region the channel flow enters the bend with a secondary circulation contrary to that which would be due to the bend alone.
3. This circulation persists at least for half the bend. It heightens the tendency for the flow curvature to fail to match the bank curvature because the necessary pressure gradient to curve the flow cannot easily develop when the flow is contained by the banks. As a result water from the channel cross-section at the bend apex (including water from the channel bed) escapes on to the downstream floodplain immediately after the bend.
4. This process invites water from the upstream floodplain to plunge vigorously not at the channel bank but near the channel centre-line. This process continues for a considerable part of the cross-over region.
5. Detailed water level measurements indicate that the free surface is far from plane. This reflects the existence of several zones of flow curvature. There are also several zones of acceleration and deceleration. These are associated with expansion/contraction phenomena postulated by Ervine and Ellis (1987).

6. Flow expelled from the main channel, e.g. at the cross-over region, will carry with it scalars (turbulence, sediment, pollutant) into a wake region on the floodplain downstream of the cross-over.

The flow mechanisms that are seen to occur have certain consequences for the success of three dimensional models. In particular:

1. The strong vertical motions suggest that adopting a hydrostatic pressure distribution may lead to unquantifiable errors. A more prudent analysis would be to initially allow for a non-hydrostatic pressure field and then to proceed to the simpler hydrostatic hypothesis checking whether its adoption significantly degrades solution accuracy.
2. Flow reversal will occur in the primary flow direction and therefore only a fully elliptic version of the Reynolds Averaged Navier-Stokes will be appropriate.
3. The rigid lid approximation will probably be a satisfactory initial hypothesis since superelevations of the water surface above the equilibrium level (uniform depth) are less than 2.5% which is lower than the 10% value suggested by McGuirk and Rodi (1977).
4. Clearly the most significant turbulence phenomenon is the strong turbulence generation at the cross-over region. Its representation is probably the most crucial factor in the turbulence modelling. Since it is primarily a strong horizontal shear layer a two equation model of turbulence with a linear stress-strain relationship will be a suitable first step.
5. A suitable computational grid is likely to be a critical factor in the successful modelling of these flows. In order that all circulations are captured,

particularly in the main channel cross-over, a very fine grid may be required. This may require significant computer resources (storage and speed). This is an interesting paradox of numerical modelling. Adopting models with more dimensions, e.g. three dimensional instead of two dimensional or two dimensional instead of one dimensional, means that computer time required increases. However, it does not only increase because a more complex model has been adopted. It further increases because now more features (eddies) can, and perhaps should, be resolved. This is an important fact which has not been appreciated in the past leading to erroneous conclusions.

7.3 Description of the Present Problem

The test case geometry is taken from Kiely (1989) which is more amenable to numerical testing than the SERC FCF geometries. The geometry is more well conditioned, i.e. the aspect ratio of the main channel and the floodplains is not as large as the FCF. Whether or not this means the experimental geometry is a better approximation to reality or not is not the issue here. What matters is that the experimental geometry is easier to model numerically. The experimental set up is depicted in figure 74. It is basically a single meander with main channel flow depth 8 cm and flood plain depth 3 cm.. The experimental setup included long straight sections before and after the meander to allow the flow to attain fully developed conditions before and after the test section. This could not be replicated in the numerical model since the grid required would be too large. The total width of the channel is 120 cm. and the width of the main channel is 20 cm. The bed slope is set at 0.001 and the flow rate is 14.1 litres/sec. The sinuosity is 1.25, the aspect ratio of the main channel is 4 and the depth ratio is 0.38. Sometimes direct comparison with the data of Kiely (1989) could not be made conveniently, owing to the differing ways in which experimental measurements and numerical

predictions are presented. In these cases the numerical predictions were compared with other experimental data for geometries with similar relative depths and sinuosities to Kiely (1989). The other results used for qualitative comparison were Schroder, Stein and Rouve (1991) and one of the S.E.R.C. Series B experiments.

7.3.1 Grid and Boundary Conditions

Because the geometry is a single meander the same procedure was adopted as Rodi and Demuren (1986), i.e. inflow velocity and turbulence quantities were set and outflow values were computed. The pressure was set to a reference datum at the outflow section and the pressure was computed throughout the channel in a effort to simulate the effect of the free surface gradient on the flow field. A relatively coarse grid was adopted, figure 75, which was cartesian and so had to be chosen to closely approximate the real geometry in a staircase fashion as also tried by McGuirk and Palma (1992).

The inflow velocity profile adopted was a very simple approximation to the experimental values. Ideally one would wish to carry out a fully developed flow calculation as described in section 2.5.2. to provide the inlet profiles. However, in this case the u velocity was simply set to 40 cm/s in the main channel and 20 cm/s in the floodplain. Turbulence parameters were computed using the following formulae,

$$k_{in} = \frac{1}{2} \frac{u^{\star 2}}{\sqrt{c_{\mu}}}$$

where,

$$u^{\star} = \sqrt{ghS_o}$$

and h is the flow depth. The turbulent energy dissipation rate, ε , was then chosen to give a turbulent viscosity of,

$$\nu_t = \frac{1}{6} \kappa h u^*$$

The crudity of these approximations for the inlet quantities is recognised. However, it is felt that as a first approximation these will at least be the correct order of magnitude.

7.4 Results

The results are presented in a semi-quantitative fashion in the same spirit as McGuirk and Palma (1992). All results are presented from a viewpoint looking downstream.

7.4.1 Primary Velocity Field

The velocity profiles in the lateral direction at several flow depths are shown in figure 76 for sections 25, 31, 35 and 39. These correspond to the first bend apex, two sections in the cross-over region and the second bend apex respectively. The bankfull level is at 5.0 cm. The results of Kiely (1989) are shown in figure 77 for section A,B and C. These correspond to the first bend apex, the cross-over region and the second bend apex respectively. Some of the mechanisms appear to be reproduced. In particular, figure 76 shows:

1. The velocities in the main channel are lower than on the floodplain.
2. The velocities on the floodplain increase with depth above the floodplain.
3. There is a transfer of fluid from the main channel to the floodplain.

4. For the downstream section in the cross-over region and at the downstream bend apex the velocity profile has a minimum mid-way between the main channel and the edge of the floodplain. This is evidence of the wake effect observed by Kiely (1989).

The complexity of the results make them difficult to visualise. To aid in the interpretation a streamline plot was constructed. This shows in figure 78 that some streamlines continue down through the main channel while others move out onto the floodplain. This verifies the observations of Sellin, Ervine and Willetts (1993).

7.4.2 Secondary Velocity Field

A direct comparison of the secondary velocity field is difficult owing to the way in which experimental data was collected along a dog-leg section in the cross-over region, Kiely (1989). As an alternative therefore, the secondary velocity field was compared qualitatively with the results of Schroder, Stein and Rouve (1991). They show how, with cross-sections perpendicular to the floodplain walls, the longitudinal and lateral velocities may be resolved into components perpendicular to the mean flow direction. Both are shown in figure 79. The comparison appears disappointing since the numerical model results give no clear indication of the same secondary flow structure as experiment. A reverse flow is observed at the channel bed but a downward plunging flow is not reproduced at the channel centre. Kiely (1989) also found it difficult to isolate the secondary flow structure owing to the dominating effect of the flow expulsion onto the floodplain. The vigorous expulsion of main channel water onto the right flood plain is captured. The flow structure is dominated by the vigorous expulsion of main channel water onto the flood plain. This prevents the plunging flow from occurring. Inadequate grid resolution is almost certainly the reason for the numerical model's inability to resolve this feature.

7.4.3 Water Surface Elevation

The total pressure in the surface cell is separated into a uniformly sloping component due to the gravitational force and a deviation from this constant slope. Figure 80(b) shows the deviation from the uniform slope. Figure 80(a) shows a contour plot of depth from one of the S.E.R.C. Series B experiments.

Qualitatively, these results are very encouraging. The computations show, in agreement with experiment, regions of maximum water level within the main channel immediately prior to the floodplain just after the bend apex. These are followed on the floodplain by regions of minimum. This provides, for the first time, mathematical evidence that the expansion contraction flow, postulated by Ervine and Ellis (1987) occurs in such systems. This phenomenon has previously been verified by experiment but had not been verified numerically. This is an important capability of the model as it will be possible to evaluate energy loss coefficients from the results. This will enable the computation of coefficients for simpler conceptual models of meandering two stage channel flow, Wark (1993).

At either end of the meander away from the main channel curvature, the surface smoothly returns to a longitudinally uniform slope.

7.4.4 Turbulence Characteristics

A direct comparison is not possible owing to the way Kiely (1989) has defined turbulence intensity. However utilising the fact that the normalised kinetic energy is roughly equivalent to the square of the turbulence intensity some observations can be made. Figure 81 shows Kiely's measured turbulence intensity and the model prediction for the normalised turbulent kinetic energy both at 1.0 cm above the floodplain bed. A favourable comparison between the two plots is observed.

Note that only the normalised turbulent kinetic energy contours above 0.01 are plotted which would correspond to turbulence intensities of 10% (0.1).

Turbulence is generated most noticeably at the cross-over region where the velocity gradients are strongest, c.f. the slot flow. The turbulence generated here is carried on to the floodplain with the mean flow expelled from the main channel. This leads to higher turbulent mixing in this region. This is the wake effect observed by Kiely (1989).

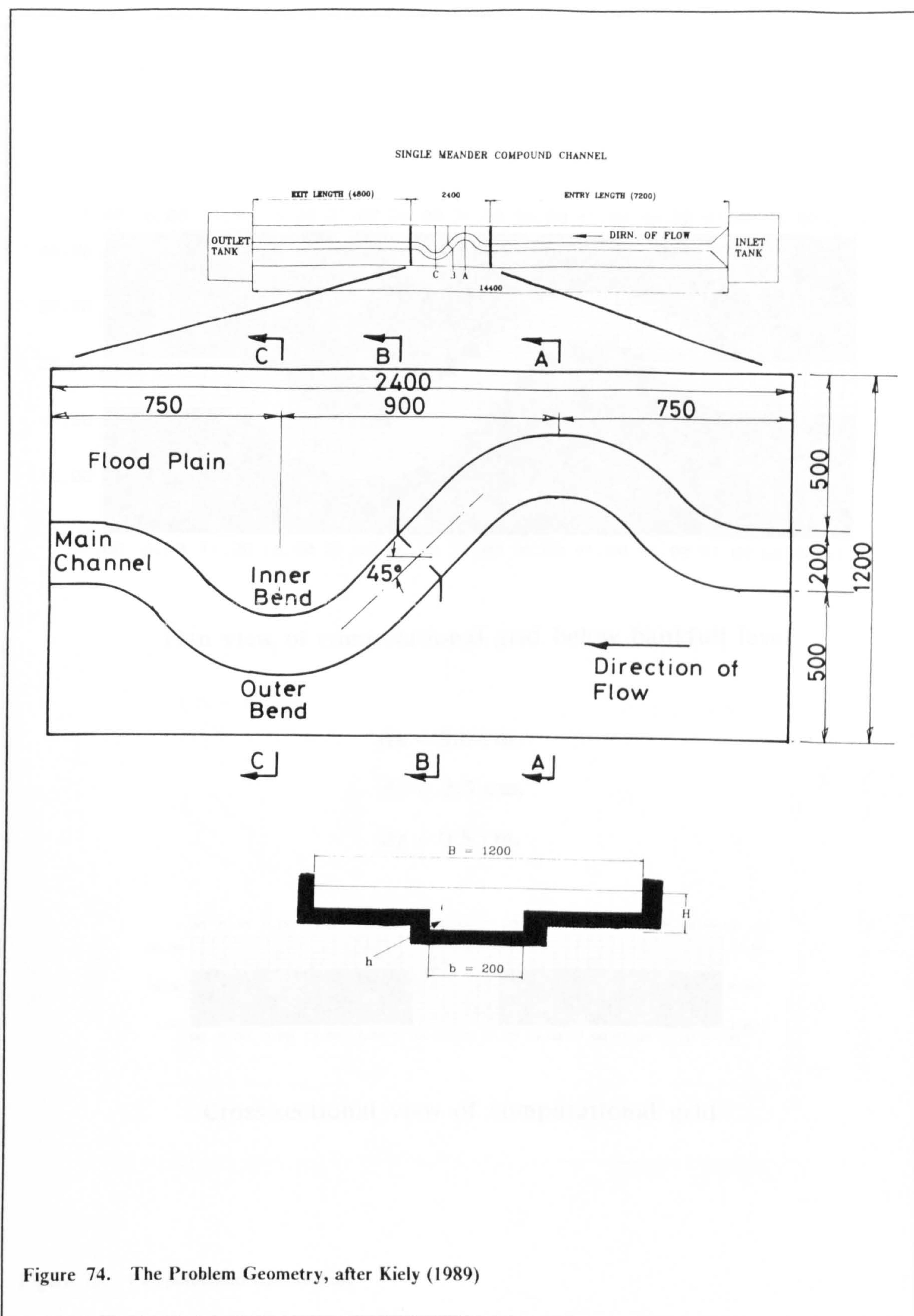
7.5 Conclusions from Results

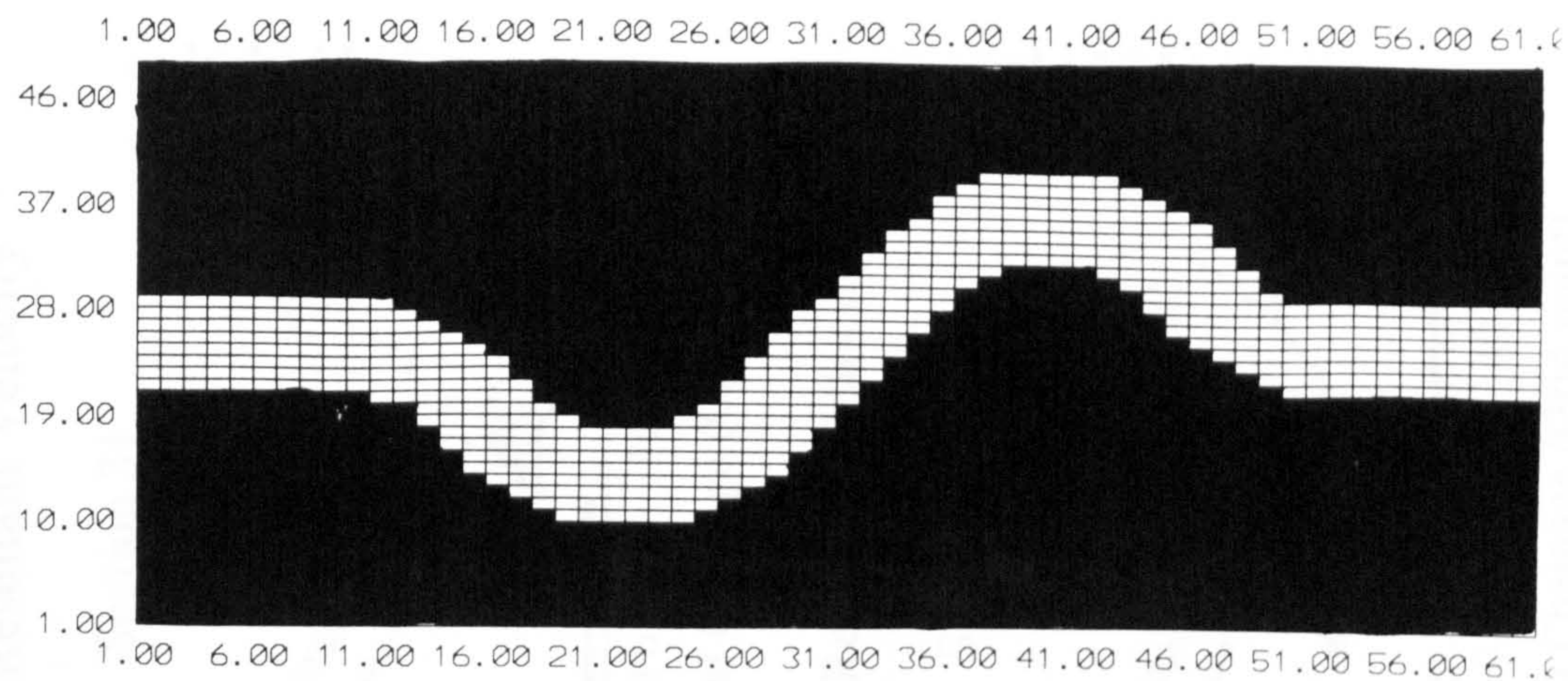
Basically, the model manages to predict some of the mechanisms occurring in a two-stage meandering channel system but fails to capture others. The surface pressure (water elevation) characteristics are captured favourably, as is the wake effect. In particular, expansion/contraction phenomena postulated by Ervine and Ellis (1987) has been shown mathematically to occur. The turbulence quantities are also predicted well considering this is the first attempt. In addition the model predicts correctly that a large portion of the main channel water ends up on the floodplain.

A disappointing trend emerges, however, when the velocity results are considered in detail. Overall the model overpredicts the expulsion of main channel water onto the floodplains. This manifests itself in the primary velocity field by underpredicting the main channel velocities and over predicting the flood plain velocities. It is observed in the secondary velocity field by the producing a secondary flow which is dominated by the expulsion of water onto the floodplain. This mechanism dominates the secondary flow field thus inhibiting the recirculation predicted by experiment. It is believed that the coarse grid in this

region (5 or 6) grid points across the main channel does not help matters in this regard. The question must be addressed however, why does the model underpredict main channel velocities and over predict flood plain velocities ?

The answer lies in the staircase approximation to the main channel skewed section, see figure 82. This approximation introduces a high artificial roughness in the main channel by basically producing lots of small elements which protrude into the flow. Lemos (1992) has previously identified this limitation of the staircase approximation. The artificial roughness induced in the main channel leads to lower velocities there. To satisfy continuity, however, the floodplain velocities are artificially enhanced by a spuriously high expansion. There are two ways that this problem could be overcome. Firstly, a much finer cartesian grid could be adopted which would approximate the non-aligned walls with smaller errors. However, a much better (though more complicated) solution would be adopting a boundary fitted transformed co-ordinate system. Simply adopting this transformed grid arrangement is not sufficient in itself. The grid would still require to be highly discretised in the cross-over region to capture the slot type recirculation. However, the mean flow could be better computed since the artificial roughness would not be present. The type of grid arrangement which would be best would probably be one which follows the dog-leg arrangement of typical experimental set ups. Figure 83 gives a possible example.



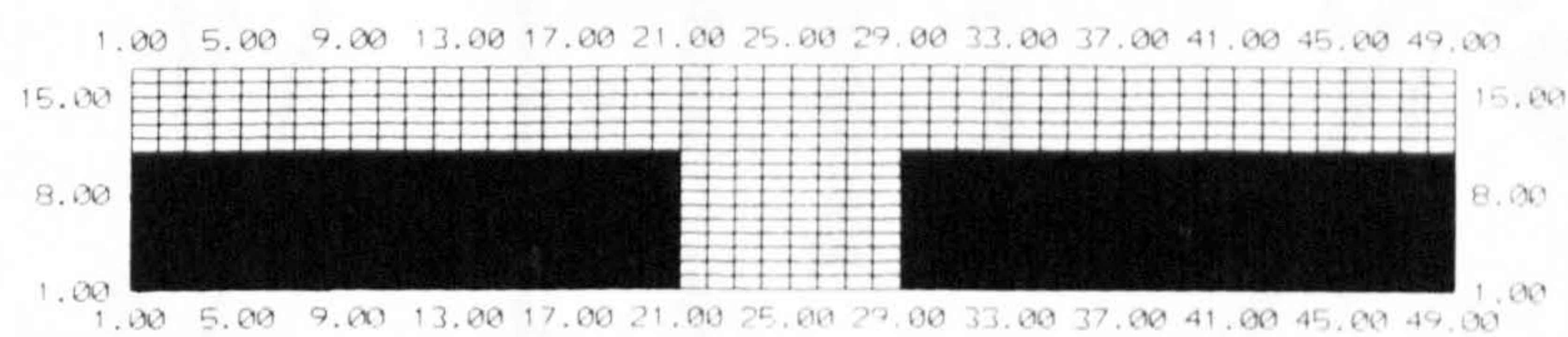


Plan view of computational grid below bankfull level

$dx = 5.0 \text{ cm.}$

$dy = 2.5 \text{ cm.}$

$dz = 0.5 \text{ cm.}$



Cross-sectional view of computational grid

Figure 75. Computational Grid Details

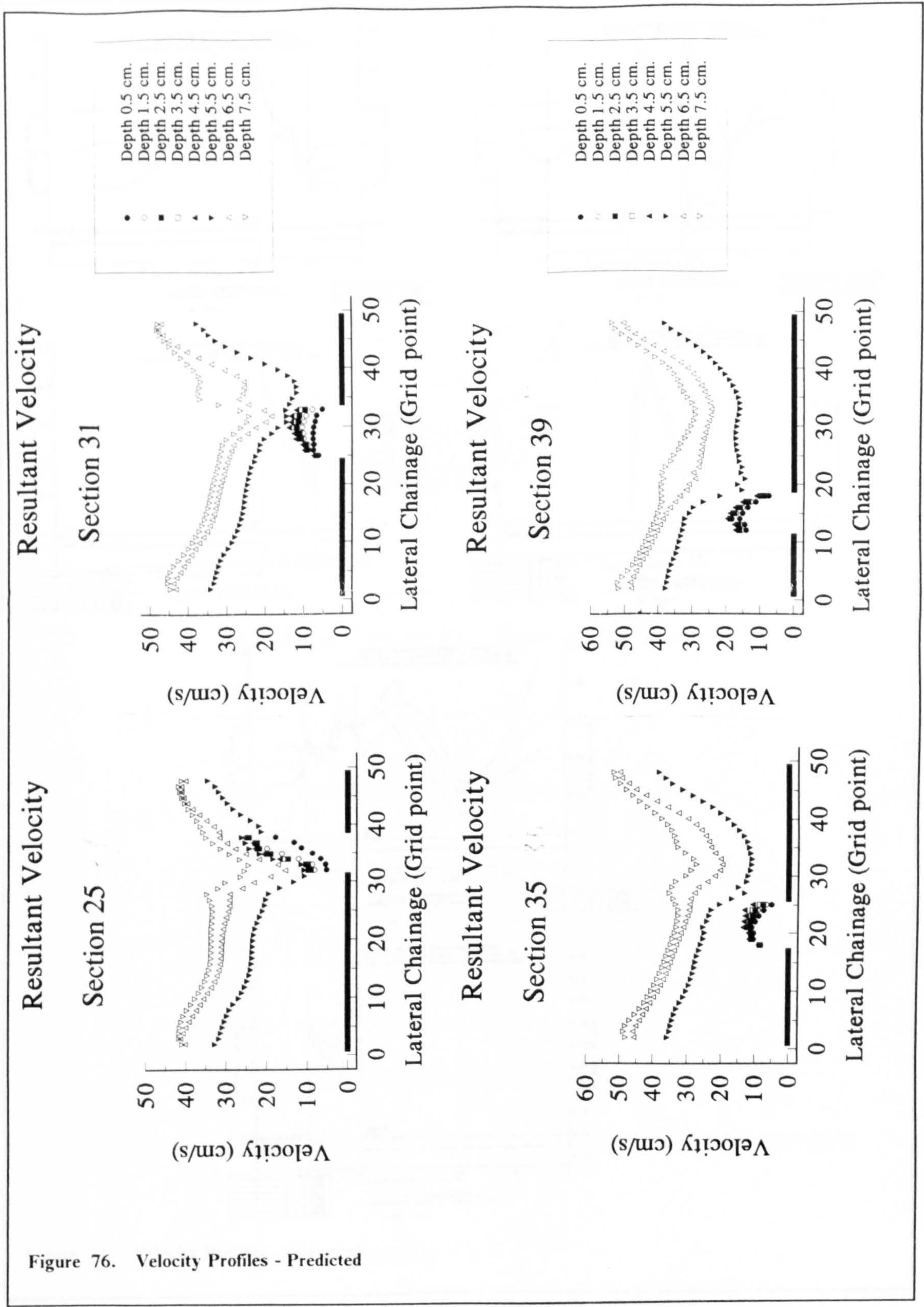


Figure 76. Velocity Profiles - Predicted

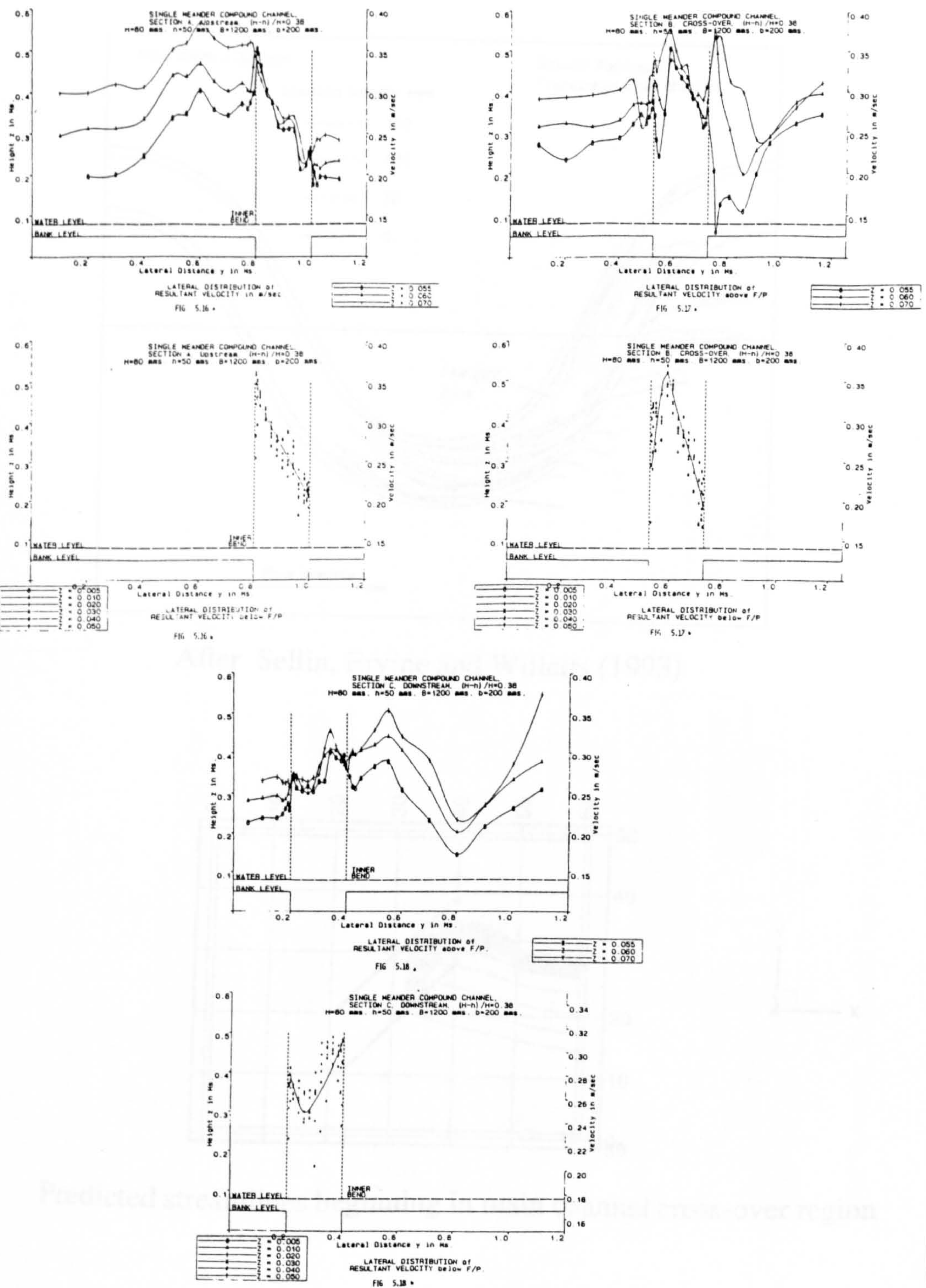
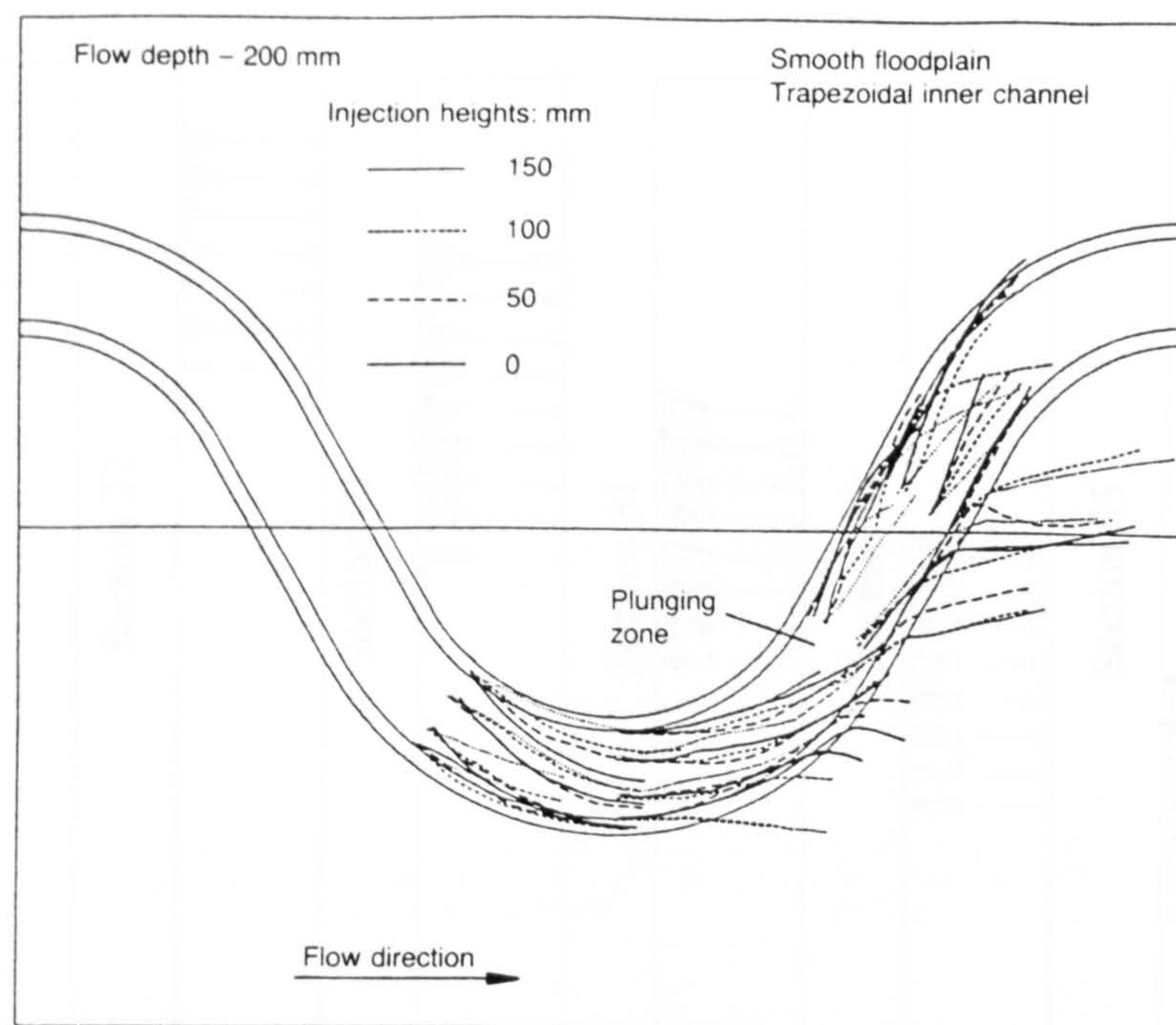
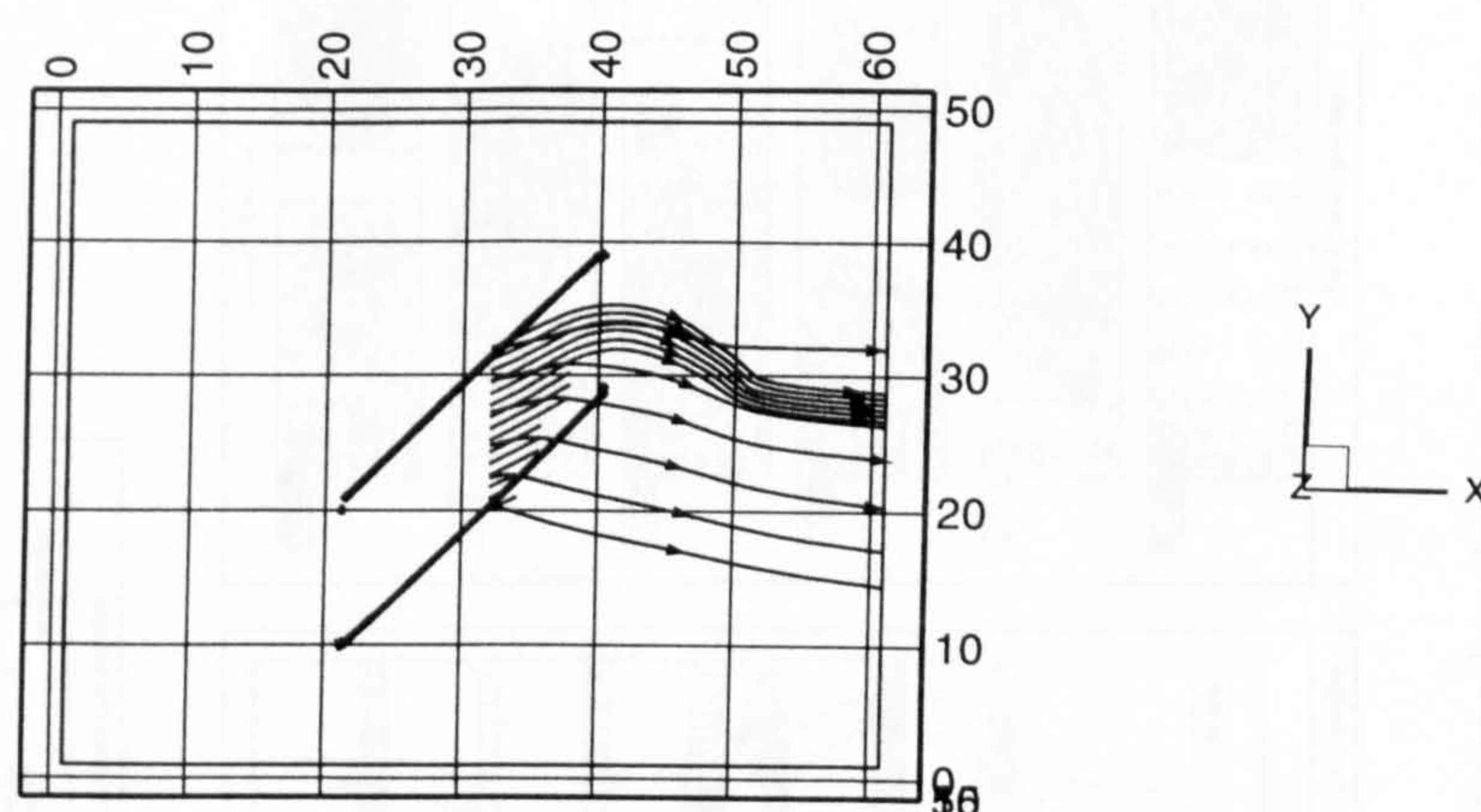


Figure 77. Velocity Profiles - Observed



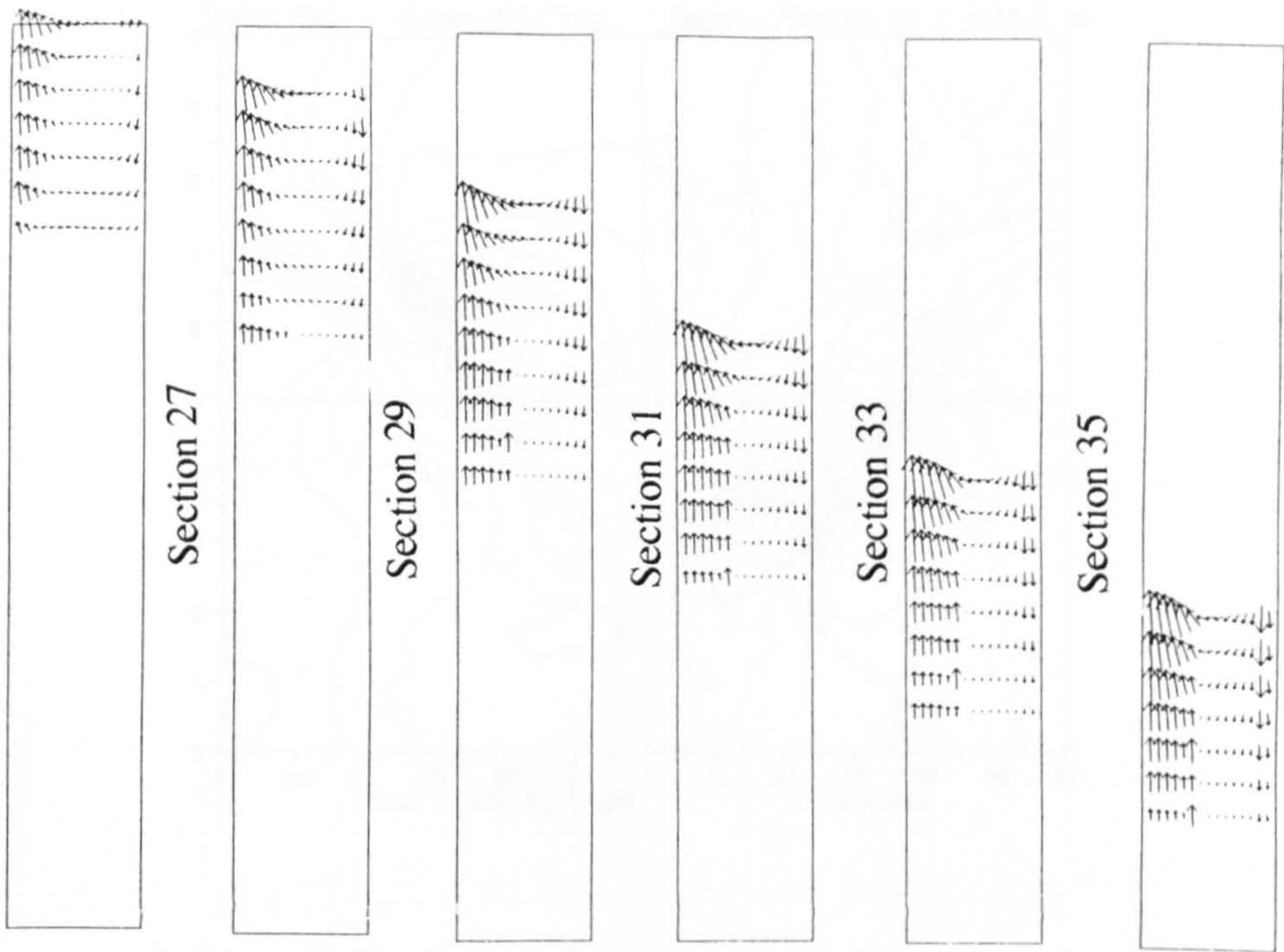
After Sellin, Ervine and Willetts (1993)



Predicted streamlines beginning in main channel cross-over region

Figure 78. Streamlines - Predicted and Observed

Figure 79. Lateral Velocity Vectors in Cross-over region - Pred and Obs



Predicted Secondary Flows Structure

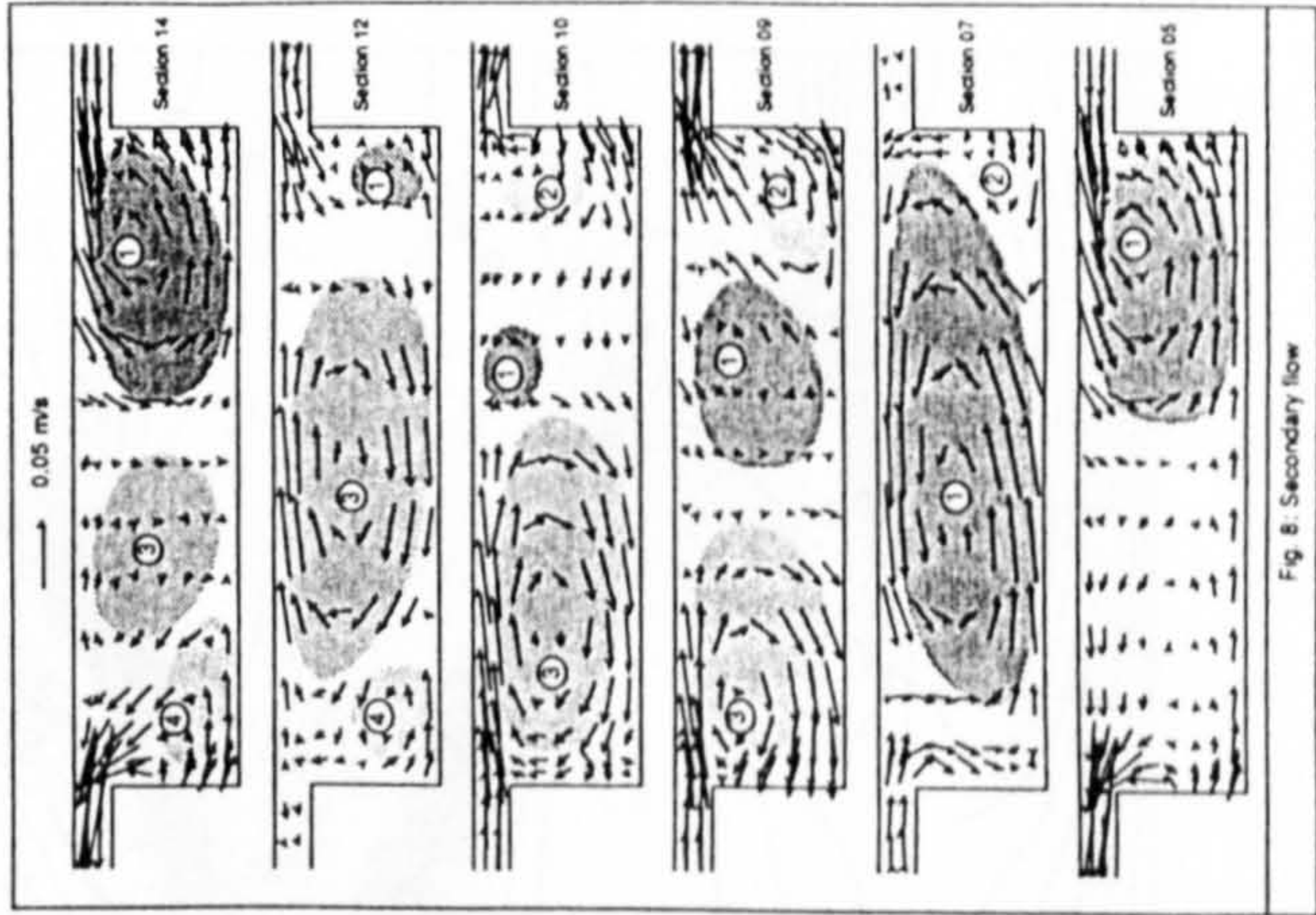
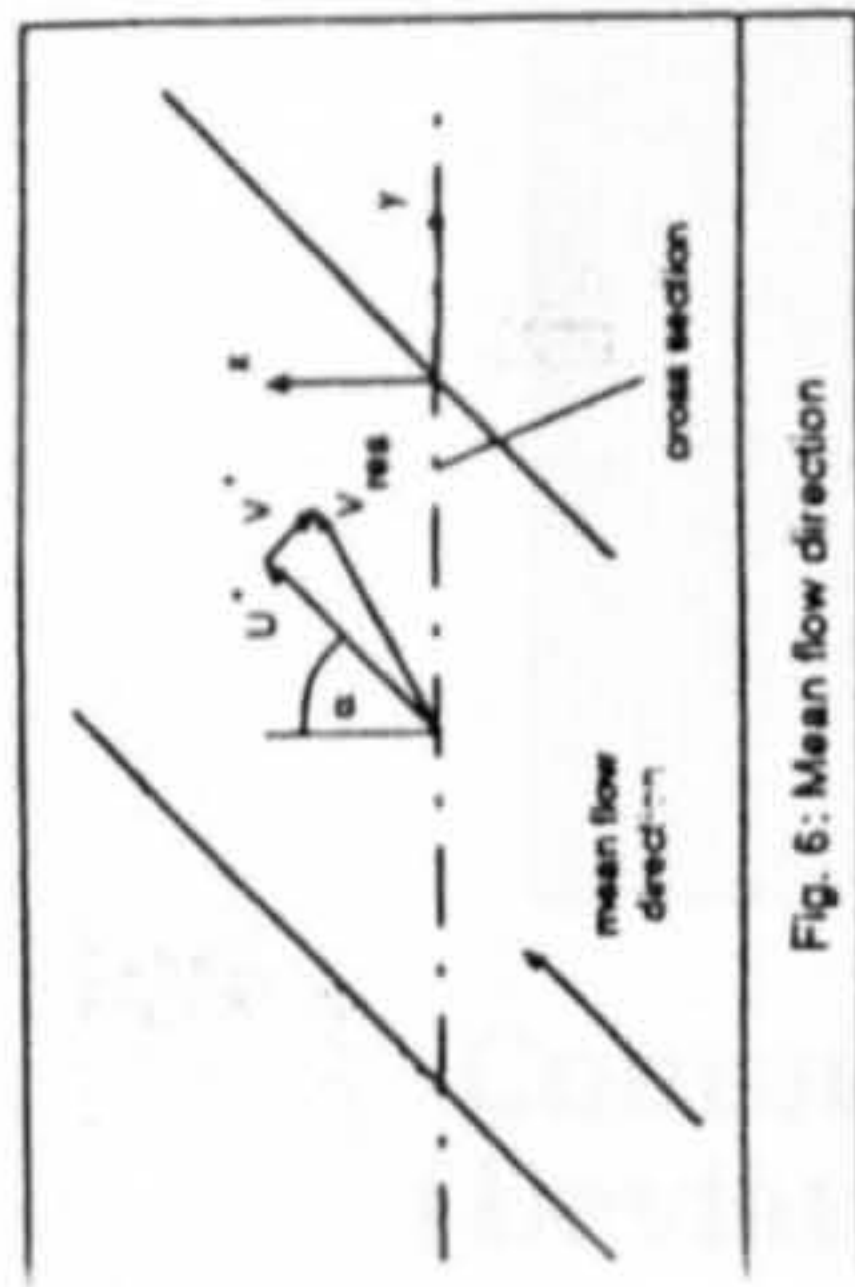
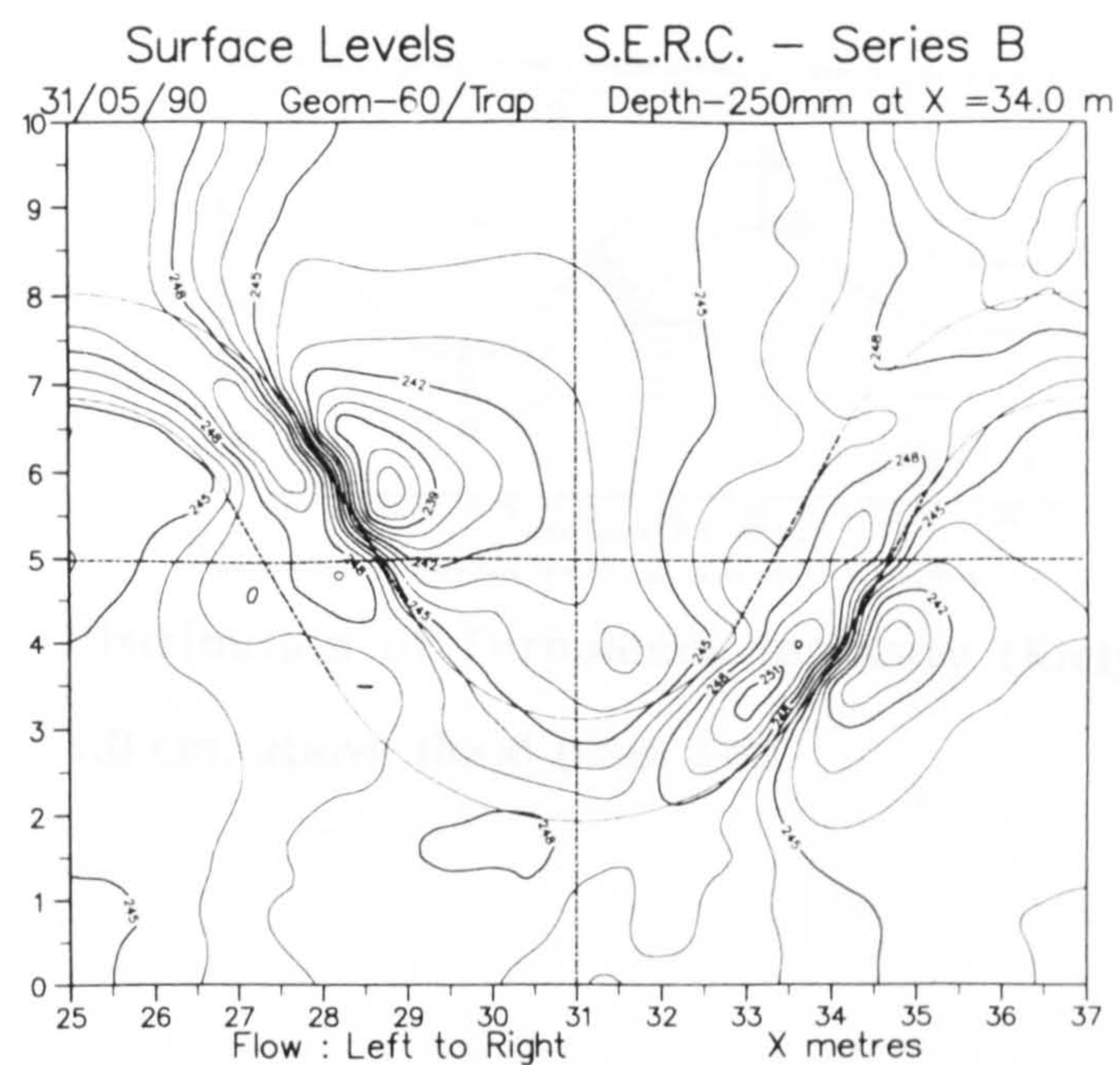


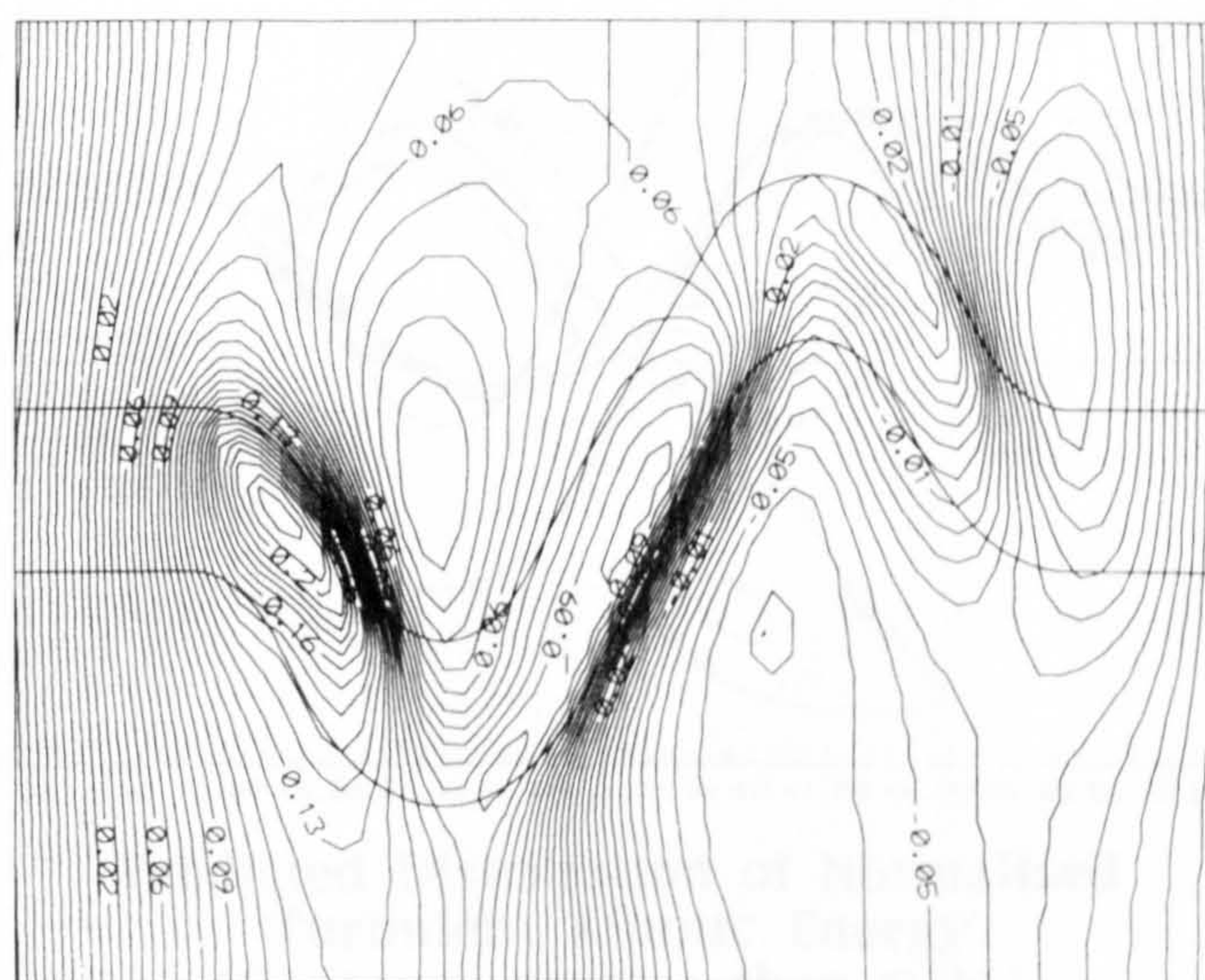
Fig. 6: Secondary flow

Fig. 7: Depth averaged velocities

After Schroder, Stein and Rouve (1991)

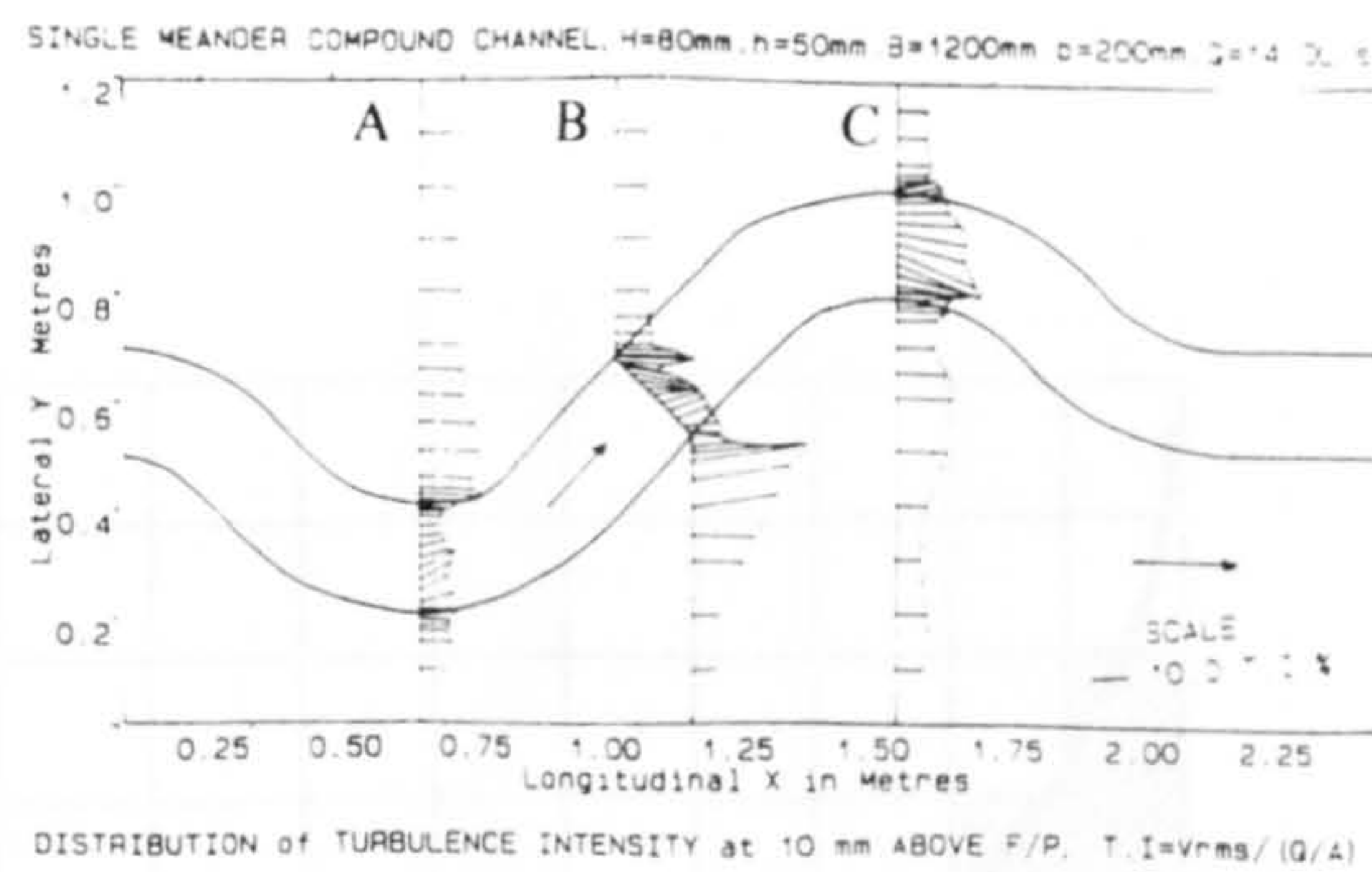


Direction of Flow →



Contours of Normalised Pressure in Surface Cell
(Deviation from Uniform Slope due to body force)

Figure 80. Comparison of water surface level



Distribution of Turbulence Intensity (Kiely, 1989)
1.0 cm. above flood plain bed

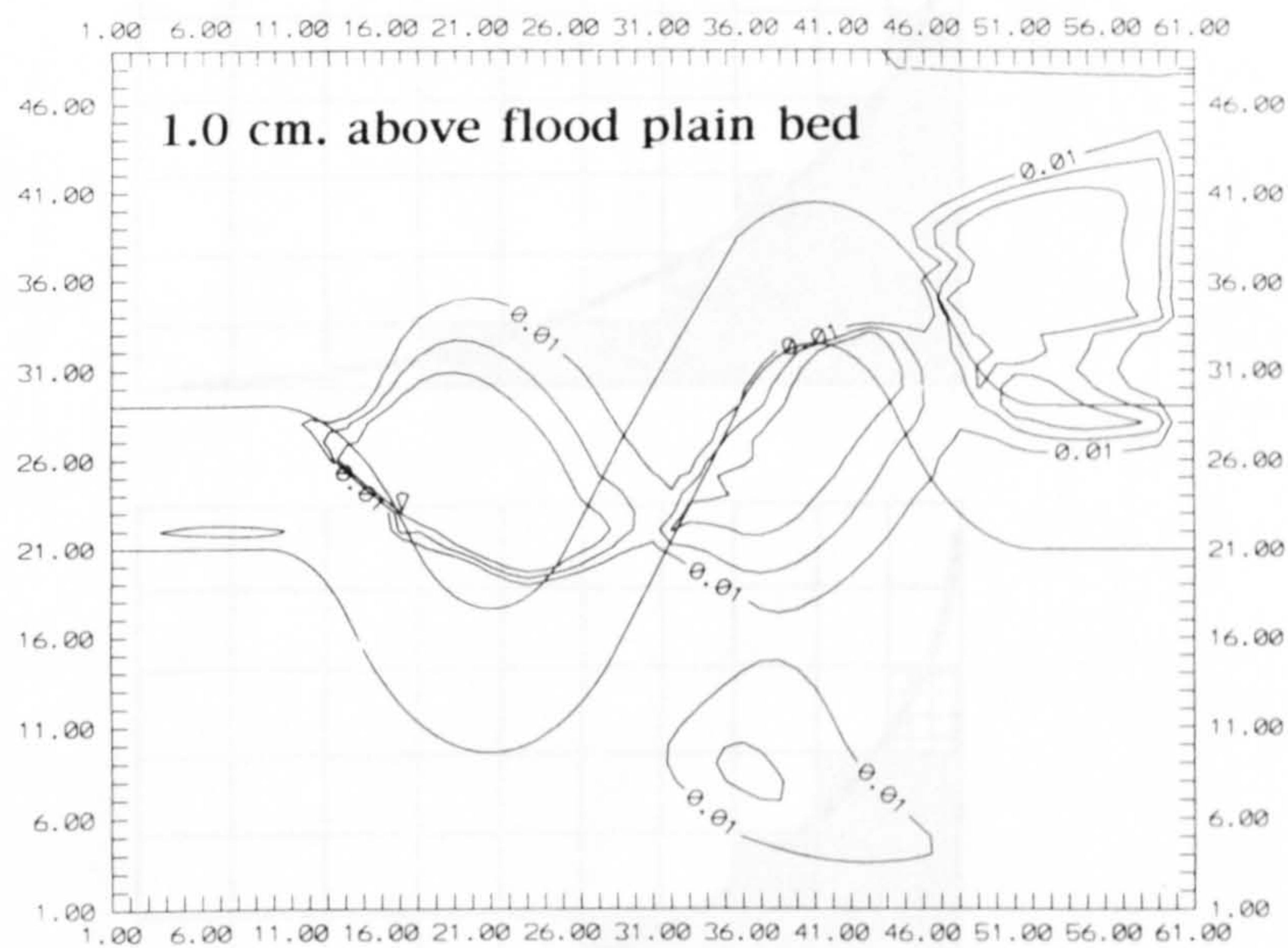


Figure 81. Comparison of turbulence above bankfull level

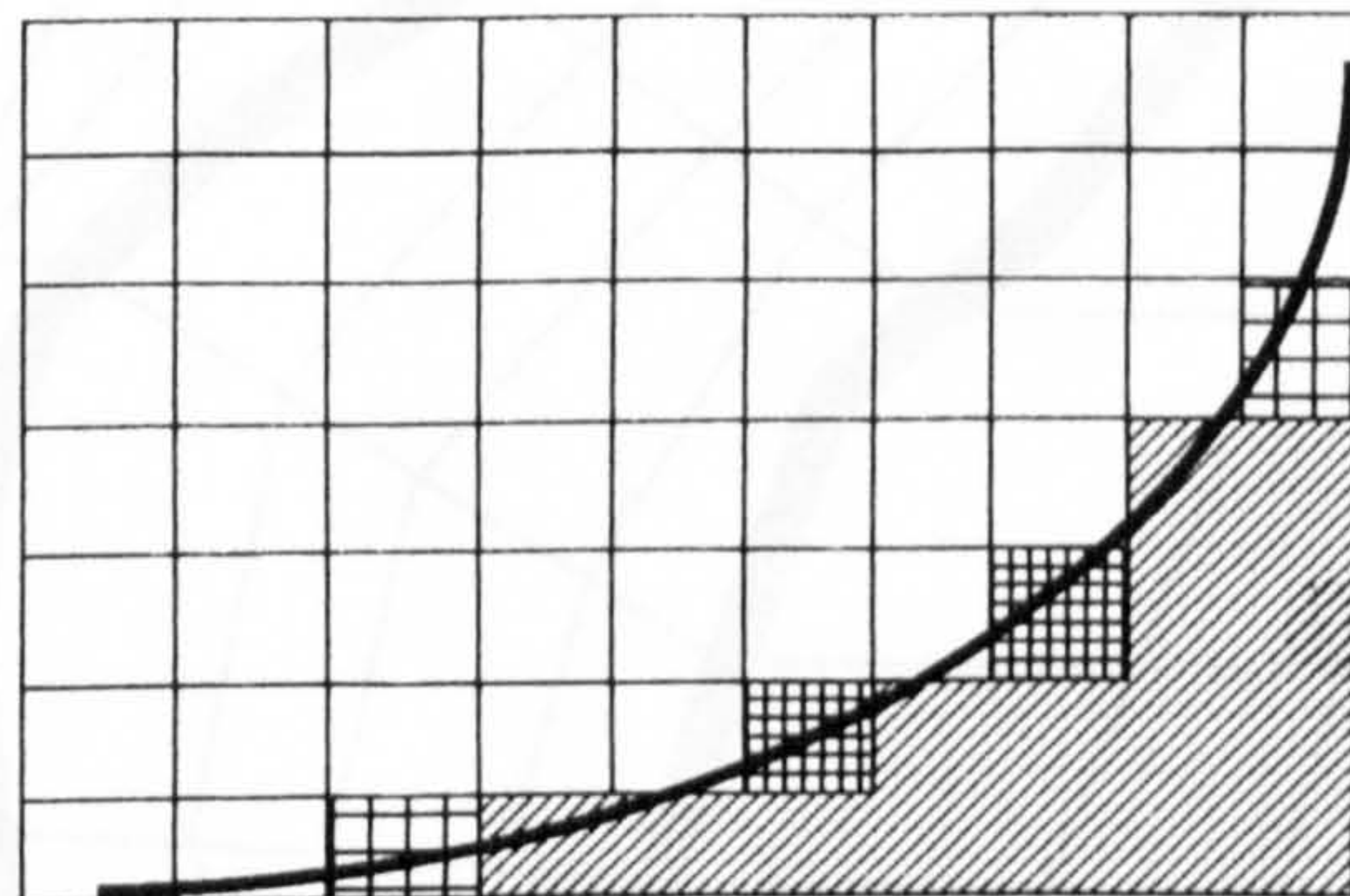
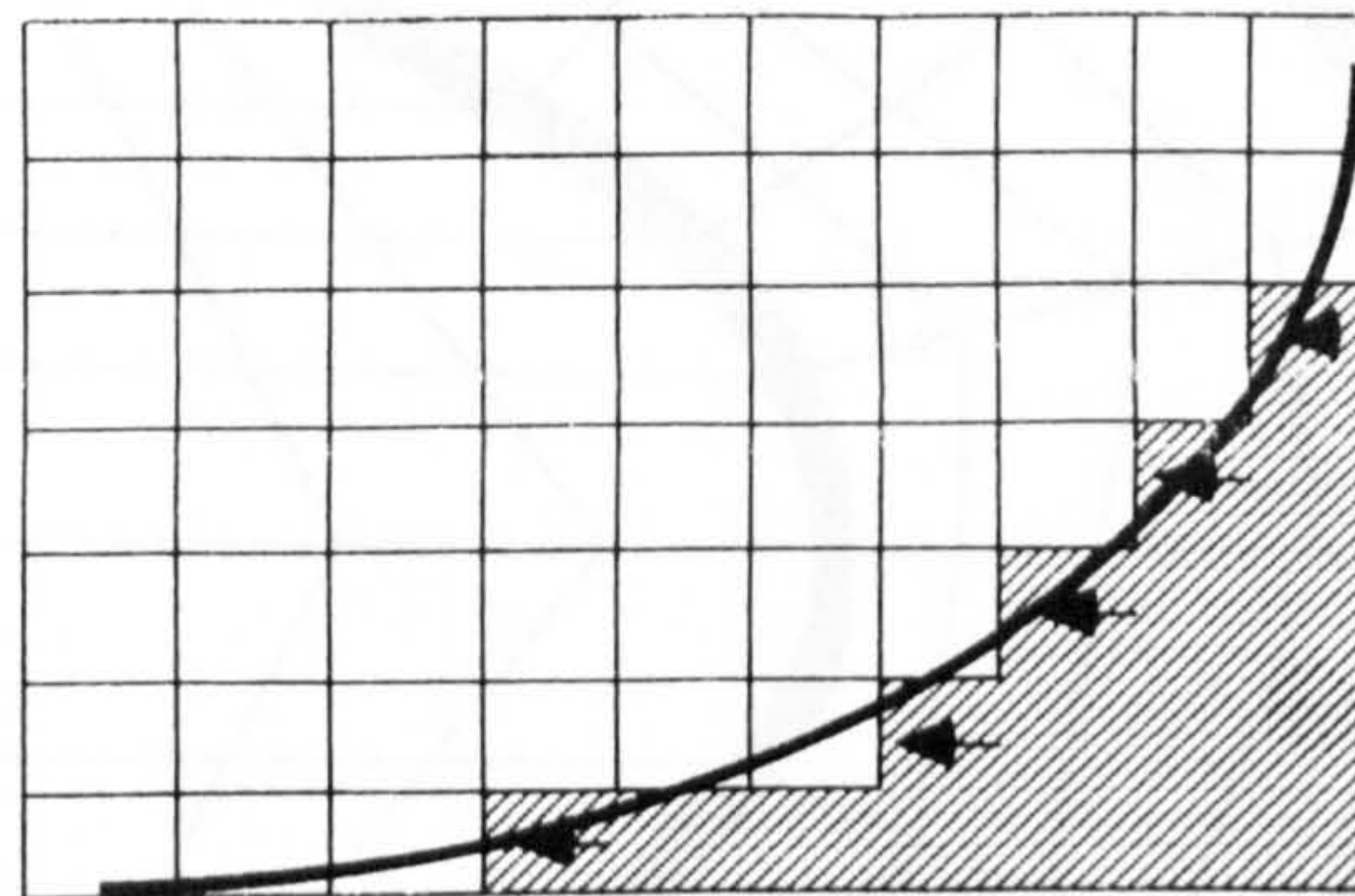
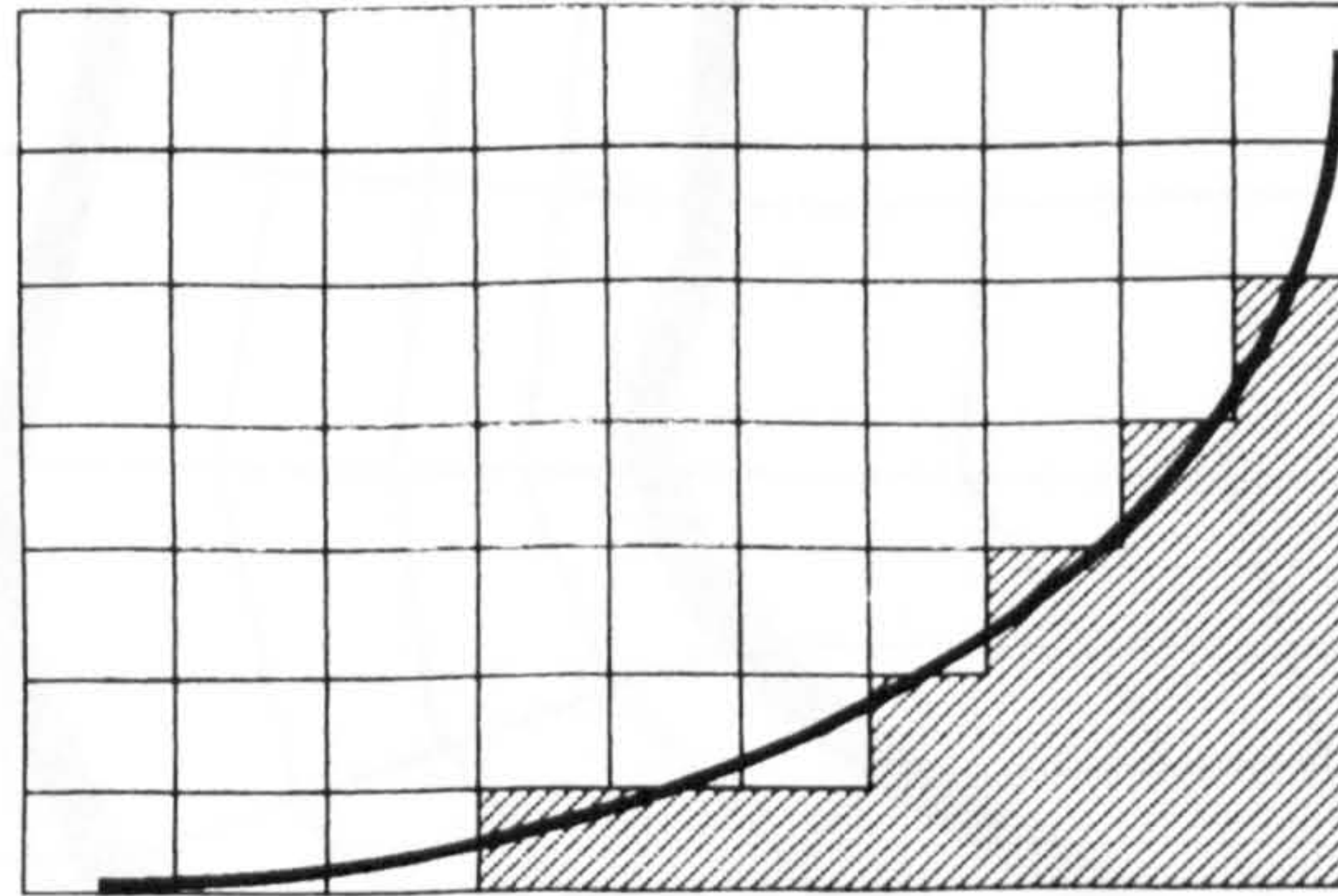


Figure 82. Staircase approximation

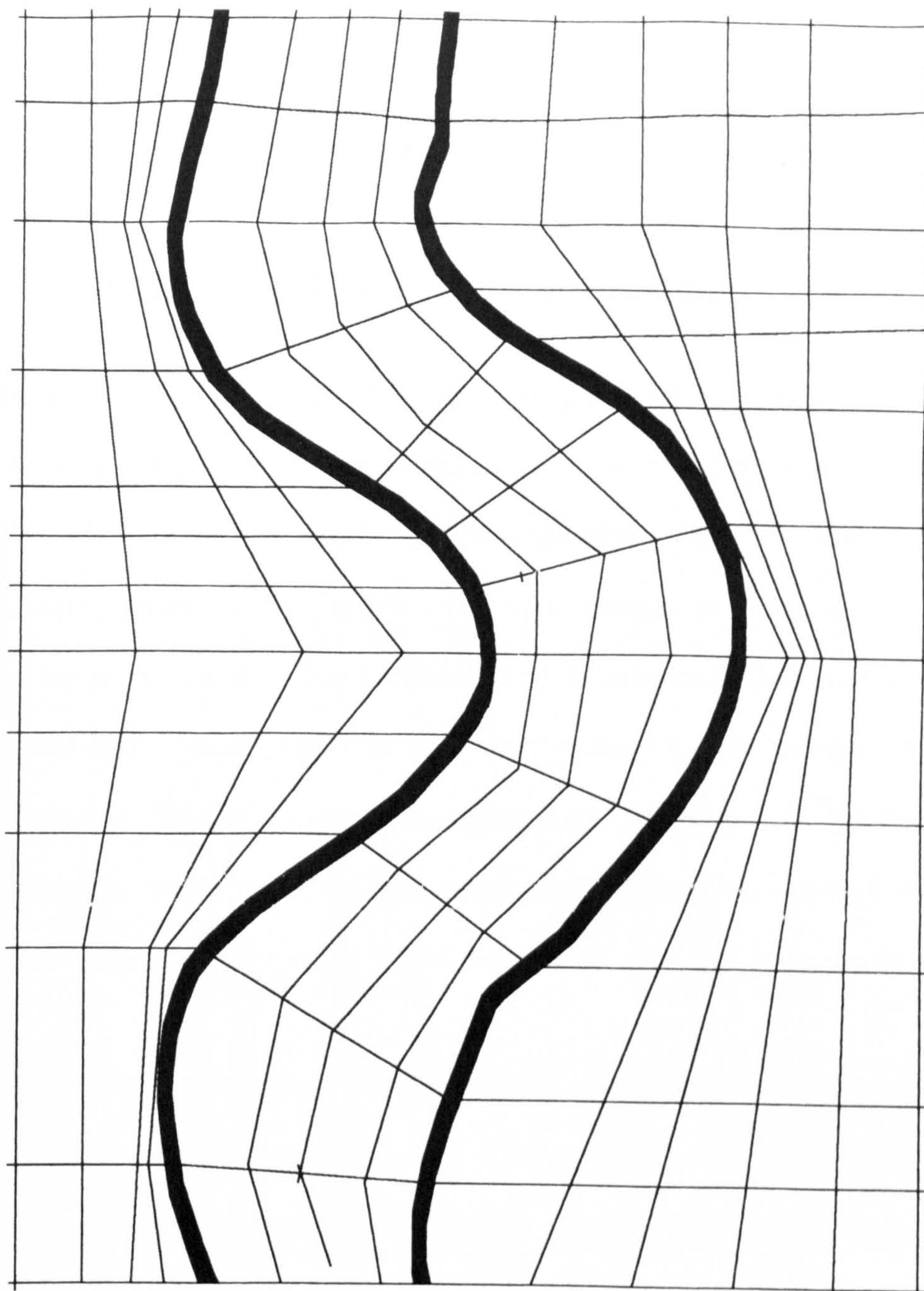


Figure 83. Possible grid for future study

8.0 Chapter 8 Closure

8.1 *Summary of Work and Conclusions*

As discussed in the previous chapters there is a need for a model that can be used to predict localised fully three dimensional flow fields at river transitions. This complex flow may be caused by natural river features, over bank flow in meandering rivers, or man made structures, bridges or weirs etc. Such a model would be useful for studying localised three dimensional flow patterns, dispersion characteristics, scour potential and thus aiding in the design of local river modifications. There are very few studies in the literature which have been aimed at producing such a model or even suggesting its viability although to be fair the computer resources for such a model have, until now, not been available.

This research was concerned with beginning the development of such a computer code for simulating free surface river flow to aid in the prediction of local three dimensional effects. It has concentrated on the hydrodynamics. The development work drew on studies in aeronautical and mechanical engineering. These disciplines have, in past research, been concerned with more sophisticated representations of turbulence and mixing characteristics and have not adopted the hydrostatic pressure assumption, common in civil engineering.

The work undertaken for this project has been,

1. A review of existing research in computational river engineering concluded that an area where more effort could be made is in the numerical prediction of very localised fully three dimensional flow features.
2. For this reason a fully three dimensional code has been developed which may form the basis of such a predictive procedure.
3. A two equation model of turbulence has been implemented to compute the eddy viscosity. Both linear and non-linear stress-strain relationships have been examined for modelling turbulence stresses.
4. The numerical treatment of the advection terms has been re-examined.
5. The model has been applied to both two dimensional (negligible lateral effects) and three dimensional problems.

8.1.1 Conclusions Regarding Numerical Methods

Formulations of traditional finite volume methods presented in the literature preclude the use of a lagrangian formulation for the advection terms. Chapter 6 demonstrates that there may be advantages in adopting the lagrangian formulation. Specific conclusions regarding numerical methods are:

1. Traditional finite volume discretisations of unsteady transport equations result in significant numerical errors in the advection terms (even with QUICK differencing) for Courant numbers greater than one.
2. Traditional finite volume discretisations of the unsteady advection terms with θ equal to one (even with QUICK differencing) result in a severe smoothing of steep profiles for all Courant numbers.

3. The present lagrangian numerical method has been shown to be superior in its treatment of the advection terms to traditional finite volume methods for accurate simulation of unsteady events at advective Courant numbers in excess of unity.
4. In dealing with the stress (or diffusion) terms an unsymmetrical differencing (upwinding) of the Oldroyd derivative terms in the non-linear model is recommended.
5. The convergence of preconditioned conjugate gradient solvers should be tested by monitoring P_{del} (the change in the dependent variable at each iteration) instead of the $Res2$ (the residual of the linear system).

8.1.2 Conclusions Regarding Turbulence Modelling

A comparison of the linear and non-linear turbulence models indicated that:

1. For strongly recirculating flows a non-linear stress-strain relationship will improve predictions of the level of the normal Reynolds stresses.
2. A numerical study of open channel flow over a backward facing step has reached similar conclusions to other investigators studying the corresponding closed channel case. Namely, the linear model underpredicts the size of the re-circulation region by about 15% and also underpredicts turbulence stresses beyond the recirculation zone. A non-linear model will improve both of these defects.
3. While, the non-linear relationship does improve predictions of the mean velocity field and turbulence quantities its adoption must be tempered by other practical factors. The question yet to be answered is: Is the non-linear

turbulence model or even more complex models useful in civil engineering practice where the uncertainties are an order of magnitude higher than the experimental studies used for testing ? Further application of linear and non-linear relationships is recommended.

8.1.3 Conclusions Regarding Two Dimensional Applications

Other tests in two dimensions using only the linear model suggested that:

1. A numerical study of slot flows has revealed a lack of understanding of this type of flow. Specifically, it appears that the flow mechanism is quite different from the backward facing step problem and it is wrong to conclude that if the forward facing step is beyond 5-7 step heights downstream of the backward facing step then re-attachment will occur within the slot. More experimental and numerical work can be done in this regard. This work is rather urgent since the existing data on slot flows, Jasem (1990), has already been incorporated into an empirical predictive procedure for discharge assessment in two-stage meandering channels, Wark (1993). No doubt this procedure would benefit from more accurate slot data.
2. The model adequately predicts the steady flow mechanisms in a settling chamber and therefore it is recommended to extend this to examine long term unsteady simulations since the present numerical method is more amenable to using large time steps.

8.1.4 Conclusions Regarding Three Dimensional Application

The three dimensional simulation was succesful in capturing the following:

1. A vigorous explusion of water from the main channel onto the floodplain.

2. Trends in the water elevation surface.
3. The wake effect, i.e. a minimum velocity on the floodplain midway between the main channel and the floodplain walls.
4. Higher turbulence levels in the wake.

The three dimensional simulation did not convincingly capture the the secondary motions in the cross-over region.

Some general conclusions regarding the three dimensional simulation of two stage channels are:

1. More work is required on the fully three dimensional simulations. Initial results are promising in some regards and disappointing in others. The staircase approximation will probably hamper future application of the model to two-stage meandering channels and the move to a boundary fitted grid system should be undertaken.
2. Regarding appropriate turbulence models for overbank flow in two stage channels the present study is inconclusive since the numerical effects have such a bearing on the final results. However, it appears that research efforts should initially concentrate on obtaining accurate grid independent solutions for a wide variety of geometries and flow rates with a linear two equation model of turbulence before (if ever) moving on to Reynolds Stress Transport Models. Although it can be argued theoretically that the RSTM captures more flow physics, in practical terms these features may not be significant. Sellin, Ervine and Willetts (1992) suggest, when considering both low and high sinosities, that,

The co-flowing lateral shear stress (zero mass transfer), so influential in the straight channel case, is insignificant at both the sinuousities here. The mechanisms arising from the cross-flow and driven by horizontal shear layers are much more important

The more complex turbulence representations may be important, however, for sediment and solute transport computation.

Appendix A - Tensors and Tensor Notation

Scalars and vectors are a special case of a more general quantity called a tensor of order m and which is made up of 3^m components. So a tensor of order 0 has 3^0 i.e. 1 component - a scalar value. A tensor of order 1 has 3^1 i.e. 3 components - a vector. Vectors are usually represented with a single index, for example, velocity,

$$u_i = \begin{bmatrix} u_1 \\ u_2 \\ u_3 \end{bmatrix} = \begin{bmatrix} u \\ v \\ w \end{bmatrix}$$

or the position vector,

$$x_i = \begin{bmatrix} x_1 \\ x_2 \\ x_3 \end{bmatrix} = \begin{bmatrix} x \\ y \\ z \end{bmatrix}$$

A tensor of ^{rank} 2 has 3^2 i.e. 9 components and is represented with two subscripts, for example, the stress tensor,

$$\tau_{ij} = \begin{bmatrix} \tau_{11} & \tau_{12} & \tau_{13} \\ \tau_{21} & \tau_{22} & \tau_{23} \\ \tau_{31} & \tau_{32} & \tau_{33} \end{bmatrix} = \begin{bmatrix} \tau_{xx} & \tau_{xy} & \tau_{xz} \\ \tau_{yx} & \tau_{yy} & \tau_{yz} \\ \tau_{zx} & \tau_{zy} & \tau_{zz} \end{bmatrix}$$

Tensor notation is a useful aid when discussing fluid dynamics since it abbreviates some rather long winded expressions. When indices are repeated this implies a summation, for example,

$$u_j u_j = u_1 u_1 + u_2 u_2 + u_3 u_3 = u^2 + v^2 + w^2$$

or,

$$\frac{\partial u_i}{\partial x_i} = \frac{\partial u_1}{\partial x_1} + \frac{\partial u_2}{\partial x_2} + \frac{\partial u_3}{\partial x_3} = \frac{\partial u}{\partial x} + \frac{\partial v}{\partial y} + \frac{\partial w}{\partial z}$$

This may be combined with a single other index as in the momentum advection terms for example,

$$u_j \frac{\partial u_i}{\partial x_j}$$

represents,

$$u \frac{\partial u}{\partial x} + v \frac{\partial u}{\partial y} + w \frac{\partial u}{\partial z}$$

$$u \frac{\partial v}{\partial x} + v \frac{\partial v}{\partial y} + w \frac{\partial v}{\partial z}$$

$$u \frac{\partial w}{\partial x} + v \frac{\partial w}{\partial y} + w \frac{\partial w}{\partial z}$$

Differential operators may be represented tensorially also, for example the gradient operator operated on a scalar gives a vector,

$$\frac{\partial}{\partial x_i} (p)$$

means,

$$\begin{bmatrix} \frac{\partial p}{\partial x} \\ \frac{\partial p}{\partial y} \\ \frac{\partial p}{\partial z} \end{bmatrix}$$

The divergence operator operated on a vector to give a scalar,

$$\frac{\partial}{\partial x_i}(u_i)$$

giving,

$$\frac{\partial u}{\partial x} + \frac{\partial v}{\partial y} + \frac{\partial w}{\partial z}$$

Appendix B - Speziale's Non-linear Stress-Strain Relationship

In tensor notation, Speziale's non-linear stress-strain relationship is,

$$-\overline{u'_i u'_j} = v_t 2 D_{ij} - \frac{2}{3} k \delta_{ij} + 4C_D C_\mu v_t T (D_{im} D_{mj} - D_{mn} D_{mn} \delta_{ij} / 3) \\ + 4C_E C_\mu v_t T (\dot{D}_{ij} - \dot{D}_{mm} \delta_{ij} / 3)$$

$$v_t = c_\mu \frac{k^2}{\varepsilon} \quad T = \frac{k}{\varepsilon}$$

$$\dot{D}_{ij} = \frac{D(D_{ij})}{Dt} - \frac{\partial u_i}{\partial x_k} D_{kj} - \frac{\partial u_j}{\partial x_k} D_{ki}$$

Here the full two dimensional expressions are given for the stresses, following Speziale and making use of the continuity equation to simplify.

$$\frac{\partial u}{\partial x} + \frac{\partial w}{\partial z} = 0$$

Stress - $\overline{u'^2}$

$$-\frac{2}{3} k + 2v_t \frac{\partial u}{\partial x} \\ + \frac{4}{3} c_\mu v_t T [(C_D - 2C_E) \left(\frac{\partial u}{\partial x} \right)^2 + \left(\frac{1}{4} C_D - 2C_E \right) \left(\frac{\partial u}{\partial z} \right)^2 \\ + \left(\frac{1}{2} C_D - C_E \right) \left(\frac{\partial u}{\partial z} \frac{\partial w}{\partial x} \right) + \left(\frac{1}{4} C_D + C_E \right) \left(\frac{\partial w}{\partial x} \right)^2] \\ + 4C_E C_\mu v_t T \left(u \frac{\partial^2 u}{\partial x^2} - w \frac{\partial^2 w}{\partial z^2} \right)$$

Stress - $\overline{w'^2}$

$$\begin{aligned}
& -\frac{2}{3}k + 2v_t \frac{\partial w}{\partial z} \\
& + \frac{4}{3}c_\mu v_t T[(C_D - 2C_E)\left(\frac{\partial w}{\partial z}\right)^2 + \left(\frac{1}{4}C_D - 2C_E\right)\left(\frac{\partial w}{\partial x}\right)^2 \\
& + \left(\frac{1}{2}C_D - C_E\right)\left(\frac{\partial u}{\partial z} \frac{\partial w}{\partial x}\right) + \left(\frac{1}{4}C_D + C_E\right)\left(\frac{\partial u}{\partial z}\right)^2] \\
& + 4C_E c_\mu v_t T\left(w \frac{\partial^2 w}{\partial z^2} - u \frac{\partial^2 u}{\partial z^2}\right)
\end{aligned}$$

Stress $-\overline{u'w'}$

$$\begin{aligned}
& v_t\left(\frac{\partial u}{\partial z} + \frac{\partial w}{\partial x}\right) \\
& - 4C_E c_\mu v_t T\left(\frac{\partial u}{\partial z} \frac{\partial w}{\partial z} + \frac{\partial u}{\partial x} \frac{\partial w}{\partial x}\right) \\
& + 2C_E c_\mu v_t T\left[u\left(\frac{\partial^2 w}{\partial x^2} - \frac{\partial^2 w}{\partial z^2}\right) + w\left(\frac{\partial^2 u}{\partial z^2} - \frac{\partial^2 u}{\partial x^2}\right)\right]
\end{aligned}$$

Bibliography

- 1 -

1988 ASCE Task Force on Turbulence Modeling
Turbulence Modeling of Surface Water Flow and Transport
Journal of the Hydraulic Engineering
Vol.114 No.9 Sept. pp.970

- 2 -

1963 A.S.C.E. Task Force
Friction Factors in Open Channels - Progress Report of
the Task Force on Friction Factors in Open Channels
Journal of the Hydraulics Division
Vol.89 HY2 March pp.97

- 3 -

1968 S.Abarbanel G.Zwas
An Iterative Finite-Difference Method for Hyperbolic
Systems
Mathematics of Computation
pp.549

- 4 -

1993 M.B.Abbott
From Modelling to Hydroinformatics
Advances in Hydro-Science and Engineering
Volume 1
Ed: S.Y.Wang

- 5 -

1962 D.E.Abbott S.J.Kline
Experimental Investigation of Sub-sonic Turbulent Flow
Over Single and Double Backward Facing Steps
Journal of Basic Engineering, ASME
Sept.

- 6 -

1985 S.M.Abdel-Gawad J.A.McCorquodale
Numerical Simulation of Rectangular Settling Tanks
Journal of Hydraulic Research
Vol.23 No.2

- 7 -

1991 P.Ackers
Hydraulic Design of Compound Channels
H R Wallingford, Oct., Report SR281
2 Volumes

- 8 -

1990 E.W.Adams W.Rodi
Modeling Flow and Mixing in Sedimentation Tanks
Journal of Hydraulic Engineering, ASCE
Vol.116 No.7 July

- 9 -

1984 R.Albanese F.Grasso C.Meola
On the Critical Problem of F.D. Pressure Treatment for
Laminar Flows Confined by Permeable Walls
International Journal for Numerical Methods in Fluids
Vol.4

- 10 -

1982 B.J.Alfrink
Value of Refined Turbulence Modelling for the Flow Over
a Trench
Proc.Symp.on Refined Modelling of Flows

- 11 -

1981 B.J.Alfrink
On the Neumann Problem for the Pressure in a
Nayier-Stokes Model
Proceedings of the 2nd Int.Conf.Num. Methods
in Laminar & Turbulent Flow
Swansea p389 Pineridge Pr

- 12 -

1983 B.J.Alfrink L.C.vanRijn
Two-Equation Turbulence Model for Flow in Trenches
Journal of Hydraulic Engineering, ASCE
Vol.109 No.3 July

- 13 -

1982 C.M.Allen
Numerical Simulation of Contaminant Dispersion in
Estuary Flows
Proceedings of the Royal Society of London
A 381

- 14 -

1978 A.M.M.Aly A.C.Trupp A.D.Gerrard
Measurements and Prediction of Fully Developed Turbulent
Flow in an Equilateral Triangular Duct
Journal of Fluid Mechanics
Vol.85 Prtl

- 15 -

1985 R.S.Amano P.Goel
Computations of Turbulent Flow Beyond Backward Facing
Steps Using Reynolds-Stress Closure
AIAA Journal
Vol.23 No.9 Sept

- 16 -

1993 M.Ammer F.Valentin
A Hierarchical Finite Element for Three Dimensional Free
Surface Flows
Refined Flow Modelling and Turbulence Measurements
Proc of the 5th International Symposium, Paris, France.

- 17 -

1970 A.A.Amsden F.H.Harlow
The SMAC Method: A Numerical Technique for Calculating
Incompressible Fluid Flows
Los Alamos Scientific Laboratory
Rep. LA-4370 Feb17

- 18 -

1968 A.A.Amsden F.H.Harlow
Transport of Turbulence in Numerical Fluid Dynamics
Journal of Computational Physics
Vol.3

- 19 -
 1970 A.A.Amsden F.H.Harlow
 A Simplified MAC Technique for Incompressible Fluid Flow
 Calculations
 Journal of Comp. Physics
 Vol 6 pp322-325

- 20 -
 1986 H.O.Anwar
 Turbulent Structure in a River Bend
 Journal of Hydraulic Engineering, ASCE
 Vol.112 No.8 Aug

- 21 -
 1980 H.O.Anwar R.Atkins
 Turbulence Measurements in Simulated Tidal Flow
 Journal of the Hydraulics Division, ASCE
 Vol.106 No.HY8 Aug

- 22 -
 1983 B.F.Armaly F.Durst J.C.F.Pereira B.Schonung
 Experimental and Theoretical Investigation of
 Backward-facing step flow
 Journal of Fluid Mechanics
 Vol.127 pp473-496

- 23 -
 1982 R.Arora K.K.Kuo M.K.Razdan
 Near-Wall Treatment for Turbulent Boundary-Layer
 Computations
 AIAA Journal
 Vol.20 No.11 Nov

- 24 -
 1988 W.Arter A.C.Newell
 Numerical Simulation of Rayleigh-Benard Convection in
 Shallow Tanks
 Physics of Fluids
 Vol.31 Part 9 Sept

- 25 -
 1987 A.Autret M.Grandotto I.Dekeyser
 Finite Element Computation of a Turbulent Flow Over a
 Two-Dimensional Backward Facing Step
 International Journal for Numerical Methods in Fluids
 Vol.7

- 26 -
 1988 J.L.T.Azevedo F.Durst J.C.F.Pereira
 Comparison of Strongly Implicit Procedures for the
 Solution of the Fluid Flow Equations in Finite
 Difference Form
 Applied Mathematical Modelling
 Vol.12 Feb

- 27 -
 1989 S.Babarutsi J.Ganoulis V.H.Chu
 Experimental Investigation of Shallow Recirculating
 Flows
 Journal of Hydraulic Engineering, ASCE
 Vol.115 No.7 July pp906

- 28 -
 1980 C.Babajimopoulos K.W.Bedford

Formulating Lake Models Which Preserve Spectral
Statistics
Journal of the Hydraulics Division, ASCE
Vol.106 No.HY1 Jan

- 29 -

1974 A.J.Baker
Navier-Stokes Solutions Using a Finite Element Algorithm
Lecture Notes in Physics - Proc.Int.Conf.on Num. Meth. in
Fluid Dynamics
Colorado

- 30 -

1983 A.J.Baker J.A.Orzechowski
An Interaction Algorithm for Three-Dimensional Turbulent
Subsonic Aerodynamic Juncture Region Flow
AIAA Journal
Vol.21 No.4 pp524

- 31 -

1983 B.R.Baliga S.V.Patankar
A Control Volume Finite-Element Method for Two
Dimensional Fluid Flow and Heat Transfer
Numerical Heat Transfer
Vol.6 pp245-261

- 32 -

1981 F.Baron J.P.Benque Y.Coefe
Turbulent Flow Induced by a Jet in Cavity - Measurements
and 3D Numerical Simulation
Turbulent Shear Flows 3
Third Int. Symp.

- 33 -

1975 D.I.H.Barr
Two Additional Methods of Direct Solution of the
Colebrook-White Function
Proc. Instn. of Civil Engineers
Prt2 Vol.59 Dec.pp827-835

- 34 -

1992 B.Basara B.A.Younis
Progress in the Prediction of Turbulent Wind Loading on Buildings
Journal of Wind Engineering and Industrial Aerodynamics
Vol.41-44 pp2863-2874

- 35 -

1976 R.M.Beam R.F.Warming
An Implicit Finite-Difference Algorithm for Hyperbolic
Systems in Conservation-Law Form
Journal of Comp. Physics
Vol22 pp87-110

- 36 -

1980 K.W.Bedford C.Babajimopoulos
Verifying Lake Transport Models with Special Statistics
Journal of the Hydraulics Division, ASCE
Vol.106 No.HY1 Jan

- 37 -

1980 S.Beltaos
Longitudinal Dispersion in Rivers
Journal of the Hydraulics Division, ASCE

- 38 -

- 1989 C.Benocci M.Skovgaard
Prediction of Turbulent Flow Over a Backward Facing Step
Numerical Methods in Laminar and Turbulent Flow, Vol.6
Proceedings of the 6th International Conference, Swansea

- 39 -

- 1987 J.R.Bennet A.H.Clites
Accuracy of a Trajectory Calculation in a Finite
Difference Circulation Model
Journal of Computational Physics
Vol.68

- 40 -

- 1989 A.C.Benim W.Zinser U.Schnell
Investigation into the Finite Element Analysis of
Enclosed Turbulent Diffusion Flames
Applied Mathematical Modelling
Vol.13 May

- 41 -

- 1982 J.P.Benque J.A.Cunge J.Feuillet A.Hauguel F.M.Holly
New Method for Tidal Current Computation
Journal of the Waterway, Port, Coastal and Ocean, ASCE
Vol.108 No.WW3 Aug

- 42 -

- 1982 J.P.Benque A.Hauguel P.L.Viollet
Engineering Applications of Computational Hydraulics: Volume II
Pitman Advanced Publishing Program

- 43 -

- 1980 J.P.Benque B.Ibler G.Labadie
A Finite Element Method for Navier-Stokes Equations
Numerical Methods for Non-Linear Problems
Proceedings of the International Conference at Swansea

- 44 -

- 1985 R.W.Benodekar A.J.H.Goddard A.D.Gosman R.I.Issa
Numerical Prediction of Turbulent Flow over
Surface-Mounted Ribs
AIAA Journal
Vol.23 No.3 Mar

- 45 -

- 1985 A.C.Benim W.Zinser
Investigation into the Finite Element Analysis of
Confined Turbulent Flows Using a k-e model of Turbulence
Computer Methods in Applied Mechanics and Engineering
51 pp507-523

- 46 -

- 1987 J.R.Bennet J.E.Campbell
Accuracy of Finite-Difference Method for Computing Lake
Currents
Journal of Computational Physics
Vol.68

- 47 -

1992 S.M.Bhallamudi M.H.Chaudhry
Computation of Flows in Open-Channel Transitions
Journal of Hydraulic Research
Vol.30 No.1

- 48 -

1992 A.F.Blumberg B.Galperin D.J.O'Connor
Modeling Vertical Structure of Open-Channel Flows
Journal of Hydraulic Engineering, ASCE
Vol.118 No.8 Aug

- 49 -

1983 A.F.Blumberg G.L.Mellor
Diagnostic and Prognostic Numerical Circulation Studies
of the South Atlantic Bight
Journal of Geophysical Research
Vol.88 No C8 pp4579-4592

- 50 -

1989 R.Booji
Depth-Averaged $k-\epsilon$ Modelling
Proc. of the XXIII IAHR Congress - Ottawa, 1989
A-199

- 51 -

1985 E.F.F.Botta M.H.M.Ellenbroek
A Modified SOR Method for the Poisson Equation in
Unsteady Free-Surface Flow Calculations
Journal of Comp. Physics
Vol.60 pp119-134

- 52 -

1987 C.Bouffinier M.Grandotto
A Comparison Study of a Turbulent Cavity Flow
in 'Turbulence Measurements and Flow Modeling'
Proceedings of the International Symposium, Iowa, U.S.A.
Eds: C.J.Chen L.-D.Chen F.M.Holly, jr.

- 53 -

1983 D.R.Boyle M.W.Golay
Measurement of a Recirculating Two-Dimensional,
Turbulent Flow and Comparison to Turbulence Model
Predictions. II: Transient Case
Journal of Fluids Engineering, ASME
Vol.105 Dec.

- 54 -

1983 D.R.Boyle M.W.Golay
Measurement of a Recirculating Two-Dimensional,
Turbulent Flow and Comparison to Turbulence Model
Predictions. I: Steady State Case
Journal of Fluids Engineering, ASME
Vol.105 Dec.

- 55 -

1877 J.Boussinesq
Mem Pres par div savants a l'acad sci Paris
Vol.23 pp.46

- 56 -

1974 W.R.Briley
Numerical Method for Predicting Three-Dimensional Steady

Viscous Flow in Ducts
Journal of Comp. Physics
Vol.14 pp8-28

- 57 -

1966 O.R.Burggraf
Analytical and Numerical Studies of the Structure of
Steady Separated Flows
Journal of Fluid Mechanics
Vol.24 Ptrl

- 58 -

1987 G.D.Byrne A.C.Hindmarsh
Stiff ODE Solvers: A Review of Current and Coming
Attractions
Journal of Computational Physics
Vol.70

- 59 -

1987 M.G.Carvalho F.Durst J.C.F.Pereira
Predictions and Measurements of Laminar Flow over
Two-Dimensional Obstacles
Applied Mathematical Modelling
Vol.11 Feb

- 60 -

1990 V.Casulli
Semi-implicit Finite Difference Methods for the Two-Dimensional
Shallow Water Equations
Journal of Computational Physics
Vol.86 pp56

- 61 -

1987 I.P.Castro J.M.Jones
Studies in Numerical Computations of Recirculating Flows
International Journal for Numerical Methods in Fluids
Vol.7

- 62 -

1978 T.Cebeci K.C.Chang
Calculation of Incompressible Rough-Wall Boundary-Layer
Flows
AIAA Journal
Vol.16 No.7 July

- 63 -

1987 I.Celik W.Rodi A.I.Stamou
Prediction of Hydrodynamic Characteristics of Rectangular
Settling Tanks
in 'Turbulence Measurements and Flow Modeling'
Proceedings of the International Symposium, Iowa, U.S.A.
Eds: C.J.Chen L.-D.Chen F.M.Holly, jr.

- 64 -

1988 I.Celik W.Rodi
Modelling Suspended Sediment Transport in
Non-equilibrium Situations
Journal of Comp. Physics
Vol.114 No10 Oct

- 65 -

1985 R.S.Chapman C.Y.Kuo
Application of the Two Equation k-epsilon Turbulence
Model to a Two Dimensional Steady, Free Surface Flow
Problem with Separation

International Journal for Numerical Methods in Fluids
Vol.5

- 66 -

1977 T.L.Chambers D.C.Wilcox
Critical Examination of Two-Equation Turbulence Closure
Models for Boundary Layers
AIAA Journal
Vol.15 No.6 Jun

- 67 -

1976 R.K.C.Chan
A Second-Order, Time Integration Scheme for Calculating
Stratified Incompressible Flows
Journal of Comp. Physics
Vol22 pp74-86

- 68 -

1976 P.C.Chatwin
Some Remarks on the Maintenance of the Salinity
Distribution in Estuaries
Estuarine and Coastal Marine Science
Vol.4

- 69 -

1983 R.S.Chapman C.Y.Kuo
Application of a High Accuracy Finite Difference
Technique to Steady, Free Surface Flow Problems
International Journal for Numerical Methods in Fluids
Vol.3

- 70 -

1970 R.K.C.Chan R.L.Street
A Computer Study of Finite-Amplitude Water Waves
Journal of Comp. Physics
Vol6 pp68-94

- 71 -

1976 C.-L.Chen
Flow Resistance in Broad Shallow Grassed Channels
Journal of the Hydraulics Division, ASCE
Vol.102 No.HY3 Mar

- 72 -

1992 Y.Chen R.A.Falconer
Advection-Diffusion Modelling Using the Modified QUICK
Scheme
International Journal for Numerical Methods in Fluids
Vol.15

- 73 -

1987 Eds: C.J.Chen L.D.Chen F.M.Holly
Turbulence Measurements and Flow Modelling
Hemisphere Publishing Corporation

- 74 -

1990 H.C.Chen V.C.Patel S.Ju
Solutions of Reynolds-Averaged Navier-Stokes Equations
for Three-Dimensional Incompressible Flows
Journal of Comp. Physics
Vol88 pp305-336

- 75 -
 1984 R.T.Cheng V.Casulli S.N.Milford
 Eulerian-Lagrangian Solution of the
 Convection-Dispersion Equation in Natural Coordinates
 Water Resources Research
 Vol.20 No.7 pp944-952 Jul

- 76 -
 1992 G.C.Cheng S.Farokhi
 On Turbulent Flows Dominated by Curvature Effects
 Journal of Fluids Engineering, ASME
 Vol.114 March

- 77 -
 1967 A.J.Chorin
 A Numerical Method for Solving Incompressible Viscous
 Flow Problems
 Journal of Comp. Physics
 Vol2 pp12-26

- 78 -
 1967 A.J.Chorin
 The Numerical Solution of the Navier-Stokes Equations
 for an Incompressible Fluid
 Bulletin of the American Mathematical Society
 Vol.73 Jan-Sept

- 79 -
 1983 D.P.Chock A.M.Dunker
 A Comparison of Numerical Methods for Solving the
 Advection Equation - I
 Atmospheric Environment
 Vol.17 No.1

- 80 -
 1985 D.P.Chock
 A Comparison of Numerical Methods for Solving the
 Advection Equation - II
 Atmospheric Environment
 Vol.19 No.4

- 81 -
 1968 A.J.Chorin
 Numerical Solution of the Navier-Stokes Equations
 Mathematics of Computation
 Vol22 pp745

- 82 -
 1959 V.T.Chow
 Open-Channel Hydraulics
 McGraw-Hill International Editions
 Civil Engineering Series

- 83 -
 1989 V.H.Chu S.Babarutsi
 Modelling the Turbulent Mixing Layers in a Shallow Open-Channel
 Proc. of the XXIII IAHR Congress - Ottawa, 1989
 A-191

- 84 -

1993 D.P.Cokljat

Turbulence Models for Non-circular Ducts and Channels

A PhD thesis submitted to City University, London in March, 1993.

Department of Civil Engineering.

- 85 -

1983 N.L.Coleman C.V.Alonso

Two Dimensional Channel Flows Over Rough Surfaces

Journal of Hydraulic Engineering, ASCE

Vol.109 No.2 Feb

- 86 -

1939 C.F.Colebrook

Turbulent Flow in Pipes, with particular reference to
the Transition Region Between the Smooth and Rough Pipe
Laws

Journal of the Inst. Civil Engineers

Vol.11 pp135-156

- 87 -

1986 S.D.Connell P.Stow

The Pressure Correction Method

Computers & Fluids

Vol.14 No.1 pp1-10

- 88 -

1993 T.J.Craft B.E.Launder K.Suga

Extending the Applicability of Eddy Viscosity Models Through
the Use of Deformation Invariants and Non-Linear Elements

Refined Flow Modelling and Turbulence Measurements

Proc of the 5th International Symposium, Paris, France.

- 89 -

1989 J.A.Cunge

Review of Recent Developments in River Modelling

Proc of 1st Int Conf on Hydraulic and Environmental Modelling
of Coastal, Estuarine and River Waters

University of Bradford, U.K.

- 90 -

1989 J.A.Cunge, F.M.Holly,jr A.Verwey

Practical Aspects of Computational River Hydraulics

Pitman Advanced Publishing Program

- 91 -

1970 B.J.Daly F.H.Harlow

Transport Equations in Turbulence

Physics of Fluids

Vol13 No11 pp2634

- 92 -

1968 B.J.Daly W.E.Pracht

Numerical Study of Density-Current Surges

Physics of Fluids

Vol11 No1 Jan pp15

- 93 -

1989 D.C.Dammuller S.M.Bhallamudi M.H.Chaudhry

Modeling of Unsteady Flow in Curved Channel
Journal of Hydraulic Engineering, ASCE
Vol.115 No.11 Nov

- 94 -

1986 A.Damaskinidou-Georgiadou K.V.H.Smith
Flow in Curved Converging Channel
Journal of Hydraulic Engineering, ASCE
Vol.112 No.6 June pp.476

- 95 -

1988 K.Dan Nguyen J.-M.Martin
A Two Dimensional Fourth Order Simulation For Scalar
Transport in Estuaries and Coastal Seas
Estuarine, Coastal and Shelf Science
Vol.27

- 96 -

1988 M.R.Davidson
Numerical Calculations of Flow in a Hydrocyclone
Operating Without an Air Core
Applied Mathematical Modelling
Vol.12 Apr

- 97 -

1980 R.W.Davis S.Deutsch
A Numerical-Experimental Study of Parshall Flumes
Journal of Hydraulic Research
Vol.18 No.2

- 98 -

1993 D.DeZeeuw K.G.Powell
An Adaptively Refined Cartesian Mesh Solver for the
Euler Equations
Journal of Computational Physics
Vol.104

- 99 -

1971 J.W.Deardorff
On the Magnitude of the Subgrid Scale Eddy Coefficient
Journal of Computational Physics
Vol.7

- 100 -

1970 J.W.Deardorff
A Numerical Study of Three-Dimensional Turbulent Channel
Flow at Large Reynolds Numbers
Journal of Fluid Mech.
Vol.41 part 2 pp.453-480

- 101 -

1987 I.Demirdzic A.D.Gosman R.I.Issa M.Peric
A Calculation Procedure for Turbulent Flow in Complex
Geometries
Computers & Fluids
Vol.15 No.3 pp.251-273

- 102 -

1983 A.O.Demuren W.Rodi
Side Discharges into Open Channels: Mathematical Model
Journal of Hydraulics Division, ASCE

- 103 -

1987 A.O.Demuren W.Rodi
Three-Dimensional Calculation of Turbulent Duct Flow
with Non-uniform Inlet Conditions
Computers & Fluids
Vol.15 No.1 pp47-57

- 104 -

1986 A.O.Demuren W.Rodi
Calculation of Flow and Pollutant Dispersion in
Meandering Channels
Journal of Fluid Mechanics
Vol172 pp63-92

- 105 -

1989 A.O.Demuren
Calculation of Sediment Transport in Meandering Channels
Proc. of the XXIII IAHR Congress - Ottawa, 1989
A-323

- 106 -

1983 A.C.Demetracopoulos H.G.Stefan
Transverse Mixing in Wide and Shallow River: Case Study
Journal of Environmental Engineering, ASCE
Vol.109 No.3 Jun

- 107 -

1985 Ph.Dewagenaere P.Esposito F.Lana P.L.Viollet
Three Dimensional Modelling of Flows with Application to
the Hot and Cold Plena of a Pool-Type LMFBR
Third Int. Conference on Reactor Thermo-dynamics, October
Paper 12 E

- 108 -

1987 D.E.Dietrich M.G.Marietta P.J.Roache
An Ocean Modelling System with Turbulent Boundary Layers
and Topography: Numerical Description
International Journal for Numerical Methods in Fluids
Vol.7

- 109 -

1991 N.Djilali I.S.Gartshore
Turbulent Flow Around a Bluff Rectangular Plate. Part I:
Experimental Investigation
Journal of Fluids Engineering, ASME
Vol.113 March

- 110 -

1991 N.Djilali I.S.Gartshore M.Salcudean
Turbulent Flow Around a Bluff Rectangular Plate. Part
II: Numerical Predictions
Journal of Fluids Engineering, ASME
Vol.113 March

- 111 -

1978 M.R.Doshi P.M.Daiya W.M.Gill
Three Dimensional Laminar Dispersion in Open and Closed
Rectangular Conduits
Chemical Engineering Science
Vol.33

- 112 -
 1990 Dotation du Centre de Calcul Vectoriel Pour la Recherche
 Modelisation et Simulation Numerique de la
 Micrometeorologie dans la couche de surface urbaine -
 Aspects dynamiques et thermiques
 Projet No 2141

- 113 -
 1983 D.E.Dougherty G.F.Pinder
 A Brief Note on Upwind Collocation
 International Journal for Numerical Methods in Fluids
 Vol.3

- 114 -
 1985 D.M.Driver H.L.Seegmiller
 Features of a Reattaching Turbulent Shear Layer in
 Divergent Channel Flow
 AIAA Journal
 Vol.23 No.2 Feb

- 115 -
 1986 A.Ecker D.H.E.Gross
 A System of Simultaneous Non-Linear Equations in
 Three-Thousand Variables
 Journal of Computational Physics
 Vol.64

- 116 -
 1976 N.D.A.El-Hadi K.S.Davar
 Longitudinal Dispersion for Flow Over Rough Beds
 Journal of the Hydraulics Division, ASCE
 Vol.102 No.HY4 Apr

- 117 -
 1959 J.W.Elder
 The Dispersion of Marked Fluid in Turbulent Shear Flow
 Journal of Fluid Mechanics
 Vol.5

- 118 -
 1992 R.C.Elliot M.H.Chaudhry
 A Wave Propagation Model for Two-Dimensional Dam-Break Flows
 Journal of Hydraulic Research
 Vol.30 No.4

- 119 -
 1970 H.W.Emmons
 Critique of Numerical Modeling of Fluid-Mechanics
 Phenomena
 Annual Review of Fluid Mechanics

- 120 -
 1984 D.A.Ervine J.I.Baird
 Resistance to Flow in Channels with Overbank Flood Plain
 Flow
 Proc of the 1st Int Conf on Channels and Channel Control Structures
 Session 4 A4 137 Springer-Verlag

- 121 -

1989 D.A.Ervine H.K.Jasem
Flood Mechanisms in Meandering Channels with Flood Plain
Flow
Proc. of the XXIII IAHR Congress - Ottawa, 1989
A-15

- 122 -

1987 D.A.Ervine J.Ellis
Experimental and Computational Aspects of Overbank
Floodplain Flow
Trans. of the Royal Society of Edinburgh: Earth Sciences
Vol.78

- 123 -

1986 P.Esposito
Tentatives De Calculs Tridimensionnels Stationnaires et
Transitoires Dans La Cuve Chaude De Super Phenix
Report - Electricite De France

- 124 -

1978 D.W.Etheridge P.H.Kemp
Measurements of Turbulent Flow Downstream of a
Rearward-Facing Step
Journal of Fluid Mechanics
Vol.86 part3 pp545-566

- 125 -

1984 R.A.Falconer
Temperature Distributions in Tidal Flow Field
Journal of Environmental Engineering, ASCE
Vol.110 No.6 Dec

- 126 -

1985 R.A.Falconer
Residual Currents in Port Talbot Harbour: A Mathematical Model Study
Proc. of the Inst.Civil.Engrs. Part 2
Vol.79 Mar

- 127 -

1990 R.A.Falconer P.H.Owens
Numerical Modelling of Suspended Sediment Fluxes in
Estuarine Waters
Estuarine, Coastal and Shelf Science
Vol.31

- 128 -

1991 R.A.Falconer D.G.George P.Hall
Three Dimensional Numerical Modelling of Wind-Driven
Circulation in a Shallow Homogeneous Lake
Journal of Hydrology
Vol.124 pp59-79

- 129 -

1992 R.A.Falconer
Flow and Water Quality Modelling in Coastal and Inland Water
Journal of Hydraulic Research
Vol.30 No.4

- 130 -

1992 R.A.Falconer G.Li

Modelling Tidal Flows in an Island's Wake Using a Two-Equation
Turbulence Model
Proceedings of the the I.C.E.
Water, Maritime and Energy
Vol 96 Issue 1 Paper 9823

- 131 -

1993 B.Farhanieh L.Davidson B.Sunden
Employment of Second-Moment Closure for Calculation of
Turbulent Recirculating Flows in Complex Geometries with
Collocated Variable Arrangement
International Journal for Numerical Methods in Fluids
Vol.16

- 132 -

1990 R.J.Fennema M.H.Chaudhry
Explicit Methods for 2-D Transient Free Surface Flows
Journal of Hydraulic Engineering, ASCE
Vol.116 No.8 Aug

- 133 -

1987 J.H.Ferziger
Simulation of Incompressible Turbulent Flows
Journal of Computational Physics
Vol.69

- 134 -

1976 J.F.Festa D.V.Hansen
A Two Dimensional Numerical Model of Estuarine
Circulation: The Effects of Altering Depth and River
Discharge
Estuarine, Coastal and Marine Science
Vol.4

- 135 -

1855 A.Fick
On Liquid Diffusion
Philos.Mag.
Vol.4 No.10 pp30

- 136 -

1991 J.I.Finnie R.W.Jeppson
Journal of Hydraulic Engineering, ASCE
Vol.117 No.11 pp30

- 137 -

1979 H.B.Fischer E.J.List R.C.Y.Koh J.Imberger N.H.Brooks
Mixing in Inland and Coastal Waters
Academic Press, Inc.

- 138 -

1988 C.A.J.Fletcher
Computational Techniques for Fluid Dynamics (2 Volumes)
Springer-Verlag

- 139 -

1990 M.Fortin S.Boivin
Iterative Stabilization of the Bilinear
Velocity-Constant Pressure Element

Int.Journal for Num. Meth. in Fluids
Vol.10 pp125-140

- 140 -

1981 M.Fortin
Old and New Finite Elements For Incompressible Flows
Int Journal for Numerical Methods in Fluids
Vol.1 pp347-364

- 141 -

1972 M.Fortin
Numerical Solution of Steady State Navier-Stokes
Equations
Numerical Methods in Fluid Mechanics (Ed.J.J.Smolderen)
Agard Lecture Series 48

- 142 -

1972 N.G.Freeman A.M.Hale M.B.Danard
A Modified Sigma Equations Approach to the Numerical
Modeling of Great Lakes Hydrodynamics
Journal of Geophysical Research
Vol77 No6 Feb pp1050

- 143 -

1985 C.J.Freitas R.L.Street A.N.Findikakis J.R.Koseff
Numerical Simulation of Three-Dimensional Flow in a
Cavity
International Journal for Numerical Methods in Fluids
Vol.5

- 144 -

1985 R.H.French
Open-Channel Hydraulics
McGraw-Hill

- 145 -

1979 M.J.Fritts J.P.Boris
The Langrangian Solution of Transient Problems in
Hydrodynamics Using a Triangular Mesh
Journal of Computational Physics
Vol.31

- 146 -

1963 J.E.Fromm
A Method for Computing Non-steady Incompressible Viscous
Flows
Los Alamos Scientific Laboratory
Rep LA-2910

- 147 -

1991 M.Fujita M.Michiue O.Hinokidani
Mathematical Simulation of Flow and Suspended Load in Open Channels
With a Trench
Proc. of Hydraulic Engineering, JSCE
Vol.35

- 148 -

1993 M.Fujita S.Komura T.Kanda
Measurements of Turbulent Flow in a Trench Using an Image Processing
Technique
Refined Flow Modelling and Turbulence Measurements
Proc of the 5th International Symposium, Paris, France.

- 149 -

1993 I.Fujita T.Kanda S.Komura Y.Yano T.Morita
Image Processing of Flows in a Trench Using a High Speed Video Camera
and Numerical Analysis by LES
Proc. of Hydraulic Engineering, JSCE
Vol.37

- 150 -

1990 B.Galperin G.L.Mellor
A Time-dependent, Three-dimensional Model of the
Delaware Bay and River System. Part 1:Description of the
Model and Tidal Analysis.
Estuarine, Coastal and Shelf Science
Vol31(3) Sept pp231-253

- 151 -

1994 P.Garcia-Navarro A.Priestley
A Conservative and Shape Preserving Semi-Lagrangian
Method for the Solution of the Shallow Water Equations
Inter.Jour.for Num.Meth.in Fluids.
Vol.18 pp273-294

- 152 -

1988 P.H.Gaskell A.K.C.Lau
Curvature-Compensated Convective Transport : SMART, a
New Boundedness-preserving Transport Algorithm
Int Journal for Numerical Methods in Fluids
Vol.8 pp617-641

- 153 -

1970 T.H.Gawain J.W.Pritchett
A Unified Heuristic Model of Fluid Turbulence
Journal of Comp.Physics
Vol5 pp383-405

- 154 -

1968 T.H.Gawain J.W.Pritchett
Turbulence in an Unbounded, Uniform Shear Flow: A
Computer Analysis
Internal Report Naval Radiological Defense Lab
6 Nov

- 155 -

1974 R.Gerard
Finite Element Solution for Flow in Noncircular Conduits
Journal of the Hydraulics Division, ASCE
Vol.100 No.HY3 Mar

- 156 -

1991 A.M.Gharangik M.H.Chaudhry
Numerical Simulation of Hydraulic Jump
Journal of Hydraulic Engineering, ASCE
Vol.117 No.9 Sept pp1195

- 157 -

1986 M.M.Gibson B.A.Younis
Calculation of Swirling Jets With a Reynolds Stress
Closure
Physics of Fluids
Vol.29 Ptrl Jan

- 158 -

1981 M.M.Gibson W.P.Jones B.A.Younis
Calculation of Turbulent Boundary Layers on Curved
Surfaces
Physics of Fluids
Vol.24 No.3 Mar

- 159 -

1979 K.Goda
A Multistep Technique With Implicit Difference Schemes
for Calculating Two- or Three-Dimensional Cavity Flows
Journal of Computational Physics
Vol.30

- 160 -

1985 J.J.Gorski T.R.Govindan B.Lakshminarayana
Computation of Three Dimensional Turbulent Shear Flows
in Corners
AIAA Journal
Vol.23 No.5 May

- 161 -

1980 A.D.Gosman C.W.Rapley
Fully Developed Flow in Passages of Arbitrary Cross-Section
in 'Recent Advances in Numerical Methods in Fluids'
Eds:Taylor Morgan
Pineridge Press

- 162 -

1987 J.Goussebaile A.Jacomy A.Hauguel J.P.Gregoire
A Finite Element Algorithm for Turbulent Flow Processing a
k- ϵ Model
in 'Turbulence Measurements and Flow Modeling'
Proceedings of the International Symposium, Iowa, U.S.A.
Eds: C.J.Chen L.-D.Chen F.M.Holly, jr.

- 163 -

1992 I.Grant E.Owens Y.-Y.Yan
Particle Image Velocimetry Measurements of the Separated
Flow Behind a Rearward Facing Step
Experiments in Fluids
Vol.12 pp238-244

- 164 -

1992 A.J.Grass
Turbulence - What are we trying to model ?
Is Turbulence Modelling of Any Use?
IAHR Seminar April 9th

- 165 -

1987 P.M.Gresho R.L.Sani
On Pressure Boundary Conditions for the Incompressible
Navier-Stokes Equations
International Journal for Numerical Methods in Fluids
Vol.7 pp1111-1145

- 166 -

1990 H.Guoqi W.Deguan X.Xieqing
A New Numerical Model For Three-Dimensional Surface
Water Flows
4th Int Symp on Refined Flow Modelling etc
China IAHR

- 167 -

1992 V.A.Gushchin V.N.Konshin

Computational Aspects of the Splitting Method for
Incompressible Flow with a Free Surface
Computers & Fluids
Vol.21 No.3

- 168 -

1984 L.P.Hackman G.D.Raithby A.B.Strong
Numerical Predictions of Flows Over Backward Facing
Steps
International Journal for Numerical Methods in Fluids
Vol.4

- 169 -

1981 L.A.Hageman D.M.Young
Applied Iterative Methods
Academic Press, New York

- 170 -

1992 M.Hall K.Shiono R.A.Falconer
Three Dimensional Layer Averaged Model for Tidal Flows
2nd Int Conf on Hydraulic Modelling and Environmental Modelling
Bradford, England.
Eds: Falconer Chandler-Wilde Liu

- 171 -

1975 P.Hamilton
A Numerical Model of the Vertical Circulation of Tidal
Estuaries and its Application to the Rotterdam Waterway
Geophys.J.R.Astr.Soc.
Vol.40

- 172 -

1991 L.S.Han
A Mixing Length Model for Turbulent Boundary Layers Over
Rough Surfaces
International Journal of Heat and Mass Transfer
Vol.34 No.8

- 173 -

1972 K.Hanjalic B.E.Launder
A Reynolds Stress Model of Turbulence and its
Application to Thin Shear Flows
Journal of Fluid Mechanics
Vol.52 part4 pp609-638

- 174 -

1959 S.M.A.Haque
The Effect of Eddy Viscosity on the Velocity Profile of
Steady Flow in a Uniform Rough channel
Journal of Fluid Mechanics
Vol.5

- 175 -

1974 F.H.Harlow A.A.Amsden
Multi-Fluid Flow Calculations at All Mach Numbers
Journal of Computational Physics
Vol16 pp1-19

- 176 -

1967 F.H.Harlow J.P.Shannon
The Splash of a Liquid Drop
Journal of Applied Physics

- 177 -

1988 H.Hara Y.Kodera K.Kanehiro
Flow Simulations by Parallel Computer
The International Journal of Supercomputer Applications
Vol2 No3 Fall pp73-80

- 178 -

1969 F.H.Harlow
Numerical Methods for Fluid Dynamics - an Annotated
Bibliography
Los Alamos Scientific Report LA-4281

- 179 -

1965 F.H.Harlow J.E.Welch
Numerical Calculation of Time-Dependent Viscous
Incompressible Flow of Fluid with Free Surface
Physics of Fluids
Vol8 Num12 pp2182 Dec.

- 180 -

1971 F.H.Harlow A.A.Amsden
A Numerical Fluid Dynamics Calculation Method for All
Flow Speeds
Journal of Computational Physics
Vol 8 pp197-213

- 181 -

1973 A.P.Hatton N.H.Woolley
Heat Transfer in Two-Dimensional Turbulent Confined
Flows
Heat and Fluid Flow
Vol.3 No.1

- 182 -

1992 P.Heinrich
Nonlinear Water Waves Generated by Submarine and Aerial
Landslides
Journal of Waterway, Port, Coastal and Ocean Engineering, ASCE
Vol.118 No.3 May/June

- 183 -

1978 W.S.Helliwell
A Fast Implicit Iterative Numerical Method for Solving
Multidimensional Partial Differential Equations
AIAA Journal
Vol.16 No.7 Jul

- 184 -

1966 F.M.Henderson
Open Channel Flow
MacMillan Series in Civil Engineering

- 185 -

1991 F.S.Henry M.W.Collins M.Ciofalo
Prediction of Swirling Flow in a Corrugated Channel
in 'Supercomputers in Engineering II'
Eds A.Brebbia D.Howard A.Peters
Computational Mechanics Publications, Elsevier Applied Science

- 186 -

1964 J.B.Herbich S.Shulits
Large Scale Roughness in Open Channel Flow
Journal of the Hydraulics Division, ASCE
Vol.90 No.HY6

- 187 -

1992 J.R.Hertzberg C.M.Ho
Time-Averaged, Three Dimensional Flow in a Rectangular
Sudden Expansion
AIAA Journal
Vol.30 No.10 Oct

- 188 -

1974 C.W.Hirt A.A.Amsden J.L.Cook
An Arbitrary Lagrangian-Eulerian Computing Method for All
Flow Speeds
Journal of Computational Physics
Vol 14 pp227-253

- 189 -

1970 C.W.Hirt J.L.Cook T.D.Butler
A Lagrangian Method for Calculating the Dynamics of an
Incompressible Fluid with Free Surface
Journal of Computational Physics
Vol.5

- 190 -

1981 C.W.Hirt B.D.Nichols
Volume of Fluid Method for the Dynamics of Free
Boundaries
Journal of Comp. Physics
Vol39 pp201-225

- 191 -

1972 C.W.Hirt J.L.Cook
Calculating Three-Dimensional Flows around Structures
and over Rough Terrain
Journal of Comp. Physics
Vol10 pp324-340

- 192 -

1968 C.W.Hirt J.P.Shannon
Free-Surface Stress Condition for Incompressible-Flow
Calculations
Journal of Comp. Physics
Vol2 pp403-411

- 193 -

1967 C.W.Hirt F.H.Harlow
A General Corrective Procedure for the Numerical
Solution of Initial-Value Problems
Journal of Comp. Physics
Vol2 pp114-119

- 194 -

1968 C.W.Hirt
Heuristic Stability Theory for Finite-Difference
Equations
Journal of Comp. Physics
Vol2 pp339-355

- 195 -

1984 F.M.Holly J.-M.Usseglio-Polatera
Dispersion Simulation in Two-Dimensional Tidal Flow
Journal of Hydraulic Engineering, ASCE
Vol.110 No.7 July

- 196 -

1970 ED: M.Holt
Proceedings of the 2nd Int Conf on Numerical Methods in
Fluid Dynamics - Lecture Notes in Physics
Springer-Verlag

- 197 -

1987 K.Horiuti
Comparison of Conservative and Rotational Forms in Large
Eddy Simulation of Turbulent Channel Flow
Journal of Computational Physics
Vol.71

- 198 -

1986 P.G.Huang
The Computation of Elliptic Turbulent Flows with Second Moment
Closure Models
PhD Thesis, University of Manchester

- 199 -

1984 J.P.Huffenus D.Khaletsky
A Finite Element Method to Solve the Navier-Stokes
Equations Using the Method of Characteristics
International Journal for Numerical Methods in Fluids
Vol.4

- 200 -

1981 J.P.Huffenus D.Khaletsky
The Lagrangian Approach of Advective Term Treatment and
its Application to the Solution of Navier-Stokes
Equations
Int Journal for Numerical Methods in Fluids
Vol.1 pp365-387

- 201 -

1981 J.A.C.Humphrey J.H.Whitelaw G.Yee
Turbulent Flow in a Square Duct with Strong Curvature
Journal of Fluid Mechanics
Vol.103 pp443-463

- 202 -

1990 N.Hur S.Thangam C.G.Speziale
Numerical Study of Turbulent Secondary Flows in Curved
Ducts
Journal of Fluids Engineering, ASME
Vol.112 June pp205

- 203 -

1987 A.G.Hutton R.M.Smith S.Hickmott
The Computation of Turbulent Flows of Industrial
Complexity by the Finite Element Method - Progress and
Prospects
International Journal for Numerical Methods in Fluids
Vol.7

- 204 -

1993 C.C.Hwang G.Zhu M.Massoudi J.M.Ekmann

A Comparison of the Linear and Nonlinear k- ϵ
Turbulence Models in Combustors
Journal of Fluids Engineering, ASME
March Vol.115 pp93

- 205 -

1992 I.A.H.R. Seminar
Is Turbulence Modelling of Any Use ?
Proceedings of a Seminar at the I.C.E.
Great George Street, London

- 206 -

1989 C.S.Ierotheou C.W.Richards M.Cross
Vectorization of the SIMPLE Solution Procedure for CFD
Problems - Part II: The Impact of Using a Multigrid
Method
Applied Mathematical Modelling
Vol.13 Sept

- 207 -

1989 C.S.Ierotheou C.W.Richards M.Cross
Vectorization of the SIMPLE Solution Procedure for CFD
Problems - Part I: A Basic Assessment
Applied Mathematical Modelling
Vol.13 Sept

- 208 -

1992 T.Ikohagi B.R.Shin H.Daiguji
Application of an Implicit Time-Marching Scheme to a
Three-Dimensional Incompressible Flow Problem in
Curvilinear Coordinate Systems
Computers & Fluids
Vol.21 No.2 pp163-175

- 209 -

1983 E.Imam J.A.McCorquodale
Simulation of Flow in Rectangular Clarifiers
Journal of Environmental Engineering, ASCE
Vol.109 No.3 Jun

- 210 -

1985 R.I.Issa
Solution of the Implicitly Discretised Fluid Flow
Equations by Operator-Splitting (PISO)
Journal of Comp. Physics
Vol62 pp40-65

- 211 -

1992 M.Jaeger G.Dhatt
An Extended k- ϵ Finite Element Model
International Journal for Numerical Methods in Fluids
Vol.14 pp1325-1345

- 212 -

1993 J.M.Janin F.Lepeintre PH.Pechon
Three Dimensional Modelling of a Free-Surface Stratified Flow
and of a Thermal Discharge
Refined Flow Modelling and Turbulence Measurements
Proc of the 5th International Symposium, Paris, France.

- 213 -

1990 H.K.Jasem
Flow in Two-Stage Channels with the Main Channel Skewed to the
Flood Plain Direction

A PhD thesis submitted to the University of Glasgow.

- 214 -

1970 H.E.Jobson W.W.Sayre
Vertical Transfer in Open Channel Flow
Journal of the Hydraulics Division, ASCE
Vol.96 No.HY3 Mar

- 215 -

1972 W.P.Jones B.E.Launder
The Prediction of Laminarization with a Two-equation
Model of Turbulence
Int Journal of Heat and Mass Transfer
Vol.15 pp301-314

- 216 -

1992 T.Kajishima Y.Miyake
A Discussion on Eddy Viscosity Models on the Basis of
the Large Eddy Simulation of Turbulent Flow in a Square
Duct
Computers & Fluids
Vol.21 No.2 pp151-161

- 217 -

1980 J.P.T.Kalkwijk H.J.DeVried
Computation of the Flow in Shallow River Bends
Journal of Hydraulic Research
Vol.18 No.4

- 218 -

1990 S.Kato S.Murakami H.Nakagawa
Numerical and Experimental Study for Horizontal
Non-isothermal 3-D Jet in Enclosed Space
The 4th Int.Symp.on Refined Flow Modelling etc
IAHR pp327

- 219 -

1989 Y.Kawahara N.Tamai
Mechanism of Lateral Momentum Transfer in Compound
Channel Flows
Proc. of the XXIII IAHR Congress - Ottawa, 1989
Fluvial Hydraulics B-463

- 220 -

1991 Y.Kaya G.McInally
Some Practical Aspects of River Modelling
River and Flood Plain Management
Scottish Hydraulics Study Group Meeting 22nd March 1991

- 221 -

1988 R.J.Keller W.Rodi
Prediction of Flow Characteristics in Main Channel/Flood
Plain Flows
Journal of Hydraulic Research
Vol26 No4 pp425

- 222 -

1978 D.S.Kershaw
The Incomplete Cholesky-Conjugate Gradient Method for
the Iterative Solution of Systems of Linear Equations
Journal of Computational Physics
Vol.26

- 223 -

1987 P.K.Khosla S.G.Rubin
Consistent Strongly Implicit Iterative Procedures for
Two-Dimensional Unsteady and Three-Dimensional
Space-Marching Flow Calculations
Computers & Fluids
Vol.15 No.4 pp361-377

- 224 -

1989 G.K.Kiely
An Experimental Study of Overbank Flow in Straight and Meandering
Compound Channels
A PhD Thesis submitted to University College, Cork, Ireland.

- 225 -

1985 J.R.Kightley I.P.Jones
A Comparison of Conjugate Gradient Preconditionings for Three
Dimensional Problems on a CRAY-1
Comp. Phys. Comm.
Vol.37 pp205-214

- 226 -

1992 S.-W.Kim T.J.Benson
Comparison of the SMAC, PISO and Iterative
Time-Advancing Schemes for Unsteady Flows
Computers & Fluids
Vol.21 No.3 pp435-454

- 227 -

1985 J.Kim P.Moin
Application of a Fractional-Step Method to
Incompressible Navier-Stokes Equations
Journal of Comp. Physics
Vol.59 pp308-323

- 228 -

1980 J.Kim S.J.Kline J.P.Johnston
Investigation of a Reattaching Turbulent Shear Layer:
Flow Over a Backward-Facing Step
Journal of Fluids Engineering, ASME
Vol.102 Sept

- 229 -

1989 M.S.Kirkgoz
Turbulent Velocity Profiles for Smooth and Rough Open
Channel Flow
Journal of Hydraulic Engineering, ASCE
Vol.115 No.11 Nov pp1543

- 230 -

1984 D.W.Knight M.E.Hamed
Boundary Shear in Symmetrical Compound Channels
Journal of Hydraulic Engineering, ASCE
Vol.110 No.10 Oct

- 231 -

1992 D.W.Knight Y.M.Yuan Y.R.Fares
Boundary Shear in Meandering Channels
Proc.Int.Symp.on Hydraulic Research in Nature and Laboratory
Wuhan, China - Nov

- 232 -

1985 D.W.Knight H.S.Patel
Boundary Shear in Smooth Rectangular Ducts
Journal of Hydraulic Engineering, ASCE
Vol.111 No.1 Jan

- 233 -

1984 D.W.Knight J.D.Demetriou M.E.Hamed
Boundary Shear in Smooth Rectangular Channels
Journal of Hydraulic Engineering, ASCE
Vol.110 No.4 Apr

- 234 -

1989 D.W.Knight P.G.Samuels K.Shiono
River Flow Simulation: Research and Developments
IWEM 89 Conference Paper
pp163

- 235 -

1991 M.H.Kobayashi J.C.F.Pereira
Numerical Comparison of Momentum Interpolation Methods
and Pressure-Velocity Algorithms Using Non-staggered
Grids.
Communications in Applied Numerical Methods
Vol7 pp173-186

- 236 -

1992 N.Kondo N.Tosaka T.Nishimura
Computation of Incompressible Viscous Flows by the
Third-Order Upwind Finite Element Method
International Journal for Numerical Methods in Fluids
Vol.15

- 237 -

1992 D.B.Kothe R.C.Mjolsness
RIPPLE: A New Model for Incompressible Flows with Free
Surfaces
AIAA Journal
Vol.30 No.11 Nov

- 238 -

1988 N.E.Kotsovinos
Secondary Currents in Straight Wide Channels
Applied Mathematical Modelling
Vol.12 Feb

- 239 -

1988 C.G.Koutitas
Mathematical Models in Coastal Engineering
Pentech Press

- 240 -

1980 C.Koutitas B.O'Connor
Modeling Three-Dimensional Wind-Induced Flows
Journal of the Hydraulics Division, ASCE
Vol.106 No.HY11 Nov

- 241 -

1978 A.Kreft A.Zuber

A Physical Meaning of the Dispersion Equation and its
Solutions for Different Initial and Boundary Conditions
Chemical Engineering Science
Vol.33

- 242 -

1986 B.G.Krishnappan Y.L.Lau
Turbulence Modeling of Flood Plain Flows
Journal of Hydraulic Engineering, ASCE.
Vol.112 No.4 April pp251

- 243 -

1972 M.Krishnamurthy B.A.Christensen
Equivalent Roughness for Shallow Channels
Journal of the Hydraulics Division, ASCE
Vol.98 No.HY12 Dec

- 244 -

1984 B.G.Krishnappan
Laboratory Verification of Turbulent Flow Model
Journal of Hydraulic Engineering, ASCE
Vol.110 No.4 Apr

- 245 -

1980 D.M.Kuehn
Effects of Adverse Pressure Gradient on the
Incompressible Reattaching Flow Over a Rearward-Facing
Step
AIAA Journal
Vol.18 No.3 Mar (TN)

- 246 -

1973 Kuipers C.B.Vreugdenhil
Calculation of Two Dimensional Horizontal Flow
Delft Hydraulics Laboratory
Report S163 part 1

- 247 -

1991 T.-W.Kuo S.Chang
Three-Dimensional Computations of Flow and Fuel
Injection in an Engine Intake Port
Journal for Engineering for Gas Turbines and Power
July Vol.113 pp427

- 248 -

1985 P.Kutler
A Perspective of Theoretical and Applied Computational
Fluid Dynamics
AIAA Journal
Vol.23 No.3 Mar

- 249 -

1986 C.J.Lai J.W.Yen
Numerical Model for Estuary with Compound Cross-Section
2nd Int Conf on Hydraulic Modelling and Environmental Modelling
Bradford, England.
Eds: Falconer Chandler-Wilde Liu

- 250 -

1986 B.Lakshminarayana
Turbulence Modelling for Complex Shear Flows
AIAA Journal

- 251 -

1981 C.K.G.Lam K.Bremhorst
A Modified Form of the k- ϵ Model for Predicting
Wall Turbulence
Journal of Fluids Engineering, ASME
Vol.103 Sept

- 252 -

1994 A.Larabi F.DeSmedt
Solving Three Dimensional Hexahedral Finite Element Groundwater
Models by Preconditioned Conjugate Gradient Methods
Water Resources Research
Vol.30 No.2

- 253 -

1975 B.E.Launder
On the Effects of a Gravitational Field on the Turbulent
Transport of Heat and Momentum
Journal of Fluid Mechanics
Vol.67 Pt3

- 254 -

1975 B.E.Launder G.J.Reece W.Rodi
Progress in the Development of a Reynolds-stress
Turbulence Closure
Journal of Fluid Mechanics
Vol.68 part3 pp537-566

- 255 -

1973 B.E.Launder W.M.Ying
Prediction of Flow and Heat Transfer in Ducts of Square
Cross-Section
Heat and Fluid Flow
Vol.3 No.2

- 256 -

1974 B.E.Launder D.B.Spalding
The Numerical Computation of Turbulent Flows
Computer Methods in Applied Mechanics and Engineering 3
pp269-289

- 257 -

1972 B.E.Launder D.B.Spalding
Mathematical Models of Turbulence (Lectures in)
Lecture Notes
Academic Press

- 258 -

1977 Y.L.Lau B.G.Krishnappan
Transverse Dispersion in Rectangular Channels
Journal of the Hydraulics Division, ASCE
Vol.103 No.HY10 Oct

- 259 -

1985 E.M.Laurenson
Friction Slope Averaging in Backwater Calculations
Journal of Hydraulic Engineering, ASCE
Vol.112 No.HY12

- 260 -

1979 G.H.Lean T.J.Weare
Modeling Two-Dimensional Circulating Flow
Journal of the Hydraulics Division, ASCE
Vol.105 No.HY1 Jan

- 261 -

1978 N.Lee A.E.Dukler
A Stochastic Model For Turbulent Diffusion
Chemical Engineering Science
Vol.33

- 262 -

1992 R.L.Lee
A Finite Element/Finite Difference Approach for Modeling
Three Dimensional Flow and Pollutant Dispersion Around Structures
Proc.Symp.on Measurement and Modeling of Environmental Flows,ASME
Anaheim, California
Eds:S.A.Sherif et al

- 263 -

1967 J.J.Leendertse
Aspects of a Computational Model for Long Period Water Wave Propagation
RAND Corporation Report, Santa Monica, California.
RM 5294-P.R.

- 264 -

1973 J.J.Leendertse R.C.Alexander S.-K.Liu
A Three Dimensional Model for Estuaries and Coastal Seas:
v1 Principles of Computation
RAND Corporation Report, Santa Monica, California.
R 1417 OWRR

- 265 -

1992 C.M.Lemos
A Simple Numerical Technique for Turbulent Flows with
Free Surfaces
International Journal for Numerical Methods in Fluids
Vol.15

- 266 -

1991 B.P.Leonard H.S.Niknafs
Sharp Monotonic Resolution of Discontinuities Without
Clipping of Narrow Extrema
Computers & Fluids
Vol19 No1 pp141-154

- 267 -

1990 B.P.Leonard S.Mokhtari
Beyond First Order Upwinding: The ULTRA-SHARP
Alternative for Non-Oscillatory Steady-State Simulation
of Convection
International Journal for Numerical Methods in Engineering
Vol.30

- 268 -

1988 B.P.Leonard
Simple High-Accuracy Resolution Program For Convective
Modelling of Discontinuities
International Journal for Numerical Methods in Fluids
Vol.8 pp1291-1318

- 269 -

1979 B.P.Leonard

A Stable and Accurate Convective Modelling Procedure
Based on Quadratic Upstream Interpolation
Computer Methods in Applied Mechanics and Engineering
Vol.19 pp59-98

- 270 -

1979 M.A.Leschziner W.Rodi

Calculation of Strongly Curved Open Channel Flow
Journal of Hydraulics Division, ASCE
Vol.105 HY10 Oct pp1297

- 271 -

1981 M.A.Leschziner W.Rodi

Calculation of Annular and Twin Parallel Jets Using
Various Discretization Schemes and Turbulence Model
Variations
Journal of Fluids Engineering, ASME
Vol.103 June

- 272 -

M.A.Leschziner

Finite-Volume Computation of Recirculating Flow with
Reynolds-Stress Turbulence Closures

Unknown Source

- 273 -

1993 M.Lesieur

Advance and State of the Art on Large Eddy Simulations
Reynolds-Stress Turbulence Closures
Refined Flow Modelling and Turbulence Measurements
Proc of the 5th International Symposium, Paris, France.

- 274 -

1963 H.J.Leutheusser

Turbulent Flow in Rectangular Ducts
Journal of the Hydraulics Division, ASCE
Vol.89 HY3 May pp1

- 275 -

1991 S.Levi Alvares

Simulation Numerique Des Ecoulements Urbains A L'Echelle
D'une Rue A L'Aide D'Un Modele k-ε
PhD Thesis Universite de Nantes

- 276 -

1990 C.W.Li

Advection Simulation by Minimax-Characteristics Method
Journal of Hydraulic Engineering, ASCE
Vol.116 No.9 Sept

- 277 -

1980 R.-M.Li J.D.Schall D.B.Simons

Turbulence Prediction in Open Channel Flow
Journal of the Hydraulics Division, ASCE
Vol.106 No.HY4 Apr

- 278 -

1989 Y.S.Li C.P.Chen

An Efficient Split-Operator Scheme for 2-D
Advection-Diffusion Simulations Using Finite Elements
and Characteristics
Applied Mathematical Modelling
Vol.13 Apr

- 279 -

1969 J.A.Liggett
Cell Method for Computing Lake Circulation
ASCE Journal of Hydraulics Division
March HY3 Vol96

- 280 -

1975 J.A.Liggett
Basic Equations of Unsteady Flow
in 'Unsteady Flow in Open Channels'
Ed: Mahmood and Yevjevich

- 281 -

B.Lin K.Shiono
Prediction of Pollutant Transport in Compound Channel
Flows
2nd Int Conf on Hydraulic Modelling and Environmental Modelling
Bradford, England.
Eds: Falconer Chandler-Wilde Liu

- 282 -

1992 C.Lin H.H.Hwung
External and Internal Flow Fields of Plunging Breakers
Experiments in Fluids
Vol.12 pp229-237

- 283 -

1990 T.M.Liou Y.Chang D.W.Hwang
Experimental and Computational Study of Turbulent Flows
in a Channel With Two pairs of Turbulence Promoters in
Tandem
Journal of Fluids Engineering, ASME
Sept Vol112 pp302-310

- 284 -

1974 S.Liu J.J.Lendertse
Multidimensional Numerical Modeling of Estuaries and
Coastal Seas
The Rand Corporation, Santa Monica

- 285 -

1977 H.Liu
Predicting Dispersion Coefficient of Streams
Journal of the Environmental Engineering Division, ASCE
Vol.103 No.EE1 Feb

- 286 -

1970 J.L.Lumley
Toward a Turbulent Constitutive Relation
Journal of Fluid Mechanics
Vol.41 part2 pp413-434

- 287 -

1983 R.Lupini T.Tirabassi
Solution of the Advection-Diffusion Equation by the
Moments Method

- 288 -

1992 D.A.Lyn W.Rodi
Density Currents and Shear-Induced Flocculation in
Sedimentation Tanks
Journal of Hydraulic Engineering, ASCE
Vol.118 No.6 June pp849

- 289 -

1991 D.A.Lyn A.L.Stamou W.Rodi
Density Currents and Shear-Induced Flocculation in
Sedimentation Tanks
Journal of Hydraulic Engineering, ASCE
Vol.118 No.6 Jun

- 290 -

1989 D.A.Lyn Z.Zhang
Boundary Fitted Numerical Modelling of Sedimentation
Tanks
Proc.of the XXIII IAHR Congress - Ottawa, 1989
A-331

- 291 -

1993 D.A.Lyn
Turbulence Measurements in Open-Channel Flows Over
Artificial Bed Forms
Journal of Hydraulic Engineering, ASCE
Vol.119 No.3 Mar

- 292 -

1990 D.A.Lyn W.Rodi
Turbulence Measurements in Model Settling Tank
Journal of Hydraulic Engineering, ASCE
Vol.116 No.1 Jan

- 293 -

1992 S.Majumdar W.Rodi J.Zhu
Three Dimensional Finite Volume Method for
Incompressible Flows With Complex Boundaries
Journal of Fluids Engineering, ASME
Vol.114 Dec

- 294 -

1988 S.Majumdar
Role of Under-relaxation in Momentum Interpolation for
Calculation of Flow with Nonstaggered Grids
Numerical Heat Transfer
Vol13 pp125-132

- 295 -

1989 M.R.Malin L.Sanchez
A Revised Version of the k-kL Turbulence Model for Near
Wall Flows
Applied Mathematical Modelling
Vol.13 Mar

- 296 -

1990 M.R.Malin B.A.Younis
Calculation of turbulent buoyant plumes with a Reynolds
stress and heat flux transport closure
Int.J.Heat Mass Transfer
Vol33 No10 pp2247-2264

- 297 -

1992 P.C.Matsoukis
Tidal Model Using Method of Characteristics
Journal of Waterway, Port, Coastal and Ocean Engineering
Vol.118 No.3 May pp233

- 298 -

1993 J.J.McGuirk J.M.L.M.Palma
The Efficiency of Alternative Pressure-Correction
Formulations for Incompressible Turbulent Flow Problems
Computers & Fluids
Vol.22 No.1

- 299 -

1981 J.J.McGuirk A.M.K.P.Taylor J.H.Whitelaw
The Assessment of Numerical Diffusion in Upwind
Difference Calculations of Turbulent Recirculating Flows
Turbulent Shear Flows
pp206 Vol

- 300 -

1978 J.J.McGuirk W.Rodi
A Depth-Averaged Mathematical Model for the Near Field
of Side Discharges into Open Channel Flow
Journal of Fluid Mechanics
Vol.86 Pt4

- 301 -

1992 J.J.McGuirk J.M.L.M.Palma
Calculations of the Dilution System in an Annular Gas
Turbine Combustor
AIAA Journal
Vol.30 No.4 Apr

- 302 -

1987 J.J.McGuirk A.K.M.Sadrul-Islam
Numerical Modelling of the Influence of a Hood on Axisymmetric
Withdrawal from a Density Stratified Environment
Proceedings of the Third International Symposium on Stratified Flows
Pasadena, California
Eds: E.J.List G.H.Jirka

- 303 -

1976 A.Melling J.H.Whitelaw
Turbulent Flow in a Rectangular Duct
Journal of Fluid Mechanics
Vol.78

- 304 -

1990 C.Mendoza H.W.Shen
Investigation of Turbulent Flow Over Dunes
Journal of Hydraulic Engineering, ASCE
Vol.116 No.4 Apr

- 305 -

1981 P.Mercier M.Deville
A Multi-dimensional Compact Higher-Order Scheme for 3-D
Poisson's Equation
Journal of Comp. Physics
Vol39 pp443-455

- 306 -

1989 S.Miller M.H.Chaudhry
Dam Break Flows in Curved Channel
Journal of Hydraulic Engineering, ASCE
Vol.115 No.11 Nov

- 307 -

1971 J.A.Miller
Laminar Incompressible Flow in the Entrance Region of
Ducts of Arbitrary Cross Section
Journal of Engineering for Power
Jan pp113 PaperNo70-GT-91

- 308 -

1974 A.C.Miller E.V.Richardson
Diffusion and Dispersion in Open Channel Flow
Journal of Hydraulic Engineering, ASCE
Vol.100 No.HY1 Jan

- 309 -

1974 A.R.Mitchell D.F.Griffiths
The Finite Difference Method in Partial Differential Equations
John Wiley and Sons

- 310 -

1987 H.Miyata T.Sato N.Baba
Difference Solution of a Viscous Flow with Free-Surface
Wave about an Advancing Ship
Journal of Computational Physics
Vol.72

- 311 -

1985 H.Miyata S.Nishimura
Finite-Difference Simulation of nonlinear ship waves
Journal of Fluid Mechanics
Vol.157 pp327-357

- 312 -

1986 H.Miyata
Finite Difference Simulation of Breaking Waves
Journal of Computational Physics
Vol.65

- 313 -

1992 H.Miyata Y.Yamada
A Finite Difference Method for 3D Flows About Bodies of
Complex Geometry in Rectangular Co-ordinate Systems
International Journal for Numerical Methods in Fluids
Vol.14 pp1261-1287

- 314 -

1985 H.Miyata S.Nishimura A.Masuko
Finite Difference Simulation of Nonlinear Waves
Generated by Ships of Arbitrary Three-Dimensional
Configuration
Journal of Comp. Physics
Vol.60 pp361-436

- 315 -

1992 K.Morinishi

A Finite Difference Solution of the Euler Equations On
Non-Body-Fitted Cartesian Grids
Computers & Fluids
Vol.21 No.3

- 316 -

1987 K.W.Morton P.K.Sweby
A Comparison of Flux Limited Difference Methods and
Characteristic Galerkin Methods for Shock Modelling
Journal of Computational Physics
Vol.73

- 317 -

1990 B.O.Moses J.F.Sini I.Dekeyser
k- ϵ Model Simulations of Vertical Jets and Plumes
in Atmospheric Environments
4th Int Symp on Refined Flow Modelling etc
IAHR China

- 318 -

1990 W.R.C.Myers E.K.Brennan
Flow Resistance in Compound Channels
Journal of Hydraulic Research
Volume 28 No 2

- 319 -

1971 P.I.Nakayama N.C.Romero
Numerical Method for Almost Three-Dimensional
Incompressible Fluid Flow and a Simple Internal Obstacle
Treatment
Journal of Computational Physics
Vol8 pp230-240

- 320 -

1987 I.Nakamura Y.Sakai M.Miyata
Diffusion of Matter by a Non-buoyant Plume in
Grid-Generated Turbulence
Journal of Fluid Mechanics
Vol.178

- 321 -

1987 H.Nakagawa I.Nezu
Experimental Investigation Into Turbulent Structure of
Backward-Facing Step Flow in an Open Channel
Journal of Hydraulic Research
Vol.25 No.1

- 322 -

1987 M.Nallasamy
Turbulence Models and their Applications to the
Prediction of Internal Flows : A Review
Computers & Fluids
Vol.15 No.2 pp151-194

- 323 -

1993 D.Naot I.Nezu H.Nakagawa
Hydrodynamic Behaviour of Compound Rectangular Open
Channels
Journal of Hydraulic Engineering, ASCE
Vol.119 No.3 Mar

- 324 -

1984 D.Naot
Response of Channel Flow to Roughness Heterogeneity
Journal of Hydraulic Engineering, ASCE

- 325 -

1982 D.Naot W.Rodi
Calculation of Secondary Currents in Channel Flow
ASCE, Journal of the Hydraulics Division
HY8 Aug pp948

- 326 -

1981 D.Naot W.Rodi
Applicability of Algebraic Models Based on
Unidirectional Flow to Duct Flow With Lateral Motion
Int Journal for Numerical Methods in Fluids
Vol.1 pp225-235

- 327 -

1969 V.W.Nee L.S.G.Kovasnay
Simple Phenomenological Theory of Turbulent Shear Flows
Physics of Fluids
Vol.12 No.3 March pp473

- 328 -

1993 J.M.Nelson S.R.McLean S.R.Wolfe
Mean Flow and Turbulence Fields Over Two-Dimensional Bed Forms
Water Resources Research
Vol.29 No.12 pp3935-3953

- 329 -

1986 I.Nezu W.Rodi
Open Channel Flow Measurements with a Laser Doppler
Anemometer
Journal of Hydraulic Engineering, ASCE
Vol.112 No.5 May

- 330 -

1984 I.Nezu H.Nakagawa
Cellular Secondary Currents in Straight Conduit
Journal of Hydraulic Engineering, ASCE
Vol.110 No.2 Feb

- 331 -

1971 B.D.Nichols C.W.Hirt
Improved Free Surface Boundary Conditions for Numerical
Incompressible-Flow Calculations
Journal of Computational Physics
Vol8 pp434-448

- 332 -

1972 B.D.Nichols C.W.Hirt
Calculating Three-Dimensional Free-Surface Flows in the
Vicinity of Submerged and Exposed Structures
Journal of Computational Physics
Vol12 pp234-246

- 333 -

1980 B.D.Nichols C.W.Hirt R.S.Hotchkiss
SOLA-VOF: A Solution Algorithm for Transient Fluid Flow
with Multiple Free Boundaries
Los Alamos Scientific Laboratory, New Mexico.
August LA-8355

- 334 -

1988 R.I.Nokes I.R.Wood
Vertical and Lateral Turbulent Dispersion: Some
Experimental Results
Journal of Fluid Mechanics
Vol.187

- 335 -

1992 H.Novelli I.Dekeyser P.Fraunie
Three-Dimensional Modelling of a Mediterranean Bay
Computer Modelling of Seas and Coastal Regions
Ed: P.W.Partridge
Computational Mechanics Publications
Elsevier

- 336 -

1964 E.M.O'Loughlin E.G.MacDonald
Some Roughness Concentration Effects on Boundary
Resistance
La Houille Blanche
No.7

- 337 -

1987 U.R.B.Obeysekare M.B.Allen R.E.Ewing J.H.George
Application of Conjugate Gradient Like Methods to a
Hyperbolic Problem in Porous Media Flow
International Journal for Numerical Methods in Fluids
Vol.7

- 338 -

1985 H.J.M.Ogink
The Effective Viscosity Coefficient in 2-D Depth
Averaged Flow Models
21st IAHR Conference, Australia
pp475

- 339 -

1992 Y.Onishi D.S.Trent
Turbulence Modelling For Deep Ocean Radionuclide
Disposal
International Journal for Numerical Methods in Fluids
Vol.15

- 340 -

1992 P.Pai T.T.H.Tsang
A Finite Element Method for a Three Dimensional
Second-Order Closure Model of Turbulent Diffusion in a
Convective Boundary Layer
International Journal for Numerical Methods in Fluids
Vol.15

- 341 -

1980 P.K.Pande R.Prakash M.L.Agarwal
Flow Past Fence in Turbulent Boundary Layers
Journal of the Hydraulics Division, ASCE
Vol.106 No.HY1 Jan

- 342 -

1987 I.S.Partom
Application of the VOF Method to the Sloshing of a Fluid
in a Partially Filled Cylindrical Container
International Journal for Numerical Methods in Fluids
Vol.7

- 343 -

1970 S.V.Patankar D.B.Spalding
Heat and Mass Transfer in Boundary Layers

- 344 -

1975 S.V.Patankar V.S.Pratap D.B.Spalding
Prediction of Turbulent Flow in Curved Pipes
Journal of Fluid Mechanics
Vol.67 Prt3

- 345 -

1980 S.V.Patankar
Numerical Heat Transfer and Fluid Flow

- 346 -

1972 S.V.Patankar D.B.Spalding
A Calculation Procedure for Heat, Mass and Momentum
Transfer in Three-Dimensional Parabolic Flows
Int.J.Heat Mass Transfer
Vol15 pp1787-1806

- 347 -

1985 M.Peric
A Finite Volume Method for the Prediction of
Three-Dimensional Fluid Flow in Complex Ducts
PhD Thesis

- 348 -

1988 M.Peric R.Kessler G.Scheuerer
Comparison of Finite-Volume Numerical Methods with
Staggered and Colocated Grids
Computers & Fluids
Vol.16 No.4 pp389-403

- 349 -

1983 R.Peret T.D.Taylor
Computational Methods for Fluid Flow
Springer-Verlag Series in Computational Physics

- 350 -

1993 J.B.Perot
An Analysis of the Fractional Step Method
Journal of Computational Physics
Vol.108 pp51-58

- 351 -

1991 J.Piquet M.Visonneau
Computation of the Flow Past Shiplike Hulls
Computers & Fluids
Vol19 No2 pp183-215

- 352 -

1982 O.Pironneau

- 353 -

1958 G.W.Platzman

A Numerical Computation of the Surge of 26 June 1954 on Lake Michigan
Geophysica
Vol6 pp407-438

- 354 -

1978 S.B.Pope

The Calculation of Turbulent Recirculating Flows in
General Orthogonal Coordinates
Journal of Comp. Physics
Vol26 pp197-217

- 355 -

1975 S.B.Pope

A More General Effective Viscosity Hypothesis
Journal of Fluid Mechanics
Vol.72 Part 2

- 356 -

1975 W.Pracht

Calculating Three Dimensional Fluid Flows at All Speeds
With an Eulerian-Lagrangian Computing Mesh
Journal of Computational Physics
Vol.17 pp132-159

- 357 -

1925 L.Prandtl

Z.A.M.M.
Vol.25 p136

- 358 -

1945 L.Prandtl

N.A.W.G.M.P. K
Kl.II p6

- 359 -

1975 V.S.Pratap D.B.Spalding

Numerical Computations of the Flow in Curved Ducts
Aeronautical Quarterly

- 360 -

1971 W.E.Pracht

A Numerical Method for Calculating Transient Creep Flows
Journal of Comp. Physics
Vol7 pp46-60

- 361 -

1976 V.S.Pratap D.B.Spalding

Fluid Flow and Heat Transfer in Three-Dimensional Duct
Flows

- 362 -

- 1960 A.Preissmann
Propagation des Intumescences dans les Canaux et Rivières
Proc of the 1st Congress de l'Assoc Francais de Calcul, Grenoble.

- 363 -

- 1985 P.Prinos R.Townsend S.Tavoularis
Structure of Turbulence in Compound Channel Flows
Journal of Hydraulic Engineering, ASCE
Vol111 No9 Sept pp1246

- 364 -

- 1990 P.Prinos
Turbulence Modelling of Main Channel - Flood Plain Flows
With an Algebraic Stress Model
Int Conf on River Flood Hydraulics, Wallingford. Sept, 1990.
pp173

- 365 -

- 1992 P.Prinos
Dispersion in Compound Open Channel Flow
2nd Int Conf on Hydraulic Modelling and Environmental Modelling
Bradford, England.
Eds: Falconer Chandler-Wilde Liu

- 366 -

- 1987 R.Raghunath S.Sengupta J.Haeuser
A Study of the Motion in Rotating Containers Using a
Boundary Fitted Co-ordinate System
International Journal for Numerical Methods in Fluids
Vol.7

- 367 -

- 1988 G.D.Raithby R.V.Elliot B.R.Hutchinson
Prediction of Three-Dimensional Thermal Discharge Flows
Journal of Hydraulic Engineering, ASCE
Vol.114 No.7 July

- 368 -

- 1992 R.Rajar
Application of the Three-Dimensional Model to Slovenian Coastal Sea
Computer Modelling of Seas and Coastal Regions
Ed: P.W.Partridge
Computational Mechanics Publications
Elsevier

- 369 -

- 1990 B.Ramaswamy
Numerical Simulation of Unsteady Viscous Free Surface
Flow
Journal of Computational Physics
Vol.90 pp396-430

- 370 -

- 1987 B.Ramaswamy M.Kawahara
Arbitrary Lagrangian-Eulerian Finite Element Method for
Unsteady, Convective, Incompressible Viscous Free
Surface Flow
International Journal for Numerical Methods in Fluids

Vol.7

- 371 -

1990 J.D.Ramshaw V.A.Mousseau
Accelerated Artificial Compressibility Method For
Steady-State Incompressible Flow Calculations
Computers & Fluids
Vol18 No4 pp361-367

- 372 -

1978 A.K.Rastogi W.Rodi
Predictions of Heat and Mass Transfer in Open Channels
Journal of the Hydraulics Division, ASCE
HY3 March Vol104 pp 397

- 373 -

1980 M.Rattray J.G.Dworski
Comparison of Methods for Analysis of the Transverse and
Vertical Circulation Contributions to the Longitudinal
Advective Salt Flux in Estuaries
Estuarine, Coastal and Marine Science
Vol.11

- 374 -

1963 R.O.Reid B.W.Wilson
Boundary Flow Along a Circular Cylinder
Journal of the Hydraulics Division, ASCE
Vol.89 HY3 May pp21

- 375 -

1992 D.E.Reeve R.A.Hiley
Numerical Prediction of Tidal Flow in Shallow Water
Computer Modelling of Seas and Coastal Regions
Ed: P.W.Partridge
Computational Mechanics Publications
Elsevier

- 376 -

1883 O.Reynolds
On the Experimental Investigation of the Circumstances Which Determine
Whether the Motion of Water will be Direct or Sinous and the Law of
Resistance in Parallel Channels
Phil Trans Roy Soc London Series A
Vol.174 pp935-982

- 377 -

1895 O.Reynolds
On the Dynamical Theory of Incompressible Viscous Fluids
and the Determination of the Criterion
Phil Trans Roy Soc London Series A
Vol.186 pp123-164

- 378 -

1983 C.M.Rhie W.L.Chow
Numerical Study of the Turbulent Flow Past an Airfoil
with Trailing Edge Separation
AIAA Journal
Vol21 No11 Nov pp1525

- 379 -

1957 R.S.Rivlin
The Relation Between the Flow of Non-Newtonian Fluids and Turbulent
Newtonian Fluids
Quart.Appl.Math.
Vol.15 pp212

- 380 -

1988 M.H.Rizk S.Menon
Large-eddy Simulations of Axisymmetric excitation
effects on a row of impinging jets
Physics of Fluids
Vol31(7) July pp1892-1903

- 381 -

1970 P.J.Roache
Sufficiency Conditions for a Commonly Used Downstream
Boundary Condition on Stream Function
Journal of Computational Physics
Vol6 pp317-321

- 382 -

1972 P.J.Roache
Computational Fluid Dynamics
Hermosa Publishing

- 383 -

1992 P.J.Roache
Validation Exercises of a One-Dimensional Flux-Based Modified
Method of Characteristics
Proceeding of the 9th International Conference on Computational
Methods in Water Resources. Vol.1

- 384 -

1980 W.Rodi
Turbulence Models and their Application in Hydraulics
IAHR State of Art Report

- 385 -

1982 W.Rodi
Examples of Turbulence Models for Incompressible Flows
AIAA Journal
Vol.20 No.7 Jul

- 386 -

1977 S.G.Rubin P.K.Khosla
Polynomial Interpolation Methods for Viscous Flow
Calculations
Journal of Computational Physics
Vol.24

- 387 -

1973 P.J.Russell A.P.Hatton
Turbulent Flow Characteristics of an Impinging Jet
Heat and Fluid Flow
Vol.3 No.1

- 388 -

1993 S.G.Sajjadi J.N.Aldridge
Second Moment Closure Modelling of Turbulent
Flow over Sand Ripples
Refined Flow Modelling and Turbulence Measurements
Proc of the 5th International Symposium, Paris, France.

- 389 -

1985 P.G.Samuels

Modelling of Flood Plain Flow Using the Finite Element Method
A PhD thesis presented to the University of Reading
in September, 1985. Department of Mathematics.

- 390 -

1990 P.G.Samuels

Cross-section Location in 1-D Models
Proc of the 1st Int Conf on River Flood Hydraulics
Ed: W.R.White
17-20 September, 1990, Wallingfor, England.

- 391 -

1981 R.L.Sani P.M.Gresho R.L.Lee D.F.Griffiths

The Cause and Cure (?) of the Spurious Pressures
Generated By Certain FEM Solutions of the Incompressible
Navier-Stokes Equations : Part 1
Int Journal for Numerical Methods in Fluids
Vol.1 pp17-43

- 392 -

1981 R.L.Sani P.M.Gresho R.L.Lee D.F.Griffiths M.Engelman

The Cause and Cure (?) of the Spurious Pressures
Generated By Certain FEM Solutions of the Incompressible
Navier-Stokes Equations : Part 2
Int Journal for Numerical Methods in Fluids
Vol.1 pp171-204

- 393 -

1983 K.V.N.Sarma P.Lakshminarayana N.S.LakshmanaRao

Velocity Distribution in Smooth Rectangular Open
Channels
Journal of Hydraulic Engineering, ASCE
Vol.109 No.2 Feb

- 394 -

1988 S.Sarraf R.Kahawita N.Eljabi

3-D General Movable Mesh in Water Circulation Modeling
Journal of Computing in Civil Engineering, ASCE
Vol.2 No.2 Apr

- 395 -

1987 S.Sarraf Kahawita R.Camarero

Three Dimensional Surface Water Modelling Using a Mesh
Adaptive Technique
International Journal for Numerical Methods in Fluids
Vol.7

- 396 -

1987 P.Sauvaget J.M.Usseglio-Polatera

Numerical Simulation of Stratified Flows in Estuaries and Reservoirs
Proceedings of the Third International Symposium on Stratified Flows
Pasadena, California
Eds: E.J.List G.H.Jirka

- 397 -

1983 D.R.Schamber B.E.Larock

Particle Concentration Predictions in Settling Basins
Journal of Environmental Engineering, ASCE
Vol.109 No.3 Jun

- 398 -

1991 M.Schroder C.J.Stein G.Rouve

Application of the 3D-LDV Technique on Physical Model of
Meandering Channel with Vegetated Flood Plain
4th Int. Conf. on Laser Anemometry - Adv. and Apps.
Aug Cleveland, Ohio

- 399 -

1991 G.A.Schohl F.M.Holly
Cubic Spline Interpolation in Lagrangian Advection
Computation
Journal of Hydraulic Engineering, ASCE
Vol.117 No.2 Feb

- 400 -

1981 W.H.Schofield
Turbulent Shear Flows Over a Step Change in Surface
Roughness
Journal of Fluids Engineering, ASME
Vol.103 June

- 401 -

1989 J.A.Schutt
Numerical Solution of the Navier-Stokes Equations for Three
Dimensional Incompressible Flows with Open Boundaries
Numerical Methods in Laminar and Turbulent Flow, Vol.6
Proceedings of the 6th International Conference, Swansea

- 402 -

1992 R.H.J.Sellin
Hydraulic Performance of Flood Channels: Meander Channel
Cross-Flow Mechanisms
SERC
Final Report GR/E76476

- 403 -

1992 R.H.J.Sellin D.A.Ervine B.B.Willetts
Behaviour of Meandering Two-Stage Channels
Proceedings of the I.C.E.
Water, Maritime and Energy
Vol 101 Issue 2 Paper 10106

- 404 -

1988 M.A.R.Sharif A.A.Busnaina
An Investigation into the Numerical Dispersion Problem
of the Skew Upwind Finite Difference Scheme
Applied Mathematical Modelling
Vol.12 Apr

- 405 -

1984 P.Shanahan D.R.F.Harleman
Transport in Lake Water Quality Modeling
Journal of Environmental Engineering, ASCE
Vol.110 No.1 Feb

- 406 -

1989 K.Shiono D.W.Knight
Transverse and Vertical Reynolds Stress Measurements in
a Shear Layer Region of a Compound Channel
7th Symp. on Turbulent Shear Flows - Stanford

- 407 -

1990 Y.Shimuzi H.Yamaguchi T.Itakura
Three Dimensional Computation of Flow and Bed
Deformation

- 408 -

1989 T.M.Shih C.H.Tan B.C.Hwang
Effects of Grid Staggering on Numerical Schemes
Int Journal for Numerical Methods in Fluids
Vol9 pp193-212

- 409 -

1991 T.M.Shih B.C.Hwang
An Algorithm that Accelerates Convergence Rates For
Incompressible Navier-Stokes Problems
International Journal for Numerical Methods in Fluids
Vol12 pp965-983

- 410 -

1990 Y.Shimizu H.Yamaguchi T.Itakura
Three-Dimensional Computation of Flow and Bed Deformation
Journal of Hydraulic Engineering, ASCE
Vol.116 No.9 Sept

- 411 -

1990 K.Shiono D.W.Knight
Mathematical Models of Flow in Two-Stage or Multi-Stage
Straight Channels
Int. Conf. on River Flood Hydraulics, 1990 HR, Wallingford.
Sept

- 412 -

1992 W.Shyy S.Thakur J.Wright
Second-Order Upwind and Central Differences Schemes for
Recirculating Flow Computation
AIAA Journal
Vol.30 No.4 Apr

- 413 -

1992 R.P.Signell B.Butman
Modeling Tidal Exchange and Dispersion in Boston Harbour
Journal of Geophysical Research
Vol.97 No.C10

- 414 -

1986 J.F.Sini I.Dekeyser
Prevision Numerique De Jets 2-D en Milieux Stratifies a
L'Aide D'un Modele

- 415 -

1989 J.F.Sini I.Dekeyser
Numerical Prediction of Turbulent Plane Buoyant Jets
Discharging in a Stratified Stagnant or Flowing Ocean
Numerical Heat Transfer
Part A Vol16 pp371-387

- 416 -

1987 J.F.Sini I.Dekeyser
Numerical Prediction of turbulent plane jets and forced
plumes by use of the k- ϵ model of turbulence.
Int.J.Heat Mass Transfer
Vol30 No9 pp1787-1801

- 417 -

1990 D.J.Skyner C.Gray C.A.Greated
A Comparison of Time-Stepping Numerical Predictions with
Whole Field Flow Measurement in Breaking Waves
Water Wave Kinematics (ED A.Torum O.T.Gudmestad)

- 418 -

1969 L.S.Slotta E.H.Elwin H.T.Mercier M.D.Terry
Stratified Reservoir Currents: Prt II The NUMAC Method
Eng.Expt.Stn. Oregon State Uni., Corvallis, Oregon.
Bulletin No 44

- 419 -

1963 J.Smagorinsky
General Circulation Experiments with the Primitive
Equations
Monthly Weather Review
Vol 91(3) pp99 March

- 420 -

1989 C.D.Smith
Some Aspects of Flood Plain Flow in a Valley with a
Meandering Channel
Proceedings of the IAHR Conference, Canada 1989
Fluvial Hydraulics B-355

- 421 -

1984 R.M.Smith
On the Finite Element Calculation of Turbulent Flow
Using the $k-\epsilon$ Model
International Journal for Numerical Methods in Fluids
Vol.4

- 422 -

1983 R.J.Sobey
Fractional Step Algorithm for Estuarine Mass Transport
International Journal for Numerical Methods in Fluids
Vol.3

- 423 -

1991 J.V.Soulis
A Numerical Method for Subcritical and Supercritical
Open Channel Flow Calculation
International Journal for Numerical Methods in Fluids
Vol.13

- 424 -

1988 P.R.Spallart
Direct Simulation of a Turbulent Boundary Layer Up to
 $Re = 1410$
Journal of Fluid Mechanics
Vol.187

- 425 -

1988 C.G.Speziale T.Ngo
Numerical Solution of Turbulent Flow Past a Backward Facing
Step Using a Nonlinear $k-\epsilon$ Model
International Journal of Engineering Science
Vol.26 No.10

- 426 -

1989 C.G.Speziale N.MacGiollaMhuiris
On the Prediction of Equilibrium States in Homogeneous
Turbulence
Journal of Fluid Mechanics
Vol.209

- 427 -

1991 C.G.Speziale
Analytical Methods for the Development of
Reynolds-Stress Closures in Turbulence
Annual Review of Fluid Mechanics
Vol.23

- 428 -

1987 C.G.Speziale
On nonlinear k-l and k- ϵ Models of Turbulence
Journal of Fluid Mechanics
Vol.178 pp459-475

- 429 -

1982 C.G.Speziale
On Turbulent Secondary Flows in Pipes of Noncircular
Cross-Section
International Journal of Engineering Science
Vol.20 No.7

- 430 -

1993 T.B.Gatski C.G.Speziale
On Explicit Algebraic Stress Models for Complex Turbulent Flows
Journal of Fluid Mechanics
Vol.254, pp59

- 431 -

1992 K.Srinivas
An Explicit Spatial Marching Algorithm for Navier-Stokes
Equations
Computers & Fluids
Vol.21 No.2 pp291-299

- 432 -

1989 A.L.Stamou E.W.Adams W.Rodi
Numerical Modeling of Flow and Settling in Primary Rectangular
Clarifiers
Journal of Hydraulic Research
Vol.27 No.5

- 433 -

1989 C.J.Stein A.Rouve
2D LDV Technique for Measuring Flow in a Meandering
Channel with Wetted Floodplains - A New Application and
First Results
International Conference on Fluvial Hydraulics
Budapest

- 434 -

1857 G.G.Stokes
On the Theories of Internal Friction of Fluids in Motion
Trans Cambridge Phil Soc
Vol.8 pp287-305

- 435 -

1968 H.L.Stone
Iterative Solution of Implicit Approximations of

Multidimensional Partial Differential Equations
SIAM Journal of Numerical Analysis
Vol5 No3 Sept pp530-558

- 436 -

1989 S.-H.Suh A.C.Benim
The Primitive Variables Formulation of the Navier-Stokes
Equations Using the Finite Analytic Method
Applied Mathematical Modelling
Vol.13 Sept

- 437 -

1989 T.Y.Su S.Y.Wang C.V.Alonso
Depth Averaging Models of River Flows
in 'Finite Elements in Water Resources'
Eds: Wang Alonso Brebbia Gray Pinder

- 438 -

1985 L.L.Takacs
A Two-Step Scheme for the Advection Equation with Minimized
Dissipation and Dispersion Errors
Monthly Weather Review
Vol.113 No.6

- 439 -

1984 N.Takemitsu
Finite Difference Method to Solve Incompressible Fluid
Flow
Journal of Comp. Physics
pp499

- 440 -

1981 C.Taylor C.E.Thomas K.Morgan
Modelling Flow over a Backward-Facing Step Using the FEM
and the Two-Equation Model of Turbulence
Int Journal for Numerical Methods in Fluids
Vol.1 pp295-304

- 441 -

1953 G.Taylor
Dispersion of Soluble Matter in Solvent Flowing Slowly
Through a Tube

- 442 -

1972 H.Tennekes J.L.Lumley
A First Course in Turbulence
The MIT Press

- 443 -

1990 S.Thangam D.D.Knight
A Computational Scheme In Generalized Coordinates for
Viscous Incompressible Flows
Computers & Fluids
Vol18 No4 pp317-327

- 444 -

1992 S.Thangam C.G.Speziale
Turbulent Flow Past a Backward Facing Step: A Critical
Evaluation of Two-Equation Models
AIAA Journal

- 445 -

1992 T.G.Thomas J.J.R.Williams D.C.Leslie
Development of a Conservative 3D Free Surface Code
Journal of Hydraulic Research
Vol.30 No.1

- 446 -

1985 H.D.Thompson B.W.Webb J.D.Hoffman
The Cell Reynolds Number Myth
International Journal for Numerical Methods in Fluids
Vol.5

- 447 -

1993 M.F.C.Thorn
The Way Forward in Practical Model Applications
Proceedings of the the I.C.E.
Water, Maritime and Energy
Vol 96 Issue 3 Paper TN 582

- 448 -

1983 T.Timin M.N.Esmail
A Comparative Study of Central and Upwind Difference
Schemes Using the Primitive Variables
International Journal for Numerical Methods in Fluids
Vol.3

- 449 -

1990 T.Tingsanchali S.Maheswaran
2-D Depth Averaged Flow Computation Near Groyne
Journal of Hydraulic Engineering, ASCE
Vol.116 No.1 Jan

- 450 -

1967 G.H.Toebes A.A.Sooky
Hydraulics of Meandering Rivers with Flood Plains
Journal of the Waterways and Harbours Division, ASCE
WW2 May pp213

- 451 -

1974 J.M.Townson
An Application of the Method of Characteristics to Tides in x-y-t
Space
Journal of Hydraulic Research
Vol.12 No.4

- 452 -

1974 J.M.Townson A.S.Donald
Numerical Modelling of Storm Surges in the Clyde Sea Area
Proceedings of the I.C.E.
Part 2 Vol.79 Dec

- 453 -

1991 J.M.Townson
Free-Surface Hydraulics
Unwin Hyman

- 454 -

1991 A.Tominaga I.Nezu
Turbulent Structure in Compound Open-Channel Flows
Journal of Hydraulic Engineering, ASCE
Vol.117 No.1 January pp.21

- 455 -

1989 A.Tominaga I.Nezu K.Ezaki
Experimental Study on Secondary Currents In Compound
Open-Channel Flows
Proc. of the XXIII IAHR Congress - Ottawa, 1989
A-15

- 456 -

1992 S.Ushijima T.Shimizu A.Sasaki Y.Takizawa
Prediction Method for Local Scour by Warmed Cooling
Water Jets
Journal of Hydraulic Engineering, ASCE
Vol.118 No.8 Aug

- 457 -

1977 E.M.Valentine I.R.Wood
Longitudinal Dispersion with Dead Zones
Journal of the Hydraulics Division, ASCE
Vol.103 No.HY9 Sept

- 458 -

1986 D.Vandromme D.H.Minh
About the Coupling of Turbulence Closure Models with
Averaged Navier-Stokes Equations
Journal of Computational Physics
Vol.65

- 459 -

1987 S.P.Vanka K.P.Misegades
Vectorised Multigrid Fluid Flow Calculations On a Cray
X-MP/48
International Journal for Numerical Methods in Fluids
Vol.7

- 460 -

1989 P.Van der Kuur A.Roelfzema G.K.Verboom
The Three Dimensional Programme TRISULA with Curvilinear
Orthogonal Co-ordinates
Advances in Water Modelling and Measurement
pp.135 Editor-M.H.Palmer

- 461 -

1980 S.P.Vanka B.C.-J.Chen W.T.Sha
A Semi-Implicit Calculation Procedure for Flows
Described in Boundary-Fitted Coordinate Systems
Numerical Heat Transfer
Vol.3 pp.1-19

- 462 -

1984 J.P.VanDoormaal G.D.Raithby
Enhancements of the SIMPLE Method for Predicting
Incompressible Fluid Flows
Numerical Heat Transfer
vol.7 pp.147-163

- 463 -

1968 G.Veronis
Large-amplitude Benard convection in a rotating fluid
Journal of Fluid Mechanics
Vol31 prt1 pp113-139

- 464 -

1971 J.A.Viecelli
A Computing Method for Incompressible Flows Bounded by
Moving Walls
Journal of Computational Physics
Vol8 pp119-143

- 465 -

1969 J.A.Viecelli
A Method for Including Arbitrary External Boundaries in
the MAC Incompressible Fluid Computing Technique
Journal of Comp. Physics
Vol4 pp543-551

- 466 -

P.L.Viollet
On the Numerical Modelling of Stratified Flows
Unknown Source

- 467 -

1981 P.-L.Viollet A.Keramsi J.-P.Benque
Modelisation Bidimensionnelle D'Ecoulements En Charge
D'un Fluide Incompressible Non Isotherme
Journal de Mechanique
Vol.20 No.3

- 468 -

1987 P.L.Viollet
The Modelling of Turbulent Recirculating Flows for the
Purpose of Reactor Thermal-Hydraulic Analysis
Nuclear Engineering and Design
Vol99 pp365-377

- 469 -

1987 P.L.Viollet
Observation and Numerical Modelling of Density Currents
Resulting from Thermal Transients in a Non-rectilinear
Pipe.
Journal of Hydraulic Research
Vol.25 No.2 pp235

- 470 -

1983 P.L.Viollet J.P.Benque J.Goussebaile
Two-Dimensional Numerical Modelling of Nonisothermal
Flows for Unsteady Thermal-Hydraulic Analysis
Nuclear Science and Engineering
Vol.84 pp350-372

- 471 -

1977 H.Vollmars J.C.Rotta
Similar Solutions of the Mean Velocity, Turbulent Energy
and Length Scale Equation
AIAA Journal
Vol.15 No.5 May

- 472 -

1982 C.B.Vreugdenhil J.H.A.Wijbenga

Computation of Flow Patterns in Rivers
Journal of the Hydraulics Division, ASCE
Vol108 HY11 Nov pp1296

- 473 -

1989 C.B.Vreugdenhil
Computational Hydraulics
Springer-Verlag

- 474 -

1993 C.Vuik
Solution of the Discretized Incompressible Navier-Stokes
Equations with the GMRES Method
International Journal for Numerical Methods in Fluids
Vol.16

- 475 -

1993 S.G.Wallis
Private Communication

- 476 -

1988 J.D.Wang S.V.Cofer-Shabica J.C.Fatt
Finite Element Characteristic Advection Model
Journal of Hydraulic Engineering, ASCE
Vol.114 No.9 Sept

- 477 -

1974 P.R.B.Ward
Transverse Dispersion in Oscillatory Channel Flow
Journal of the Hydraulics Division
Vol.100 HY6 June

- 478 -

1990 J.B.Wark P.G.Samuels D.A.Ervine
A Practical Method of Estimating Velocity and Discharge
in Compound Channels
1st International River Flood Hydraulics Conference
Wallingford, England.

- 479 -

1990 J.B.Wark
The Equations of River and Flood Plain Flow
University of Glasgow, PhD Progress Report
December 1988

- 480 -

1993 J.B.Wark
Discharge Assessment in Straight and Meandering Compound Channels
A PhD thesis submitted to the University of Glasgow, July 1993.

- 481 -

1980 A.J.Ward-Smith
Internal Fluid Flow - The fluid dynamics of flow in
pipes and ducts
Clarendon Press, Oxford.

- 482 -

1984 G.Weber M.Schatzmann
Transverse Mixing in Open Channel Flow
Journal of Hydraulic Engineering, ASCE
Vol.110 No.4 Apr

- 483 -

1992 D.J.Weber J.E.Danberg
Correlation of Mean Velocity Measurements Downstream of
a Swept Backward Facing Step
AIAA Journal
Vol.30 No.11 Nov

- 484 -

1965 J.E.Welch F.H.Harlow J.P.Shannon B.J.Daly
The MAC Method: A Computing Technique for Solving
Viscous Incompressible Transient Fluid Flow Problems
Involving Free Surfaces
Los Alamos Scientific Laboratory
Rep LA-3425

- 485 -

1991 F.M.White
Viscous Fluid Flow
McGraw-Hill

- 486 -

1985 J.H.A.Wijbenga
Steady Depth-Averaged Flow Calculations on Curvilinear
Grids
2nd Int Conf on The Hydraulics of Floods & Flood Control
pp373

- 487 -

1985 J.H.A.Wijbenga
Determination of Flow Patterns in Rivers with
Curvilinear Coordinates
21st IAHR Congress Australia
pp131

- 488 -

1991 B.B.Willetts
The Hydraulics of Meandering Channels
River and Flood Plain Management
Scottish Hydraulics Study Group Meeting 22nd March 1991

- 489 -

1988 D.C.Wilcox
Multiscale Model for Turbulent Flows
AIAA Journal
Vol.26 No.11 Nov

- 490 -

1988 D.C.Wilcox
Reassessment of the Scale-Determining Equation for
Advanced Turbulence Models
AIAA Journal
Vol.26 No.11 Nov

- 491 -

1988 P.Wilders Th.L.VanStijn G.S.Stelling G.A.Fokkema
A Fully Implicit Splitting Method for Accurate Tidal
Computations
Inter.Journ.for Num.Meth. in Fluids
Vol.26

- 492 -

1969 G.P.Williams
Numerical Integration of the Three-Dimensional
Navier-Stokes Equations for Incompressible Flow
Journal Fluid Mechanics
Vol37 prt4 pp727-750

- 493 -

1992 J.J.R.Williams
Large Eddy Simulation
Is Turbulence Modelling of Any Use?
IAHR Seminar April 9th

- 494 -

1988 P.Wormleaton
Determination of Discharge in Compound Channels using the Dynamic
Equation for Lateral Velocity Distribution
Proc Int Conf on Fluvial Hydraulics
Vitaki, Budapest

- 495 -

1987 H.C.Yee
Construction of Explicit and Implicit Symmetric TVD
Schemes and Their Applications
Journal of Computational Physics
Vol.68

- 496 -

1972 G.-T.Yeh
Unified Formulation of Wall Turbulence
Journal of the Hydraulics Division, ASCE
Vol.98 HY12 Dec pp 2263

- 497 -

1973 B.C.Yen
Open Channel Flow Equations Revisited
Journal of the Engineering Mechanics Division, ASCE
Vol.99 No.EM5 Oct

- 498 -

1973 C.-L.Yen D.E.Overton
Shape Effects on Resistance in Flood-Plain Channels
Journal of the Hydraulics Division, ASCE
Vol.99 HY1 Jan pp219

- 499 -

1990 Y.Yongquan W.Chigong
An Investigation on ASM Turbulence Model in Predicting
Non-isotropic Turbulent Flows
4th Int Symp on Refined Flow Modelling etc
China IAHR

- 500 -

1993 A.Yoshizawa
Derivation of a Model Reynolds-Stress Transport Equation
Using the Renormalization of the Eddy-Viscosity Type
Representation
Physics of Fluids - A
Vol.5(3) Mar

- 501 -

1989 B.A.Younis O.E.Abdellatif
Modeling Sediment Transport in Rectangular Ducts with a
Two-Equation Model of Turbulence
Sediment Transport Modeling - Proc.Int.Symp.ASCE '89
Aug. Louisiana

- 502 -

1992 B.A.Younis
Some Turbulence Models
Is Turbulence Modelling of Any Use?
IAHR Seminar April 9th

- 503 -

1991 B.A.Younis
Turbulence Modelling for Non-Circular Ducts and Channels
SERC CFD Community Club Seminar 9 July 1991

- 504 -

1992 N.A.Zaghloul
A Computer Model to Calculate Flow Resistance in Open
Channels with Movable Boundaries
Advances in Engineering Software
Vol.14

- 505 -

1983 M.Zedan G.E.Schneider
A Three-Dimensional Modified Strongly Implicit Procedure
for Heat Conduction
AIAA Journal
Vol.21 No.2 Feb pp295

- 506 -

1991 C.-X.Zhang
Simulation Numerique D'Ecoulements Turbulents Autour
D'Un Obstacle
PhD Thesis Universite de Nantes

- 507 -

1992 S.Zhou J.A.McCorquodale
Modeling of Rectangular Settling Tanks
Journal of Hydraulic Engineering, ASCE
Vol.118 No.10 Oct

- 508 -

1991 J.Zhu
A Low-Diffusive and Oscillation-Free Convection Scheme
Communications in Applied Numerical Methods
Vol7 pp225-232